IN TWO SECTIONS—SECTION TWO

Transactions

of the

A.S.M.E.

SOCIETY RECORDS—Part III

(Including Indexes to Publications)

[*Part I of Society Records for the year 1940 (containing Council and Committee Personnel and other general information) was issued as Section Two of the Transactions for February, 1940, and Part II (Memorial Biographies) October, 1940.*]

JANUARY, 1941

VOL. 63, NO. 1

Transactions

of The American Society of Mechanical Engineers

Published on the tenth of every month, except March, June, September, and December

Published monthly by The American Society of Mechanical Engineers. Publication office at 20th and Northampton Streets, Easton, Pa. The editorial department located at the headquarters of the Society, 29 West Thirty-Ninth Street, New York, N. Y. Cable address, "Dynamic," New York. Price $1.50 a copy, $12.00 a year; to members and affiliates, $1.00 a copy, $7.50 a year. Changes of address must be received at Society headquarters two weeks before they are to be effective on the mailing list. Please send old as well as new address.... By-Law: The Society shall not be responsible for statements or opinions advanced in papers or .... printed in its publications (B13, Par. 4).... Entered as second-class matter March 2, 1928, at the Post Office at Easton, Pa., under the Act of August 24, 1912....

Depositories for A.S.M.E. Transactions in the United States, Including Territories and Dependencies

BOUND copies of the complete Transactions of The American Society of Mechanical Engineers will be found in the libraries in the United States and other countries which are listed on the following pages.

Alabama

Auburn.......... Engineering Library, Alabama Poly. Inst.
Birmingham..... Public Library
University....... Library, University of Alabama

Arizona

Tucson.......... Library, University of Arizona

Arkansas

Fayetteville...... Engineering Library, University of Arkansas

California

Berkeley......... Library, University of California
Long Beach...... Public Library
Los Angeles...... Public Library
University of Southern California
Oakland......... Oakland City Library
Teachers' Professional Library
Pasadena........ Library, California Institute of Technology
Santa Clara...... Library, University of Santa Clara
San Diego....... Public Library
San Francisco.... Public Library (Civic Center)
Engineers Club of San Francisco
Mechanics Institute
Stanford Univ.... Library, Stanford University

Colorado

Boulder.......... Library, University of Colorado
Denver.......... Public Library
Fort Collins...... Colorado State Agricultural College

Connecticut

Bridgeport....... Public Library
Hartford......... Public Library
New Haven...... Public Library and Yale University
Waterbury....... Silas Bronson Library

Delaware

Newark.......... University of Delaware
Wilmington...... Wilmington Free Institute

District of Columbia

Washington...... Scientific Library, U. S. Patent Office; Library of Congress; Bureau of Standards Library; George Washington and Catholic Universities

Florida

Gainesville....... University of Florida
Jacksonville...... Free Public Library
Miami........... Public Library
Tampa.......... Public Library

Georgia

Atlanta.......... Carnegie Public Library
Georgia School of Technology
Savannah........ Public Library

Hawaii

Honolulu........ University of Hawaii Library

Idaho

Moscow......... University of Idaho

Illinois

Chicago......... John Crerar Library; Western Society of Engineers; Library, Illinois Institute of Technology; Museum of Science and Industry; Public Library of Chicago
Evanston........ Northwestern University
Moline.......... Public Library
Peoria........... Public Library
Urbana.......... University of Illinois

Indiana

Evansville....... Public Library
Fort Wayne...... Public Library
Indianapolis..... Public Library and Indiana State Library
Notre Dame..... Library, University of Notre Dame
Terre Haute..... Rose Polytechnic Institute
West Lafayette... Library, Purdue University

Iowa

Ames............ Iowa State College
Des Moines...... Public Library
Iowa City........ State University of Iowa

Kansas

Kansas City..... Public Library, Huron Park
Lawrence........ Library, University of Kansas
Manhattan...... Kansas State College
Wichita.......... Wichita City Library

Kentucky

Lexington........ University of Kentucky
Louisville........ Speed Scientific School
University of Louisville

Louisiana

Baton Rouge..... Louisiana State University
New Orleans..... Howard Memorial Library
Louisiana Engineering Society
Public Library
Tulane University

Maine

Orono........... University of Maine

Maryland

Annapolis........ United States Naval Academy
Baltimore........ Johns Hopkins University
Engineers Club of Baltimore
Public Library
College Park..... Library, University of Maryland

Massachusetts

Boston.......... Engineering Societies of New England
Northeastern University
Boston Public Library
Cambridge....... Harvard University (Engineering Library)
Massachusetts Institute of Technology
Fall River....... Public Library
Lynn............ Free Public Library
New Bedford..... Free Public Library
Springfield....... Springfield City Library
Tufts College.... Tufts College
Worcester........ Worcester Polytechnic Institute
Free Public Library

Michigan

Ann Arbor....... University of Michigan
Detroit.......... Public Library
Cass Technical High School
Highland Park Public Library
University of Detroit
East Lansing..... Michigan State College
Flint............ Public Library
Grand Rapids.... Public Library
Houghton........ Michigan College of Mining & Technology
Jackson.......... Public Library

Minnesota

Duluth.......... Public Library
Minneapolis...... University of Minnesota
Minneapolis Public Library (Engineering and Circulating Libraries)
St. Paul......... James Jerome Hill Reference Library

Mississippi

State College..... Mississippi State College

Missouri

Columbia........ University of Missouri
Kansas City..... Public Library
Rolla............ Missouri School of Mines and Metallurgy
St. Louis......... Engineers Club of St. Louis; Public Library; Washington University; Mercantile Library

Montana

Bozeman........ Montana State College

Nebraska
- Lincoln.......... University of Nebraska
- Omaha.......... Public Library

Nevada
- Reno............ University of Nevada Library

New Hampshire
- Durham......... University of New Hampshire

New Jersey
- Bayonne......... Free Public Library
- Camden......... Free Public Library
- Elizabeth........ Free Public Library
- Hoboken......... Stevens Institute of Technology
- Jersey City...... Free Public Library
- Newark.......... Newark College of Engineering
  - Free Public Library
- New Brunswick.. Rutgers University
- Paterson......... Free Public Library
- Princeton........ Princeton University
- Trenton......... Free Public Library

New Mexico
- Albuquerque..... University of New Mexico

New York
- Albany.......... New York State Library
- Brooklyn........ Polytechnic Institute
  - Pratt Institute
  - Brooklyn Public Library
- Buffalo.......... The Grosvenor Library
  - Engineering Society of Buffalo
  - Buffalo Public Library
- Ithaca........... Cornell University
- Jamaica, L. I..... Queens Borough Public Library
- New York....... Engineering Societies Library
  - Public Library
  - College of the City of New York
  - Cooper Union
  - Columbia University
  - New York Museum of Science and Industry
  - New York University Library
- Potsdam......... Clarkson College of Technology
- Rochester........ Rochester Engineering Society
- Schenectady..... Union College
- Syracuse......... Syracuse University
  - Public Library
- Troy............ Rensselaer Polytechnic Institute
- Utica............ Public Library

North Carolina
- Chapel Hill...... University of North Carolina
- Durham......... Duke University
- Raleigh.......... North Carolina State College

North Dakota
- Fargo........... North Dakota State Agricultural College
- Grand Forks..... University of North Dakota

Ohio
- Ada............. Ohio Northern University
- Akron........... Public Library
  - University of Akron
- Canton.......... Public Library
- Cincinnati....... University of Cincinnati
  - Public Library
  - Engineers Club of Cincinnati
- Cleveland........ Public Library
  - Case School of Applied Science
  - Cleveland Engineering Society
  - Fenn College
- Columbus........ State of Ohio Library
  - Public Library
  - Ohio State University
- Dayton.......... Engineers Club of Dayton
- Toledo.......... Public Library
  - University of Toledo
- Youngstown..... Public Library

Oklahoma
- Norman......... Oklahoma University
- Oklahoma City... Public Library
- Stillwater........ Oklahoma A.&M. College
- Tulsa............ Public Library

Oregon
- Corvallis......... Oregon State Agricultural College
- Portland......... Portland Library Association

Pennsylvania
- Allentown........ Free Library
- Bethlehem....... Lehigh University
- Easton.......... Public Library
  - Lafayette College
- Erie............. Public Library
- Lewisburg....... Bucknell University
- Philadelphia..... Engineers Club
  - Drexel Institute
  - The Free Library
  - University of Pennsylvania
  - Franklin Institute
- Pittsburgh....... University of Pittsburgh
  - Engineers' Society of Western Pennsylvania
  - Carnegie Institute of Technology
  - Carnegie Library (Schenley Park)
  - Carnegie Free Library of Allegheny
- Reading......... Public Library
- Scranton......... Public Library
- State College..... Pennsylvania State College
- Swarthmore...... Swarthmore College
- Villanova........ Villanova College
- Wilkes-Barre..... Public Library

Puerto Rico
- Mayaguez....... University of Puerto Rico

Rhode Island
- Kingston........ Rhode Island State College
- Providence....... Brown University
  - Providence Engineering Society
  - Public Library

South Carolina
- Clemson College.. Library, Clemson College

South Dakota
- Brookings........ South Dakota State College

Tennessee
- Kingsport........ Public Library
- Knoxville........ University of Tennessee
- Memphis........ Goodwin Institute
- Nashville........ Vanderbilt University

Texas
- Austin........... University of Texas
- College Station... Agricultural & Mechanical College of Texas
- Dallas........... Public Library
  - Southern Methodist University
- El Paso.......... Public Library
- Fort Worth...... Carnegie Public Library
- Houston......... Rice Institute
  - Public Library
- Lubbock......... Texas Technological College
- San Antonio..... Carnegie Library

Utah
- Salt Lake City... University of Utah
  - Public Library

Vermont
- Burlington....... University of Vermont

Virginia
- Blacksburg....... Virginia Polytechnic Institute
- Charlottesville... University of Virginia
- Lexington....... Virginia Military Institute
- Norfolk.......... Public Library
- Richmond....... Virginia State Library

Washington
- Pullman......... State College of Washington
- Seattle.......... Public Library
  - Engineers Club
  - University of Washington
- Spokane......... Public Library
- Tacoma......... Public Library

West Virginia
- Morgantown..... West Virginia University

Wisconsin
- Madison......... Library, University of Wisconsin
- Milwaukee....... Public Library
  - Vocational School Library
  - Marquette University

Wyoming
- Laramie......... Wyoming University

Depositories for A.S.M.E. Transactions Outside the United States

Argentine

Buenos Aires.....Biblioteca de la Sociedad Cientifica

Australia

Adelaide.........Public Library of Adelaide
Melbourne.......Public Library of Victoria
Perth...........University of Western Australia Library
Sydney..........Public Library, N. S. W., Sydney

Belgium

Louvain.........University of Louvain

Brazil

Rio de Janeiro...Bibliotheca da Escola Polytechnica
Bibliotheca Nacional
São Paulo........Bibliotheca da Escola Polytechnica

Canada

Montreal........McGill University
Engineering Institute of Canada
Toronto.........University of Toronto, Library

Chile

Santiago.........Universidad de Chile, Facultad de Ciencias Fisicas y Matematicas (Engg. School)

China

Peiping..........College of Technology of Peiping University

Cuba

Havana..........Cuban Society of Engineers

Denmark

Copenhagen......The Royal Technical College

England

Birmingham.....Birmingham Public Libraries
Bristol..........University of Bristol
Cambridge.......University of Cambridge
Leeds...........University of Leeds
Liverpool........Public Library of Liverpool
Liverpool Engineering Society
London..........City and Guild Engineering College
Institution of Automobile Engineers
The Institution of Mechanical Engineers
Institution of Civil Engineers
Institution of Electrical Engineers
The Junior Institution of Engineers
The Royal Aeronautical Society
Manchester......Manchester Public Libraries (Reference Library)
Oxford..........Oxford University
Newcastle-upon-Tyne..........The North-East Coast Institution of Engineers and Shipbuilders
Sheffield.........Sheffield Public Libraries

France

Lyons...........University of Lyons
Paris............École Nationale des Arts et Metiers
École Nationale Supérieure de L'Aeronautique
École Centrale des Arts et Manufactures de Paris
Société des Ingénieurs Civils de France

Germany

Berlin...........Verein deutscher Ingenieure
Bibliothek der Technischen Hochschule
Breslau..........Bibliothek der Technischen Hochschule
Cologne (Köln)...Universitäts- und Stadtbibliothek
Dresden.........Bibliothek der Technischen Hochschule

Germany (Continued)

Düsseldorf.......Bücherei des Vereines deutscher Eisenhüttenleute
Frankfort........Technische Zentralbibliothek
Hamburg........Bibliothek der Technischen Staatslehranstalten
Hanover.........Bibliothek der Technischen Hochschule
Karlsruhe........Bibliothek der Technischen Hochschule
Leipzig..........Stadtbibliothek
Munich..........Bibliothek der Technischen Hochschule
Bibliothek des Deutschen Museums
Stuttgart........Bibliothek der Technischen Hochschule

Holland

Amsterdam......Koninklijke Akademie von Wetenschappen
Delft............Bibliotheek der Technische Hoogeschool
The Hague.......Koninklijk Instituut van Ingenieurs
Rotterdam.......Nationaal Technisch Scheepvaartkundig Instituut

India

Bangalore........Mysore Engineers Association
Calcutta.........Bengal Engineering College
Poona...........Poona College of Engineering
Rangoon.........University of Rangoon

Ireland

Belfast..........Queen's University of Belfast

Italy

Milan...........Biblioteca de la R. Scuola d'Ingegneria
Comitato Autonomo per l'Esame della Invenzioni
Naples..........Biblioteca della R. Scuola d'Ingegneria
Rome...........Biblioteca della R. Scuola d'Ingegneria
Consiglio Nazionale delle Ricerche presso il Ministero della Educazione Nazionale
Turin...........Biblioteca della R. Scuola d'Ingegneria

Japan

Kobe............Kobe Technical College
Tokyo...........Imperial University Library
The Society of Mechanical Engineers
Yokohama.......Library of Yokohama

Mexico

Mexico City.....Asociacion de Ingenieros y Arquitectos de Mexico
Library of the Escuela de Ingenieros Mecanicos y Electricistas

Norway

Oslo.............Den Polytekniske Forening

Portugal

Lisbon...........Institute Superior Technico

Rumania

Bucharest........Scoala Polytechnica din Bucharest

Scotland

Glasgow.........Royal Technical College
Mitchell Library

South Africa

Cape Town......University of Cape Town
Johannesburg....South African Institute of Engineers

Sweden

Stockholm.......Kungl. Tekniska Hogskolan
Svenska Teknologföreninger
Gothenburg......Chalmers Tekniska Institut

Switzerland

Zurich...........Bibliothek der Eidg. Technischen Hochschule

Turkey
Istanbul.........Robert College

U.S.S.R.
Kharkov.........Supreme Economic Council of Ukraine
Leningrad........Leningrad Polytechnic Institute
Moscow.........Supreme Council of National Economy
Tomsk..........Tomsk Polytechnic Institute

Wales
Cardiff..........Cardiff Public Library

Indexes to A.S.M.E. Papers and Publications

THIS and the following pages will serve as a guide to the current publications of the A.S.M.E. during the calendar year 1940, and also to publications developed by the technical committees.

Regular Society Publications, 1940

Mechanical Engineering, monthly (see index on page RI-79)
A.S.M.E. Transactions, monthly (see index on page RI-89)
Mechanical Catalog and Directory, 1941 edition

Special Publications Issued in 1940

1939 Oil Engine Power Cost Report
1940 Proceedings of the Oil and Gas Power Division
Autobiography of an Engineer by William LeRoy Emmet
Autobiography of John Fritz

Boiler Construction Code, 1940 Edition

Locomotive Boiler Code
Low-Pressure Heating Boiler Code
Miniature Boiler Code
Power Boiler Code Including Rules for Inspection
Unfired Pressure Vessel Code
Specifications for Materials
Suggested Rules for Care of Power Boilers

Power Test Codes

Evaporating Apparatus
Steam Locomotives

Auxiliary Sections

Part 3—Temperature Measurement, Chapter 8
Part 5—Chapter 4, Flow Measurement by Means of Standardized Nozzles and Orifice Plates
Part 11—Determination of Quality of Steam

How to Find Papers Presented at 1940 A.S.M.E. Meetings

THE technical programs of the meetings of the Society and of its Professional Divisions have been published in *Mechanical Engineering* and may be located by consulting the index on pages RI-79–88. A majority of these papers were published, or will be published, in *Mechanical Engineering* or the Transactions (including the *Journal of Applied Mechanics*) and may be located by reference to the indexes of these publications. Several additional papers and reports included in these 1940 programs were not published during the year in either Transactions or *Mechanical Engineering*, but were issued in mimeographed or photo-offset form.

Complete sets of these are on file for reference purposes at the office of the Society and the Engineering Societies Library, under the title of "Miscellaneous Papers Presented at A.S.M.E. Meetings, 1940." Photostat copies of any of the papers may be secured from the Library at twenty-five cents a page to members.

Publications Developed by the Technical Committees

THE Society's technical committees, the first of which was organized many years ago and all of which have been continuously at work on codes, standards, research, and other special reports, have developed a series of publications of permanent value to the membership. The following list is presented here for record and for ready reference. This list covers the entire group of publications of these committees completed to date which are now available.

To assist the members in securing copies of these publications the sale price is also given. A discount of 10 per cent is allowed to A.S.M.E. members on standards and a 20 per cent discount on all other publications except where otherwise noted.

AMERICAN STANDARDS

Bolt, Nut, and Rivet Proportions

Large Rivets (B18.4—1937), $0.65
Plow Bolts (B18f—1928), $0.35
Round Unslotted-Head Bolts (B18.5—1939), $0.50
Slotted-Head Proportions: Machine Screws, Cap Screws, and Wood Screws (B18c—1930), $0.45
Small Rivets (B18a—1927), $0.30
Socket Set Screws and Socket-Head Cap Screws (B18.3—1936), $0.40
Tinners', Coopers', and Belt Rivets (B18g—1929), $0.35
Track Bolts and Nuts (B18d—1930), $0.40
Wrench-Head Bolts and Nuts and Wrench Openings (B18.2—1933), $0.50
Price of Set of Standards on Bolt, Nut, and Rivet Proportions, including binder, $4.55

Piping and Pipe Fittings

Brass Fittings for Flared Copper Tubes (A40.2—1936), $0.35
Cast-Iron Pipe Flanges and Flanged Fittings for 25 Lb Maximum Saturated Steam Pressure (B16b2—1931), $0.40
Cast-Iron Pipe Flanges and Flanged Fittings for 125 Lb Maximum Saturated Steam Pressure (B16a—1939), $0.60
Cast-Iron Pipe Flanges and Flanged Fittings for 250 Lb Maximum Saturated Steam Pressure (B16b—1928), $0.50
Cast-Iron Pipe Flanges and Flanged Fittings for 800 Lb Maximum Hydraulic Pressure (B16b1—1931), $0.35
Cast-Iron Soil Pipe and Fittings (A40.1—1935), $0.65
Cast-Iron Long Turn Sprinkler Fittings for 150 and 250 Lb Maximum Saturated Steam Pressure (B16g—1929), and Addendum (B16g1—1937), $0.50
Cast-Iron Screwed Fittings for 125 and 250 Lb Maximum Saturated Steam Pressure (B16d—1927), $0.35
Code for Pressure Piping (no discount) (B31.1—1935), $1.00
Face-to-Face Dimensions of Ferrous Flanged and Welding End Valves (B16.10—1939), $0.55
Malleable-Iron Screwed Fittings for 150 Lb Maximum Saturated Steam Pressure (B16c—1939), $0.50
Pipe Plugs (B16e2—1936), $0.35
Scheme for the Identification of Piping Systems (A13—1928), $0.50
Steel Pipe Flanges and Flanged Fittings for 150 to 2500 Lb Maximum Steam Service Pressure (B16e—1939), $1.25
Wrought-Iron and Wrought-Steel Pipe (B36.10—1939), $0.50

Letter and Graphical Symbols and Charts

Aeronautical Symbols (Z10e—1929), $0.35
Drawings and Drafting-Room Practice (Z14.1—1935), $0.50
Engineering and Scientific Charts for Lantern Slides (Z15.1—1932), $0.50
Graphical Symbols for Electric Power and Wiring (Z10g2—1933), $0.20

Graphical Symbols for Electrical Traction Including Railway Signaling (Z10g5—1933), $0.40
Graphical Symbols for Plumbing, Piping, Pipe Fittings and Valves, Heating and Ventilating, Heat-Power Apparatus, Conventional Rivets, etc. (Z14.2—1935), $0.45
Graphical Symbols for Radio (Z10g3—1933), $0.20
Graphical Symbols for Telephone and Telegraph Use (Z10g6—1929), $0.20
Letter Symbols for Electrical Quantities (Z10g1—1929), $0.20
Symbols for Electrical Equipment of Buildings (C10—1924), $0.20
Symbols for Heat and Thermodynamics (Z10c—1931), $0.30
Symbols for Mechanics, Structural Engineering, and Testing Materials (Z10a—1932), $0.25
Symbols for Photometry and Illumination (Z10d—1930), $0.20
Time Series Charts (Z15.2—1938), $1.25

MISCELLANY

Fire-Hose Coupling Screw Thread (B26—1925), $0.25
Production and Inspection of Fire-Hose Coupling Screw Thread (1925), $0.25
Gear Materials and Blanks (B6.2—1933), $0.50
Hose Coupling Screw Threads (B33.1—1935), $0.25
Indicating Pressure and Vacuum Gages (B40—1939), $0.40
Rolled Threads for Screw Shells of Electric Sockets and Lamp Bases (C44—1931), $0.35
Shaft Couplings (B49—1932), $0.35
Spur Gear Tooth Form (B6.1—1932), $0.45

Small Tools and Machine Tool Elements

Machine Tapers (B5.10—1937), $0.50
Milling Cutters (B5c—1930), $0.75
Taps—Cut and Ground Threads (B5.4—1939), $1.25
Terminology and Definitions for Single-Point Cutting Tools (B5.13—1939), $0.40
Adjustable Adapters (B5.11—1937), $0.50
Chucks and Chuck Jaws (B5.8—1936), $0.45
Circular and Dovetail Forming Tool Blanks (B5.7—1936), $0.40
Involute Splines, Side Bearings (B5.15—1939), $0.65
Jig Bushings (B5.6—1935), $0.35
Lathe Spindle Noses (B5.9—1936), $0.50
Rotating Air Cylinders and Adapters (B5.5—1932), $0.35
Tool Holder Shanks—Tool Post Openings (B5b—1929), $0.25
T-Slots, Their Bolts, Nuts, Tongues, and Cutters (B5a—1927), $0.35
Ball and Roller Bearings (B3.1, 2, 3—1930–1933), $0.40
Code for Design of Transmission Shafting (B17c—1927), $0.75
Shafting and Stock Keys (B17.1—1934), $0.45
Screw Threads for Bolts, Nuts, Machine Screws, and Threaded Parts (B1.1—1935), $0.60
Tolerances, Allowances, and Gages for Metal Fits (B4a—1925), $0.50
Woodruff Keys, Keyslots, and Cutters (B17f—1930), $0.35
Price of Set of Standards on Small Tools and Machine-Tool Elements, including binder, $9.85

BOILER CONSTRUCTION CODE—1940

Locomotive Boiler Code, $0.55
Low-Pressure Heating Boiler Code, $0.75
Miniature Boiler Code, $0.65
Power Boiler Code Including Rules for Inspection, $2.25
Unfired Pressure Vessel Code, $1.50
Specifications for Materials, $2.00
Suggested Rules for Care of Power Boilers, $1.00
Price of complete set of Boiler Codes including binder, $8.50
Boiler Code Interpretations
Price obtainable upon request

JOINT CODE

API-ASME Code for Unfired Pressure Vessels for Petroleum Liquids and Gases (1938 with 1940 Addenda), $1.25

POWER TEST CODES AND AUXILIARY SECTIONS

Test Codes for

Atmospheric Water-Cooling Equipment (1930), $0.45
Compressors and Exhausters (1935), $0.95
Displacement Compressors, Vacuum Pumps, and Blowers (1939), $0.75
Evaporating Apparatus (1940), $0.50
Feedwater Heaters (1927), $0.35
Gas Producers (1928), $0.55
Hydraulic Prime Movers (1938), $0.60
Internal-Combustion Engines (1930), $0.55
Liquid Fuels (1930), $0.35
Reciprocating Steam Engines (1935), $0.65
Reciprocating Steam-Driven Displacement Pumps (1927), $0.65
Refrigerating Systems (1927), $0.55
Solid Fuels (1931), $0.55
Speed-Responsive Governors (1927), $0.45
Stationary Steam-Generating Units (1936), $0.60
Steam Condensing Apparatus (1938), $0.65
Steam Locomotives (1940), $0.55

Auxiliary Sections

Definitions and Values (1931), $0.40
General Instructions (1929), $0.35
Part 1—General Consideration (1935), $0.35
Part 2—Pressure Measurement; Chapter 2, Static and Total Pressure, Static Holes and Tubes, Impact Tubes, and Chapter 3, Pipes for Pressure Measurement (1936), $0.65
Part 2—Pressure Measurement; Chapter 4, Bourdon, Bellows, Diaphragm, and Deadweight Gages (1938), $0.65
Part 3—Temperature Measurement; Chapter 1, General; Chapter 5, Pyrometric Cones; Chapter 6, Liquid-in-Glass Thermometers, and Chapter 7, Bourdon Tube Thermometers (1931), $0.75
Part 3—Temperature Measurement; Chapter 2, Radiation Pyrometers (1936), $0.55
Part 3—Temperature Measurement; Chapter 8, Optical Pyrometers (1940), $0.35
Part 4—Head Measuring Apparatus (1933), $0.35
Part 5, Chapter 4—Flow Measurement by Means of Standardized Nozzles and Orifice Plates (1940), $2.75
Part 6—Electrical Measurements (1934), $1.25
Part 9—Heat of Combustion (1932), $0.40
Part 10—Flue and Exhaust Gas Analyses (1936), $1.35
Part 11—Determination of Quality of Steam (1931), $0.45
Part 12—Measurement of Time (1932), $0.35
Part 13—Speed Measurements (1939), $0.45
Part 14—Linear Measurements (1936), $0.55
Part 15—Measurement of Surface Areas (1937), $0.75
Part 16—Density Determinations (1931), $0.30
Part 17—Determination of the Viscosity of Liquids (1931), $0.45
Part 18—Humidity Determinations (1932), $0.50
Part 20—Smoke-Density Determinations (1936), $0.65
Part 21—Leakage Measurement, Chapter 1, Condenser Leakage Tests (1928), $0.35
Part 21—Leakage Measurement; Chapter 2, Boiler and Piping; Chapter 3, Steam Engine Leakage (1932), $0.35

RESEARCH

Dynamic Loads on Gear Teeth (1932), $1.50
Fluid Meters:
Part 1—Theory and Application (1937), $3.00
Part 2—Description of Meters (1931), $1.75
Part 3—Selection and Installation (1933), $1.50
Report of the AGA-ASME Committee on Orifice Coefficients (1935), $2.75
Tests on Electrical Equipment for Drilling Rotary Drilled Oil Wells (1933), $0.85
Tests on Steam Equipment for Drilling Rotary Drilled Oil Wells (1932), $0.85
Bibliography on Cutting of Metals (1866–1930), $1.25
Bibliography on Deterioration of Condensing Equipment (1845–1930), $1.25
Bibliography on Effect of Temperature Upon Properties of Metals (1928–1931), $1.25
Bibliography on Management Literature and Supplement (1903–1935), $2.75
Bibliography on Mechanical Springs (1678–1927), $1.25
Bibliography on Woods of the World (1928), $1.25
Bibliography on Marketing Research (1935), $1.00
Bibliography on Machining of Wood (1939) $1.25

SAFETY CODES

Safety Code for Elevators (A17.1—1937) (10 per cent discount), $1.00
Elevator Inspectors' Manual (A17.2—1937) (10 per cent discount), $0.75
Safety Code for Mechanical Power-Transmission Apparatus (10 per cent discount) (B15—1927), $0.35
Compressed-Air Machinery and Equipment (B19—1938), $0.30

BIOGRAPHIES

BIOGRAPHIES issued under the sponsorship of the A.S.M.E. Biography Advisory Committee are as follows:

Autobiography of John A. Brashear (1924), $5.00
Autobiography of an Engineer, by W. LeR. Emmet (1940), $3.50
Autobiography of John Fritz (1940), $3.25
Biography of James Hartness, by Joseph W. Roe (1937), $4.00
Biography of John Stevens, by Archibald Douglas Turnbull (1928), $5.00
Biography of John Edson Sweet, by A. W. Smith (1925), $4.50
Biography of Robert Henry Thurston, by William F. Durand (1929), $5.00
Life of Henry Laurence Gantt, by L. P. Alford (1934), $5.00

BOOKS ON SPECIAL SUBJECTS

Aeronautical Dictionary (1929), $1.65
Corrosion-Resistant Metals (1936), $1.25
Engineering's Part in the Development of Civilization (1939), $1.50
General Discussion on Lubrication (1938) (no discount), $6.50
Hydraulic Laboratory Practice (1929), $10.00
Hydraulic Structures (1937), $18.00
Manual on Cutting of Metals (1939), $5.00
1941 A.S.M.E. Mechanical Catalog and Directory, $3.00 (sent gratis to members, upon request)
1939 Oil Engine Power Cost Report (1940), $1.00
Theoretical Steam Rate Tables (1937), $1.25

Hydraulic Couplings for Internal-Combustion-Engine Applications

By N. L. Alison,[1] R. G. Olson,[2] and R. M. Nelden[3]

This paper deals with hydraulic couplings of the hydrokinetic type used for the transmission of power from internal-combustion engines in marine, traction, and industrial applications. The units described are of the two-element type, having a one-to-one torque ratio, and although mention is made of certain applications of the hydraulic torque converter, such as the original Föttinger speed transformer, the detail discussion is confined to the two-element transmitter or hydraulic coupling.

The first installation of the hydraulic coupling in connection with internal-combustion engines was made in the geared Diesel cargo ship *Vulcan* in 1923. Since that time its field of application has been constantly widening and this paper has been prepared in an effort to record some of the developments that have been made, as well as to explain some of the basic characteristics and principles of this type of drive. Because of the wide scope of the paper, embracing marine, traction, and industrial applications, it makes no attempt to go deeply into the problems discussed, but rather to outline the way hydraulic couplings are used and the results obtained.

Both hydraulic couplings and torque converters are of the hydrokinetic type and have their origin in the Föttinger speed transformer invented by Doctor Föttinger when on the engineering staff of the Vulcan Company in the early 1900's. The Föttinger transformer was used as a speed reducer between a marine steam turbine and a propeller, providing a speed reduction of about five to one with an efficiency in the neighborhood of 85 per cent. Prior to the introduction of the helical reduction gear the Vulcan Company produced Föttinger speed transformers aggregating about 220,000 hp, but because of the higher efficiency and lower cost of the helical gear it completely replaced the hydraulic type.

The development then remained at a standstill for a number of years, until Dr. Bauer, marine engineer and director of the Vulcan Company, foreseeing the scope for the high-speed geared Diesel engine, perfected the two-element transmitter on the Föttinger principle, but with a one-to-one torque ratio. This became known as the "Vulcan coupling" and when combined with mechanical gearing was called the "Vulcan gear."

The next important period in the development of the hydraulic coupling began in 1928, when Harold Sinclair, of Isleworth, England, in cooperation with the Vulcan Company adapted the fluid circuit to two new designs of couplings: (1) The "traction" type for automotive applications, and (2) the "scoop-tube" type for variable-speed industrial applications. The American participation began in 1932.

[1] General Manager, Hydraulic Coupling Division, American Blower Corporation, Detroit, Mich.

[2] Staff Engineer, Hydraulic Coupling Division, American Blower Corporation, New York, N. Y.

[3] Test and Development Engineer, Hydraulic Coupling Division, American Blower Corporation, Detroit, Mich. Jun. A.S.M.E.

Presented at the National Meeting of the Oil and Gas Power Division, Asbury Park, N. J., June 19–22, 1940, of The American Society of Mechanical Engineers.

1—MARINE APPLICATIONS

Although the field for the application of the hydraulic coupling has now extended to include practically every use of the internal-combustion engine, as well as numerous electric-motor drives, it was first used aboard ship and the marine engineer has contributed much to its development and present wide acceptance.

To take advantage of the lower weight, higher efficiency, and smaller space requirement of the medium-speed and high-speed Diesel engine, and at the same time profit by the higher efficiency of a low-speed propeller, the need arose for a reduction element in the propulsion system. As far back as 1908 mechanical reduction gears were used for this purpose. The earliest installation on record is a side-wheel boat on the river Volga in Russia, but it was not until after the World War that geared Diesels were used in ships with screw propellers. The first installations of this type were made in Germany, utilizing submarine engines that had been completed after the close of the World War. Although the first of these installations made with the engines connected to the gears through mechanical couplings proved successful, the general acceptance and wide use of this method of drive began when Dr. Bauer evolved the idea of connecting the engines to the gears by means of hydraulic couplings. Since that time more than 75 commercial vessels have been equipped with this method of drive, and at the end of 1939 the combined commercial and naval applications were in excess of two million horsepower.

As used in marine applications, the hydraulic coupling consists of two radially vaned rotating elements known as the primary and secondary rotors, one of which is connected to the engine crankshaft and the other to the shaft of the pinion gear. There is no mechanical connection between the driving and the driven members and power is transmitted by the kinetic energy of the fluid which circulates between the radial passages in the rotating elements. A cover known as the secondary-rotor housing, enclosing the back of the runner to retain the working fluid, is bolted to and rotates with the impeller. Fig. 1 shows the impeller and runner, while Fig. 2 is a section through the hydraulic coupling and pinion of a typical marine gear. Fig. 3 shows a diagrammatic arrangement with two medium-speed Diesel engines connected through helical gears and hydraulic couplings to the propeller shaft.

Referring to Fig. 2, it will be seen that the hydraulic coupling is enclosed in a stationary casing which is, in turn, connected to a sump tank. A motor-driven pump delivers oil from the sump tank through a hole in the pinion shaft into the working circuit of the coupling. When it is desired to disconnect one or the other engine from the gear, the oil inlet valve is closed, and the coupling empties through calibrated nozzles provided in the periphery of the secondary-rotor housing.

The fluid used is mineral lubricating oil, and it is customary to use the same oil in the coupling as is used for reduction gear or engine lubrication. Frequently the coupling sump tank is combined with the gear or engine sump tanks.

The functions performed by the hydraulic coupling in connection with geared Diesel marine drives are as follows:

(*a*) Prevents the transmission of torsional vibrations, thus

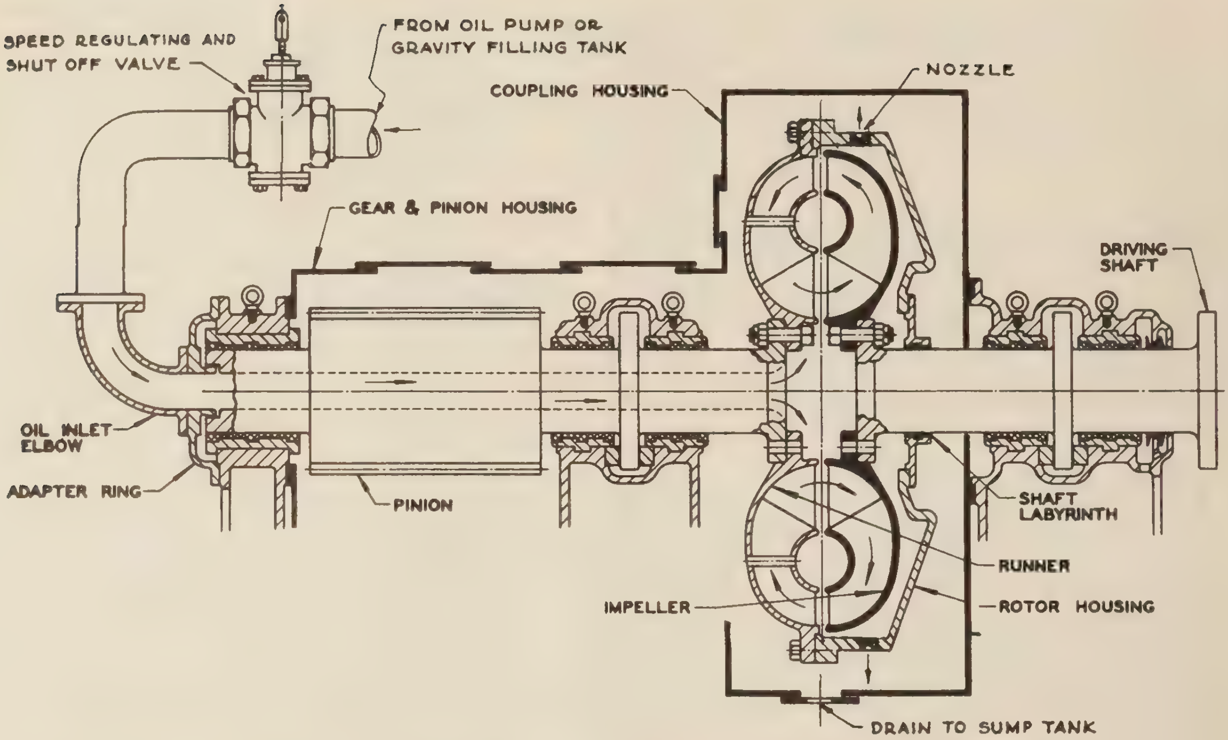

Fig. 2 Hydraulic Coupling and Pinion Gear of a Typical Marine Installation

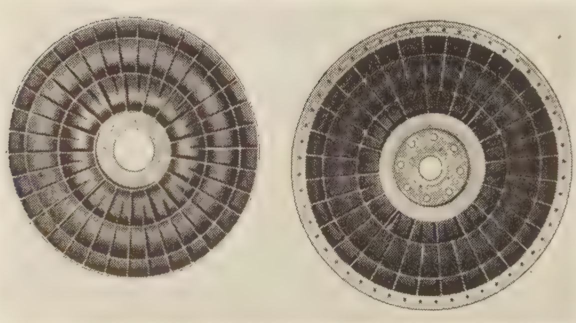

Fig. 1 Impeller and Runner of a Hydraulic Coupling

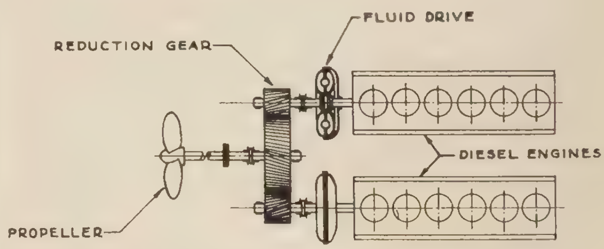

Fig. 3 Two Medium-Speed Diesels Connected Through Hydraulic Couplings and Helical Reduction Gears to a Propeller Shaft

completely divorcing the vibrating system of the engine from that of the gears, propeller, and shafting.

(*b*) As there is no mechanical connection between the driving and driven members, the coupling protects the engine and gears from damage due to sudden shock loads which might result from the seizure of a piston or in case the propeller becomes fouled.

(*c*) Permits rapid declutching so that in the case of a multiple-engine drive, an engine can be readily disconnected when minor repairs are required at sea, or when it is desired to operate the vessel at reduced speed for extended periods. Engines can also be operated in port for warming up and adjustment without being connected to the propeller shaft.

(*d*) Large clearances between rotating members provide a considerable degree of flexibility and make extremely accurate alignment unnecessary.

(*e*) By regulating the quantity of oil in the working circuit, the coupling can be used to provide variable speed, such as might be required in the case of hopper dredges, fishing boats, or vessels operating in shallow rivers.

Performance

Exhaustive tests conducted abroad as well as in this country show that the efficiency of the marine coupling always equals 100 minus the slip in per cent and that the torque input is equal to the torque output for all conditions of speed and filling. Although the coupling can be selected to operate with a slip as low as 1 per cent, corresponding to an efficiency of 99 per cent, it is customary in marine service to use couplings having a slip of between $2^1/_2$ and 3 per cent in order to keep down the over-all diameter. As the power required by the oil-circulating pump amounts to approximately $^1/_4$ per cent of the engine horsepower, the over-all efficiency of the coupling will be approximately 97 per cent. Since the rotating members are totally enclosed and all bolts are shrouded, loss due to windage is negligible.

Slip is the difference in speed between the driving and driven members of the coupling, measured in per cent. Therefore, if the engine speed is 500 rpm and the slip of the coupling is 3 per cent, the output shaft speed will be 485 rpm. An important characteristic is that the slip remains practically constant for all engine speeds, due to the fact that the power-transmitting capac-

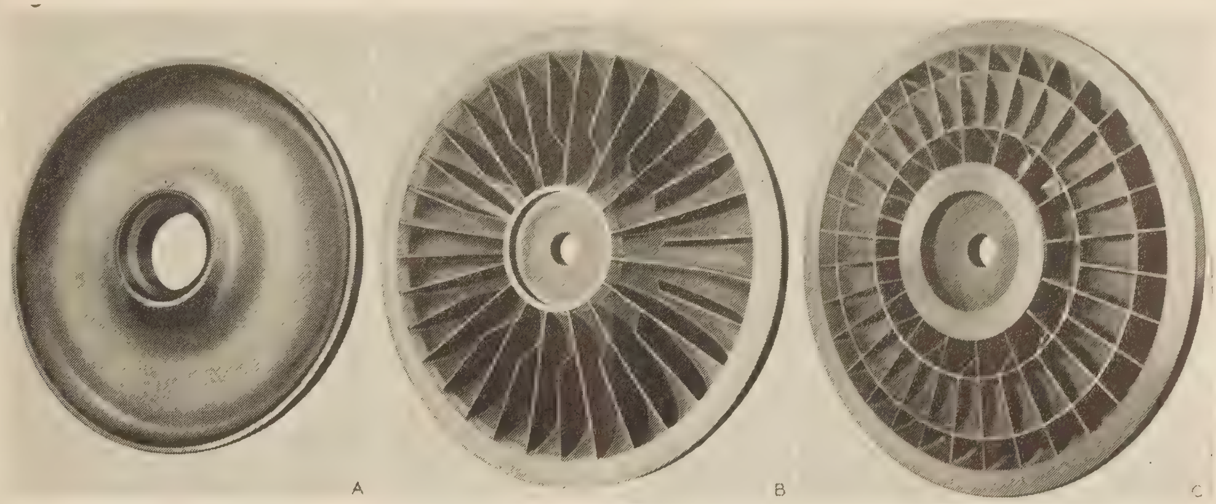

Fig. 4 Stages in the Manufacture of Hydraulic Couplings

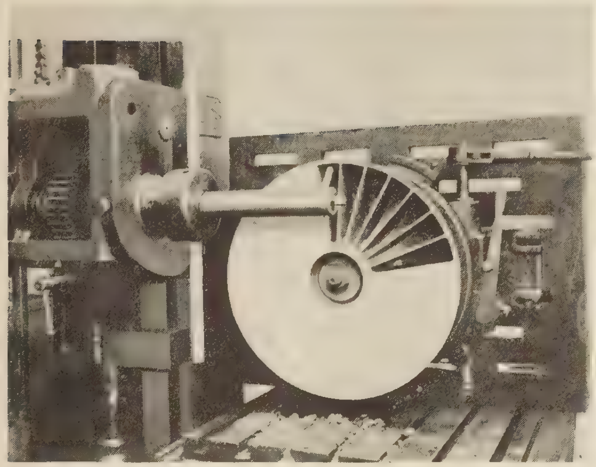

Fig. 5 Rotating Members of Hydraulic Couplings for High-Speed Installations Are Machined From Solid Steel Blocks

ity of the coupling and the power required by the propeller both vary as the cube of the speed.

Construction

Hydraulic couplings are built of welded steel, cast iron, or cast steel, according to the requirements of each installation. For use with high-speed Diesel engines, where relatively light weight and low WR^2 are desirable, welded couplings are generally used, while large low-speed couplings such as are now being used in U. S. Maritime Commission C-2 cargo vessels are of cast construction. Due to the smoother surfaces and the thinner vanes of the welded couplings their slip is somewhat lower, especially in the smaller sizes, but in the case of large low-speed couplings this difference in slip becomes negligible. In all sizes, the lower slip of the welded couplings can be compensated for by only a small increase in the diameter of the cast couplings. The latter construction is appreciably lower in cost and is more readily adaptable to the higher WR^2 requirements of the low-speed engine.

Fig. 4 shows a welded steel coupling during various stages of fabrication. The view on the left shows the die-formed bowl or shell of a coupling impeller before the radial blades are welded in place. The center view shows the bowl with the long and short blades in place, while the right-hand view shows a completed runner after the semicircular sections, forming the core ring, have been welded in place.

For extremely high speeds, such as are encountered where the hydraulic coupling is used as a disconnecting clutch between the main and cruising turbines in certain types of naval vessels, the rotating members are made from solid steel blocks, the radial passages being machined out by a milling operation, as shown in Fig. 5. After this machining operation is completed, the small

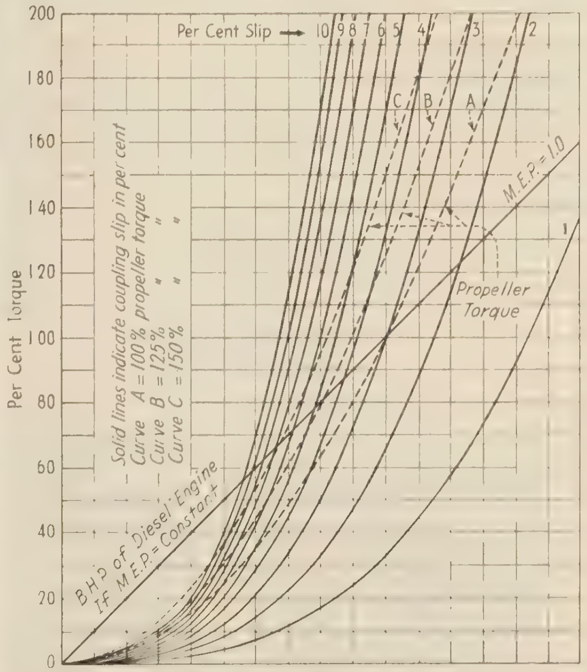

Fig. 6 Relation of Output Torque and Slip for Hydraulic Couplings

(At 100 per cent engine speed and 100 per cent engine output, slip is 3 per cent.)

steel sections, which form the semicircular core ring, are welded in place.

When the coupling is used for driving engine-attached scavenging blowers, and cast construction is used, the driving member may be made of cast aluminum as a means of keeping the WR^2 of this member as low as possible.

Relation of Output Torque and Slip

Fig. 6 shows a set of curves from which coupling slip and engine speed may be determined for any condition of operation where two or more engines are connected to a single propeller through hydraulic couplings and reduction gears. The curves are drawn up on the basis of 3 per cent coupling slip with all engines operating and the propeller absorbing designed torque. It will be noted that in addition to the propeller curve representing designed torque, two additional propeller-torque curves are shown, one based on 125 per cent, the other 150 per cent of designed torque, to indicate a possible foul-bottom condition or the ship operating with a heavy tow.

To illustrate the use of the curves we can assume a two-engine drive with both hydraulic couplings operating with 3 per cent slip, assuming designed torque on the propeller. The curve shows the propeller torque varying as the square of the speed, and on this basis the slip of the hydraulic couplings will remain approximately constant at 3 per cent for all engine speeds.

Therefore the curve for 3 per cent slip and the brake-horsepower curve intersect on the graph at 100 per cent torque and 100 per cent engine speed. By moving horizontally to the left on the graph from this point of intersection to the 125 per cent propeller-torque curve, thence vertically downward to the brake-horsepower curve, a point is reached which indicates that at 125 per cent propeller torque the slip of the couplings increases to 3.7 per cent, and the engine speed drops to 90 per cent. For 150 per cent propeller torque, the coupling slip is $4^1/_2$ per cent and the engine speed has dropped to about 82 per cent of full speed.

Now, if the hydraulic coupling connected to one of the engines is emptied and the ship continues under way on the remaining engine, the input torque will be about 0.5, the slip of the coupling will be in the neighborhood of 6 per cent, and the engine speed 71 per cent, assuming that the propeller torque is in accordance with the designed requirement.

Special Couplings

Fig. 7 shows a hydraulic coupling of the double or twin type which is used in certain marine installations where space limitation does not permit using a standard single coupling. This design permits decreasing the outside diameter of the rotating parts in the neighborhood of 15 per cent, so that, for example, instead of using a size-42 single coupling for transmitting 900 hp at an engine speed of 700 rpm, a size-36 coupling of the double type can be used.

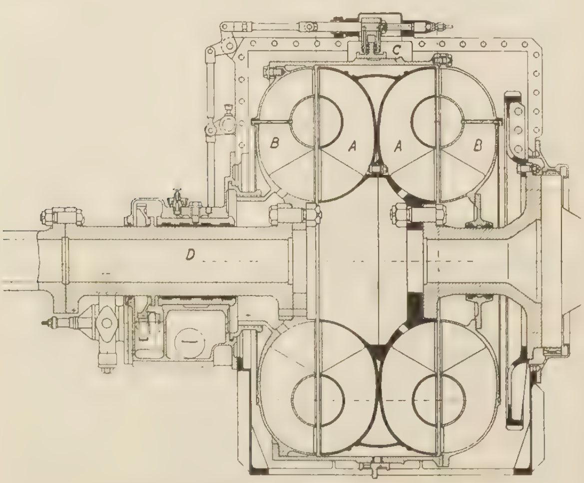

Fig. 7 A Double Hydraulic Coupling

In the coupling shown in Fig. 7 the two primary members A are connected to the driving shaft, while the secondary rotors B, carried by the drum C, are flanged to the secondary shaft D. The position of the two members can be reversed so that the primary becomes the secondary, and vice versa, without any loss of transmission efficiency or change in performance. Also, the outer member can be mounted directly on the engine flywheel as is done in the case of standard traction couplings, and a ball or roller bearing can be located in the center of the coupling to hold the primary and secondary rotors in proper relation to each other.

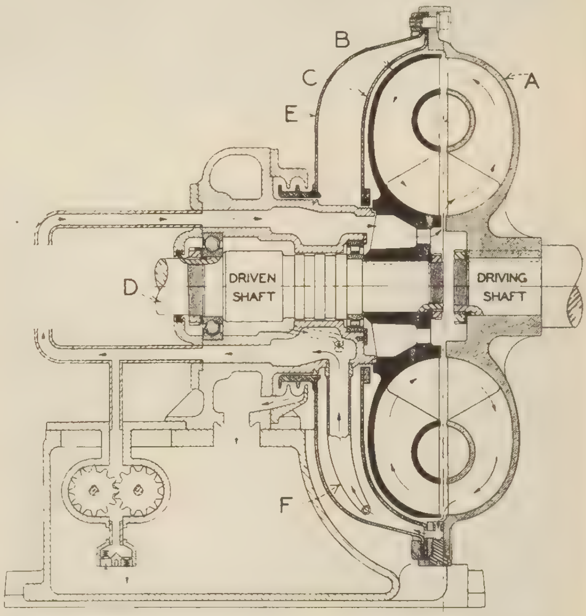

Fig. 8 A Scoop-Tube Variable-Speed Hydraulic Coupling

A type of coupling widely used for variable-speed drive in connection with constant-speed motor applications is the scoop-tube type shown in Fig. 8. In addition to the primary rotor A, secondary rotor B, and rotor housing C of the regular marine couplings, this coupling has a second rotor housing E, known as the "outer casing." A stationary scoop tube F, supported by an external manifold, is located in the chamber formed between the inner and outer casings. Calibrated leak nozzles in the periphery of the inner casing allow oil to leak continuously from the coupling working circuit into the scoop-tube chamber. The oil is thrown out through the nozzles by centrifugal force, due to the rotation of the coupling, and this oil is picked up by the scoop tube from whence it is delivered through an oil cooler and back into the working circuit. The action of the scoop tube can be compared to the scoop under a steam locomotive picking up water out of a trough.

The scoop-tube coupling is provided with an oil pump driven by a reversible motor, and this pump serves to fill or empty the coupling when it is desired to clutch or declutch. When variable output speed is desired the hydraulic coupling can be operated with the working circuit only partially filled, and by this means speed regulation can be obtained over a range of five to one.

The reversible pump only operates when it is desired to add to or remove oil from the coupling circuit, and at all other times the pump remains idle and circulation through the oil cooler is maintained by the action of the scoop tube. If desired, the scoop tube can be arranged to discharge directly into the sump tank with the motor-driven pump operating continuously to make up the oil which circulates through the nozzles and scoop tube. Where this method of control is used, declutching is accomplished by closing the oil inlet valve and allowing the scoop tube to drain the working circuit.

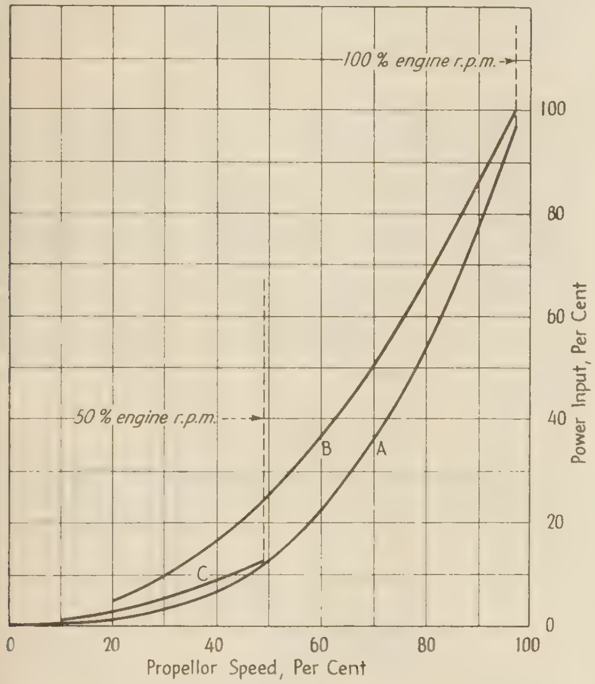

Fig. 9 Variable-Speed Performance Curve

(Curve A—propeller horsepower. Curve B—hydraulic-coupling input horsepower with engine running at maximum speed. Curve C—hydraulic-coupling input horsepower with engine running at 50 per cent speed.)

As in the case of other designs of hydraulic couplings, either the inner wheel or the outer wheel carrying the two casings can be connected to the engine shaft and the other member to the gear or propeller shaft.

Variable-Speed Operation

Although hydraulic couplings of both the scoop tube and scoop control types are used extensively for the variable-speed drive of fans, turboblowers, pumps, as well as machines requiring constant torque, the characteristics of the coupling when used for variable-speed propeller drive are perhaps not so well known. Curve A in Fig. 9 indicates the power required by a ship propeller in percentage of full power over a range from 100 per cent down to zero speed assuming that the load varies as a cube function of the speed. Curve B shows the power input to the hydraulic coupling based on the assumptions that the engine is running at maximum speed and the regulation of propeller speed is obtained entirely by varying the quantity of oil in the coupling circuit. It will be seen that the power input drops off rapidly and that the difference between curve A and curve B, representing the loss of power in the hydraulic coupling, varies from a maximum of 16 per cent of full power at 65 per cent speed to approximately 5 per cent at 20 per cent speed.

Curve C in Fig. 9 shows the power input to the hydraulic coupling assuming that the engine speed is reduced to 50 per cent of maximum and that the propeller speed is reduced down to 10 per cent of maximum by means of the hydraulic coupling. In this case the maximum power loss in the coupling, represented by the difference between curves A and C, is only slightly in excess of 2 per cent of full power, so that the heat to be dissipated is actually less than the normal slip loss of the coupling at full power. In this example it is assumed that the quantity of oil in the coupling would only be changed when propeller speeds below 50 per cent were desired.

It is believed that the variable-speed function of the coupling would be particularly useful in the case of hopper dredges, fishing boats, and river boats where lower speeds than could be conveniently obtained with the engine alone might be desirable. The variable filling of the coupling would also give extra protection to the propeller in the case of vessels operating in shallow rivers or in ice.

Another type of vessel where the variable-speed feature of the hydraulic coupling might be used to advantage is the geared-Diesel-drive tugboat. Its value here would be in always permitting the engine to operate at maximum speed regardless of how heavy a tow was being handled. In other words, instead of reducing the engine speed as a result of increased propeller torque, the filling of the coupling would be adjusted to allow the engine to operate at maximum speed and permit the propeller to rotate at a speed corresponding to full engine torque. If desired, a thermostat could be provided in the engine exhaust which would automatically adjust coupling filling to limit exhaust temperature to the maximum recommended by the engine manufacturer.

Hydraulic Coupling Fluids

As stated earlier in this paper, the fluid recommended for use in the hydraulic coupling is straight mineral lubricating oil having a maximum viscosity of about 180 Saybolt seconds at 130 F. Water has also been used, but because of its lubricating qualities, stability, long life, and availability, oil has been found to be the most satisfactory all-around fluid. Other fluids have been investigated, but to date none has been found that offers all of the advantages of oil. A heavy liquid known as "Aroclor" has been used experimentally with quite satisfactory results. It has the advantage of high specific gravity, low viscosity, and low vapor pressure. Its principal disadvantage lies in its rather high cost and the fact that it gives off objectionable fumes at high temperatures. Mercury has frequently been proposed because it is about fifteen times as heavy as oil, but its cost is probably prohibitive, and it would have a rather undesirable effect on the nonferrous materials in the coupling and cooler.

Thrust

The axial thrust of the hydraulic coupling when full of oil acts in the outward direction tending to separate the two members, while with the coupling only partially filled the thrust acts in the opposite direction tending to draw the two members together. Therefore, it is necessary to provide bearings to take the thrust in both directions, and in marine applications this is usually handled by thrust collars on the driving and driven shafts.

The coupling thrust can also be handled by a ball or roller thrust bearing located in the center of the coupling, or by a bearing between the rotor housing and the driven shaft. The latter arrangement is frequently used in traction-type hydraulic couplings described later in this paper.

Quick-Emptying Valves

Fig. 2 shows a coupling provided with constant-leak nozzles. This coupling is used principally in connection with single-engine drives and other applications where rapid declutching is not re-

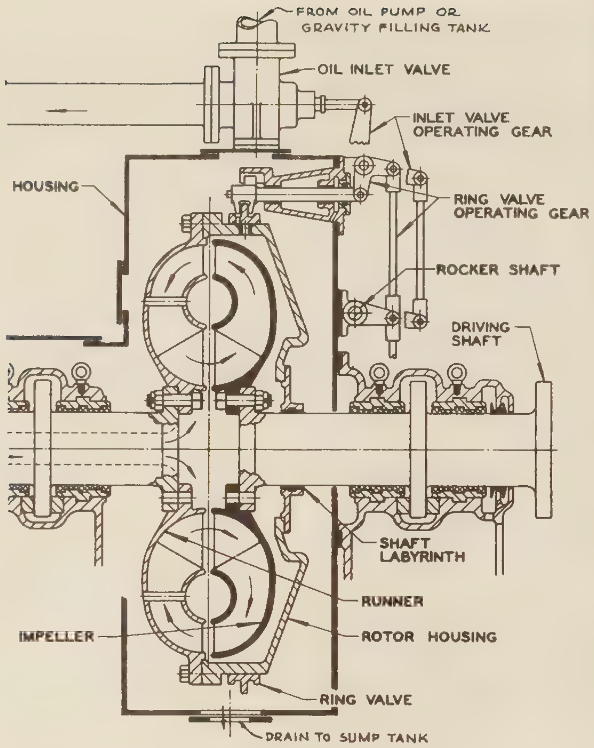

Fig. 10 Hydraulic Coupling With Ring-Type Quick-Emptying Valve

quired. Declutching is accomplished by stopping the oil-supply pump or closing the oil inlet valve and permitting the coupling to empty through the nozzles provided in the periphery of the rotor housing. Depending upon the size and speed, this coupling requires between 2 and 5 minutes to empty completely.

Fig. 10 shows a marine coupling provided with ring-type dumping valve which permits declutching in from 3 to 5 sec. Nozzles in the rotor housing are covered by a steel ring which is keyed to and rotates with the coupling. By means of three claws and linkage mounted on the stationary enclosing casing, the ring can be moved axially a sufficient amount to uncover the nozzles, thus permitting a rapid escape of oil from the coupling. The ring valve is interconnected with the oil-supply valve so that when the former is closed the latter is open and vice versa.

A more recently developed quick-emptying coupling is the piston-valve type shown in Fig. 11. In this coupling there is a series of piston valves around the periphery of the rotor housing which are held normally in the closed position by springs. By means of air or oil pressure admitted to the valves as shown, the pistons are moved axially so as to uncover drain ports, allowing the coupling to empty. Where extremely rapid declutching is not required, the piston-valve coupling offers the advantage of greater simplicity and lower cost.

As in couplings with constant-leak nozzles, the ring-valve and piston-valve types are arranged to circulate sufficient oil for cooling under normal operation or where the coupling is used for variable speed.

Oil Piping and Auxiliaries

Fig. 12 shows a typical layout of oil piping and auxiliaries for an installation where two Diesel engines are connected through hydraulic couplings and a reduction gear to the propeller shaft

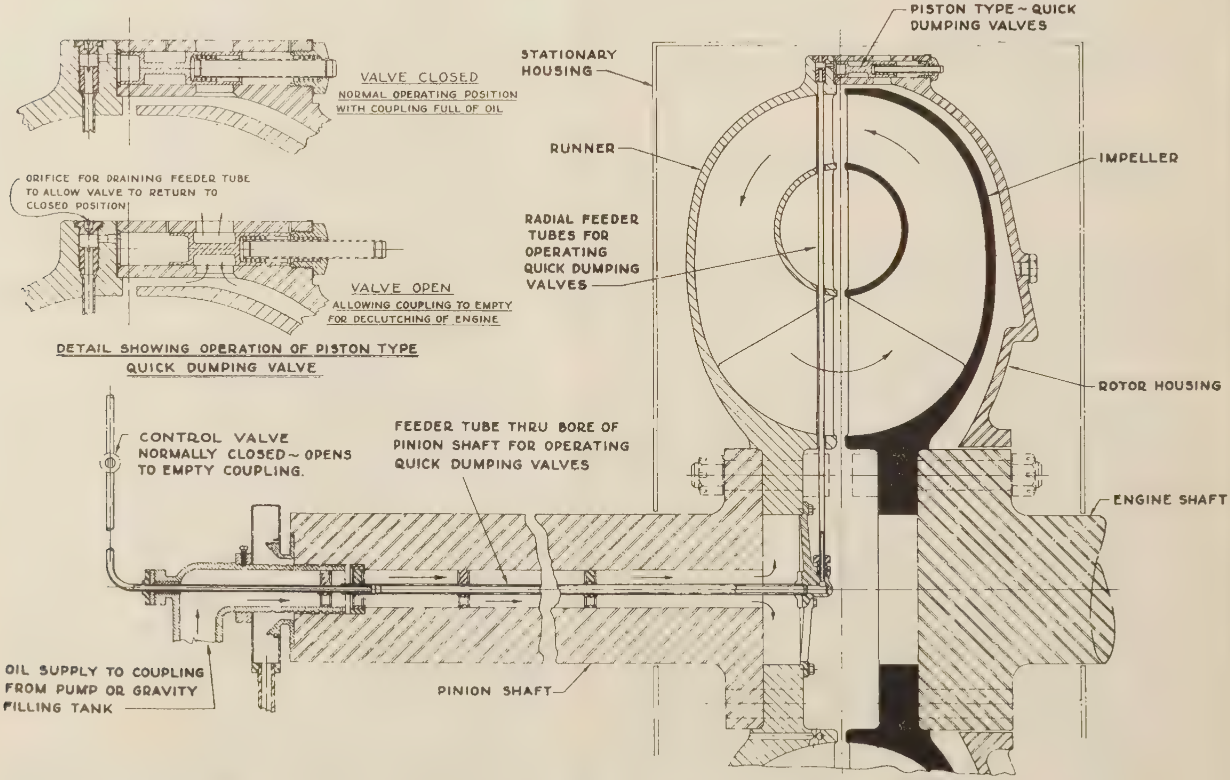

Fig. 11 Hydraulic Coupling With Piston-Type Quick-Emptying Valves

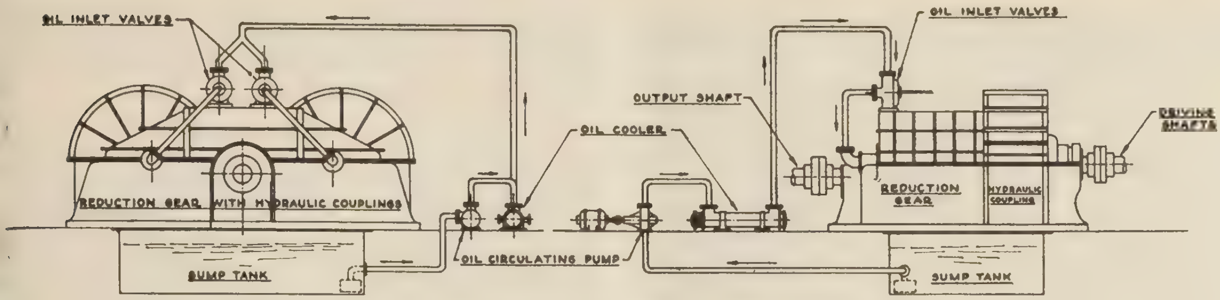

Fig. 12 Piping and Auxiliaries for Hydraulic Couplings

The auxiliaries shown consist of an oil strainer, a motor-driven oil-circulating pump, a shell-and-tube oil cooler, and two oil-inlet or speed-regulating valves. The pump delivers oil to the couplings through the hollow pinion shafts and this oil returns to the sump tank, where it is again picked up by the pump and a continuous circulation is maintained. During normal operation the pump needs only to handle the oil which leaks out at the periphery of the couplings, and in order to have greater capacity for filling when starting up, the pump can be driven by a two-speed motor. The pump and motor are selected for a maximum pressure of 25 psi.

Another arrangement of piping and auxiliaries that has been used widely in commercial vessels utilizes an overhead gravity filling tank as a means of rapid filling. Where this system is used, it is customary to combine the oil for coupling filling with that for gear lubrication, and the gravity tank is made of sufficient capacity so that in the event of pump failure there will be enough oil in the tank to insure a supply of oil to the gears for a period of 5 min. It seems doubtful that the gravity tank will be used to any great extent in the future, because in most cases it is not essential and the arrangement shown in Fig. 12 offers a less complicated system of piping and generally at lower cost.

2—INDUSTRIAL AND TRACTION APPLICATIONS

Since 1928 the hydraulic coupling has been used commercially for various automotive, traction, and industrial applications, and in total horsepower these applications now account for an aggregate equal to that of the marine coupling. The first automobile to use the hydraulic coupling was the Daimler in England under the name "fluid flywheel," and now in this country we have fluid drive and Hydra-Matic drive as used, respectively, by Chrysler and General Motors. In industrial and traction applications, this coupling is known as the "traction type" as conceived and developed by Harold Sinclair, and it will be referred to by this name in the remaining part of this paper.

The traction coupling differs from the marine type in that in it no provision is made for completely disconnecting the driving from the driven member. It is a self-contained unit and is usually mounted directly on the engine flywheel or on an extension of the crankshaft as shown in Fig. 13. It consists of a driving member or impeller (1), a driven member or runner (2), enclosing cover (3), reservoir (4), thrust bearing (5), driven side stub shaft (6), and oil seal (7). The coupling operates with a fixed quantity of oil in the working circuit and does not require an external tank or pump. Heat generated within the coupling is dissipated by radiation. When starting up the coupling is filled with light lubricating oil to the level of the filling plug in the enclosing cover.

The characteristics of the traction coupling, used as a power take-off in connection with an internal combustion engine, are shown in Fig. 14. Curve *C-D* shows the slip of the coupling from 100 per cent to 40 per cent engine speed when delivering maximum engine torque to the driven machine, and it will be seen that this slip increases from $2^1/_2$ per cent at point *D* to 100 per cent at point *C*. This represents a full-throttle condition. Curve *A-B* represents the torque output from the coupling with the runner stalled and the engine operating at reduced speed. For example, in starting up, the drag torque at point *A* is zero and as the engine increases in speed the torque of the coupling immediately builds up toward point *B* setting the driven shaft in motion, after which the slip of the coupling rapidly decreases and falls to about 2 or 3 per cent in the range of normal speed and load.

The ability of the coupling to prevent engine stalling is shown by curve *C-D* indicating how the effect of overload is to pull down

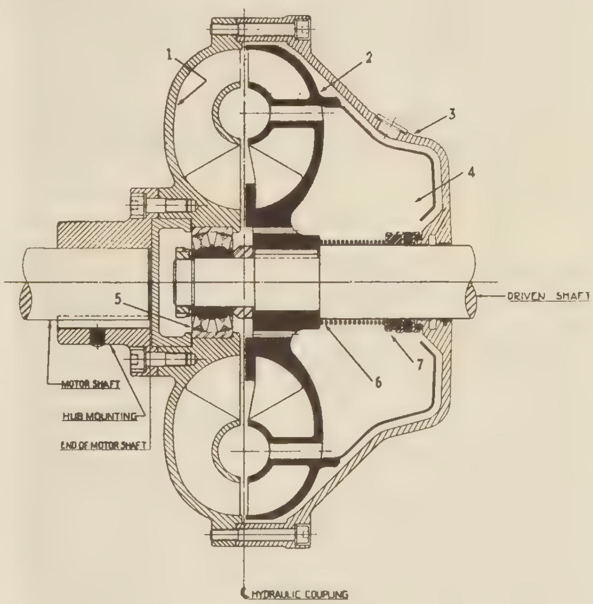

Fig. 13 Section Through a Traction Coupling

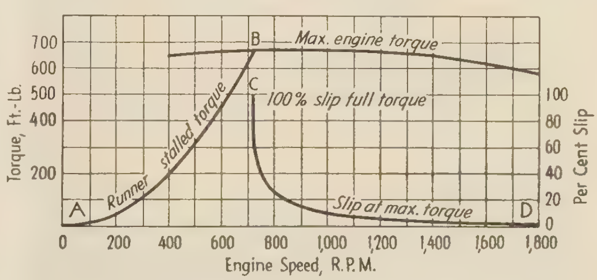

Fig. 14 Traction Coupling Performance Curve

the engine speed until point C is reached, when the slip rises to 100 per cent and the output shaft stalls while transmitting the full torque of the engine.

The absence of any physical connection between the driving and driven members of the coupling reduces wear to a minimum and prevents the transmission of torsional vibration and shocks.

In the traction coupling a ring-shaped baffle is attached to the coupling at the inner profile diameter, and serves to impede the oil circulation when working at high slip or when stalled, thus reducing the drag torque. The baffle has no effect on the slip at normal load and speed, and by varying its diameter the point of coupling stall when delivering full torque can be changed to best suit the operating characteristics of the engine.

The reservoir on the back of the runner serves as an expansion chamber; consequently, there is no possibility of building up excessive pressure due to overheating of the oil in case the coupling is allowed to remain stalled for long periods with the engine developing full torque.

Applications of the traction-type hydraulic coupling have been made in the fields of power shovels and draglines, oil-well drilling, marine drives where declutching is not essential, rail traction, and ore trucks.

Rail Traction

Although relatively little progress has been made in the rail-traction field in the United States, hydraulic couplings and hydraulic torque converters have been used widely for locomotive and rail-car drive in nearly every other part of the world, with the greatest number of hydraulic coupling units originating in England, and those of the torque-converter type being most prominent in Germany. In this connection it is interesting to note that up to February, 1939, one English manufacturer had produced about 1200 couplings totaling 165,000 hp for rail-traction applications, while a German manufacturer of torque converters had manufactured over 800 units totaling about 225,000 hp. The largest hydraulic coupling unit was 380 hp while the largest torque converter was a locomotive unit rated at 1380 hp. Most of the rail-car applications of the hydraulic coupling made abroad have been in connection with constant-mesh gearboxes of the epicyclic type in rail cars for branch-line service.

In this country, interest in rail-traction applications has increased during the last two years, and several switching locomotives ranging in size from 20 tons to 40 tons equipped with hydraulic torque converters have been built.

Scoop Control Coupling

Another type of self-contained unit used for certain Diesel-engine drives is the scoop control coupling shown in Fig. 15. It consists of an impeller to which is bolted an inner casing enclosing the runner, and an outer casing which acts as a reservoir and is of sufficient capacity to receive the contents of the working circuit. Calibrated nozzles in the inner casing allow a continuous flow of oil from the coupling circuit into the reservoir from where it is picked up by a scoop tube mounted on the external manifold. The scoop tube is connected to an external handle which can be moved through an arc of about 70 deg. With the scoop in its fully extended position, the coupling circuit is full of oil and minimum slip is obtained, while with the scoop in its retracted position all of the oil is in the reservoir and the coupling is completely disconnected. Thus, this coupling can serve as a disconnecting clutch, and if variable output speed is desired this can be obtained by placing the control lever in an intermediate position. The oil handled by the scoop tube can be circulated through an oil cooler where extra cooling is required.

When used for marine drive, the scoop control coupling provides a means of declutching and variable output speed. With the scoop tube in the engaged position, the characteristics of the coupling are the same as those of the traction type previously described.

The scoop control coupling used in connection with Diesel drilling rigs performs the same functions as the traction coupling with regard to parallel operation and the damping of vibrations and shocks. For "fishing" operations, it performs the added function of accurately controlling output speed, and when used for slush-pump drive, can be equipped with oil cooler to permit the engine to be run for long periods with the pump stalled.

The scoop control coupling is usually constructed with cast-iron impeller and runner, and spun-steel inner casing and rotating reservoir. When the coupling is stationary, the oil rests in the lower half below the level of the shaft and, consequently, no oil

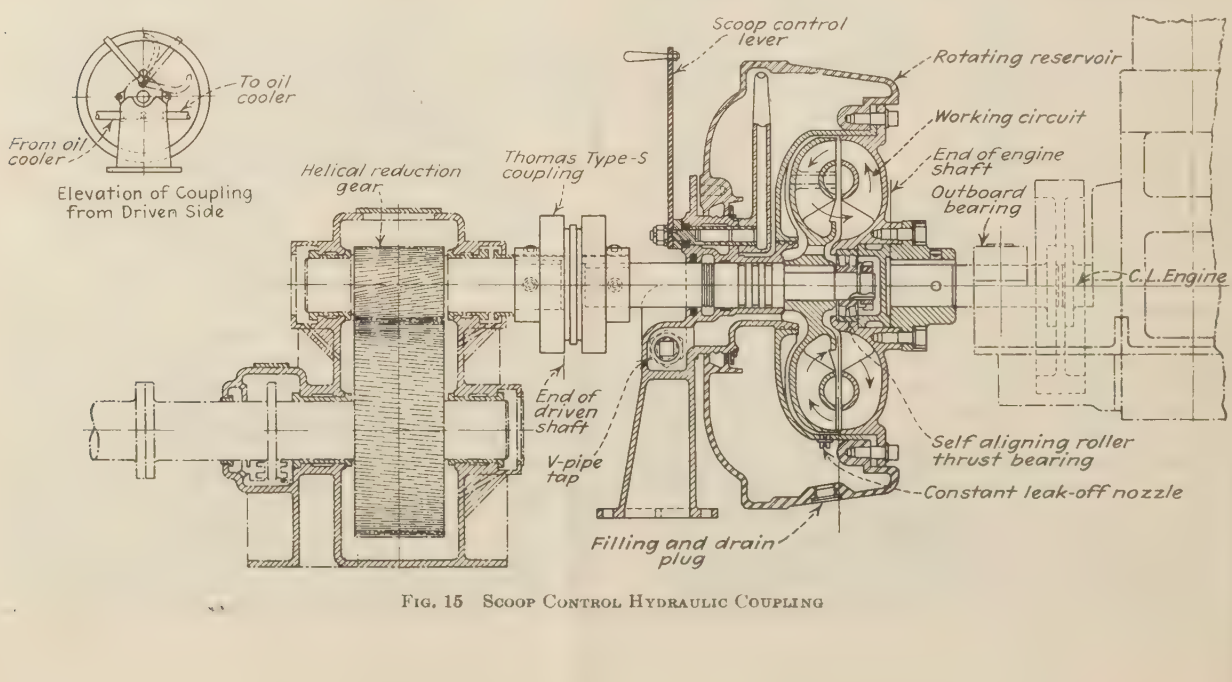

Fig. 15 Scoop Control Hydraulic Coupling

seal or gland is required. Thrust is provided for by means of a self-aligning roller bearing located in the impeller hub, and no external thrust bearings are needed.

Summary

Summarizing briefly, the uses of hydraulic couplings for internal combustion engine drives can be placed in three general divisions: (1) Marine, (2) traction, (3) industrial. In addition to the applications listed in the paper, marine couplings are used for dredge pump drives while traction couplings have been used widely in connection with capstans, winches, cranes, hoists, portable compressors, engine-generator sets, road rollers, tractors, and buses.

BIBLIOGRAPHY

"Geared Diesel Marine Applications," by W. D. Leggett, presented at the annual meeting of the Society of Naval Architects and Marine Engineers, November 16–17, 1939.

"Recent Developments in Ship Propulsion by Geared Diesel and Hydraulic Couplings," by G. Bauer, *Marine Engineer*, vol. 61, 1938, pp. 4, 35, 61, 127, 153, 225.

"Some Problems in the Transmission of Power by Fluid Couplings," by Harold Sinclair, Proceedings of The Institution of Mechanical Engineers, vol. 139, 1938, p. 83.

"Recent Developments in Hydraulic Couplings," by Harold Sinclair, Proceedings of The Institution of Mechanical Engineers, vol. 130, 1935, p. 75.

Discussion

Austin Kuhns.[4] It has been the writer's privilege during the last few years to be intimately connected with the application and installation of by far the majority of hydraulic couplings in the marine field in the United States. Unfortunately, censorship prevents any disclosure of the development of these designs for government use and limits any remarks which may be made to the category of generalities.

The hydraulic clutch or coupling has given absolutely continuous and satisfactory performance in every installation with which the writer is personally familiar. It has accomplished to the fullest extent its required function and from torsiograph analysis has confirmed all claims of vibration separation and protection of connected machinery under unusual loads and abuse. Its control has been convenient of operation, positive, and sensitive and no maintenance whatsoever has been required on any of these installations.

It is the writer's personal opinion that the field of service for the hydraulic clutch or coupling lies with the medium and higher engine speeds. The history of the Continental installations shows that most of these couplings have been for slow-speed applications where large sizes and excessive volumes of oil or operating fluid are required. In this country we have taken advantage of the fact that the power-transmitting capacity of the hydraulic coupling goes up as the cube with the speed, and also of the fact that the progress in Diesel-engine development has proceeded toward higher and higher rotative speeds. With Diesel engines running between 700 and 800 rpm, the size of the hydraulic clutch or coupling, the volume of oil, the space required, and the complexity of the fluid system become problems of minor importance and the simplicity of this type of clutch, the physical strength of the rotating elements, and the absence of maintenance items make it unusually attractive to the marine engineer.

C. A. Neracher[5] and D. F. Toot.[5] The wide application of the hydraulic coupling has necessitated that it be treated in the authors' paper in a very general manner. However, since the outstanding improvement in the American automobile in recent years has been the introduction of the hydraulic coupling and, since the automobile is of such universal use, it has been considered appropriate to outline briefly some of the characteristics of the coupling as applied to that industry. This consideration is further influenced by the fact that many thousands of automobiles equipped with hydraulic couplings have been in the hands of users for a sufficiently long period of time to demonstrate that this is not a passing fancy.

The automobile engine is fundamentally a high-speed power source; at low speeds its power output is small and it is impossible to couple it directly to a stationary load. Even the conventional dry-plate clutch must "slip" until the automobile has attained a speed such that the corresponding input speed of the transmission is at least as great as the stall speed of the engine; otherwise, the engine will "die." Probably the greatest advantage of the hydraulic coupling is that it will allow the engine to operate at idling speeds even though the connection between load and power source remains unbroken. Furthermore, it will perform in this manner for long periods of time with no harm whatever to itself. Here is a coupling, or clutch, which at low speed is no coupling at all and yet, when the engine speed is increased, becomes almost as perfect a coupling as the dry-plate clutch; a metamorphosis which requires neither thought nor effort on the part of the operator.

This property of the hydraulic coupling opens a field of driving art, or technique, which is entirely new to car operators. In the first place, it allows the car to be stopped and held stationary, as at a traffic signal, without either declutching or shifting to neutral. Then, it makes it possible for the engine to acquire a speed at which it can supply its maximum torque for the purpose of starting the car—a time at which a high torque is most needed.

Let us consider the importance of these two points to car operation. The American driving public has grown to depend more and more upon high-powered engines rather than upon multiple-speed transmissions for acceleration and performance. At the present time, most of the driving in this country, whether it be city or rural, is done in high gear. It is seldom that a person shifts into second gear at any speed above 15 or possibly even 10 mph. In European cars, the engines are very small and four-speed transmissions are common. Furthermore, all of these gears are used and used often. With our large engines, while we still equip cars with three-speed transmissions, many drivers rarely use more than two. During the last two years, owners of cars equipped with an overdrive transmission and a hydraulic coupling have learned to avoid using any forward gear ratios except direct and overdrive, in other words, the two top gear ratios.

For all ordinary starts in a car equipped with a hydraulic

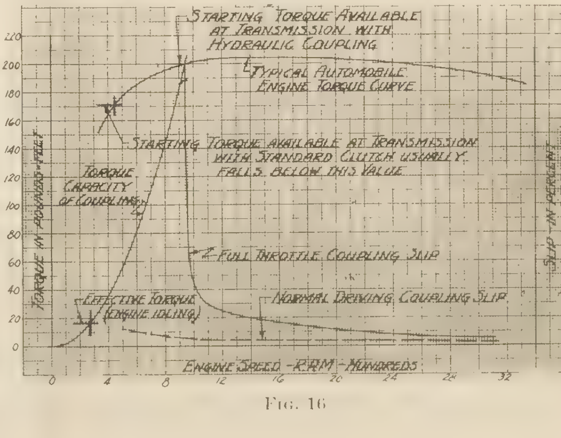

Fig. 16

[4] Farrel-Birmingham Company, Inc., Buffalo, N. Y.

[5] Chrysler Corporation, Detroit, Mich.

coupling, it is no longer necessary to have an over-all gear ratio of 10 to 1, since the engine is allowed to operate at a speed very near its peak torque output, Fig. 16 of this discussion. Thus, at the instant of "breakaway," the engine is delivering a great deal more torque than is the case with a plate clutch. Because of this fact, former breakaway performance can be equaled by using an over-all ratio of about 6 to 1. If now we use a combination of rear axle and transmission which has an automatic shift from, let us say, an over-all ratio of 5 or 6 to 1 to one of 3 or 4 to 1, we shall have sufficient breakaway torque and yet maintain a normal driving gear ratio comparable with the present-day overdrive.

This transmission can be built so that below about 10 mph the transmission will stay in the top gear or shift into the lower or "kick-down" gear, depending upon throttle operation. In other words, at these low car speeds, the driver can make the transmission shift to the lower ratio either by releasing the accelerator entirely or depressing it to its extreme position. Between these two extreme throttle positions, the car continues to operate in top gear. Between 10 mph and 50 mph, the shift to the lower gear ratio can be obtained only by depressing the accelerator as far as possible. Above 50 mph, direct drive is maintained at all throttle positions. This together with a manually operated emergency low gear and reverse gear is, in a word, the new transmission made possible by the hydraulic coupling. With such a unit all normal forward driving can be done by operating only the accelerator and the brake.

The advantage of the hydraulic-coupling installation, which is most noticeable to the driver, is that now he can operate the brake pedal with his left foot since he does not have to operate the clutch pedal. The old difficulty of starting on a hill is gone since he can hold the car with his left foot and with the transmission "in gear," operate the accelerator with his right foot; the clutch pedal need not be touched. In this way, he always has definite control of the car since he need not release the brake until sufficient torque is applied to the rear wheels to move the car forward. This is a distinct advantage also when operating the car in close quarters, such as parking, where a fine control of speed is required. In heavy city traffic where the present driving method requires that the right foot be moved from brake to accelerator and back to brake again, the new "left-foot braking system" is a definite boon. Due to the elimination of this tiring operation, and since fatigue is a major contributor to traffic accidents, it is felt that the coupling is an important safety improvement.

The hydraulic coupling contributes further to safety by making skidding on icy pavements a rarity rather than a not unusual occurrence. The slipping characteristic of the coupling, which allows the car wheels to rotate very slowly while the engine is continually applying driving effort, makes it possible to maintain a condition of rolling friction. With the present rigid coupling the rear wheels must rotate at approximately 40 rpm even in the lowest possible gear ratio. This means that, in starting on ice, very careful clutch "feathering" is necessary to prevent the wheels from reaching this speed instantly, thereby slipping on the ice. Of course, once the tires begin sliding instead of rolling, the coefficient of friction becomes lower, and skidding continues. That the hydraulic coupling has enabled the average driver to overcome this driving hazard is evidenced by the large number of comments received from owners of cars so equipped expressing great pleasure with their newly acquired sense of security on icy roads.

Effect of Variations in Atmospheric Conditions on Diesel-Engine Performance

By JESSE S. DOOLITTLE,[1] STATE COLLEGE, PA.

This paper presents the variations obtained in fuel rates and maximum power output of a two-cycle Diesel engine when there were changes in the temperature, pressure, and humidity of the supply air and in the exhaust pressure. The author found the engine to be quite insensitive to any of these changes at light loads. At loads in excess of the load of minimum fuel rate, any changes in intake or exhaust conditions that affected the air supply to the engine measurably changed the fuel rate and maximum power output.

IT HAS long been realized that variations in atmospheric conditions may affect the power output of internal-combustion engines. For the carburetor type of engine, the amount of this effect has been more or less agreed upon and formulas have been developed to express this effect (1).[2]

For the Diesel engine, on the other hand, although considerable work has been done (2, 3, 4, 5), there is no general agreement of the effect of variations in atmospheric conditions on the engine performance. For the most part, work on the Diesel engine has been confined to the four-cycle engine. As the two-cycle Diesel engine is used extensively, it was believed desirable to investigate the effect of variations in atmospheric conditions on the performance of a two-cycle engine. For a period of over a year, work has been carried out on this subject in the mechanical engineering laboratory of The Pennsylvania State College.

Test Setup

The engine used for this test was a horizontal single-cylinder single-acting two-cycle type, having direct injection. The engine was 9 × 12-in. in size and was operated at 300 rpm. Scavenging air was compressed by the crank side of the piston, in a compartment separated from the crankcase.

The variations in atmospheric conditions are (*a*) pressure, (*b*) temperature, and (*c*) humidity, and the test setup was made to measure the effect of these variables. In addition, the effects of variations in exhaust pressure could be studied.

Fig. 1 shows a schematic layout of the general setup. A surge chamber, about $1^3/_4$ ft in diameter and 18 ft in length, was connected to the intake of the engine by means of a 3-ft length of 4-in. pipe. In the further end of this surge chamber was placed a finned-type heater. A water and steam supply, connected to the heater, permitted the obtaining of any air temperature at the engine intake between 70 F and 120 F. A 3-in. valve at the intake of the surge chamber controlled the air flow to the chamber and regulated the air pressure at the engine intake. A steam line was run into the intake of the surge chamber to permit increasing the relative humidity of the incoming air to as high a value as 100 per cent if desired. To obtain air pressures above atmospheric, a compressed-air line was connected to the intake of the surge chamber. Baffles located in the surge chamber insured a uniform mixture going to the engine and trapped any water that might have condensed out.

Intake and exhaust pressures were measured by use of water manometers. The intake pressure was measured at the engine side of the surge chamber, and the exhaust pressure in the exhaust line, close to the engine. Wet- and dry-bulb temperatures of the incoming air were measured by thermometers located in the 4-in. supply pipe, directly above the engine. The amount of fuel used was measured by use of a 1000-cc measuring burette, graduated in 10-cc divisions. As the distance between divisions was about $^1/_4$ in., the amount of fuel used was determinable within $^1/_2$ per cent when 350 cc were used per run. The power output of the engine was measured by use of a prony brake. The maximum error in the measurement of the brake horsepower was about 1 per cent, this error due at the lower loads to the inability to read the load closer than $^1/_2$ lb and at the higher loads to the inability to control the brake load closer than 1 lb. The engine speed was regulated by a governor, which was adjusted before each run to about 300 rpm. The total revolutions per run were obtained by use of a revolution counter. The length of the runs was measured by a stop watch.

Test Procedure

Before attempting the main runs, preliminary tests were made to find the effect of variations in injection-advance angle and also in injection-valve opening pressures. Over the range obtainable with the engine in operation, very little effect was found by a change in the injection advance angle. Hence, this angle was set so that there was not an unreasonable amount of knocking for normal running conditions. This adjustment was not changed for the rest of the tests.

As it was found that both the fuel rate and the smoke in the exhaust were excessive at the recommended injection-valve opening pressure of 2500 lb per sq in., this pressure was increased to about 2900 lb per sq in. This pressure was maintained throughout the tests. Although somewhat better results were obtained with higher valve-opening pressures, the low fuel viscosity (32 Saybolt seconds at 100 F) made it desirable to avoid these higher pressures. The valve-opening pressures were determined by use of a Bosch injection-pressure tester.

During all runs the jacket-water outlet temperature was kept at about 130 F. The length of runs varied somewhat with the load, averaging about 6 min. At least 350 cc of fuel were used during each run. Care was taken to see that the engine had reached operating temperatures before any readings were made. Although the power output of the engine was changed in values of only 1 or 2 hp at a time, the engine was held at the new load for a period of 5 to 10 min before readings were taken.

Preliminary runs showed that the variations in exhaust pressure of $^1/_2$ in. Hg did not appreciably affect the engine performance. As the normal variations in barometric pressure during the runs were not greater than this, the exhaust pressure was not controlled except in those runs where the effects of large variations were studied.

Three series of runs were made to study the effects of variations in (*a*) the humidity of the supply air, (*b*) the incoming-air tempera-

[1] Assistant Professor of Mechanical Engineering, The Pennsylvania State College. Mem. A.S.M.E.

[2] Numbers in parentheses refer to the Bibliography at the end of the paper.

Presented at the National Meeting of the Oil and Gas Power Division, Asbury Park, N. J., June 19–22, 1940, of The American Society of Mechanical Engineers.

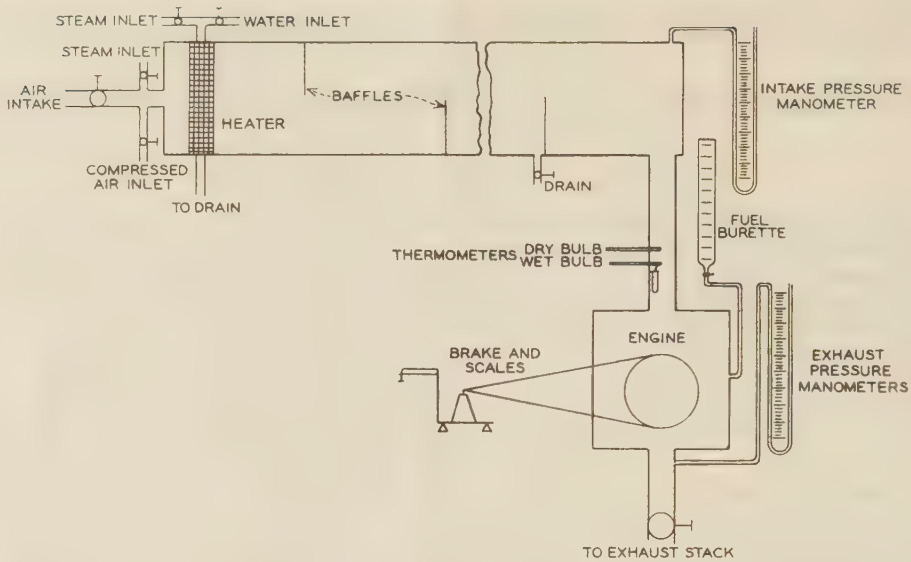

Fig. 1 Arrangement of Apparatus to Determine the Effect of Atmospheric Conditions of Diesel-Engine Performance

ture, and (c) the atmospheric pressure. For each run, with these variables held constant, fuel rates were obtained for at least ten different loads varying from about 30 per cent of rated load to the maximum obtainable with steady operation.

To investigate the effect of humidity, runs were made with intake air temperatures of 80 F and 120 F. At 80 F, two series of runs were made, one having an incoming-air relative humidity of 48 per cent and the other a relative humidity of 90 per cent. At 120 F, relative humidities of 27 and 90 per cent were used. The intake air pressure was held at 28 in. Hg abs.

To study the effect of variations in intake-air temperatures, runs were made to obtain variations in fuel rate with load at intake-air temperatures of 80 F and 120 F. Runs were also made with intake-air temperatures of 45 F by taking air from outdoors but, unfortunately, it was not realized at the time that the most significant part of the fuel-rate curve was that at very high loads. By the time the importance of the high-load runs was discovered, outside temperatures were too high to obtain the desired air temperature.

The effect of intake-pressure variations was studied by varying the absolute intake pressure from 22.5 to 33.5 in. Hg, holding the exhaust pressure constant. To simulate increased barometric pressures, three series of runs were made with equal intake and exhaust pressures, varying from an absolute pressure of 29.4 to 31 in. Hg. A series of runs were also made by increasing the absolute exhaust pressure from 29 to 31 in. Hg, the intake pressure being held constant.

As the revolutions per minute of some of the foregoing runs varied as much as 8 rpm from the mean value of 300 rpm, the engine was calibrated for the effect of speed. It was found that this small change in speed did not measurably affect the engine performance.

Discussion of Results

A change in atmospheric conditions may affect two prime factors which influence engine performance, namely, the amount of air supplied to the engine and the work required to get the air into the combustion chamber. For maximum efficiency, there must be sufficient excess air present so that every particle of fuel comes in contact and can unite with a particle of oxygen as nearly as possible at a dead-center position of the piston. Providing that this minimum amount of excess air is present, any change in the air supplied should not materially change the efficiency of combustion. However, a decrease in the intake air below this minimum excess value results in incomplete combustion and an increased fuel rate. Furthermore, a decrease in the intake pressure or an increase in the exhaust pressure may increase the work required to get a given weight of air into the combustion cylinder and increase the fuel rate.

Figs. 2 to 7 show that the results obtained substantiate this line of reasoning.

An increase in atmospheric humidity displaces some of the air in the engine cylinder; hence it decreases the amount of oxygen present. The maximum amount of vapor that can be present changes with temperature. At 80 F, standard barometer, and 100 per cent relative humidity, 3.5 per cent of the incoming air is water vapor, by volume. Thus, normal changes in atmospheric humidity at 80 F cannot materially affect the oxygen supply to the engine and should not change the fuel rate or the maximum power output. Fig. 2a shows that test results confirm this line of reasoning. At 120 F, on the other hand, the incoming air may contain as much as 11.5 per cent water vapor, by volume; hence, the humidity may be large enough to affect the amount of oxygen present. At the lower loads, there is much excess air present and the decrease in oxygen content due to the increased amount of water vapor present does not measurably affect the fuel rate. At loads higher than the load of minimum fuel rate, there is normally a deficiency of oxygen in contact with the fuel; hence, any increase in water vapor increases this deficiency and causes the fuel rate to increase. This effect may be seen in Fig. 2b.

The same line of reasoning may be applied to the effect of variations in atmospheric temperatures. A change in air density as effected by a temperature change does not affect the fuel rate provided there is a large excess of air present. However, if the engine is so loaded that there is a deficiency of excess air, a change in air temperature will affect the amount of air present and the fuel rate will be changed. Fig. 3 shows this effect. Although not shown in Fig. 3, it was found that when runs were made at an inlet air temperature of 45 F, the fuel rates obtained were the same as those at air temperatures of 80 and 120 F at loads up to that load for minimum fuel rate.

Fig. 4 shows the effect of variations in intake pressure when the exhaust pressure is held constant. Fig. 4*a* illustrates the effect of long suction lines, suction lines containing valves, elbows, air filters, and other restrictions, and throttled intake, and shows that, at light loads, there is very little effect on fuel rate until the intake

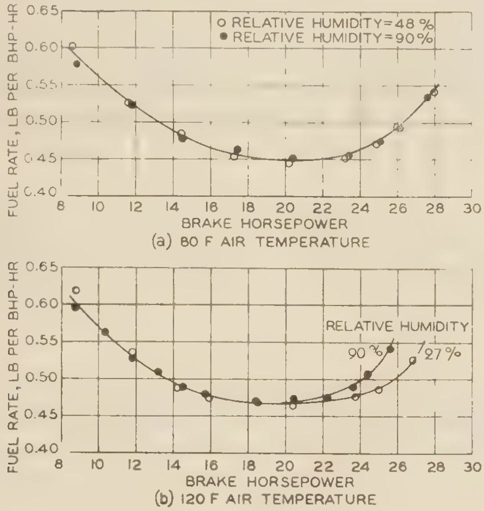

FIG. 2 EFFECT OF RELATIVE HUMIDITY ON ENGINE PERFORMANCE

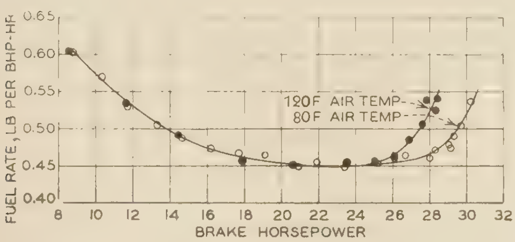

FIG. 3 EFFECT OF VARIATION IN AIR TEMPERATURE ON ENGINE PERFORMANCE

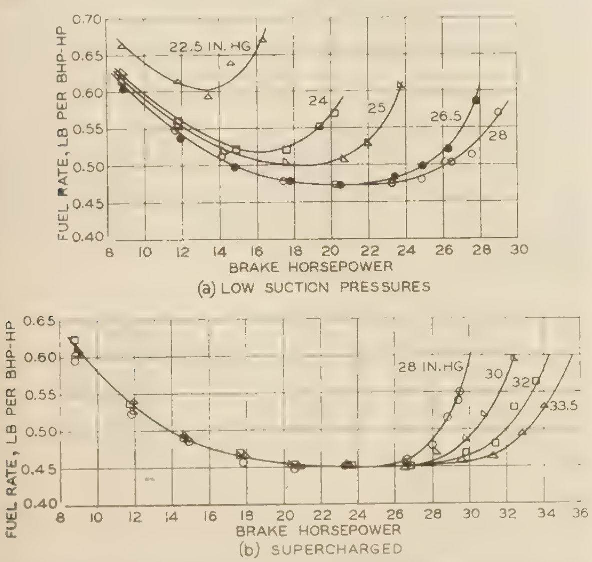

FIG. 4 EFFECT OF VARIATION IN INTAKE PRESSURE ON ENGINE PERFORMANCE AT ATMOSPHERIC-EXHAUST PRESSURE

pressure is decreased more than 4 to 5 in. Hg below normal atmospheric pressure. With this low suction pressure, the combined effect of decreased oxygen supply and the larger pumping losses operate to increase the fuel rate. At high loads these two factors decrease the power output as the suction is increased and also increase the fuel rate. The results of supercharging are shown in Fig. 4*b*. It should be noted that no allowance has been made for the power required for the supercharging. Within the range of these tests, an increase in the intake pressure produced no change on the fuel rates until high loads were reached. At the higher loads, due to an increase of the air supply to the cylinder with increased intake pressure, the deficiency of oxygen that formerly existed was eliminated; hence, the maximum power obtainable was increased, together with a decrease in fuel rate.

Fig. 5 shows the results obtained when both the intake and exhaust pressures were increased, such as might take place if the engine were used in a deep mine.

Although not comparable on an absolute basis, some conclusions may be drawn from a relative comparison of Figs. 4*b* and 5.

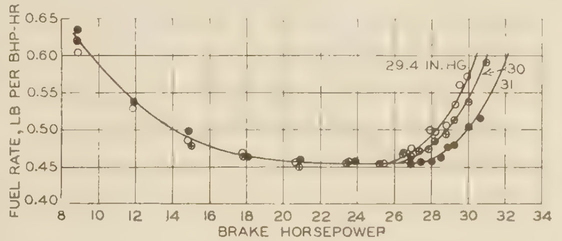

FIG. 5 EFFECT OF VARIATIONS IN INTAKE PRESSURE ON ENGINE PERFORMANCE, WITH EXHAUST PRESSURE EQUAL TO INTAKE

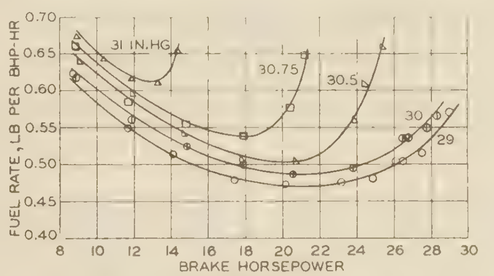

FIG. 6 EFFECT OF VARIATION IN EXHAUST PRESSURE ON ENGINE PERFORMANCE AT A CONSTANT INTAKE PRESSURE OF 28 IN. HG

The difference between these two figures is that for Fig. 5 the exhaust pressure was increased as the intake pressure increased, while for Fig. 4*b* the exhaust pressure remained unchanged. On this basis it appears that the engine performance is rather insensitive to changes in exhaust pressure.

Fig. 6 shows, however, that under certain conditions, a small change in exhaust pressure will cause a large decrease in power output and a corresponding increase in the fuel rate. It also shows that when the exhaust pressure was increased from 30 to 31 in. Hg (intake pressure remaining constant at 28 in. Hg), the fuel rate was increased 15 to 20 per cent and the maximum power output was halved. On the other hand, an increase in exhaust pressure from 29 to 30 in. Hg produced little change in maximum power and only about 4 per cent increase in the fuel rate. The reason for this is that the air flow to the engine is a function of the difference in the pressure in the main cylinder and the pressure of the compressed air in the precompression chamber. As the exhaust pressure is increased, the pressure in the main cylinder is increased and the pressure difference between the air in the pre-

compression cylinder and the gases in the main cylinder is decreased. Because the flow of air varies as the square root of this pressure difference, a given drop in pressure does not produce much change in flow if the pressure differential is high but does cause a large change in flow when the pressure differential is small. Thus, when the pressure differential is large, the engine is rather insensitive to changes in exhaust pressure. However, as this pressure differential is decreased by building up the back pressure, the air flow falls off rapidly with the previously mentioned attendant results. These results show that long exhaust lines, exhaust lines with various fittings causing frictional resistance to flow, and partially closed valves may cause serious loss in power.

Within the range covered by these tests, it appears that if the engine were so loaded that changes in atmospheric conditions affected the fuel rate, the change in fuel rate was proportional to the change in oxygen content per unit volume of the atmosphere, providing the pressure difference between intake and exhaust was not changed. Thus, an increase in air temperature, an increase in humidity, or a decrease in atmospheric pressure that produced a given change in the oxygen content of a given volume of air, produced about the same increase in fuel rate at any one load. However, no general correlation can be made between fuel rates and air densities, as a given change in air density produces no measurable change in fuel rate at light loads, a small change at high loads, and a large change at maximum load.

Due to unknown reasons, it was impossible to duplicate results exactly when a test was repeated after a lapse of a month or so, even when apparently all conditions were duplicated. The deviations between fuel rates were insignificant at light loads but varied up to as much as 6 per cent in some cases at the highest load. However, after a lapse of another month, original test results were duplicated in many cases. Because of this variation in engine performance, considerable care was taken to see that the results obtained when investigating any one variable were consistent and could be checked at any time throughout the series of runs with a maximum variation of $2^1/_2$ per cent. Thus, the various curves in any one figure may be compared with one another but should not be compared with similar curves in another figure.

Conclusions

It appears from the results of these tests that the outstanding factor affecting the performance of the two-cycle engine is the amount of air present in the cylinder at time of combustion. These results show that if sufficient air is present so that each particle of fuel may come in contact with oxygen at the desired time, other factors, such as air density, air temperature, and humidity, are immaterial. Thus, two general statements may be made, relating engine performance to the amount of air present:

1 If the engine is operated at loads lower than the load of minimum fuel rate, there may be changes in air density as high as 15 per cent without materially affecting the fuel rate.

2 If the engine is operated at loads in excess of the load giving minimum fuel rate, any change in intake air pressure, temperature, or humidity, or exhaust pressure will influence the amount of air taken into the cylinder and, due to the insufficiency of air present under these conditions, will influence both the fuel rate and the maximum power output.

In addition, one more conclusion may be drawn which is particularly applicable to two-cycle engines, namely: If, due to the engine design, setup, or operation, the pressure differential between the scavenging air and main-cylinder pressure is abnormally small, then changes in either the exhaust or intake pressures will measurably affect the air flow to the engine and will change both the fuel rate and maximum power output.

Due to the fact that the rated horsepower of a given-size engine varies with the design of the engine as well as with the manufacturer, no single statement can be made concerning the effect of variations in atmospheric conditions on the performance of engines in general. However, it may be stated that if an engine is conservatively rated, i.e., at a load below the load of minimum fuel rate, normal changes in barometric pressure will not affect its performance up to rated load, and changes in elevation, at which the engine is operated, of 4000 to 5000 ft may be made without measurably changing the engine performance. On the other hand, for the engine that is overrated, any change in barometric pressure, air temperature or humidity, or elevation will influence the fuel rate at rated load and may even prevent the engine delivering its rated load.

Acknowledgment

This project was sponsored by the Engineering School of The Pennsylvania State College and at the same time served as a basis of a master's thesis for Robert S. Boone. The author wishes to thank the various members of the Engineering School and particularly Mr. Boone for their kind cooperation.

BIBLIOGRAPHY

1 "Internal Combustion Engines," by L. C. Lichty, McGraw-Hill Publishing Co., Inc., New York, N. Y., 1939, p. 459.

2 "Reducing the Performance of a Solid-Injection Diesel Engine to Standard Conditions," by H. A. Everett, *Diesel Power*, vol. 11, no. 9, September, 1933, p. 541.

3 "A Rational Basis for Comparing Diesel Engine Performances," by E. S. Dennison, *S.A.E. Journal*, vol. 36, no. 6, June, 1935, p. 210.

4 "Compression-Ignition Engine Performance at Altitudes," by C. S. Moore and J. H. Collings, Jr., *S.A.E. Journal*, vol. 40, no. 6, June, 1937, p. 263.

5 "Correcting Diesel Engine Performance to Standard Atmospheric Conditions," by C. F. Taylor, *S.A.E. Journal*, vol. 41, no. 1, July, 1937, p. 312.

Discussion

A. J. Blackwood[3] and G. H. Cloud.[3] The author's report that the effect of atmospheric conditions on Diesel-engine performance under normal conditions is small should be most satisfying to the operators of Diesel equipment.

Tests in the research division of the Esso Laboratories on high-speed automotive engines have confirmed generally the author's results with respect to the effect of changes in atmospheric conditions. Changes in engine condition with time (mechanical adjustment and general engine condition) have been found to affect performance much more than day-to-day variations in atmospheric conditions.

Referring to the effect of exhaust pressures on engine performance, recent tests on a supercharged two-cycle automotive Diesel engine have shown that variations in exhaust pressures change power output and fuel economy appreciably. The following table shows some of the writers' experimental data obtained at full load, 1700 rpm:

Exhaust pressure, in. mercury	Decrease in maximum power, per cent	Increase in fuel consumption, per cent
0.0	0.0	0.0
0.9	1.7	2.0
2.2	2.9	6.0
3.4	4.1	8.0
6.1	8.7	13.0
7.3	9.5	15.0
9.0	12.3	18.0
11.9	16.5	24.0

The percentage of decrease in maximum power output with

[3] Esso Laboratories, Linden, N. J.

increase in exhaust pressure was not nearly as great in this engine as was shown in Fig. 6 of the paper. However, the differences between the results cited and the author's are no doubt due to the greater differential between the scavenging and exhaust pressures in the high-speed engine. These results confirm the author's observations that considerable loss in power may occur when exhaust pressures are permitted to become excessive. As shown by the following table, compiled from data obtained from Diesel units in automotive service, there are cases where inadequate exhaust systems raise exhaust pressures sufficiently at the higher speeds to interfere seriously with engine performance:

	Full-load back pressure In. mercury at rpm		
Engine unit	400	1200	2000
A	0.1	0.3	0.7
B	0.1	0.4	2.2
C	0.1	0.7	3.5
D	0.1	0.8	4.6
E	0.2	2.8	15.8

Some American manufacturers of automotive Diesel equipment have tended to set their engine outputs quite close to their maximum in order to compete with gasoline units in truck and bus service. This practice of increasing the maximum output up to the critical range often results in smoking, poor fuel economy, and rapid engine fouling. The author's work should help to discourage this practice by showing that it makes the equipment sensitive to slight changes in atmospheric conditions or exhaust pressures.

Author's Closure

The author wishes to thank Messrs. Blackwood and Cloud for the additional information they have given on this subject. Their second table is of particular value as it brings out the fact that changes in engine speed produce dissimilar changes in exhaust pressures for various engines. Thus, the conclusion may be drawn that a change in speed would not affect the maximum output and fuel rate of these various engines in the same manner.

It is desirable that much more information be made available so that both the designer and operator of Diesel engines may know what to expect when operating conditions are changed.

The Significance of Diesel-Exhaust-Gas Analysis[1]

By JOHN C. HOLTZ[2] and M. A. ELLIOTT,[3] PITTSBURGH, PA.

Data on exhaust-gas composition, obtained in a study of the hazards that might attend the use of Diesel engines underground, are discussed in relation to combustion in the Diesel engine. Two engines were tested throughout a wide range of fuel-air ratios, and the results indicated that combustion was essentially complete in the normal operating range although even under these conditions low but significant concentrations of carbon monoxide, aldehydes, and free carbon were present in the exhaust gases. The concentration of carbon monoxide, determined by precise analytical methods, was a minimum at a fuel-air ratio of approximately 0.03 lb per lb and was affected by engine design and to a slight extent by factors that varied with speed. The coexistence of aldehydes and free carbon indicated that direct oxidation and destructive combustion of the fuel were occurring simultaneously. The calculation of combustion efficiency from data on the products of incomplete combustion is illustrated.

Increasing interest in the use of Diesel engines[4] as the source of power for haulage equipment in mines and tunnels in the United States has led to a study by the Bureau of Mines of the hazards that might be involved. The ultimate object of this study is to develop recommendations that may serve to establish safe practices in the use of these engines underground. In such an application the discharge of harmful or objectionable gases into working places might constitute a significant hazard unless adequate ventilation were supplied. Therefore it is important to examine the exhaust gases produced by American Diesel engines operated under various conditions. Data on one aspect of this study were obtained in tests to determine the composition of exhaust gases produced at various speeds and loads by two four-stroke-cycle engines in proper mechanical condition.[5] The results of these tests have been discussed (1)[6] in relation to the use of Diesel engines underground. Inasmuch as some of the harmful and objectionable constituents also are products of incomplete combustion, the results furnish data on the combustion process in the Diesel engine. The significance of these data in studying the combustion performance of engines is discussed in the present paper.

[1] Published by permission of the Director, Bureau of Mines, United States Department of the Interior, Washington, D. C.

[2] Gas Engineer, Explosives Division, Central Experiment Station, Bureau of Mines, U. S. Department of the Interior. Jun. A.S.M.E.

[3] Associate Gas Engineer, Explosives Division, Central Experiment Station, Bureau of Mines, U. S. Department of the Interior.

[4] The designation "Diesel" engine is used instead of the more descriptive term "compression-ignition" engine because mine locomotives equipped with these engines usually are referred to as "Diesel mine locomotives."

[5] An engine adjusted and maintained in accordance with the manufacturer's recommendations is considered to be in proper mechanical condition.

[6] Numbers in parentheses refer to the Bibliography at the end of the paper.

Presented at the National Meeting of the Oil and Gas Power Division, Asbury Park, N. J., June 19–22, 1940, of The American Society of Mechanical Engineers.

Test Equipment

Engines and Dynamometer. The two Diesel engines tested are described in Table 1. Each engine was mounted in a "power unit," including radiator, fan, clutch, fuel system, and starting mechanism. In the tests, each unit was coupled to an electric dynamometer rated at 45 hp from 1200 to 2500 rpm.

TABLE 1 DESCRIPTION OF ENGINES TESTED

Engine	*A*	*B*
Type	Four-stroke cycle	Four-stroke cycle
Number of cylinders	4	4
Cylinder bore, in.	4 1/4	4
Piston stroke, in.	5 1/2	4 1/2
Piston displacement, cu in.	312.1	226.2
Maximum rated speed, rpm	1400	2600
Maximum rated brake horsepower, without accessories	44	70
Fuel pump	Individual pump for each cylinder; fuel delivery controlled by pump - plunger by-pass	Individual pump for each cylinder; fuel delivery controlled by pump - plunger by-pass
Type of injection valve	Single - hole orifice; flat-faced valve seat	Circumferential orifice (pintle nozzle); conical valve seat
Opening pressure of injection valve discharging into air at atmospheric pressure, lb per sq in.	1500	1650
Combustion system	Cylindrical precombustion chamber with cone-shaped ends	Spherical turbulence or air-swirl chamber
Cooling system	Positive circulation, thermostatically controlled	Positive circulation, thermostatically controlled

TABLE 2 CHEMICAL AND PHYSICAL PROPERTIES OF FUEL

Flash point (P.M.C.C.), F	Above 200
Water and sediment	Trace
Viscosity S. U. at 100 F, sec	48
Carbon residue	Trace
Ash	Trace
Gravity, deg A.P.I.	38.8
Pour point (upper), F	50
Cetane number (knockmeter delay method)	78
Sulphur, per cent	Trace
Hydrogen, per cent	14
Carbon, per cent	86
Nitrogen, per cent	0
Heating value, Btu per lb	19,910

Fuel. The chemical and physical properties of the fuel are shown in Table 2.

Method of Testing

As the engines were new when received, each was run in for 100 hr at various speeds and loads before any tests were made. In the tests an engine was operated at the desired speed and load for 1 hr. During the last 15 min the fuel consumption was measured, and the exhaust gases were sampled. One sample was analyzed in either a Haldane apparatus or a Bureau of Mines Orsat apparatus to determine the percentage of carbon dioxide, oxygen, carbon monoxide, hydrogen, and methane. Nitrogen was determined by difference. Other samples were analyzed by special methods to determine carbon monoxide, aldehydes, and oxides of nitrogen. Details of the sampling equipment, methods of analysis, and testing procedure have been reported (1).

Relation of Exhaust-Gas Composition to Fuel-Air Ratio

Previous studies (2, 3, 4, 5) of the exhaust gases from internal-combustion engines have shown that the composition of these gases is chiefly a function of air-fuel ratio. In fact, it has been

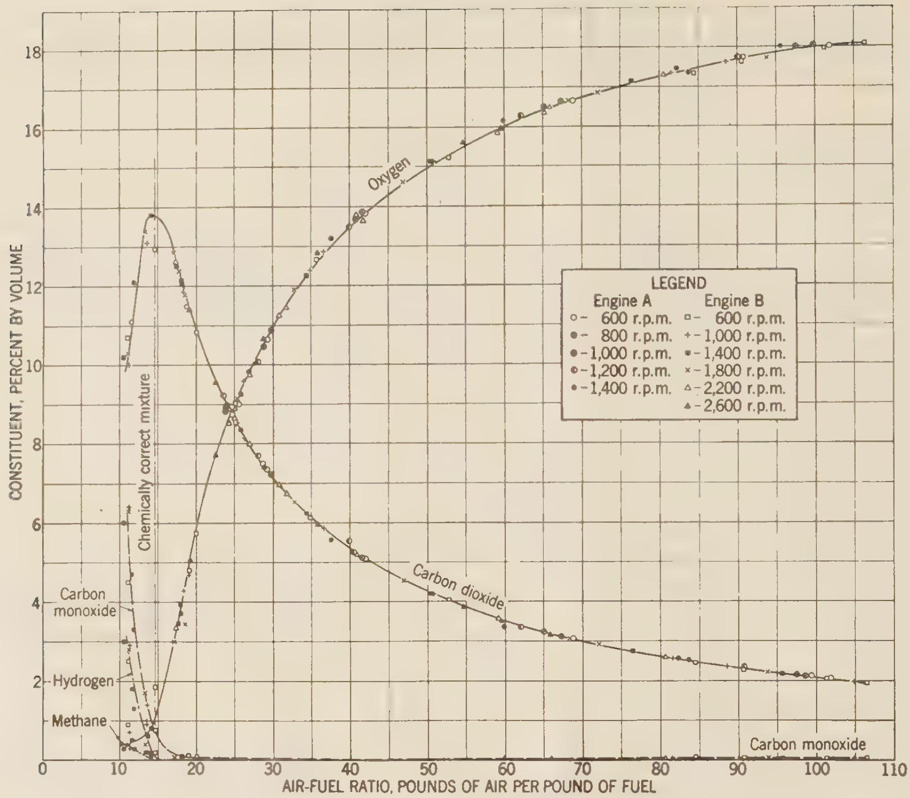

Fig. 1 Relation of Composition of Exhaust Gas to Air-Fuel Ratio

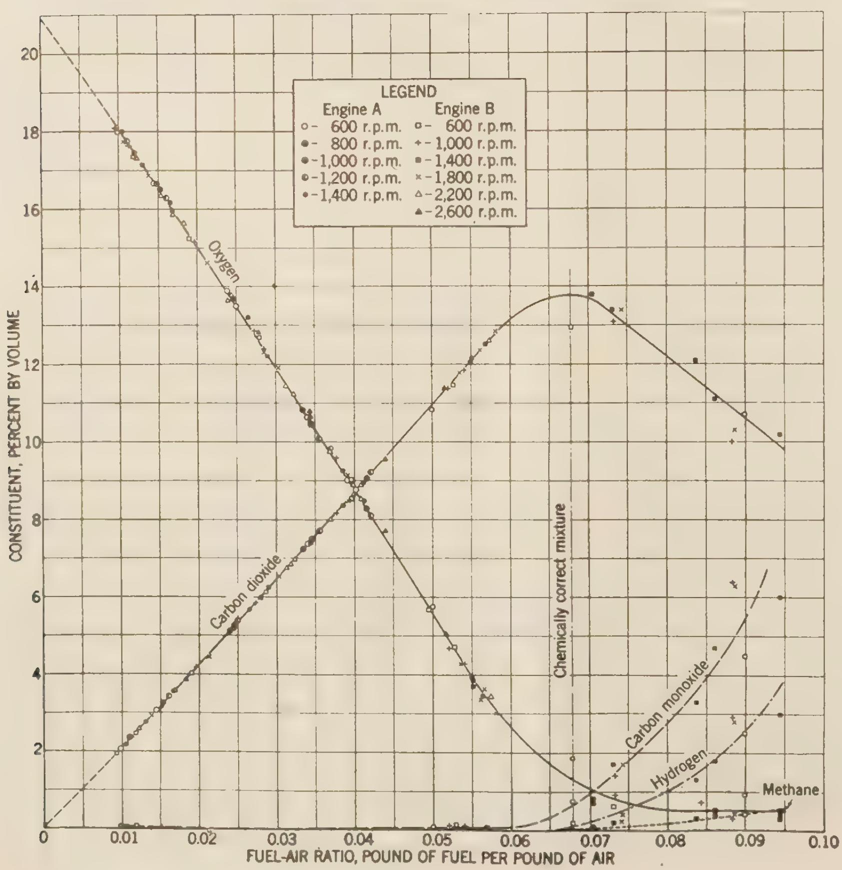

Fig. 2 Relation of Composition of Exhaust Gas to Fuel-Air Ratio

TABLE 3 TYPICAL EXPERIMENT RESULTS[a]

Test no.	B-13	B-14	B-15	B-16	B-12	B-70	B-72	B-69
Engine speed, rpm	1400	1410	1400	1410	1400	1400	1400	1400
Net power output, bhp	0[b]	8.8	17.5	26.4	37.80	40.20	41.0	40.6
Fuel used, lb per hr	4.56	6.89	9.56	12.45	18.12	21.29	24.41	29.63
Volume of dry exhaust gas, cu ft per hr[c]	4500	4460	4180	4050	3950	3700	3650	4050
Fuel-air ratio, lb per lb	0.013	0.020	0.029	0.039	0.056	0.070	0.084	0.094
Composition of dry exhaust gas:[d]								
CO_2, per cent by volume	2.74	4.19	6.22	8.36	12.400	13.8	12.1	10.2
O_2, per cent by volume	17.14	15.13	12.20	9.26	3.440	0.8	0.3	0.3
CO,[e] per cent by volume	0.041	0.028	0.024	0.027	0.058	0.7[f]	3.5[f]	6.0[f]
H_2, per cent by volume	....	....	....	....	....	0.1	1.3	3.0
CH_4, per cent by volume	0	0	0	0	0.03	0.1	0.3	0.4
N_2, per cent by volume	80.08	80.65	81.56	82.35	84.07	84.5	82.7	80.1
Oxides of nitrogen, parts per million[g]	167	267	378	448	364	346	277	186
Aldehydes, parts per million[h]	4	1	1	1	4	1	2	0

[a] Results are from tests on engine *B*.
[b] Power output of engine consumed by mechanical losses and in driving accessories. Under these conditions the power unit (engine and accessories) may be considered to be operating at no load.
[c] Calculated as dry exhaust gas at 60 F and 29.92 in. Hg.
[d] Gas analyses in tests B-69, B-70, and B-72 made in Bureau of Mines Orsat apparatus; in other tests Haldane apparatus was used.
[e] Determined by iodine-pentoxide method unless otherwise indicated. In calculating nitrogen by difference, values were expressed to nearest unit in second decimal place to conform with results of analysis in Haldane apparatus.
[f] Determined by absorption or combustion.
[g] As equivalent NO_2; not included in sum of percentages of other gases.
[h] As formaldehyde; not included in sum of percentages of other gases.

demonstrated (6) that the air-fuel ratio of internal-combustion engines can be calculated from exhaust-gas composition with an accuracy of ±2 per cent. Because of the convenience of such a procedure, the air-fuel relationships in the present investigation have been calculated by equations based on the stoichiometry of the combustion reactions and on material balances. These equations are given in the Appendix.

The variation of exhaust-gas composition with calculated air-fuel ratio, shown in Fig. 1, agrees in general with the observations of others, but the present investigation includes a much greater range of air-fuel ratios than has been studied heretofore. With such a wide range of air-fuel ratios there appears to be some advantage in correlating exhaust-gas composition with fuel-air ratio, as shown in Fig. 2, because, in the normal operating range of the Diesel engine, power output is a direct function of fuel-air ratio whereas it is an inverse function of air-fuel ratio. Therefore it is easier to visualize the relation of exhaust-gas composition to engine load when the results are correlated with fuel-air ratio, and the subsequent discussion will be conducted on this basis.

Fig. 2 shows that comparatively little carbon monoxide and no significant concentrations of hydrogen and methane were observed in the exhaust from the two engines at fuel-air ratios less than the chemically correct.[7] However, at fuel-air ratios greater than this the air present is inadequate to burn the fuel completely, and the concentration of products of incomplete combustion increased rapidly with an increase in fuel-air ratio. Fig. 2 shows also that the variation of the concentration of carbon dioxide and of oxygen with fuel-air ratio is nearly linear at those ratios less than 0.06 lb per lb. The general relationships indicated by Fig. 2 are similar to those obtained by replotting the data of D'Alleva and Lovell (3), using the Taylor method (7).

Although Fig. 2 presents data on exhaust-gas composition at fuel-air ratios on the rich side, such conditions of operation are not normal and were obtained in these tests by changing the adjustment of the stop limiting the travel of the rack on the fuel pump of engine *B*. After this change the fuel injected at full throttle was increased by approximately 60 per cent. When the engines were operated in their normal range the fuel-air ratio never exceeded 0.042 and 0.058 lb per lb for engines *A* and *B*, respectively.

Table 3 presents data typical of those used in plotting the figures in this paper.

[7] At the "chemically correct" or "stoichiometric" fuel-air ratio there is just sufficient air to burn the fuel completely. For the fuel used in these tests the chemically correct ratio was 0.0679 lb of fuel per lb of air.

Relation of Exhaust-Gas Composition to Combustion Performance

Despite the favorable conditions for completing combustion in the normal operating range of the Diesel engines tested, products of incomplete combustion were present in the exhaust gases, although the concentration of such products generally was low and could be determined only by sensitive methods of gas analysis. The importance of a knowledge of the products of incomplete combustion in relation to the combustion process in the Diesel engine has been emphasized by Boerlage and Broeze (8) who state that "analysis of the products of incomplete combustion may be a guide toward a better understanding of the Diesel process. From a practical point of view these products hold one of the biggest problems in Diesel development."

Products of Incomplete Combustion

The products of incomplete combustion observed in the exhaust gases of the two engines and discussed in the following are carbon monoxide, aldehydes, free carbon, hydrogen, and methane. Other products of combustion and losses from incomplete combustion are also discussed.

Carbon Monoxide and Aldehydes. The concentration of carbon

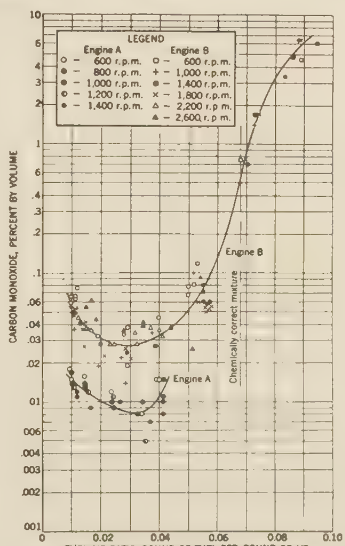

Fig. 3 Relation of Carbon-Monoxide Concentration in Exhaust Gas to Fuel-Air Ratio

monoxide in the exahust gas from each engine is shown in Fig. 3 in relation to fuel-air ratio. When the engines were operated in the range of fuel-air ratios for which they were adjusted by their respective manufacturers, the concentration of carbon monoxide was always less than 0.12 per cent. Despite such low concentrations, significant differences were observed in the carbon monoxide produced by each engine. The analytical method was precise enough to show that the carbon-monoxide concentration decreased slightly as the fuel-air ratio increased from the lowest values to an intermediate value of approximately 0.03 lb per lb. Further increase in fuel-air ratio was accompanied by an increase in carbon-monoxide concentration until, at the fuel-air ratios greater than the chemically correct one, the concentrations reached values comparable to those observed in the exhaust gases from gasoline engines.

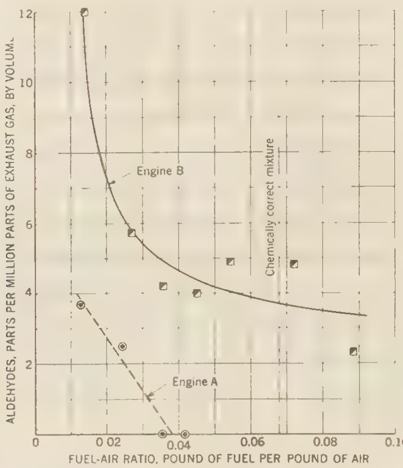

FIG. 4 TREND OF ALDEHYDE CONCENTRATION IN EXHAUST GAS WITH FUEL-AIR RATIO

This variation of carbon-monoxide concentration with fuel-air ratio is significant when considered in relation to the outline of the combustion process proposed by Boerlage and Broeze (8, 9), who suggest that two processes occur simultaneously: (*a*) The direct oxidation of hydrocarbons in the fuel by a series of reactions in which partly oxidized compounds are formed as intermediate products; and (*b*) the thermal decomposition (cracking) of the fuel followed by oxidation of the destruction products. The first process is referred to as direct oxidation and the second as destructive combustion.

If the reactions in the direct-oxidation process are chilled before oxidation is complete, carbon monoxide, aldehydes, and organic acids will be present in the exhaust gas. If the reactions occurring in destructive combustion are chilled soot also will be present. Under overrich conditions carbon monoxide and hydrogen are formed by either process.

The presence of aldehydes in the exhaust, shown in Fig. 4,[8] indicates that direct-oxidation reactions were occurring and that these reactions were chilled. The increase in the concentration of aldehydes and of carbon monoxide as the fuel-air ratio decreased from intermediate to low values indicates that chilling was more pronounced at the low fuel-air ratios. Obviously at low fuel-air ratios conditions are more favorable for chilling because average temperatures during combustion are comparatively low.

The increase in carbon-monoxide concentration with fuel-air ratio at ratios greater than approximately 0.03 lb per lb but less than the chemically correct ratio, shown in Fig. 3, probably occurs because the tendency to form locally overrich regions, which may give rise to carbon monoxide, is much greater as the fuel-air ratio increases and the concentration of oxygen approaches low values. Such locally overrich regions exist at fuel-air ratios on the lean side because uniform mixture of fuel and air throughout the combustion space is difficult to obtain under the heterogeneous conditions attending the injection of liquid fuel. At fuel-air ratios greater than the chemically correct value, carbon monoxide is produced because the air present is inadequate for complete combustion. Under these conditions the presence of free oxygen in the exhaust probably is indicative of imperfect mixing of fuel and air.

Although an average curve has been drawn in Fig. 3 to represent the variation of carbon-monoxide concentration with fuel-air ratio, close examination of the points indicates that the results were affected slightly by engine speed. It is probable that some of the differences observed were caused not only by differences in engine speed but also by the effects of other factors, such as turbulence and engine temperature. The significance of engine temperature was indicated by an increase of 350 per cent in carbon-monoxide concentration shown by a recorder when the temperature of the jacket water was decreased momentarily.

Aldehydes, in addition to being significant in relation to combustion, also are of interest in relation to the so-called acrid exhaust from Diesel engines because the odor and irritation of aldehydes can be detected at extremely low concentrations (10). In these tests the concentration of aldehydes, expressed as equivalent formaldehyde, ranged from 0 to 5 parts per million in the exhaust from engine *A* and from 0 to 31 parts per million in the exhaust from engine *B*. In preliminary tests a correlation has been observed between aldehyde concentration and odor and irritating properties of the exhaust.

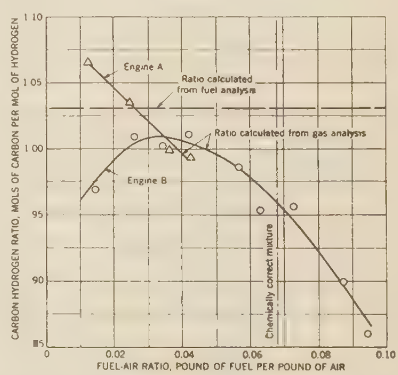

FIG. 5 COMPARISON OF CARBON-HYDROGEN RATIOS CALCULATED FROM EXHAUST-GAS ANALYSIS AND FROM FUEL ANALYSIS

Free Carbon. When the exhaust gas from either engine was passed through filter paper, a material resembling soot or free carbon was always deposited even though the final exhaust was clear. An analysis of a sample of such material collected in a test at a high fuel-air ratio indicated 99.1 per cent carbon, 0.7 per cent hydrogen, and traces of other materials.

If significant quantities of free carbon were present in the exhaust gas, the carbon-hydrogen ratio calculated from the gas analysis should be less than that calculated from the fuel analysis. The comparison of these ratios in Fig. 5 shows that this was generally true. However, an exception was observed in the tests with engine *A* at the lowest fuel-air ratios, under which conditions the carbon-hydrogen ratios calculated from the gas

[8] Each point in Fig. 4 is an average of several tests at different speeds in the same fuel-air ratio range.

TABLE 5 LOSSES FROM INCOMPLETE COMBUSTION, AND COMBUSTION EFFICIENCY FOR ENGINE *B*

Fuel-air ratio, lb per lb	CO		H_2		CH_4		Free carbon		Total		Combustion efficiency per cent
	Btu per lb of fuel	Per cent	Btu per lb of fuel	Per cent	Btu per lb of fuel	Per cent	Btu per lb of fuel	Per cent	Btu per lb of fuel	Per cent	
0.01	246	1.24	0	0	0	0	848	4.26	1094	5.5	94.5
0.02	62	0.31	0	0	0	0	481	2.42	543	2.7	97.3
0.03	37	0.19	0	0	0	0	269	1.35	306	1.5	98.5
0.04	32	0.16	0	0	0	0	297	1.49	329	1.7	98.3
0.05	40	0.20	0	0	0	0	410	2.06	450	2.3	97.7
0.06	93	0.47	0	0	0	0	622	3.12	715	3.6	96.4
0.07	528	2.65	119	0.60	185	0.93	933	4.69	1765	8.9	91.1
0.08	1876	9.42	512	2.57	320	1.61	1287	6.46	3995	20.1	79.9
0.09	2578	12.95	1230	6.18	591	2.97	1683	8.46	6082	30.6	69.4

TABLE 4 FREE CARBON IN THE EXHAUST GASES FROM ENGINE *B*

Fuel-air ratio, lb per lb	Carbon-hydrogen ratio from gas analysis (r_g), mols per mol	Free carbon in dry exhaust gases	
		Lb per lb of fuel	Lb per 1000 cu ft[a]
0.01	0.960	0.060	0.047
0.02	0.991	0.034	0.053
0.03	1.008	0.019	0.046
0.04	1.006	0.021	0.068
0.05	0.996	0.029	0.117
0.06	0.978	0.044	0.213
0.07	0.952	0.066	0.361
0.08	0.922	0.091	0.576
0.09	0.888	0.119	0.815

[a] Dry exhaust gas calculated at 60 F and 29.92 in. Hg.

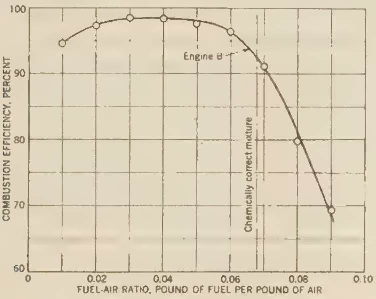

Fig. 6 Relation of Combustion Efficiency of Engine *B* to Fuel-Air Ratio

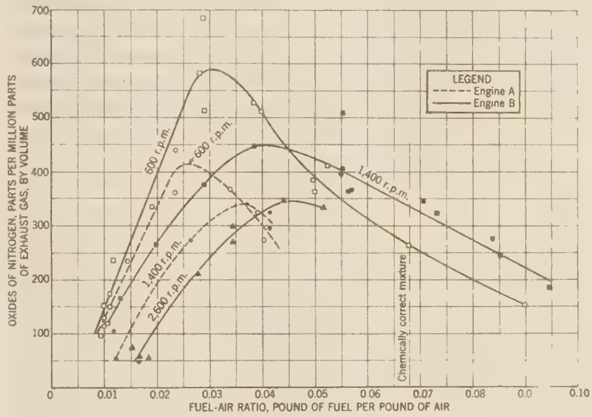

Fig. 7 Relation of Concentration of Oxides of Nitrogen in Exhaust Gas to Fuel-Air Ratio

analysis were greater than those calculated from the fuel analysis. The reason for this exception is not entirely clear, although the difference indicated at the lowest fuel-air ratio may be significant because the point shown is an average of 13 tests. In fact, each point in Fig. 5 is an average of several tests at different speeds in the same range of fuel-air ratio. The carbon-hydrogen ratios for the individual tests were calculated by equations given in the Appendix.

Using average values of the carbon-hydrogen ratios from the curve for engine *B* in Fig. 5 and equations given in the Appendix, the proportion of the fuel appearing as free carbon in the exhaust has been calculated and is given in Table 4. The results indicate that free carbon may be a relatively important factor in studying combustion. In such studies it would be preferable to determine the free carbon directly instead of by calculation as illustrated here.

In relating the concentration of free carbon in Table 4 to the appearance of the exhaust, it was observed that smoke was easily noticeable when the exhaust gas contained more than approximately 0.3 lb of carbon per 1000 cu ft.

Hydrogen and Methane. At fuel-air ratios less than 0.06, hydrogen was never indicated by the gas-analysis data, and methane was never present in significant concentrations. At higher fuel-air râtios the concentration of each of these gases increased. With regard to hydrogen, these observations agree with the results of others. However, in the present investigation the concentration of methane was not constant as previously reported by other investigators (4, 6).

Losses From Incomplete Combustion. Using average data on the products of incomplete combustion the potential heat lost in the exhaust gases from engine *B* has been calculated by equations given in the Appendix. The results are presented in Table 5, which also shows the losses expressed as a percentage of the higher heating value of the fuel. The combustion efficiency, also given in Table 5, was obtained by subtracting from 100 the total losses expressed as a percentage. These results are presented to illustrate the value of precise gas analysis in studying combustion performance; no attempt has been made to show the minor effect of factors that vary with speed.

Fig. 6 shows that the combustion efficiency of engine *B* reached a maximum at fuel-air ratios ranging from approximately 0.03 to 0.04 lb per lb. In this range of fuel-air ratios it is probable that the quantity of excess air is sufficient to minimize the formation of locally overrich regions without causing excessive chilling of the combustion reactions. In the normal operating range of engine *B* the combustion efficiency was between 94.5 and 98.5 per cent. At fuel-air ratios above this range, combustion efficiency decreased rapidly with an increase in fuel-air ratio. This decrease in efficiency also was apparent from measurements of power output and fuel consumption. For example, in tests at 1400 rpm on the rich side no significant increase in power output was observed despite an increase of 40 per cent in the fuel injected.

Oxides of Nitrogen. Oxides of nitrogen are among the harmful gases that must be considered in providing ventilation for Diesel engines used underground. Consequently, the concentration of these gases was determined in this investigation.

The oxides of nitrogen include: (*a*) Nitric oxide (NO), which is formed at the high temperatures associated with combustion; and (*b*) nitrogen peroxide (NO_2), which is formed at comparatively low temperatures by the reaction of nitric oxide and oxygen. In this investigation, concentrations of oxides of nitrogen are reported as equivalent nitrogen peroxide, although both oxides probably are present in the cooled exhaust gases.

Fig. 7 shows the concentration of oxides of nitrogen in rela-

tion to fuel-air ratio. The results indicate that the concentration of these gases may be affected by both speed and engine design. The occurrence of a maximum at fuel-air ratios between 0.025 and 0.045 can be explained by the effects of temperature and oxygen concentration on the equilibrium of the reaction of oxygen and nitrogen to form nitric oxide. The concentrations shown in Fig. 7 are within the range of those observed by other investigators (11, 12) using an experimental compression-ignition engine.

The possible significance of oxides of nitrogen in relation to internal-combustion-engine operation has been suggested by Hanson and Egerton (13), who have shown that the rate of oxygen absorption by lubricating oil at 220 C is influenced greatly by the presence of nitrogen peroxide in concentrations comparable to those observed during combustion. According to these investigators, this may account for certain differences in the results of engine tests of lubricating oils.

Under some conditions, oxides of nitrogen may contribute to engine corrosion and to the odor and irritating properties of the exhaust.

Oxides of Sulphur. The fuel used in these experiments was free of sulphur; therefore, oxides of sulphur were not present in the exhaust gases. However, if a fuel contains sulphur the exhaust gases will contain both sulphur dioxide and sulphur trioxide, which are significant chiefly in relation to engine corrosion and to the odor and irritating properties of the exhaust. The equations given in the Appendix should be modified when the fuel contains appreciable quantities of sulphur.

Summary

In an investigation by the Bureau of Mines of the hazards that might attend the use of Diesel engines underground the composition of the exhaust gases from two four-stroke-cycle four-cylinder Diesel engines in proper mechanical condition has been determined by precise analytical methods for fuel-air ratios ranging from approximately 0.01 to 0.09 lb per lb. This paper discusses the significance of these results in relation to combustion in the Diesel engine.

The variation of exhaust-gas composition with fuel-air ratio is shown and indicates that combustion was essentially complete when excess air was present. When the two engines were operated in their normal range of fuel-air ratios the concentration of carbon monoxide never exceeded 0.12 per cent, and hydrogen and methane were never present in significant concentrations.

Despite such low concentrations of carbon monoxide it was observed that the concentration of this gas was affected not only by fuel-air ratio but also by engine design and to a slight extent by factors that varied with engine speed. In tests of both engines the concentration of carbon monoxide reached a minimum at a fuel-air ratio of approximately 0.03 lb per lb.

Aldehydes, which are intermediate products formed in the direct oxidation of hydrocarbons, were present in the exhaust gases from both engines. The concentration of these compounds never exceeded 31 parts per million and tended to increase as the fuel-air ratio was decreased. Preliminary studies have indicated that aldehydes may be partly responsible for the so-called acrid exhaust from Diesel engines.

Throughout the normal operating range of both engines, free carbon was collected on filter paper through which exhaust gas was passed. Under these conditions the final exhaust generally was clear, although the calculated quantity of free carbon in the exhaust gas from one of the engines ranged from 2 to 6 per cent by weight of the fuel. Free carbon in the exhaust increased rapidly at fuel-air ratios greater than the maximum ratio in the normal operating range, and when the concentration of free carbon reached approximately 0.3 lb of carbon per 1000 cu ft of exhaust gas, smoke was easily noticeable.

The presence of aldehydes in the exhaust is indicative of chilling of direct oxidation reactions, and the presence of free carbon at fuel-air ratios on the lean side is indicative of chilling of destructive (cracking) combustion reactions occurring in locally overrich regions. These observations support the outline of the combustion process in the Diesel engine suggested by Boerlage and Broeze (8, 9).

In the normal operating range of one engine the potential heat lost in the products of incomplete combustion was between 1.5 and 5.5 per cent of the energy in the fuel. Such low losses might not be detected unless precise methods of analysis were used to determine the products of incomplete combustion.

The significance of oxides of nitrogen and oxides of sulphur in relation to the operation of internal-combustion engines is discussed briefly.

Acknowledgments

The authors gratefully acknowledge the advice and guidance given by A. C. Fieldner, chief, Technologic Branch; D. Harrington, chief, Health and Safety Branch; and Wilbert J. Huff, consulting explosives chemist, Explosives Division, Bureau of Mines.

The Health Division and the Explosives Division are cooperating in this investigation, and the authors acknowledge the valuable assistance of H. H. Schrenk, chief chemist, and L. B. Berger, associate chemist, Health Division. The authors are also indebted to individual members of the Explosives and Health Divisions for their part in operating the engines and sampling and analyzing the exhaust gases. The National Bureau of Standards and the Coal Analysis Laboratory of the Bureau of Mines furnished data on the properties of the fuel.

Appendix

Calculation of Results

The following nomenclature applies to the terms in the equations given in this section:

CO_2, CO, CH_4, H_2, O_2, N_2 = respectively, the percentage by volume of carbon dioxide, carbon monoxide, methane, hydrogen, oxygen, and nitrogen in the dry exhaust gas

H_2O = water vapor in exhaust, mols per 100 mols of dry exhaust gas

c = carbon in fuel, per cent by weight

h = hydrogen in fuel, per cent by weight

V = volume of dry exhaust gas, cu ft (at 60 F and 29.92 in. Hg) per lb of fuel

a = air-fuel ratio, lb of air per lb of fuel

f = fuel-air ratio, lb of fuel per lb of air

r_0 = carbon-hydrogen ratio calculated from gas analysis, mols per mol

r = carbon-hydrogen ratio calculated from fuel analysis, mols per mol

M_c = mols of carbon per 100 mols of dry exhaust gas, calculated from exhaust-gas analysis

M_h = mols of hydrogen per 100 mols of dry exhaust gas, calculated from exhaust-gas analysis

U = free carbon in exhaust, per cent by weight of fuel

Y = free carbon in exhaust, pounds per 1000 cu ft (at 60 F and 29.92 in. Hg) of dry gas

In deriving the equations, the following constants were used:

Mol volume = 379.4 cu ft of dry gas at 60 F and 29.92 in. Hg

Weight of 1 lb-mol of air = 28.98 lb

Composition of air, percentages by volume: Carbon dioxide = 0.03; oxygen = 20.93; nitrogen (including other inert gases) = 79.04.

The volume of exhaust gas per pound of fuel can be calculated from the stoichiometry of the combustion reactions by either of three methods:

1 By a carbon balance, which assumes that all of the carbon in the fuel appears as carbon-containing gases determined in the exhaust-gas analysis.

2 By a hydrogen balance, which assumes that all of the hydrogen in the fuel appears as hydrogen-containing gases determined in the gas analysis or as water vapor which can be calculated from the exhaust-gas analysis by an oxygen balance.

3 By a combined carbon and hydrogen balance, which assumes that all of the carbon and hydrogen in the fuel can be accounted for in the gas analysis either directly or by calculation. A further assumption is that the fuel contains only carbon and hydrogen.

The ultimate analysis of the fuel is required in the first and second methods but not in the third. The three methods are illustrated in the following:

Volume of Dry Exhaust Gas per Pound of Fuel

Method 1—Carbon Balance. Mols of carbon from the fuel per 100 mols of dry exhaust gas

$$M_c = CO_2 + CO + CH_4 - 0.03^9 \qquad [1]$$

Mols of carbon per pound of fuel

$$\frac{c}{100 \times 12.01} \qquad [2]$$

Mols of dry exhaust gas per pound of fuel

$$\frac{c}{12.01\, M_c} \qquad [3]$$

Cubic feet of dry exhaust gas per pound of fuel

$$V = \frac{379.4c}{12.01\, M_c} \qquad [4]$$

Method 2—Hydrogen Balance. Mols of hydrogen as water vapor per 100 mols of dry exhaust gas

$$H_2O = 2\left(\frac{20.96 N_2}{79.04} - CO_2 - O_2 - \frac{1}{2} CO\right) \qquad [5]$$

Total mols of hydrogen per 100 mols of dry exhaust gas

$$M_h = H_2O + H_2 + 2CH_4 \qquad [6]$$

Cubic feet of dry exhaust gas per pound of fuel

$$V = \frac{379h}{2.016 M_h} \qquad [7]$$

Method 3—Carbon-Hydrogen Balance. Pounds of carbon and hydrogen per 100 mols of dry exhaust gas

$$12.01\, M_c + 2.016 M_h \qquad [8]$$

Cubic feet of dry exhaust gas per pound of fuel

$$V = \frac{379.4 \times 100}{12.01 M_c + 2.016 M_h} \qquad [9]$$

[9] Average concentration of carbon dioxide in intake air. This correction is of importance only at low fuel-air ratios and when precise analytical methods are used.

In this investigation the carbon balance, method 1, was used at fuel-air ratios less than the chemically correct ratio. At higher fuel-air ratios the hydrogen balance, method 2, was used to avoid errors that would have been caused by the comparatively large quantities of free carbon present but not determined in the gas analysis. Considering only random errors in gas analysis it was estimated that the error in V calculated by the hydrogen balance probably would be four or five times greater than the error in V calculated by the carbon balance. Therefore, even though the exhaust gas may contain free carbon at fuel-air ratios less than the chemically correct one, there is no net advantage in using the hydrogen balance in calculating the results of a single test unless the proportion of the fuel appearing as free carbon is greater than the probable error in calculating V. There would be an advantage in using the hydrogen balance when the results of a large number of identical tests are averaged.

Method 3 was not used in this investigation but has been included for comparison.

Fuel-Air Ratio

The fuel-air ratio was calculated from the volume of dry exhaust gas using a nitrogen balance, or

$$f = \frac{1}{a} = \frac{379.4 \times 79.04}{28.98\, VN_2} = \frac{1035}{VN_2} \qquad [10]$$

Carbon-Hydrogen Ratio

The carbon-hydrogen ratio was calculated from the gas analysis as follows

$$r_g = \frac{M_c}{M_h} \qquad [11]$$

where M_c and M_h may be calculated from Equations [1] and [6], respectively.

The relation used to calculate the carbon-hydrogen ratio from the fuel analysis is

$$r = \frac{2.016c}{12.01h} \qquad [12]$$

Free Carbon in Exhaust Gas

The free carbon in the exhaust gas, per cent by weight of fuel, is

$$U = c - \frac{12.01\, r_g h}{2.016} \qquad [13]$$

Free carbon in exhaust gas, pounds per 1000 cu ft of dry exhaust gas, is

$$Y = \frac{U}{100\, V} \qquad [14]$$

Potential Heat Lost in Exhaust Gas

Potential heat in carbon monoxide

$$\text{Btu per pound of fuel} = \frac{321(CO)V}{100} \qquad [15]$$

Potential heat in free carbon

$$\text{Btu per pound of fuel} = \frac{14140\, U}{100} \qquad [16]$$

Potential heat in hydrogen

$$\text{Btu per pound of fuel} = \frac{324(H_2)V}{100} \qquad [17]$$

Potential heat in methane

$$\text{Btu per pound of fuel} = \frac{1012(CH_4)V}{100} \quad \ldots\ldots [18]$$

BIBLIOGRAPHY

1 "Diesel Engines Underground. I—Composition of Exhaust Gas From Engines in Proper Mechanical Condition," by J. C. Holtz, L. B. Berger, M. A. Elliott, and H. H. Schrenk, Bureau of Mines, Report of Investigations No. 3508, U. S. Department of the Interior, 1940.

2 "Carburetor Adjustment by Gas Analysis," by A. C. Fieldner and G. W. Jones, *Industrial and Engineering Chemistry*, vol. 14, 1922, pp. 594–600.

3 "Relation of Exhaust Gas Composition to Air-Fuel Ratio," by B. A. D'Alleva and W. G. Lovell, *S.A.E. Journal*, vol. 38, 1936, pp. 90–98, 116.

4 "Interrelation of Exhaust Gas Constituents," by H. C. Gerrish and F. Voss, National Advisory Committee for Aeronautics, 24th Annual Report No. 616, 1938, p. 139.

5 "Interpretation of Exhaust Gas Analysis," by S. H. Graf, G. W. Gleeson, and W. H. Paul, Bulletin Series, No. 4, Engineering Experiment Station, Oregon State Agricultural College, 1934. Includes an extensive bibliography on investigations of exhaust-gas composition.

6 "Relation of Hydrogen and Methane to Carbon Monoxide in Exhaust Gases From Internal-Combustion Engines," by H. C. Gerrish and A. M. Tessman, National Advisory Committee for Aeronautics, 20th Annual Report No. 476, 1934, p. 53.

7 "The Internal Combustion Engine," by C. F. Taylor and E. S. Taylor, International Textbook Company, Scranton, Pa., 1938, p. 60.

8 "The Combustion Process in the Diesel Engine," by G. D. Boerlage and J. J. Broeze, *Chemical Reviews*, vol. 22, 1938, pp. 61–85.

9 "Combustion Qualities of Diesel Fuel," by G. D. Boerlage and J. J. Broeze, *Industrial and Engineering Chemistry*, vol. 28, 1936, pp. 1229–1234.

10 "Intensities of Odors and Irritating Effects of Warning Agents for Inflammable and Poisonous Gases," by S. H. Katz and E. J. Talbert, Bureau of Mines Technical Paper No. 480, U. S. Department of the Interior, 1930.

11 "Nitrogen Oxides in Internal Combustion Engine Gases," by T. K. Hanson and A. C. Egerton, Proceedings of the Royal Society of London, series A, vol. 163, 1937, pp. 90–100.

12 "The Combustion Process in the Compression-Ignition Engine," by J. W. Drinkwater and A. D. Egerton, Proceedings of The Institution of Mechanical Engineers, vol. 138, 1938, pp. 415–459.

13 "Influence of Catalysts on Oxidation of Oils," by T. K. Hanson and A. C. Egerton, The Institution of Mechanical Engineers, Lubrication Discussion, Group IV, October, 1937, pp. 146–150.

Discussion

H. E. Degler.[10] The writer does not agree with the author in the statement that the air-fuel ratio of internal-combustion engines can be calculated from the exhaust-gas composition with an accuracy of ±2 per cent. However, it is true that such a procedure is convenient and probably of some relative value for the purposes of their paper. It is generally agreed that combustion in the internal-combustion engine is not perfect, but the incompleteness, as evidenced by the presence of carbon monoxide in the exhaust gases, is not very marked. The uncertainty of determining accurately the small percentages of carbon monoxide in engine exhaust gases is well known. In addition, chemical tests on the condensed water vapor from the exhaust often reveal the presence of aldehydes (CH_nO compounds) and other partly oxidized organic materials, as mentioned in the paper. For these reasons, it is the writer's opinion that the air-fuel ratios supplied to the engine cannot be computed from the exhaust-gas composition with the 2 per cent accuracy stated. In general, it is found that this discrepancy becomes greater as the supplied air-fuel ratios become larger.

From the comparative results obtained on the two engines tested, there is no doubt but that the form of the combustion chamber and the type of fuel-injection system are important considerations in the matter of obtaining efficient (more complete) combustion of the fuel. The authors did not state the general design of the two engines used for making these tests. The writer would like to inquire if engine *A* is an auxiliary-combustion-chamber type and engine *B* a direct-injection (open-combustion) design. It is unfortunate that investigators continue to use uncertain terminology in connection with the appearance of the Diesel-engine exhaust, such as "clear exhaust," "generally clear," "easily noticeable," etc. A year ago the writer presented a paper[11] in which he asked the question: "What is clear exhaust?" This was defined as, "a smoke standard established with the use of a smoke-density meter; clear exhaust being the condition when the smoke meter shows 50 per cent smoke density, which is the point when the exhaust becomes visible to the naked eye."

Engine manufacturers and operators have been increasing jacket-water temperatures in recent years, some as high as 212 F at atmospheric pressure, thus taking advantage of the latent-heat cooling effect in addition to the sensible-heat removal. These higher temperatures will reduce the "chilling of direct oxidation reactions," as mentioned by the authors, and assure lower CO, decrease aldehydes, and reduce the free carbon in the engine exhaust. There are possibilities of using sealed-water systems under pressure for cooling purposes. In liquid-cooled aircraft engines the coolant is generally ethylene glycol because of its high boiling (345 F) and low freezing (2 F) points, but it is inferior to water in other properties.

In the usual combustion of hydrocarbons, there is a race between thermal decomposition and hydroxylation. If the conditions favor hydroxylation, such as the use of a preheated hydrocarbon-air mixture and the allowance of sufficient time for the entrance of oxygen into the hydrocarbon molecule, there would be no soot. However, if conditions favor cracking, as for example, whenever the hydrocarbons and oxygen of the air are not thoroughly mixed, the heat from the combustion of part of the hydrocarbon cracks the remainder.

The problem of ascertaining the nature of the active intermediates is one of the most complicated in the field of the kinetics of gas reactions. Experimental evidence has been used to determine these radicals and the most probable sequence of the chain reactions. The initiation of these reactions depends upon the presence of reaction centers, hot or actuated molecules at an energy level above the mass average, from which combustion spreads chainwise. A consideration of the absorption of energy in quanta and its correlation with the number of molecules reacting is necessary to account for the fact that combustion reactions do not follow the laws of mass action, as deduced from simple stoichiometric equations. The success of some recent analysis to explain the larger number of experimental facts justifies the hope that the technology of combustion may be advanced from its present empirical state to a more scientific basis.

W. H. Sanders.[12] The data presented appear particularly valuable since they have been secured by unusually skillful technique in a type of experiment which has received comparatively little attention. It seems probable that work like this will become increasingly important as fuel-air ratios are raised in an effort to make smaller and lighter engines; also as need to understand the Diesel combustion process becomes more urgent.

Computation of fuel-air ratios from exhaust-gas analysis has been found quite satisfactory. Measurements were made on a four-stroke-cycle industrial Diesel by three methods: (*a*) a large

[10] Professor of Mechanical Engineering, University of Texas, Austin Tex. Mem. A.S.M.E.

[11] "Interpretation of Smoky Exhaust of Diesel Engines," A.S.M.E. Oil and Gas Power Division, Proceedings of National Conference, Ann Arbor, Mich., paper No. 19, 1939.

[12] Naval Research Laboratories, Washington, D. C.

laboratory-type wet-test gas meter for intake air, and customary fuel-consumption measurements; (*b*) exhaust samples collected in evacuated bulbs for analysis with the Shepherd apparatus; (*c*) the method of addition of a foreign substance, with analysis before and after its mixing with the intake. Agreement to the order of 5 per cent was obtained. It was thought the agreement could have been improved by more precise gas analysis. In this particular case it was much more convenient to use gas-analysis apparatus than an orifice and surge tank large enough to insure steady flow.

Authors' Closure

The statement that the air-fuel ratio of internal-combustion engines can be calculated from exhaust-gas composition with an accuracy of ±2 per cent is based upon the results of tests of the N.A.C.A. (6) in which this order of agreement was observed in comparisons of the air-fuel ratio, calculated from the exhaust-gas analysis, and the air-fuel ratio determined by weighing the fuel and measuring the air. These results were cited only to indicate the probable order of accuracy to be expected in calculating air-fuel ratio from exhaust-gas composition; it was not our intention to infer that this accuracy would be attained under all conditions. In fact, in a previous paper (1) we pointed out that, even when excess air was present, the exhaust gases in our tests contained free carbon which, because it was not determined in the gas analysis, could lead to errors of as much as 5 per cent in the calculated fuel-air ratio when the carbon balance was used. This same conclusion is evident from the results presented in column 9 of Table 5 of the paper, which show the proportion of the fuel appearing in the exhaust as free carbon.

The attainment of a high degree of accuracy in results calculated from the exhaust-gas analysis was not of vital importance in our investigation, although some consideration was given to this factor in an earlier paper (1). Inasmuch as Professor Degler has raised the question of the accuracy of calculating fuel-air ratio from exhaust-gas composition, the following comments may be of interest:

The accuracy of methods of calculating fuel-air ratio from exhaust-gas analysis by means of material balances and chemical stoichiometry depends upon the three following factors:

(*a*) The validity of the assumption that all of the particular material in question is determined or can be accounted for by the results of the gas analysis.

(*b*) The accuracy of the methods of sampling and analyzing exhaust gases.

(*c*) The accuracy of methods of fuel analysis.

From a study of the results of gas analysis, it was established that determinations of carbon-dioxide and oxygen concentration were, respectively, within ±0.04 per cent and ±0.06 per cent of the most probable value 99 per cent of the time. If these errors in gas analysis were the only consideration, it can be shown that the fuel-air ratio calculated by a carbon balance will be within ±0.3 per cent of the most probable value at the chemically correct fuel-air ratio and within ±2 per cent at the lowest fuel-air ratio. Corresponding values for the probable accuracy of fuel-air ratios, calculated from a hydrogen-oxygen balance, would be ±1.5 per cent and ±9 per cent, respectively. This effect of random errors in gas analysis may be of interest in conjunction with Professor Degler's statement that the discrepancy in calculated air-fuel ratios becomes greater as the air-fuel ratios become larger (fuel-air ratios lower).

The principal source of error in calculating fuel-air ratio from exhaust-gas analysis lies in deviations from the assumption that the analytical procedure determines or accounts for all of the material on which the material balance is based. Our results show that free carbon was present in the exhaust gas. In addition, unburned fuel and, as Professor Degler points out, aldehydes and other partly oxidized hydrocarbon may also be present. Any of these compounds if undetermined would contribute to inaccuracies in the calculations of fuel-air ratio. In so far as aldehydes soluble in water are concerned, these were determined in our tests and, therefore, cannot be considered as a source of error. Furthermore, we do not agree with Professor Degler's statement that "the uncertainty of determining small percentages of carbon monoxide in engine exhaust gases is well known," because a method[13] is available for determining, with an accuracy of ±0.003 to 0.005 per cent, low concentration of carbon monoxide in mixtures of engine exhaust and air. This method was used in our tests.

With reference to Professor Degler's question regarding the general design of the engine, this information is given in Table 1 under "combustion system." As indicated in that table, both engines are of the auxiliary-chamber type.

[13] "The Determination of Carbon Monoxide in Air Contaminated With Motor Exhaust," by M. C. Teague, *Industrial and Engineering Chemistry*, vol. 14, 1920, pp. 964–968.

Lateral Stiffness and Vibration in Engine Structures

By RUSSELL PYLES,[1] OLEAN, N. Y.

The forces tending to produce horizontal vibration in engine frames may be obtained from the bearing-load diagrams. For an eight-cylinder nine-bearing engine, the dominant forces occur at the center main bearing and bearings Nos. 3 and 7. The first major horizontal critical speed is the eighth order, which will come into resonance when the engine speed is one eighth the natural horizontal frequency of frame.

In view of the difficulty of predicting the horizontal frequency of the complicated frame structure, a simplified empirical method of comparing stiffness of frames is given.

INCREASED engine speed accompanied by higher brake mean effective pressure and a lower total weight of the unit, accentuates engine-vibration problems. Vibration occurs principally in the combustion chamber, crankshaft, and engine structure. Rough-running engines may result from any one or a combination of these.

Combustion control and torsional vibration have been the subjects of much study and methods have been developed for handling these problems. This is not so true of frame vibration, probably because it has not in the past been generally troublesome. However, this type of vibration is not new. Eighteen years ago, Ricardo[2] briefly discussed synchronous vibration of crankcases, particularly with respect to six-cylinder automotive engines. At this time, the six-cylinder engine was beginning to displace the four. The longer crankcase resulted in a lower natural frequency of the frames and without additional stiffness, resonant vibration was more probable. Cylinders were cast in pairs or threes, and bolted to the crankcase. This construction added no stiffness to the crankcase, and left it relatively flimsy at the middle. The advent of the enbloc crankcase seemed to remedy this trouble, because the stiffness of the cylinder box added to the crankcase raised the natural frequency of the structure, moving serious critical speeds above the then prevailing running speeds. Larger stationary and marine engines have been relatively free from pronounced frame vibration because of low speeds and excessive weights, permitting the use of a large amount of metal with little regard for its efficient disposition. Heavy foundations also contribute some stiffness to the engine base. The trend to higher speeds and lighter engines will raise the frequency of the exciting forces, lower the natural frequency of the engine structure, and thus make the possibility of resonance more probable. In very light high-speed designs, crankcase deflections of serious magnitude may even result without resonance, but as a forced vibration.

The broad function of the engine frame or crankcase and base is to carry the imposed loads and maintain proper alignment of all moving parts, principally pistons, rods, and crankshaft. Deflection of bearing supports alters the normal load capacity of the bearing and at the same time permits crankshaft deflection which imposes additional bending stresses in the shaft. The question naturally arises as to what deflections are permissible. Considering the bearings, displacements of one bearing with respect to the others should be less than the oil-film thickness unless deflection of the shaft is allowed. Some deflection of the crankshaft is undoubtedly permissible, this being limited by shaft stress. Frame stress due to vibration deflection is not likely to be generally serious although frame failures have occurred. An important limiting factor appears to be the general discomfort experienced with vibration, enhanced by the appearance of relative movement in the engine structure. Vibratory movement to the average eye is always magnified and appears to have several times its actual amplitude.

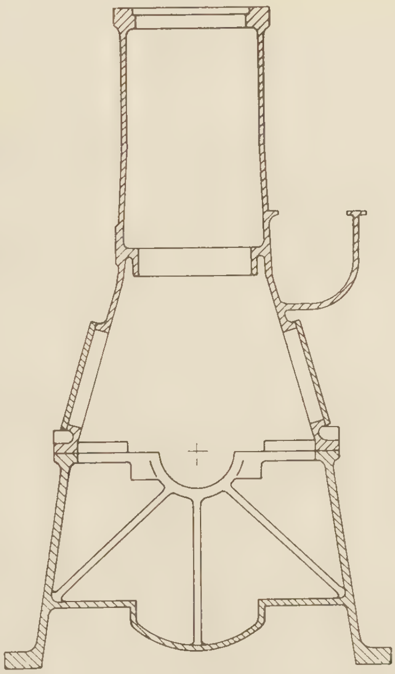

Fig. 1 Conventional Frame and Base Form

Fig. 1 indicates the conventional form of base and upper crankcase, bored for cylinder liners. Consider the base to be supported at each end and a vertical load applied at the center main bearing. Stiffness in this plane is obviously great because of the depth of the continuous side walls of the water jacket and base. Now apply the bearing load in a horizontal plane and it is evident that resistance to bending is smaller. No deep sections exist in the horizontal plane to contribute to rigidity. Side walls of the base and frame are relatively flexible under horizontally applied load. Obviously, the critical bending plane is horizontal and this is borne out by experience. For this reason, this discussion

[1] Engineer, Clark Bros. Co., Inc.

[2] "The Internal Combustion Engine," by H. R. Ricardo, Blackie & Son Limited, London, England, vol. 1, 1922, p. 205.

Presented at the National Meeting of the Oil and Gas Power Division, Asbury Park, N. J., June 19–22, 1940, of The American Society of Mechanical Engineers.

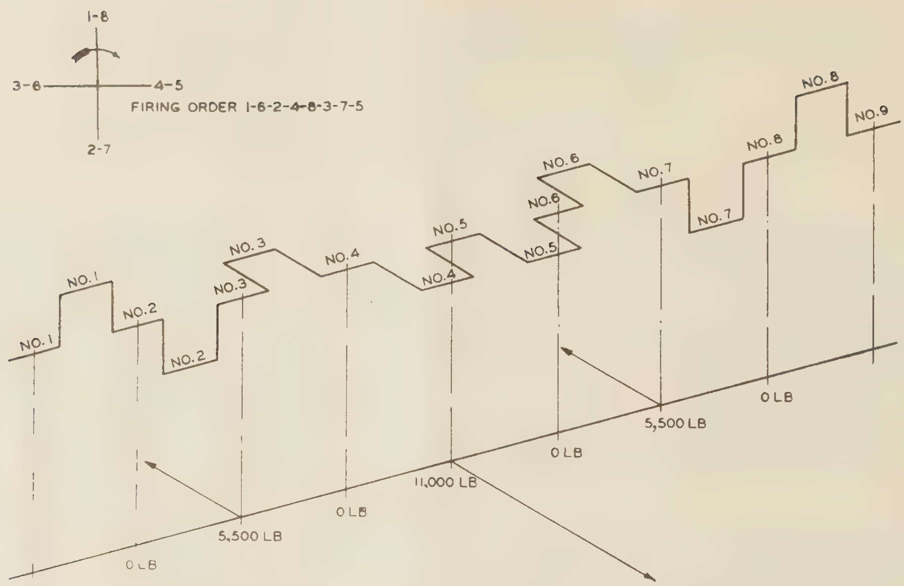

Fig. 2 Crank Arrangement and Horizontal Loading for an Eight-Cylinder Engine

is restricted to a consideration of horizontal forces and stiffness only.

Forces Acting at Bearings

Lateral forces within the frame spring from three sources, (*a*) gas pressure, (*b*) inertia forces of reciprocating parts, and (*c*) centrifugal force of rotating masses.

Horizontal components of gas pressure and inertia are due to the angularity of the connecting rod. The forces are transmitted through the rod to the crankpin and thence to the bearings. Centrifugal forces transfer directly to the bearings through the crank webs. These forces are transmitted to the base and frame structure through the bearing supports.

A polar diagram of bearing loading, made in a conventional manner, shows the effect of the combined gas pressure, inertia, and centrifugal force all taken in their proper phase relationship. If we take horizontal components of the polar diagram at various crank angles and plot them—a curve of horizontal force versus crank angle is obtained. This may be done for each main bearing. When these curves are considered in their proper phase, depending upon firing order and crank arrangement, a fair picture is given of horizontal loading on the engine structure.

This general method has been used here and applied to an eight-cylinder four-cycle engine. The eight-cylinder engine may be more susceptible to frame vibration than a four or six because the extreme length will result in a lower natural frequency of the frame. Fig. 2 shows the crank arrangement and firing order for such an engine. The horizontal components at the bearings are indicated for the crank positions shown at a speed of 720 rpm.

Figs. 3*a* and 3*b* show the polar diagram and horizontal components for an intermediate bearing with cranks at 180 deg, that is, bearings Nos. 2, 4, 6, and 8. Note that the horizontal components are small and the complete cycle takes up 720 deg of crank angle.

The diagrams for the other intermediate bearings (Nos. 3 or 7) with cranks at 90 deg apart are shown in Figs. 4*a* and 4*b*. The scales for these curves are one half those used for the intermediate bearing with cranks 180 deg apart. Comparison of the maximum values of the horizontal components brings out the

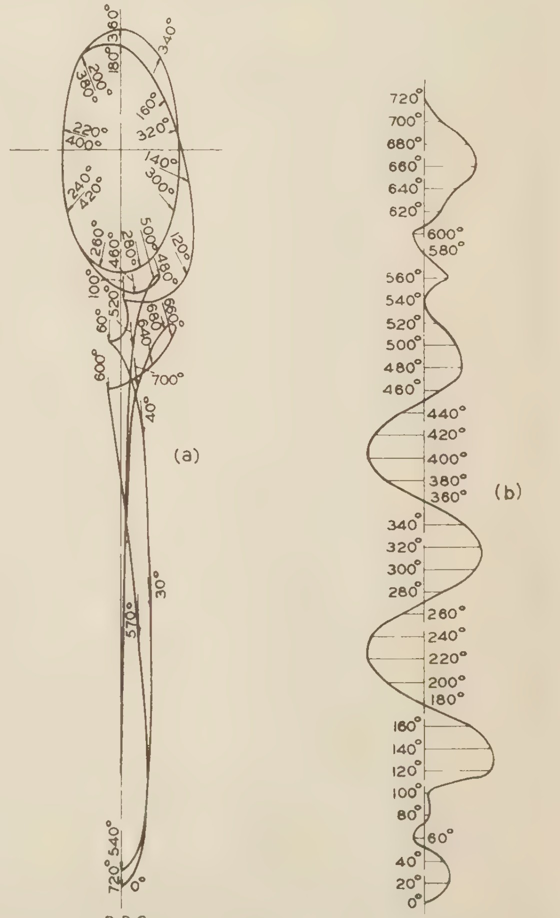

Fig. 3 Polar Diagram and Horizontal Components of Loads on Intermediate Main Bearings of an Eight-Cylinder Engine at 900 Rpm, Cranks at 180 Deg
(Scale: 1 in. = 4000 lb.)

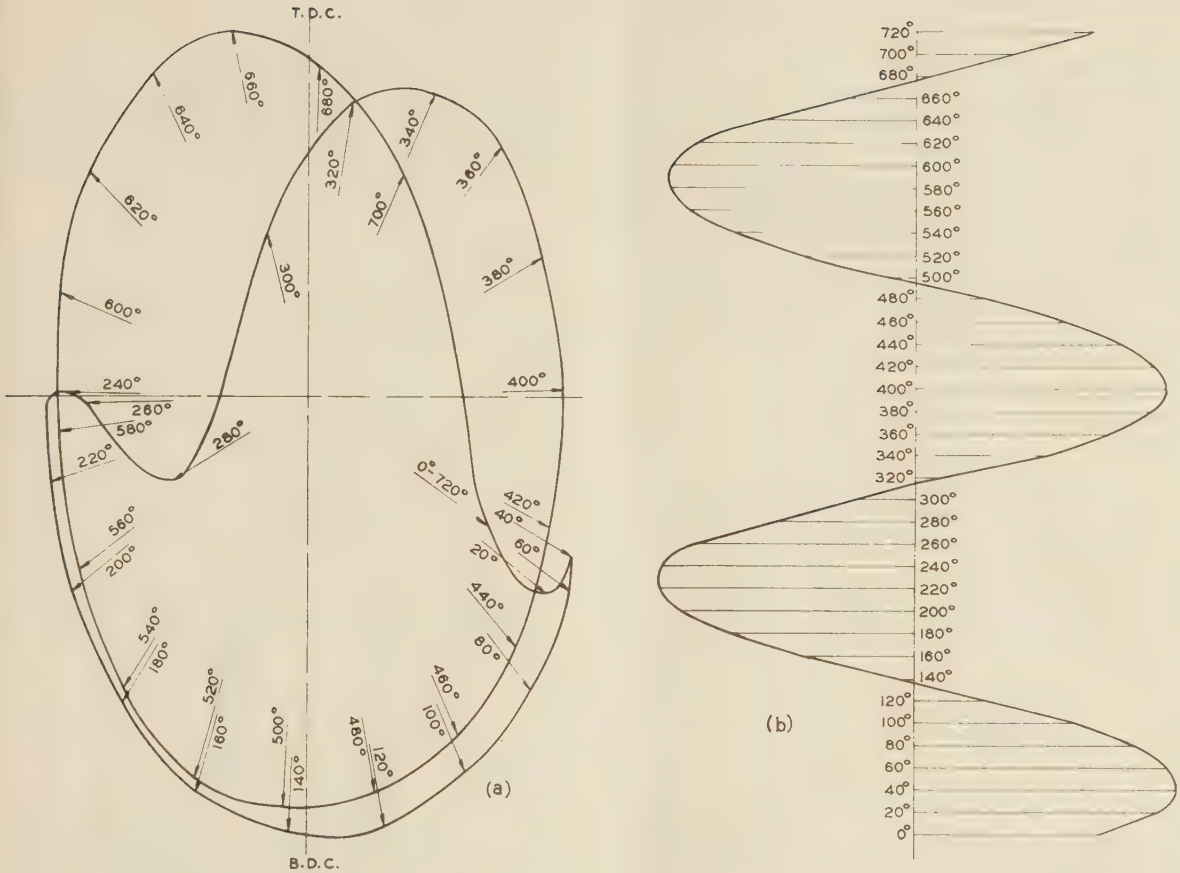

Fig. 4 Polar Diagram and Horizontal Components of Loads on Intermediate Main Bearings of an Eight-Cylinder Engine at 900 Rpm, Cranks at 90 Deg

(Scale: 1 in. = 8000 lb.)

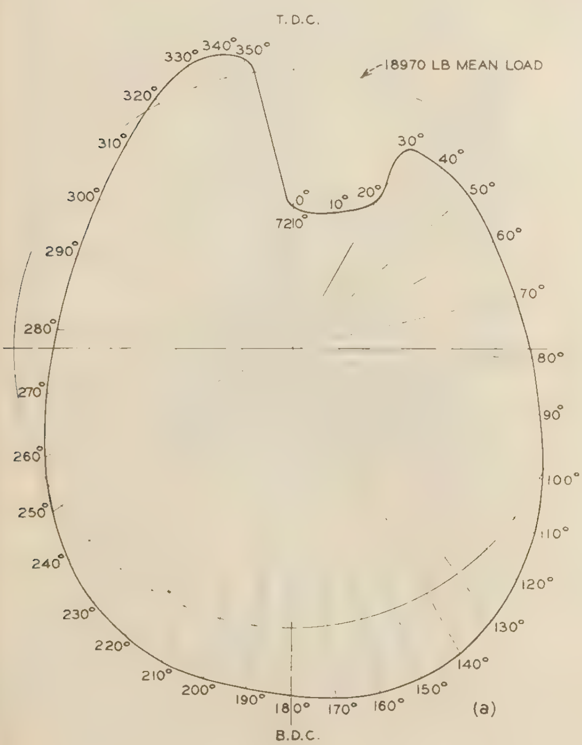

Fig. 5a

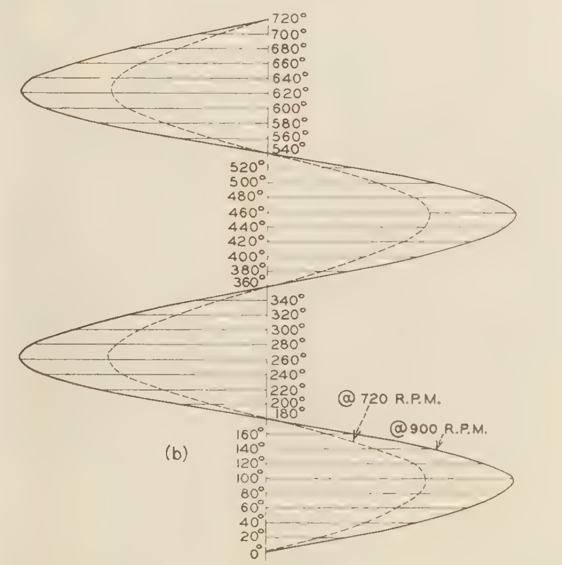

Fig. 5b

Fig. 5a left and 5b right: Polar Diagram and Horizontal Components of Loads on Intermediate Main Bearings of an Eight-Cylinder Engine at 900 Rpm, Cranks in Line

(Scale: 1 in. = 12,000, lb.)

insignificant effect of bearings Nos. 2, 4, 6, and 8 on horizontal frame loading. It will also be noted that the horizontal-component frequency at bearings Nos. 3 and 7 is engine speed. The condition at the center main bearing is similar, as indicated by Figs. 5*a* and 5*b*. The magnitudes of the loads and horizontal components are much greater due to the cranks at each side of the bearing being in line, centrifugal forces adding directly. Horizontal components again have a frequency of engine speed.

Loads on the end bearings are not shown because the mean load is even smaller than that of the intermediate bearing with cranks 180 deg apart. Furthermore, considering the horizontal frame deflections, it seems logical to fix the base at each end.

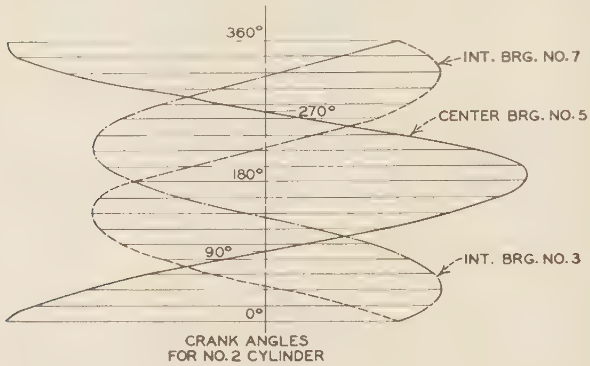

Fig. 6 Phase Angles of Horizontal Components of Bearing Loads

It is evident from inspection of the horizontal-component curves that only three bearings can have any major influence on horizontal vibration. These are the intermediate bearings Nos. 3 and 7, and the center bearing No. 5. In Fig. 6, the horizontal components for these three bearings are shown in their proper phase relation for the firing order 1–6–2–4–8–3–7–5 of Fig. 2. The frequencies are all engine speed, and at any instant during the cycle, there are forces at two bearings acting in one direction, while the force at the other bearing is opposite. If the frame structure is considered as a simple beam fixed at the ends, these fundamental loads will produce deflection curves which reverse. Such curves correspond to the elastic curves for the second and third mode of vibration. The natural frame frequencies for the second and third modes of vibration are higher than the natural frequency for the first mode of vibration. But for vibration of the first mode, which is the lowest natural frequency, it is necessary that the fundamental forces, or their harmonics, act in phase in the same direction. Each of the curves of Fig. 6 may be broken down by a Fourier analysis into a series of sine curves which, when added, give the original curves. This is the same procedure as used in determining the harmonic coefficients in torsional-vibration work. At no time are the fundamental forces of Fig. 6 all in phase, but the harmonics of some order may come into phase. The phase angles for the harmonics up to the eighth order are given in Table 1.

TABLE 1 PHASE ANGLES

Bearing No.	Loading angle, deg	Orders 1	2	3	4	5	6	7	8
3	0	0	0	0	0	0	0	0	0
5	135	135	270	45	180	315	90	225	0
7	270	270	180	90	0	270	270	90	0

All harmonics are not in phase until the eighth order. This is the first major critical for vibration of the first mode. In other words, the first critical speed occurs when the engine speed is one eighth the horizontal natural frequency of the frame structure. It is further possible, by methods similar to those used in torsional-vibration work, to evaluate the energy of bending due to the eighth-order harmonics. However, to determine the amplitude of horizontal vibration requires a knowledge of the horizontal natural frequency of the structure as well as the amount of damping present. Herein lies the rub.

Stiffness and Frequency of Structure

Analytical determination of the horizontal natural frequency of the frame structure must be based upon values for lateral stiffness and the mass taking part in vibratory movement. Because of the generally complicated construction, it appears impossible to arrive at a true method of establishing stiffness. Frame and base sections near the horizontal plane of the bearings contribute their full stiffness to the structure. However, the contribution of the A-frame legs, the upper crankcase, and lower base is problematical. Rigidity is further effected by the base support. An engine grouted into concrete certainly is more rigid than the same engine mounted on relatively light channels

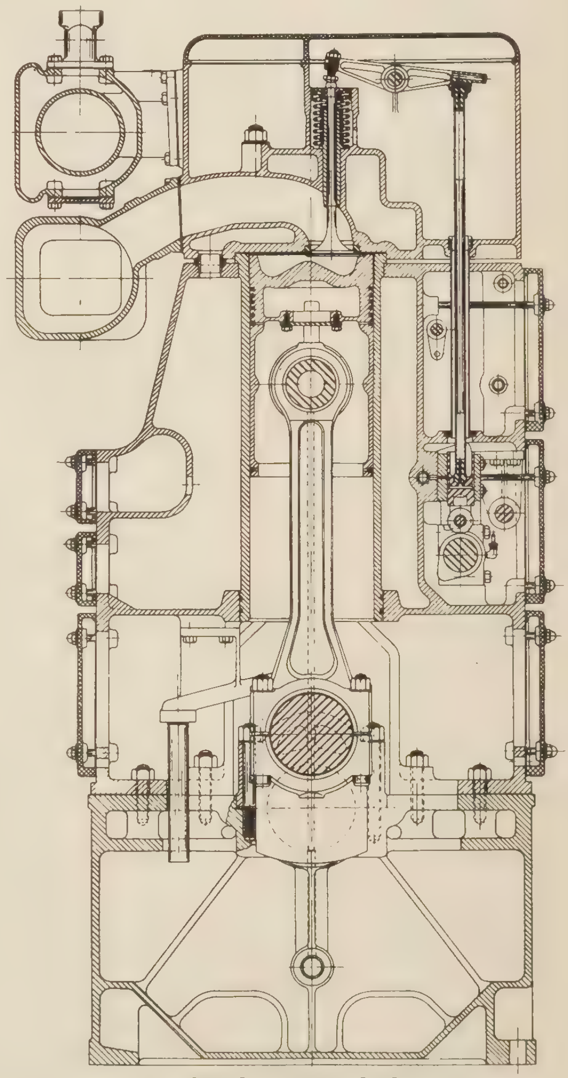

Fig. 7 Stationary Engine With Stiffening Webs at the Horizontal Plane of the Crankshaft

in a locomotive. Estimation of the effective engine mass vibrating horizontally is equally difficult. Horizontal-vibration amplitudes should be a maximum adjacent to the plane of load application, that is, at the horizontal center line of the crankshaft. Cylinder heads and the upper frame being elastically

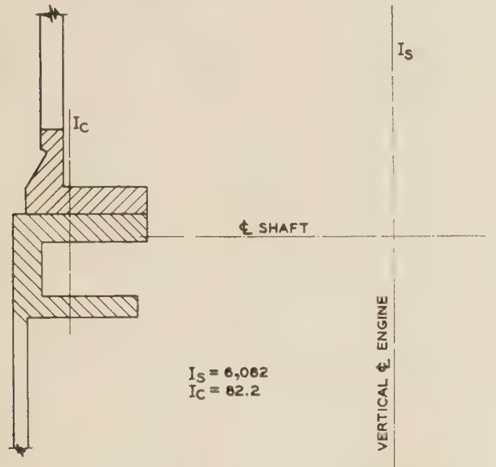

FIG. 8 FRAME SECTION OF A STATIONARY ENGINE

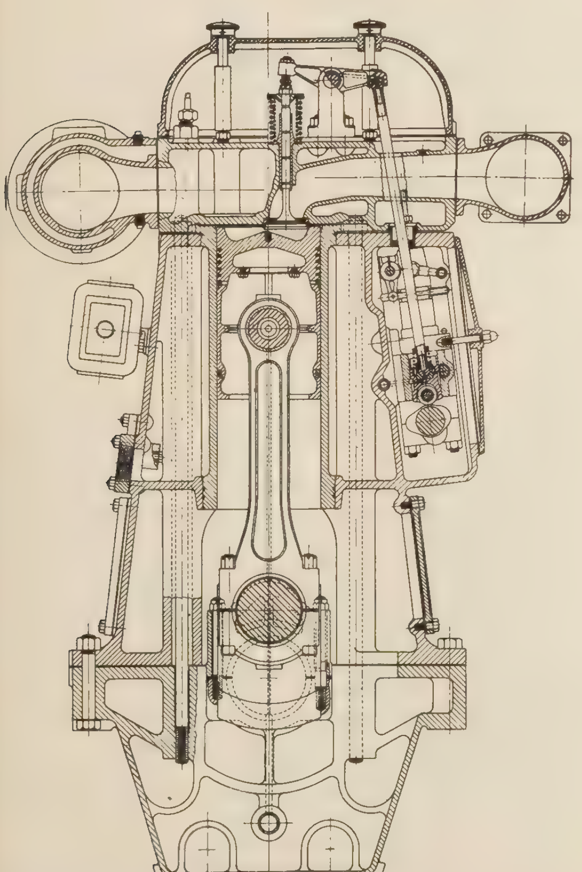

FIG. 9 MARINE-TYPE 8 × 10½-IN. ENGINE WITH HORIZONTAL STIFFENING WEBS

connected do not attain the amplitudes existing at the plane of the crankshaft.

Simplifications may be made by taking moments of inertia of those sections adjacent to the bearings and neglecting the stiffness contribution of the upper frame and bottom of the base. Fig. 7 is a section through a 10 × 12-in. 720-rpm engine, and Fig. 8 is an enlarged view of the sections in the horizontal plane of the crankshaft. If it is assumed that the sections at each side are rigidly connected through the vertical sections under the bearings, moments of inertia can be evaluated about the center line of the crankshaft. The structure can thus be reduced to a simple beam supported at the ends. The natural frequency of such a beam can be calculated when the weight of the beam is known. This is done in the following Appendix.

The limits for the effective weight of the beam are: (*a*) Minimum, when the weight is only that of the beam excluding all other engine weight; and (*b*) maximum, when the total engine weight is assumed distributed along the beam.

For condition (*a*), the calculated natural frequency horizontally is $F_n = 19{,}260$ cycles per min, and for (*b*) $F_n = 3750$ cycles per min. These limits are so far apart as to be of little use from a design standpoint. Actually, this engine at 720 rpm exhibits no sign of lateral vibration, which places its natural horizontal frequency as definitely above (8 × 720) 5760 cycles per min.

After an engine is built, its horizontal frequency can be determined experimentally by using a variable-speed motor-driven rotating weight mounted on the side of the base, at the same time taking vibrograph records. However, this is too late to be of any use in the design stage.

Briefly summarizing the theoretical aspects, the forces and their frequencies acting to produce horizontal vibration may be determined. The reaction characteristics of the frame structure to these forces are not readily predictable, within practical limits

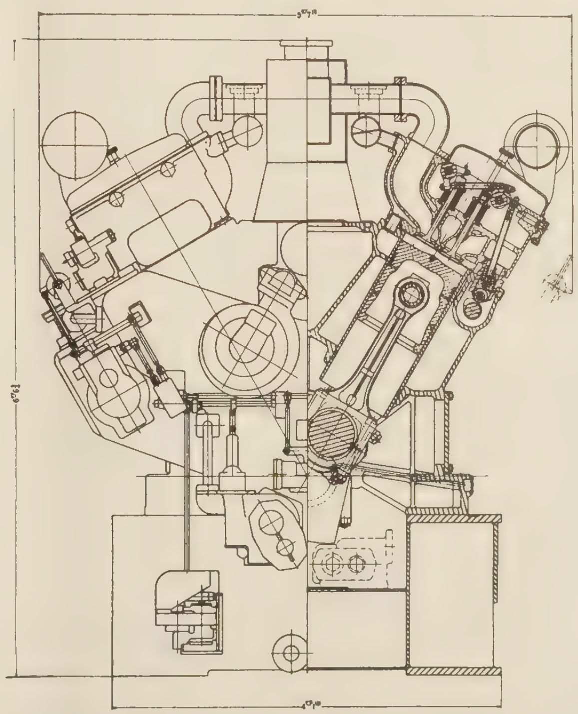

FIG. 10 LOCOMOTIVE-TYPE 9 × 12-IN. V-ENGINE WITH HORIZONTAL STIFFENING WEBS IN THE CAST-STEEL CRANKCASE, AND A WELDED BASE

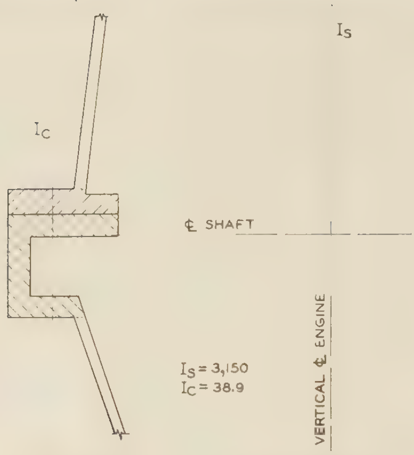

Fig. 11 Frame Section of the Marine-Type Engine Shown in Fig. 9

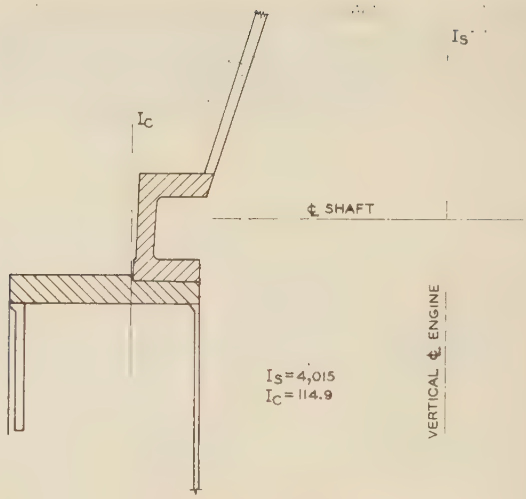

Fig. 13 Horizontal Stiffening Sections of a 9 × 12-In. Vertical Locomotive-Type Engine

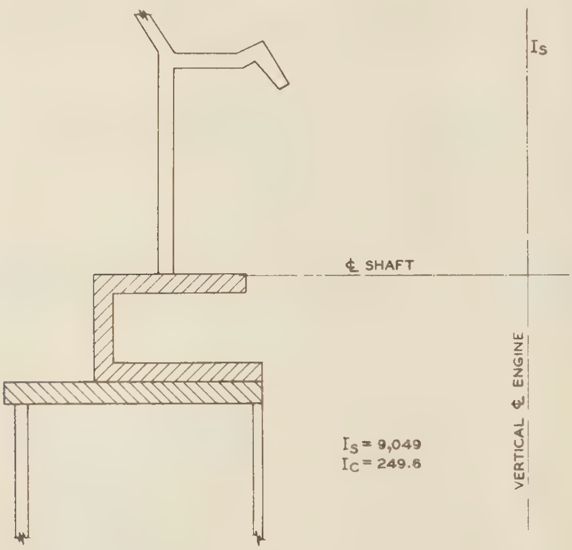

Fig. 12 Frame Section of the Locomotive-Type Engine Shown in Fig. 10

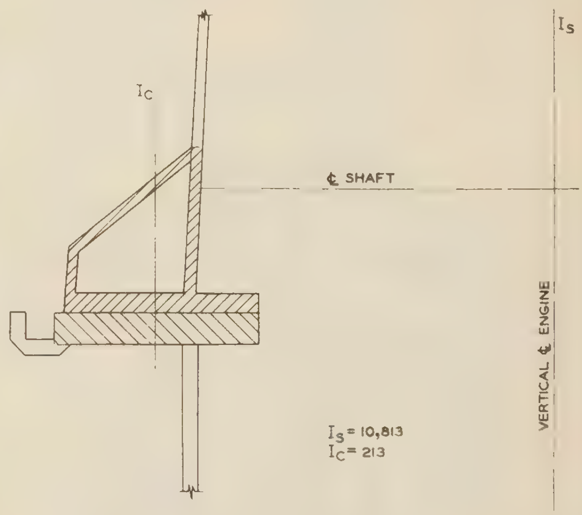

Fig. 14 Horizontal Stiffening Sections of a 12 × 12-In. Locomotive V-Type Engine

Simplified Design Check Method

The designer is thus forced to rely upon experience and practice, tempered with a little theory. For some time prior to this investigation, an empirical method has been used for checking lateral stiffness of engine structures. Because the method has in every case resulted in frames of adequate lateral rigidity, it is given here.

The frame is reduced to a simple beam supported at each end. Moments of inertia are taken about the center line of the crankshaft using those sections of the base and frame which run the full length of the engine, and lie in the region of the horizontal center line of the shaft. These sections provide the main horizontal stiffness near the region of load application. Cross sections of an $8 \times 10^1/_2$-in. engine and a 9×12-in. V-engine are shown in Figs. 9 and 10, respectively. The sections considered for horizontal stiffness are given in Figs. 11 and 12, respectively. Additional horizontal stiffening sections are shown in Fig. 13 for a 9×12-in. vertical engine, and in Fig. 14 for a 12×12-in. V-engine. Characteristics of these engines are given in Table 2.

It has been shown that the maximum horizontal load on the structure is due to the center main bearing. It is also true that the values of the harmonics will be proportional to the magnitude of the fundamental force at the center main bearing. For comparing engines of a similar crank arrangement, for instance sixes, or twelve-cylinder V-engines, simplification permits considering only the center-bearing horizontal load. On these premises, any deflection values calculated cannot be considered literally but only comparatively.

The loads at the center main bearings being known from the

TABLE 2 ENGINE CROSS SECTIONS

Figure No.	No. of cylinders	Speed, rpm	Bore and stroke, in.	Frame and base material
8	6	720	10 × 12	Both high-tensile cast iron
11	6	900	8 × 10$^1/_2$	Both high-tensile cast iron
12	12-V	900	9 × 12	Frame—cast steel Base—welded steel
13	6	900	9 × 12	Frame—cast steel Base—welded steel
14	12-V	800	12 × 12	Both steel casting

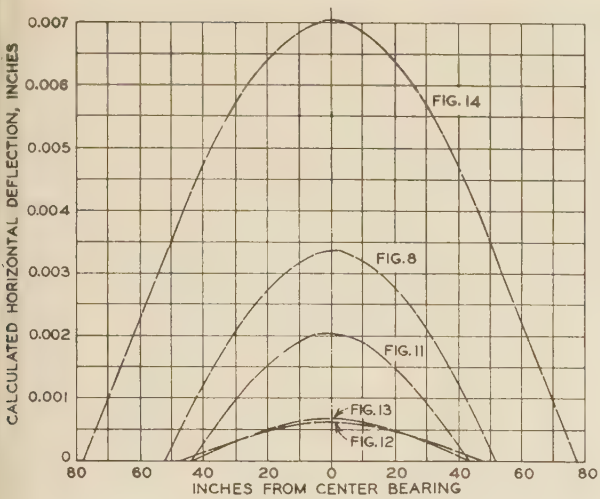

Fig. 15 Deflection Curves for Frame Sections Shown in Figs. 8, 11, 12, 13, and 14

bearing-load polar diagrams, and the moment of inertia of the simple structure evaluated, a deflection curve for the simple beam may be calculated from

$$f_{\max} = \frac{Pl^3}{48\,EI_s}$$

These deflection curves are shown in Fig. 15 for the various engine sections. All of these engines except Fig. 14 have operated over extended periods with entire absence of any lateral vibration difficulties. Frame failure did occur in Fig. 14 and was remedied by changes in the base to increase stiffness. From these very limited data, it can only be concluded that deflections as calculated of as much as 0.007 in. may be dangerous, and inversely, that deflections of 0.0035 in. or less are likely to result in satisfactory rigidity.

Appendix

The natural frequency of a bar with hinged ends is given by[3]

$$F_n = \frac{\pi n^2}{2l^2}\sqrt{\left(\frac{EIg}{As}\right)}\ldots\ldots\ldots\ldots\ldots\ldots[1]$$

where n = mode of vibration = first; l = length of bar = 105 in.; E = modulus of elasticity = 15,000,000; A = cross-section area = 26.63 sq in.; s = specific weight of bar material = 0.26 lb per cu in.; g = acceleration of gravity = 386 in. sec^2; and I = moment of inertia = 6082 in.^{4}

Considering only the weight of the bar, and substituting in Equation [1] gives

$$F_1 = 321 \text{ cycles per sec} = 19{,}260 \text{ cycles per min}$$

This is the high limit for natural frequency.

The lower limit of frequency obtains when the whole weight of the engine is considered as distributed along the length of the bar, in which case As in Equation [1] is replaced by engine-weight/engine-length, in this case 20,000/105 = 190 lb per in. of length. Substituting in Equation [1] gives

$$F_1 = 62.4 \text{ cycles per sec} = 3750 \text{ cycles per min}$$

This is the lower limit for natural frequency.

[3] "Vibration Problems in Engineering," by S. Timoshenko, D. Van Nostrand & Co., Inc., New York, N. Y., 1927, p. 229.

BIBLIOGRAPHY

"Engine Roughness—Its Cause and Cure," by P. M. Heldt, *S.A.E. Journal*, vol. 38, February, 1936, p. 47.
"Engine Block Design," by D. Gerdan, *Automotive Industries*, vol. 75, August 22, 1936, p. 242.
"Diesel Engine Design," by H. F. P. Purday, D. Van Nostrand & Co., Inc., New York, N. Y., 1937, Chapter 12.

Discussion

C. I. Burns.[4] The horizontal forces instigating frame deformations in vertical engines are applied at the running-gear reactions. At the cylinder or crosshead guide occur the side-thrust reactions, comprising the gas pressure and inertia-force horizontal components. At the crank main bearings the side-thrust reactions occur, combined with the centrifugal force of the rotating parts.

The side-thrust loads, which are of variable intensity, direction and point of application, impose cantilever-beam deflections and stresses on the conventional engine structure, resulting in transverse deformations at the cylinder heads, accompanied by tensile and compressive stresses normal to the bearing-load beam stresses discussed in the paper. Thus, the longitudinal crankcase members are subjected to two-dimensional stresses. In the vicinity of the stressed transverse members, the longitudinals are submitted to three-dimensional primary stresses which materially complicates an accurate analysis. Where the unit combined stresses run high, just below the endurance limit or the elastic limit of material, failure of the frame may be caused by abrupt discontinuity in cross section or by surface finish and high notch sensitivity of material. Fatigue frame failures are progressive and originate at points of high stress concentrations.

Rapid combustion subjects the engine structure to a shock loading which may be considerably in excess of the apparent static load and an approximate coefficient of impact may be obtained by considering the time rate of pressure rise of the main bearing load and side-thrust diagrams.

With a view toward the reduction of forced crankcase-vibration amplitudes, the importance of a prudent combination of bearing loadings is suggested by a consideration of a few characteristics. For completely counterbalanced opposed-crank throws, the polar bearing-load diagram for four-stroke engines would indicate that the predominant load both in intensity and rate of change is downward, due principally to the gas pressure; the horizontal loads, which are gradually applied, arise from secondary inertia forces. When in-line throws are employed, as in the case of center bearing of six-cylinder engines, the loads are of high intensity and the polar diagrams are nearly constant in form, due to the high centrifugal force. The intermediate-bearing polar diagrams invariably show the most erratic characteristics both as to form and intensity. Several rapid reversals in direction and of moderate intensity usually occur at intermediate bearings of six-cylinder engines. The end main bearings generally are the least in magnitude but have several directional variations. The deflection effects on the crankcase beam are dependent upon the relative positions of the crankpins, the cyclic relation of each, the engine speed, and the nature of the combustion process.

In both V- and W-type engines, polar main-bearing diagrams reveal markedly greater horizontal force components but this is compensated for by the inherently stiffer shape of the housings for accommodating the cylinder banks. In very large marine engines, frame stresses and deflections originating from rolling and impact, should be analyzed.

The manner of fitting the engine mounting, in addition to the relative stiffness of frame and foundation, has a pronounced ef-

[4] Assistant Engineer, New York Navy Yard, Brooklyn, N. Y.

fect on the degree of integrated rigidity between the engine structure and the seating upon which depends the resultant stresses, deformations, and natural frequency of vibration. For example, the maximum-deflection ratio of a beam fixed at both ends to a beam simply supported is 1 to 4 when a concentrated central static load is applied.

Some additional variables which contribute to the dilemma of a rational analysis are secondary stresses, rate of loading of each member, elastic and resilient moduli, degree of discontinuity of sections, variations in individual cylinder working-substance performance and variations of load and speed within the operating range of the engine.

P. M. Heldt.[5] The writer's experience has been confined to automotive engines, and what follows has reference to this type. In the development of these engines, as we passed from the single- and the two-cylinder to the four, the six, and the eight-in-line, each increase in length and accompanying increases in speed and combustion pressure made certain vibration problems more acute. Trouble arose from both torsional vibration of the crankshaft and transverse vibration of the engine block. Engines, in which this latter type of vibration is pronounced, are usually referred to as "rough." It took a long time to realize that a vertical engine will vibrate more readily in the horizontal than in the vertical direction, since both of the exciting forces, the gas pressure and the inertia, are vertical. It is the writer's belief that the discovery that the vibration of rough engines is predominantly horizontal was made only after vibration-recording instruments had been made available to the engine builders.

Six-cylinder engines were used in stock automobiles in this country as far back as 1905, and the eight-in-line was introduced in 1921. However, up to the late 1920's, most crankcases of six- and eight-cylinder automobile engines were mere shells, with a number of transverse bulkheads supporting the bearings. What little transverse horizontal rigidity these crankcases had was due mainly to the deck carrying the cylinders, and to the flange running around the lower edge. At first this flange was made only sufficiently wide to support the gasket, but in some of the later engines its width was practically doubled. So far as the writer's recollection goes, the first engine with a crankcase obviously designed to provide great transverse rigidity was a bus engine with an aluminum crankcase brought out by Waukesha in 1929. In this there was a substantial box section extending along the bottom of the crankcase on either side. In addition to transverse rigidity, great vertical rigidity also was aimed at, by making the crankcase of more than the usual depth and submerging the lower half of the cylinder block in it. With aluminum, of course, a greater stiffness of form is necessary, because the modulus of elasticity is less than that of cast iron. While the box section at the bottom of the crankcase sides has been adopted by a number of other designers, the use of channels, as shown in the author's Figs. 7 and 8, is now more common. In the automobile engine, these channels form part of the crankcase itself, rather than of the base. Also, the channel may be open either to the outside or the inside, and if the latter, the upper flange usually blends into the side of the crankcase with a large radius.

Owing to the complicated shape of the crankcase, it is, of course, impossible to make an accurate calculation of its transverse rigidity. The author's method of calculating it, by considering only the principal sections contributing to it, is interesting and should give satisfactory results, especially if a check can be made by applying the method to data from engines which proved successful and others which failed because of insufficient block stiffness.

[5] Engineering Editor, *Automotive Industries*, Philadelphia, Pa.

The Combustion-Gas Turbine

By J. T. Rettaliata,[1] Milwaukee, Wis.

The numerous obstacles in the path of the development of the modern combustion-gas turbine have been adequately surmounted. Years of metallurgical and aerodynamical research, resulting in better materials and an efficient compressor, are the factors which contributed most to the realization of a commercial gas turbine. Its advantages, when compared with other methods of power production, are manifold. Many new uses to which it can be profitably applied are anticipated when additional experience is obtained.

This paper deals with the development and theory of the gas turbine, as well as the features which make it possess attractive potentialities for certain classes of service.

At present the combustion type of gas turbine is receiving publicity both in this country and abroad. Such recent attention may cause it to be erroneously regarded as an invention of modern times, whereas, in reality, the first patents were taken out on one during the latter part of the eighteenth century. Even at that early date engineers appreciated the advantages of a prime mover having rotary motion and also being devoid of the complexities existing in a steam plant. With a background of so many years it is natural to inquire why the cycle has not found practical application before now.

In the early days the main difficulties with the gas turbine unit were the lack of available materials to withstand the high temperatures needed to produce good over-all thermal efficiencies, and a compressor of adequate efficiency so as to make the cycle feasible. Only in recent years have these two obstacles been overcome—today's better materials enable temperatures of 1000 F to be used; and an axial compressor, upon which years of aerodynamical research have been spent, affords the necessary high-efficiency compressor unit.

Strangely enough, the advent of the steam turbine both inhibited and aided the development of the gas turbine. Interest in the gas turbine waned in favor of the steam turbine, but it is primarily the progress in the development of materials for the latter that has been responsible for the realization of a commercial gas turbine. Its present stage of development and its future prospects were discussed recently by A. Meyer (1)[2] whose company, Brown-Boveri, has pioneered in the development of the gas turbine.

Gas-Turbine Axial-Compressor Unit

A modern gas-turbine axial-compressor unit is shown in Fig. 1. A five-stage reaction-type gas turbine A is directly coupled to B, a fifteen-stage axial compressor. Air from the atmosphere enters the compressor where its pressure is raised. Part of the air discharged from the compressor is used for combustion purposes in the oil burner C; the remaining air flowing through the annular space and cooling the products of combustion to a satisfactory turbine inlet temperature. The gas, a mixture of air and combustion products, then expands through the turbine from which it is exhausted to the atmosphere. The power developed by the turbine is greater than that required by the compressor and the excess power is supplied to the generator D. In order to start the unit from a standstill, a motor E is provided to bring the unit up to about 25 per cent of normal speed at which point the turbine is capable of driving the compressor.

The unit is controlled by a speed governor connected to the fuel-oil supply. In this way the inlet-gas temperature to the turbine is varied, thus changing the power developed by the turbine. An emergency governor actuates a by-pass valve around the turbine when a designated overspeed is exceeded. The turbine and compressor are connected through a solid coupling which enables their equal axial thrusts to neutralize each other, thus eliminating the necessity of balance pistons.

In Fig. 2 is shown a view of a partially assembled gas-turbine axial compressor with the top half of the casing removed. This unit is rated at 23,000 cfm of air at standard conditions. The turbine, at the left, is mounted on a common bedplate with the compressor at the right. Proceeding from left to right along the

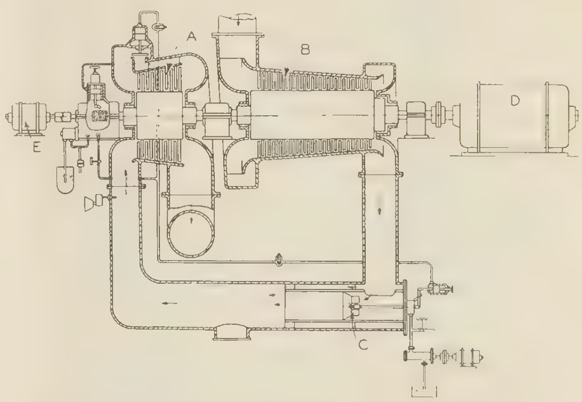

Fig. 1 The Gas-Turbine Power Unit
(A—gas turbine; B—axial compressor; C—oil burner; D—generator; E—starting motor.)

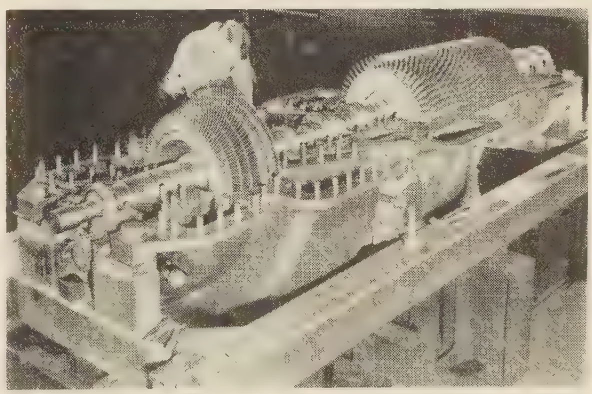

Fig. 2 Partially Assembled Gas-Turbine Axial-Compressor Unit

[1] Steam Turbine Department, Allis-Chalmers Manufacturing Company. Jun. A.S.M.E.

[2] Numbers in parentheses refer to the Bibliography at the end of the paper.

Presented at the National Meeting of the Oil and Gas Power Division, Asbury Park, N. J., June 19–22, 1940, of The American Society of Mechanical Engineers.

turbine shaft are located: The emergency governor and the exposed head of its stop bolt whose radial movement releases the trip mechanism of the by-pass valve upon the attainment of a predetermined overspeed; a turbine shaft bearing; a labyrinth sealing gland composed of radially projecting fins on the shaft which rotate with close clearances in narrow grooves in the casing; the turbine inlet opening; six rows of radial clearance reaction blading; the turbine exhaust opening; a labyrinth sealing gland (not visible); a shaft bearing; and one half of the solid coupling at the end of the turbine shaft.

Continuing in the same direction along the compressor shaft can be seen: The compressor half of the coupling which engages the half coupling on the end of the turbine shaft; a shaft bearing; a labyrinth sealing gland similar in construction to that previously described in the case of the turbine; the compressor intake; twenty-one rows of blading; the discharge opening; a labyrinth sealing gland (not visible); a shaft bearing; and coupling to which a reduction gear is connected.

Supplementing the turbine and compressor with a generator, combustion chamber, fuel controls, and a lubrication system completes the power plant.

The turbine cylinder is made of molybdenum cast steel and is split on the horizontal center line. Both inlet and outlet nozzles are located in a vertical plane; the inlet nozzle being cast in one piece with the upper cylinder half and the exhaust nozzle being

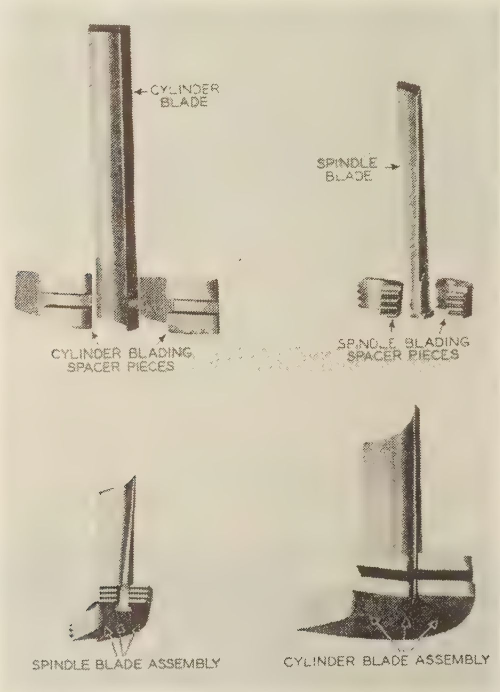

Fig. 3 Stainless-Steel Cylinder and Spindle Blading for the Gas Turbine

cast in one piece with the lower cylinder half. A by-pass connection is furnished joining the inlet and exhaust through a safety valve.

The casing is provided with a sufficient number of ribs and stay bolts designed to maintain its shape yet permitting it to expand freely.

The gas-turbine spindle is made of a solid chrome-nickel-steel forging. The bladed spindle can be seen in Fig. 2.

Cylinder and spindle blades are made of stainless steel. These blades, with spacer pieces, are shown in Fig. 3. The cylinder blades are made from a straight rolled section, whereas, the tapered spindle blades are milled from solid bar stock. The cylinder blades are held in place by the combined action of spacer pieces and the coincidence of a slot in the blade and a projecting ring in the groove. The spindle blades are securely fastened by the engaging of the upset end of the blade with serrated spacer pieces.

Labyrinth glands are provided where the spindle ends pass through the casing. Sealing air is taken from the compressor

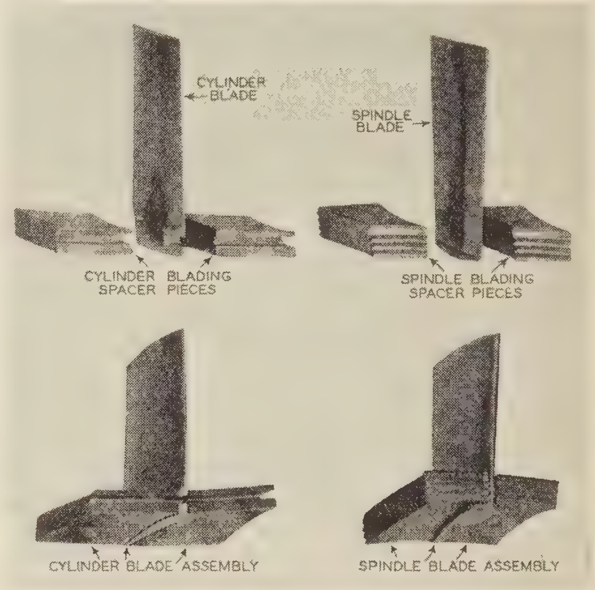

Fig. 4 Cylinder and Spindle Blading for the Axial Compressor

discharge and injected at a suitable point along the labyrinth in order to prevent gas from leaking to atmosphere. Separate valves are provided in the sealing lines to both glands.

The turbine spindle is carried by two special roller bearings. Lubricating oil is supplied to individual spray nozzles at a pressure of 25 to 30 psi, gage.

A solid coupling is provided to transmit the torque from the turbine to the compressor.

The compressor casing consists of a cast-iron cylinder, horizontally split, with inlet and outlet openings directed vertically upward and cast together with the upper half.

The compressor rotor is of forged steel consisting of two parts: a drum with one shaft end, and a shaft end having a hollow cylinder for the spindle proper. The hollow cylinder is shrunk onto the drum and locked. Labyrinth sealing glands are provided on the rotor ends where the shaft emerges from the casing. The bladed rotor can be seen in Fig. 2.

The cylinder and spindle blades, shown in Fig. 4, for the compressor are made of 5 per cent nickel steel. The types of root fastening are similar to those described for the gas turbine. The cylinder blades are milled and cam ground to varying sections that increase in area in a radial direction toward the center of rotation. Such contours are required by aerodynamic theory in order to give a high-efficiency axial compressor.

The Gas Cycle

The combustion-gas turbine operates on the Brayton cycle consisting of two isentropic and two isobaric lines.

The theoretical cycle on the pressure-volume plane is shown in Fig. 5. The isentropic compression in the compressor is represented by AB. The isobaric addition of heat in the combustion chamber is shown by BC. Line CD depicts the isentropic expansion in the turbine. The assumption of a closed cycle requires

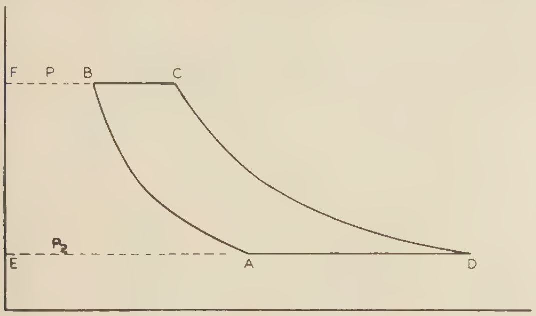

Fig. 5 The Theoretical Cycle on a Pressure-Volume Plane for the Combustion-Gas Turbine

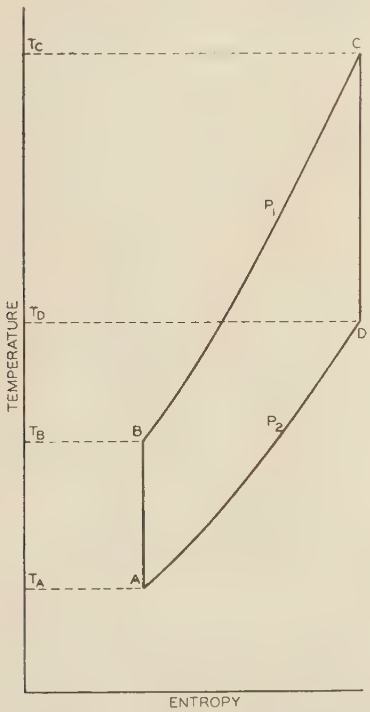

Fig. 6 The Theoretical Cycle on a Temperature-Entropy Plane for the Combustion-Gas Turbine

that the exhaust gas be cooled along the constant-pressure line DA. The energy theoretically required to compress one pound of air in the compressor is represented by the area $EFBA$. The energy liberated by one pound of gas expanding in the turbine is shown by the area $EFCD$. Consequently, the difference between these two areas, $ABCD$, would represent the theoretical excess energy available for power purposes.

In a steady-flow reversible process the compressive and expansive energies per pound are equivalent to area

$$EFBA = \int_{P_2}^{P_1} V_{AB}\,dP \qquad [1]$$

and area

$$EFCD = \int_{P_2}^{P_1} V_{CD}\,dP \qquad [2]$$

respectively; therefore, the excess energy may be expressed as area

$$ABCD = \int_{P_2}^{P_1} V_{CD}\,dP - \int_{P_2}^{P_1} V_{AB}\,dP \qquad [3]$$

Using perfect gas relationships, Equation [3], upon integration and substitution of limits, becomes, in units of Btu per pound

$$\Delta h_{ABCD} = \frac{144}{778}\,\frac{k}{k-1}\,P_1\,(V_C - V_B)\left[1-\left(\frac{P_2}{P_1}\right)^{\frac{k-1}{k}}\right] \qquad [4]$$

where k = isentropic exponent of fluid in cycle; P_1 = pressure at compressor discharge and turbine inlet, psi, abs; P_2 = pressure at compressor intake and turbine exhaust, psi, abs; V_C and V_B = specific volumes, at turbine inlet and compressor discharge, respectively, cu ft per lb.

The theoretical cycle on the temperature-entropy plane is shown in Fig. 6. The nomenclature is similar to that used in Fig. 5. The excess energy, in Btu per pound, will be

$$\Delta h_{ABCD} = c_p\,[(T_C - T_D) - (T_B - T_A)] \qquad [5]$$

where c_p = specific heat of fluid at constant pressure; and T_A, T_B, T_C, T_D = temperatures, in degrees Fahrenheit abs, at compressor intake and discharge, and turbine inlet and exhaust, respectively.

Referring to Equation [5], the excess energy in Btu per pound is equivalent to the product of the specific heat at constant pressure and the difference, expressed in degrees Fahrenheit, between the lengths of the lines AB and CD in Fig. 6. Thus the net useful output of the cycle is a function of the divergence of the constant-pressure lines on the temperature-entropy plane.

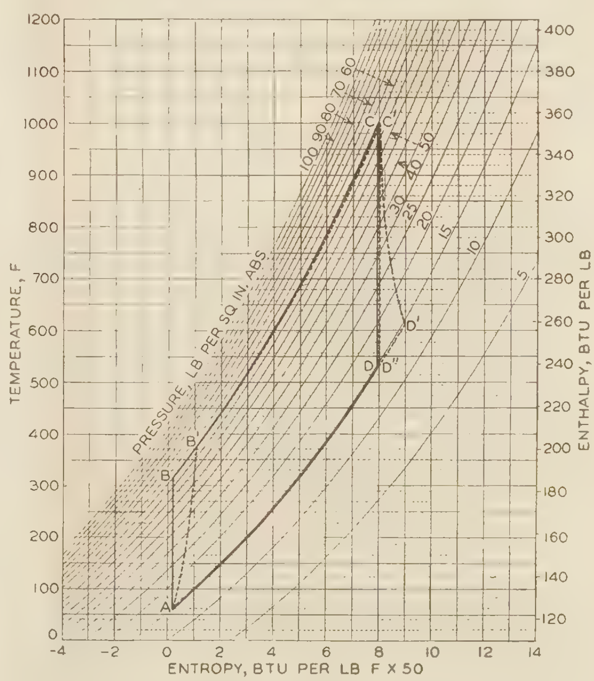

Fig. 7 Combined Temperature-Entropy Enthalpy-Entropy Diagram Showing Theoretical and Actual Cycles

It must be remembered that the previous discussion on the

gas cycle, in the interest of simplicity, has involved only theoretical considerations. In actual operation other factors which reduce materially the output energy must be taken into account when ascertaining the real excess power obtainable.

For example, the efficiencies of the turbine and compressor must be considered, and also the drop in pressure between the compressor and turbine. The isentropic exponent k must be the ratio of the mean value of the variable specific heats for the temperature ranges involved. There must be a further, although slight, correction made for the larger quantity of gas flowing through the turbine due to the fuel added for raising the temperature of the air. The true excess energy then will involve these modifications and will be less than that given by Equations [4] and [5].

A theoretical and actual gas-turbine cycle are shown in Fig. 7 on a combined temperature-entropy and enthalpy-entropy diagram for air, based on the Partington and Shilling (2) equations for variable molar specific heat.

The incorporation of the enthalpy scale at the right facilitates the use of the diagram by eliminating the operation, shown in Equation [5], of multiplying the specific heat at constant pressure by the absolute temperature; the product being enthalpy. For convenience, the temperature scale reads directly in degrees Fahrenheit.

For purposes of simplification, the composition of the gas in the turbine is taken as the same as the air in the compressor. This is essentially correct for a power cycle as the amount of fuel added to raise the temperature of the air is less than 1 per cent of the quantity of air flowing through the compressor.

The theoretical cycle is shown by $ABCD$ in Fig. 7, whereas $AB'C'D'$ represents the actual cycle after losses have been taken into account.

Assuming the fuel required to be 1 per cent of the quantity of air compressed, the effect of losses will result in an actual excess energy equivalent to

$$\left[\frac{1.01\ \Delta h_{C'D'} - \Delta h_{AB'}}{1.01\ \Delta h_{CD} - \Delta h_{AB}}\right] \times 100 \qquad [6]$$

per cent of the theoretical. In the actual cycle depicted in Fig. 7, 63 per cent of the theoretical excess energy is not realized, thus demonstrating the importance of a highly efficient turbine and compressor and also the necessity of maintaining small pressure drops in the combustion chamber.

In the example just discussed, the composition of the gas in the turbine was assumed to be identical with that of the air in the compressor. Some cases arise, however, wherein the turbine receives gas of an entirely different composition, such as products from a chemical process. In these instances the energy per pound of expanding fluid cannot be obtained from Fig. 7 but must be determined from the thermodynamic properties of the particular gas in question.

Axial-Compressor Characteristics

As mentioned previously, the governing of a power unit is accomplished by controlling the quantity of fuel supplied to the combustion chamber and thus varying the temperature of the gas entering the turbine. Other factors remaining constant, the absolute pressure at the turbine inlet would vary approximately as the square root of the absolute inlet temperature.

The characteristics (3) of the axial-flow compressor are such that when operating at constant speed the volume of air at the intake varies only slightly with discharge pressure, as shown in Fig. 8. An examination of the curve will reveal that as the discharge pressure falls a small increase in suction volume results.

When the power required by the compressor is exactly balanced by the power delivered by the turbine, that is, when the excess power is zero, the temperature at the turbine inlet will be about 650 F. Consequently, using the relationship between pressure and temperature stated previously, and correcting for the slight increase in gas quantity at reduced pressure, the absolute inlet pressure under this new condition will be approximately 10 per cent less than the design value.

Therefore, the entire operating range of the unit, from no load to full load, is confined to that portion of the curve, Fig. 8, included between the normal point and point A. Thus, regardless of the electrical load, the unit operates very nearly at design values of pressure and gas flow.

Although a reaction turbine and an axial compressor bear a physical resemblance to one another, the design problems associated with each are quite different. For instance, in the case of a fluid expanding in a turbine, the reheating effect, caused by friction in the blade passages, results in an over-all internal efficiency better than the stage efficiency, whereas, in a compressor the reheat due to friction has a negative effect, and consequently depreciates the over-all efficiency to a value less than the individual-stage efficiency.

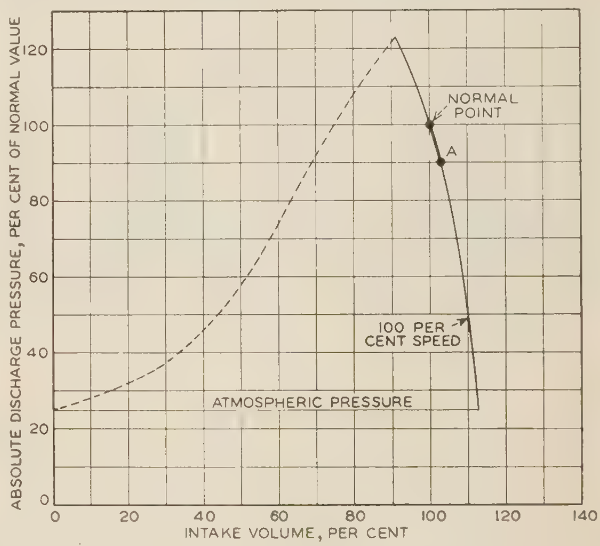

Fig. 8 Axial-Compressor Characteristics

The axial type of compressor has a limited stable operating range at any given speed. At full speed stable operation will only exist down to about 90 per cent volume, beyond which point the compressor will commence "pumping." This phenomenon occurs at reduced volumes because then the small axial velocity component causes the air to enter the blades at an extremely glancing angle, which results in loss of contact on the backs of the blades and subsequent unstable conditions. The axial compressor may be operated stably at reduced volumes, however, by decreasing the speed. In Fig. 8 the region of unstable operation is represented by the area to the left of the broken line.

In contrast with the type of operation exhibited by the axial compressor is that of the centrifugal compressor with its stable range extending to approximately 50 per cent volume or lower at full speed. However, owing to its lower efficiency the centrifugal compressor, unless it were elaborately water-cooled, could not replace the axial type for the application under consideration. Furthermore, due to the fact that temperature and not quantity control is used on these units and, as previously discussed, the operating range is limited to a relatively small portion of the

pressure-volume curve, the axial type of compressor is well adapted to this class of service.

Thermal Efficiency

For any given turbine-inlet temperature there is one compressor pressure ratio for which the thermal efficiency of the unit will be a maximum, as shown in Fig. 9.

The sensitivity of the cycle to temperature is effectively displayed by a doubling of thermal efficiency when the temperature is increased from 600 to 800 F.

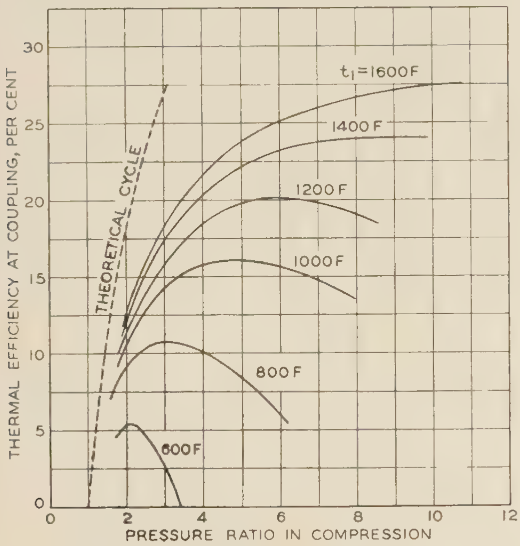

Fig. 9 Thermal Efficiency as a Function of Pressure Ratio for Various Turbine Inlet Temperatures—Nonregenerative Cycle

(t_1 = turbine inlet temperature.)

Another reason for the gas turbine remaining in the background during its long development period may be had from the lower temperature curves in Fig. 9. The poor thermal efficiencies shown by these curves must be decreased still further when the lower efficiencies of the earlier turbines and compressors are taken into account. Small wonder then if the developers of the early gas turbines made slow progress when such limited temperatures were imposed by inferior materials.

The highest normal operating temperature of any of the gas-turbine units built to date has been 1000 F. The higher-temperature curves are exhibited to demonstrate the possibilities of projected development. Research on blading materials, however, indicates that increased temperatures may be considered as practical in the not too distant future.

Reference to Fig. 7 will reveal that the turbine exhaust gas is discharged at 612 F into the atmosphere. Such degradation of energy naturally hinders economical operation. One of the various methods by which the thermal efficiency of the gas cycle may be improved is by the use of a heat exchanger. In this manner the exhaust gas from the turbine may be utilized in raising the temperature of the air discharged from the compressor.

The introduction of a heat exchanger must be undertaken with caution, however, as an excessive pressure drop through it may easily nullify any increase in efficiency that could otherwise be realized. Nevertheless, when properly designed, improved performance is readily attainable.

By the addition of a heat exchanger (4) having a size of about 11 sq ft per excess horsepower, the thermal efficiency of a unit operating with a turbine admission temperature of 1000 F may be increased approximately 50 per cent.

Thermal efficiency as a function of pressure ratio for various efficiencies of turbine and compressor is shown in Fig. 10. The importance of high turbine and compressor efficiencies is strikingly brought out, for increasing these efficiencies from 0.75 to 0.90, a 20 per cent change, results in a 400 per cent increase in maximum thermal efficiency obtainable.

The curves are all based on a turbine inlet temperature of 1000 F. Their trend will naturally be upward when future materials warrant safe operation at higher temperatures.

It will be noticed that the peaks of the various curves occur at different values of pressure ratio, thus signifying the dependence of maximum thermal efficiency upon the correct association of pressure ratio with combined efficiency of turbine and compressor.

Here again is emphasized the need of a highly efficient turbine and compressor. Only because the modern gas-turbine axial-compressor unit possesses this necessary high efficiency is the cycle commercially practicable today.

The effect on thermal efficiency of a drop in pressure from the compressor discharge to the turbine inlet for various turbine efficiencies is shown in Fig. 11. No regenerator is included in the

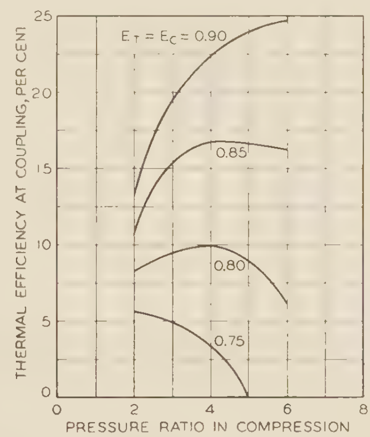

Fig. 10 Thermal Efficiency as a Function of Pressure Ratio for Various Efficiencies of Turbine and Compressor—Nonregenerative Cycle

(E_T = turbine efficiency, and E_C = compressor efficiency.)

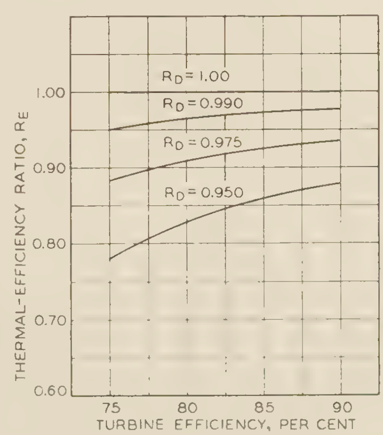

Fig. 11 Effect of Pressure Drop on Thermal Efficiency—Nonregenerative Cycle

[R_D = (turbine inlet pressure)/(compressor discharge pressure); R_E = (thermal efficiency with pressure drop)/(thermal efficiency without pressure drop).]

cycle and the turbine inlet temperature is assumed to be 1000 F.

The pressure drop is expressed as a ratio of turbine inlet pressure to compressor discharge pressure. Similarly, the effect of this pressure drop is signified by the ordinate scale showing the ratio of the thermal efficiency obtainable with a pressure drop to that which would exist in a cycle without a drop in pressure.

The curves indicate the effect of pressure drop on thermal efficiency to be more pronounced at lower turbine efficiencies. Furthermore, the slopes of the curves increase with increasing pressure drops.

Selecting values from the curves shows that a 5 per cent drop in pressure with a turbine efficiency of 80 per cent causes a 17 per cent decrease in thermal efficiency.

Fig. 11 quite effectively demonstrates the importance of a design free from any serious restrictions to flow. A study of the curves will show how the use of a heat exchanger with a prohibitive pressure drop would have a deleterious effect on the thermal efficiency possible of attainment with a properly designed regenerator.

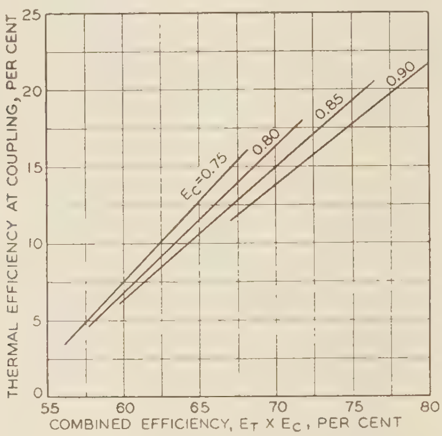

FIG. 12 THERMAL EFFICIENCY AS A FUNCTION OF COMBINED EFFICIENCY FOR VARIOUS COMPRESSOR EFFICIENCIES—NONREGENERATIVE CYCLE

(E_T = turbine efficiency; E_C = compressor efficiency.)

In certain chemical processes gas-turbine axial-compressor units are used for supercharging. High-temperature gas returned from the process is furnished the turbine for the development of power. In some of these instances the pressure drop in the process is high enough to reduce to zero the excess power which would otherwise be obtainable with a moderate drop in pressure. Such inefficiency is only tolerated, however, in these special cases where the primary concern is the delivery of air and not the production of power.

Thermal efficiency as a function of the combined efficiency of the turbine and compressor for various compressor efficiencies is shown in Fig. 12. The curves are computed on basis of a pressure ratio of four and a turbine admission temperature of 1000 F.

One important feature to recognize is that lower compressor efficiencies yield higher thermal efficiencies for any given combined efficiency. This results from the turbine handling larger quantities of energy than the compressor. Therefore, if the level of combined efficiency is fixed it is more advantageous to favor the turbine than the compressor. For instance, an assumed combined efficiency of 64 per cent could be obtained by turbine and compressor efficiencies of 80 per cent each, but higher thermal efficiency would result from an arrangement having the same combined efficiency yet consisting of turbine and compressor efficiencies of 82 and 78 per cent, respectively.

An examination of Fig. 12 will reveal why the axial type of compressor was selected to operate in conjunction with the gas turbine instead of the centrifugal type. In general, in the range of pressures and volumes in which gas-turbine units operate, the highest adiabatic efficiency likely to be obtained with a multi-stage centrifugal compressor is about 75 per cent, whereas, for the axial compressor it is approximately 83 per cent or slightly higher. Using these figures and assuming a turbine efficiency of 85 per cent, combined efficiencies of 63.8 and 70.5 per cent can be obtained with multi-stage centrifugal and axial compressors, respectively. Therefore, the maximum thermal efficiency that could normally be realized when using a centrifugal compressor in the cycle would be about 12.5 per cent, as compared with a value of 16 per cent, an increase of 28 per cent, obtainable with an axial compressor.

Thus, the early inventor endeavoring to achieve success when employing the centrifugal compressor was doubly penalized: first, by the natural limitations of a cycle operating under temperatures not sufficiently high; and, second, by the inherent inefficiency of the compressor itself. His colleague using the axial compressor fared but slightly better, for he labored under the same temperature restrictions and his type of compressor did not reach its present efficient state until comparatively recently.

Excess Power

The excess power of a unit as a function of compressor efficiency for various turbine efficiencies is shown in Fig. 13. The curves are based on a cycle with no regenerator and a turbine admission temperature of 1000 F.

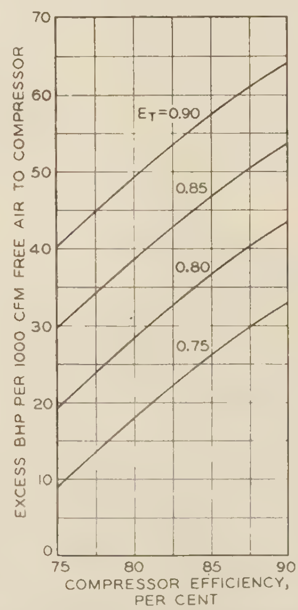

FIG. 13 EXCESS POWER AS A FUNCTION OF COMPRESSOR AND TURBINE EFFICIENCIES

(E_T = turbine efficiency.)

A manifestation of the importance of high turbine and compressor efficiencies is presented by the curves. A 20 per cent increase in a turbine efficiency of 75 per cent entails a 300 per cent increase in excess power with a compressor efficiency of 75 per cent.

At a given turbine efficiency the excess power increases approximately linearly with compressor efficiency.

By reason of its molecular weight and isentropic exponent

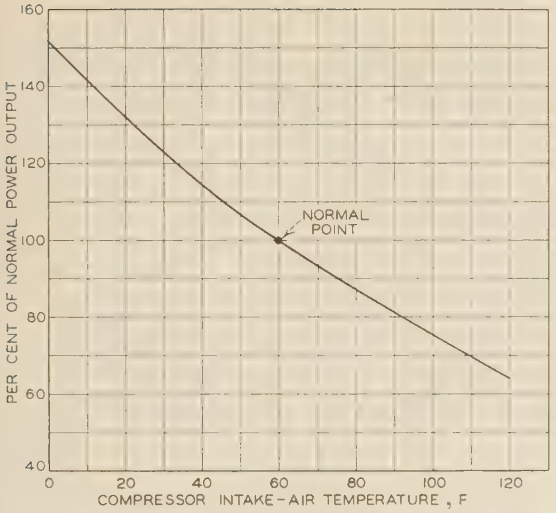

Fig. 14 Effect of Intake-Air Temperature on Excess Power

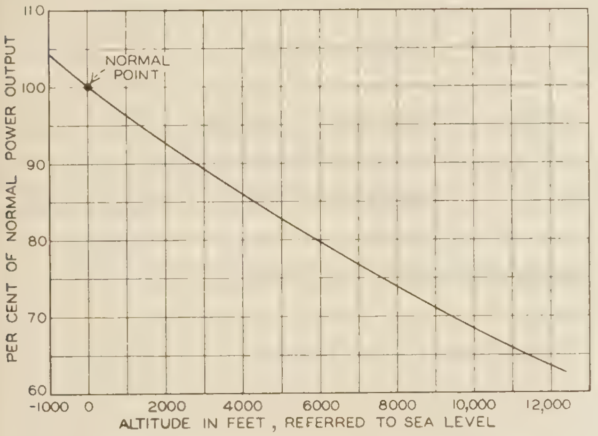

Fig. 15 Effect of Altitude on Excess Power

(when in superheated vapor state) being less than that of air, water injected into the combustion chamber will increase the excess power developed by a given size of gas-turbine axial-compressor unit. Such a procedure, while augmenting the output of the unit, is nevertheless an inefficient practice owing to the latent-heat-of-vaporization loss at the turbine exhaust. If indulged in extensively the concomitant reduction in over-all thermal efficiency may prove prohibitive.

The effect of intake-air temperature on the power delivered by a unit is shown in Fig. 14. As may be seen from the curve, an increase in temperature decreases materially the output of a given unit. On the other hand, a unit designed for normal operation with an intake-air temperature of 60 F will develop approximately 50 per cent more than rated power when the air temperature is reduced to 0 F.

The output of a unit as affected by altitude is illustrated by the curve in Fig. 15. Upon examination it can be seen that high altitudes have an adverse effect on the power obtainable.

If the unfavorable effect of temperature and altitude is of a temporary nature, as may be the case, for instance, in locomotive or marine applications, it may be remedied by water injection. As mentioned before, however, such practice should be resorted to only when absolutely necessary because of the ensuing decreased economy of operation at such periods.

Applications

At the present time the principal commercial application of the gas-turbine axial-compressor unit in the United States has been in oil refineries. Air discharged from the compressor is used in a process and the resulting high-temperature gases are expanded in the turbine, producing power, the excess of which is supplied to a generator. In this arrangement, no combustion chamber is required as the process itself acts in this capacity.

Many gas-turbine axial-compressor units operate as superchargers in the Velox boiler, developed by Brown-Boveri, where the boiler-exhaust gases drive the turbine.

A 4000-kw unit has been installed in an emergency stand-by power station in the city of Neuchâtel, Switzerland. Its simplicity and independence of water facilities ideally adapt the gas turbine to this class of service. Recently published tests, conducted by Stodola (5) indicate a coupling thermal efficiency, based on lower heating value of fuel, of 18.04 per cent for this unit when operating on a nonregenerative cycle with a turbine inlet temperature of 1000 F. This is the first unit built for the primary purpose of producing power.

A 2200-hp gas-turbine locomotive, with electrical transmission, is being built by Brown-Boveri for Swiss Federal Railways.

In this country Allis-Chalmers, licensees of Brown-Boveri, is engaged in an engineering study (6) of the possibilities of the gas-turbine as a drive for locomotives of larger output. Both electrical and mechanical transmissions are being studied as well as the merits of the hydraulic coupling. One mechanical-drive locomotive is rated at 5000 hp at the power turbines. At an efficiency of 90 per cent this corresponds to 4500 hp at the axle.

The over-all length is approximately 87 ft, the height over the cab is 15 ft, and the width 10 ft 4 in. The total operating weight is about 500,000 lb, or 112 lb per hp at the axle.

There are two driving axles on each truck, the drivers being 52 in. diameter and the total weight on them 280,000 lb. The wheel base is 78 ft, which permits turning on an 80-ft turntable, so the cab and transmissions are designed for one-way operation.

The power plant has been divided into two units of 2500 hp each, being lighter and better adapted to uniformly distribute the weight along the frame than a single 5000-hp unit, and also permitting a lower and better arrangement of the various elements, especially the transmissions.

The use of separate power turbines improves the performance as the compressor and its driving turbine can operate independently at the best speed for the conditions regardless of the speed of the locomotive and the power turbine.

The speed and power of the locomotive are controlled by a combination of manual and governor control of the fuel burned in the combustion chamber and by throttling the power turbine.

Numerous other natural and favorable applications of the gas-turbine axial-compressor unit will develop from time to time and probably include marine propulsion, blast-furnace plants, wind tunnels, special power plants, and other special applications.

BIBLIOGRAPHY

1 "The Combustion-Gas Turbine," by A. Meyer, *Mechanical Engineering*, vol. 61, September, 1939, pp. 645–652.

2 "The Specific Heat of Gases," by J. R. Partington and W. G. Shilling, D. Van Nostrand Co., Inc. New York, N. Y., 1924.

3 "Axial Compressors," by J. Avery, Allis-Chalmers *Power Review*, August, 1939.

4 "The Combustion-Gas Turbine: Its History, Development, and Prospects," by A. Meyer, Proceedings of The Institution of Mechanical Engineers, May, 1939.

5 "Load Tests of a Combustion Turbine," by A. Stodola, *Power*, vol. 84, February, 1940, p. 74.

6 "An Engineering Study of the Combustion Turbine Locomotive," by J. L. Ray, Allis-Chalmers Bulletin No. B-6066, Allis-Chalmers Mfg. Co., Milwaukee, Wis., September 6, 1939.

Discussion

W. R. New.[3] The 6 or more years of impending hostilities in Europe, prior to September 3, 1939, revived interest in power cycles other than the steam cycle in which pressures had already been increased to the critical value with initial temperatures of almost 1000 F. The threatened necessity for operation of large power plants in bombproof shelters without access to sufficient water; inadequate supply of petroleum derivatives, particularly internal-combustion-engine fuels; and adherence to even more rigid national economies provided them with real incentives for this work.

In this country, without these incentives, suggestions to consider other power cycles as an alternative to the conventional steam plant have proceeded almost invariably from some very restricted viewpoint. The author's paper seems to fall within this category.

The simplest arithmetical calculations of the exhaust-annulus dimensions of gas turbines, dicharging to the atmosphere, compared, for example, with those discharging at an elevated-pressure level, convinced the writer long ago that only a closed system need be considered for anything but small plants or small propulsion equipment where refinements could be sacrificed in the interest of great simplicity.

The apparent necessity of excluding nonadiabatic operations from the turbine and continuous-flow compressor, coupled with the simplicity and adequacy of constant-pressure processes for heat exchange, immediately suggests the Joule or Brayton cycle, shown idealized in the author's *P-V* and *T-S* diagrams in Figs. 5 and 6, as the simplest choice. With the irreversibilities inherent in heat addition from the source and rejection to the environment through the entire ranges of temperature *B-C* and *D-A*, respectively, this cycle can command little attention from those interested in primary-power generation where plant thermal efficiencies of almost 32 per cent have already been reached with initial temperatures somewhat less than 1000 F. With the attainment of high thermal efficiency of the entire cycle as a major objective, thermal regeneration between the gas streams is not to be introduced as of secondary importance. In effect, regeneration modifies the entire structure of the analysis, and is, for example, much more important than seeking the ultimate in efficiency of turbine and compressor.

In the interest of brevity, detailed criticism of what the author has presented can be omitted in favor of directing attention to the inadequately emphasized limitations of a thermal power plant, functioning on the simple Joule cycle, with atmospheric pressure as the lower limit. The objection may, of course, be raised that such an enlargement of the point of view falls without the scope of the present treatment. On the other hand, at this time, when many members of the profession, less acquainted with the development of thermal cycles in general, and the steam-and-gas turbine in particular, may be inclined to consider the author's contribution as a general treatment of a new type of thermal prime mover, it seems appropriate to point out some of the scales with which to measure the stature of such information.

Lybrand Smith.[4] Reliability is the great essential for marine machinery, in which the writer is primarily interested. Common sense would indicate that a rotating machine, with the only rubbing parts being the two bearings, would be more reliable than a reciprocating machine with its inherent great multiplicity of rubbing and tapping parts. So far as marine practice is concerned, all data which the writer has ever been able to gather confirms common sense. Marine-turbine machinery is more reliable than reciprocating machinery, whether the latter be steam or internal combustion. As a matter of fact there is very little trouble with marine turbines in themselves. There is much more trouble with their necessary adjuncts, such as condensers and boilers. Since the gas turbine would eliminate condensers and boilers, it would eliminate such troubles at the same time.

Gas turbines as power generators are too new in the field to have developed actual data for operating reliability. However, inquiries about gas turbines used by oil companies indicate an extraordinary reliability.

Fuel economy is very important. The data given by the author indicate that we could not expect an immediate fuel economy as good as that of Diesel engines or as of the very best steam plants. However, there are very few central power stations with a thermal efficiency in excess of 30 per cent, and practically no marine-steam installations with a thermal efficiency in excess of 25 per cent. All of these very efficient steam installations use heat traps, such as preheaters, economizers, and feedwater heaters to the utmost. Considering figures given in the paper, it does not appear that any gas turbine we could build immediately would have a fuel economy as good as our best steam plants, but it looks as though we might start by equaling mediocre steam plants and have an excellent possibility of surpassing the best in the not very distant future.

The matter of weight is very important for a marine installation. Since little attention has yet been given to making a gas turbine as light as possible, reliable data are not available on how such weights will compare with the weights of other marine installations. It would appear probable, however, that the weight of a gas-turbine installation would be comparable to that of a steam-turbine installation. Until actual plans are made in detail for a ship installation, such an estimate can be little more than a hunch.

Air supply and combustion-gas exhaust will be a special problem for marine work. With boilers, or with internal-combustion engines, we only need enough air to burn fuel. With the existing gas turbines, it is proposed to use 5 or 6 times as much air as is required for combustion, in order to keep the blades cool. This means that an enormously greater amount of intake air, and an enormously greater amount of exhaust products must pass through the deck of the ship than is the case in any existing ships. Provision for such supply and exhaust will require considerable changes in the ship's structure, particularly if we are not to suck in half the ocean when a wave breaks aboard.

Speed control is very important in marine work. It is desirable to be able to control the propeller from full speed ahead to full speed astern by stepless gradations. The present gas turbine does not lend itself to such results without the use of very heavy and complicated electrical transmission. If the speed of a turbine is varied by controlling inlet-gas temperature, as suggested by the author, we might expect violent changes in efficiency, as would be indicated by the various curves in the author's Fig. 9. These changes in efficiency would not be so important in a unit generally operated near full power, but would be intolerable in a unit which operated at low power a considerable amount of time. The problem of speed control must be given great study in connection with any marine application.

It appears that the combustion-gas turbine offers great prospects of being developed into a reliable, economical, and lightweight unit for high powers, such as are used in marine propulsion. It appears to be good enough now for some applications. It will improve with every advance in metallurgy enabling higher temperatures to be used; with advances in applied mechanics, enabling blades to be cooled; with advances in design, enabling

[3] Research Engineer, Westinghouse Electric & Manufacturing Company, South Philadelphia, Pa.

[4] Captain, U. S. Navy, Head of Research Branch, Bureau of Ships, Navy Department, Washington, D. C.

heat traps to recover more waste heat. It is believed that there is a wide field of usefulness for gas turbines in the future. It is hoped that all manufacturers whose work in any way would be involved in gas turbines or their auxiliaries will devote considerable attention to them, and will make practical developments, whenever possible.

Author's Closure

In view of the present national-defense program, it is difficult to agree with Mr. New that we in this country lack the incentive to consider bombproof power plants. When and if the time should come for the construction of such plants, the gas turbine would manifestly receive favorable attention as being ideally suited for this application, especially in remote localities where this type of plant is likely to be situated.

Obviously unfounded is Mr. New's intimation that the author is propounding the gas turbine as a universal substitute for the conventional steam plant. On the contrary, the limitations of the gas turbine are well recognized and, for this reason, it was deemed advisable to state the special applications for which it is particularly adaptable. In the opinion of the author, a review of these applications, given in the latter part of the paper, will reveal that they are not excessively inclusive, thereby invalidating Mr. New's relegation of the paper to the restricted-viewpoint category.

The closed system, mentioned by Mr. New, has certain advantages but their attainment is only at the expense of that desideratum of all power-generation equipment, namely, simplicity. The absence of water for any purpose whatsoever is one of the attractive features associated with the combustion turbine described in the paper. Practical operation of the closed system, however, demands a source of water to cool the gas entering the compressor. The principal advantage of this system lies in the use of increased densities with a concomitant reduction in dimensions. Since both systems operate on the same basic cycle, their thermal efficiencies should be essentially equal under similar temperature conditions. The only published information on the closed system which has come to the author's attention has been of a descriptive nature and he awaits with interest test results on such a plant.

The gas turbine, discussed in the paper, enjoys a distinctive advantage in that it might well be considered independent of geographical location as its sphere of application; air is universally available and no special sites near water-supply systems are necessary. This makes it especially fitted for certain classes of service, among which may be included locomotive applications and also installations in remote localities having natural gas or oil available but where the water problem is acute.

Mr. New is evidently of the opinion that the merits of the regenerative cycle were insufficiently stressed in the paper and consequently consigned to a position of secondary importance. The author is aware of the value of regeneration as a means of increasing cycle thermal efficiency and the magnitude of a representative increase is given in the paper as a function of heat-exchanger surface. In the interest of avoiding repetition the author purposely refrained from making extended references to regeneration as it had been previously covered in papers by Marks and Danilov (7),[5] Meyer (4), Jendrassik (8), Tucker (9), Rettaliata (10), and others.

The author takes exception to Mr. New's statement regarding the alleged inadequate emphasis placed upon the limitations of the gas turbine described in the paper. It is not believed any unreasonable claims were made for either performance or field of application. In fact, based upon Stodola's (5) tests, the thermal efficiencies given in Fig. 9 of the paper are actually on the conservative side.

Mr. New's attempt to caution the less informed members of the profession regarding the antiquity of the combustion turbine appears to be of questionable necessity when it is stated in the very first paragraph of the paper that patents were taken out on this type of unit as early as the eighteenth century.

The author is grateful for the constructive and authoritative comments of Captain Smith regarding the marine application of the combustion-gas turbine.

It is appreciated that reliability is of primary importance in all types of vessels and this is especially true of combatant ships. Based upon the remarkable record of trouble-free service, established by the oil-refinery units, as mentioned by Captain Smith, there appears to be good reason to believe the gas turbine is capable of fulfilling the requirement of reliability.

The thermal efficiency of the basic cycle, operating with a turbine admission temperature of 1000 F, will be less than that obtainable with a modern steam plant. However, with the adoption of regeneration, reheat, and elevated temperatures, it is possible for the thermal efficiency of the gas-turbine plant to equal or even surpass that of today's best central stations. Although the present limit in operating temperature is 1000 F, there are indications that it may soon be possible to go to increased temperatures by resorting to special materials and a primary turbine stage of the impulse type so as to confine the highest temperatures to a stationary-nozzle element.

A preliminary investigation of a marine application of the gas turbine operating at 1000 F discloses that the weight will exceed that of a modern ship with steam-turbine-propulsion equipment. The use of higher temperatures, however, will result in a reduction of the weight of the gas-turbine drive below that of the steam installation for a stipulated capacity.

Captain Smith raises an interesting point by calling attention to the intake and exhaust problem associated with a marine application of the gas turbine. Undoubtedly the large volumes of air involved will necessitate modifications in existing ship design. The utilization of advanced temperatures will minimize the intensity of this problem to a certain extent, however, by reducing the quantity of air required in the cycle for a given output.

The type of gas-turbine-propulsion equipment which would be used for marine applications would consist of a double-turbine arrangement. One turbine, driving the compressor, would deliver just sufficient power to effect compression. The other turbine, connected to the propeller shaft, would receive the excess gas not being used by the compressor turbine. By this method, efficiencies at reduced powers could be improved over those obtainable with the single-turbine system, because the compressor and its driving turbine could operate at their optimum speed, independent of the power turbine. Consequently, the double-turbine arrangement would have a flatter efficiency versus load characteristic.

The author shares Captain Smith's opinion regarding the future prospects of the combustion-gas turbine. Improved materials, enabling higher temperatures to be employed, should offer the necessary stimulus for the further advancement of this type of prime mover especially in its natural fields of application.

[5] Numbers (7) to (10) refer to the Bibliography at the end of this closure; other references are to the Bibliography at the end of the paper.

BIBLIOGRAPHY

7 "Gas Turbines," by L. S. Marks and M. Danilov, Trans. A.S.M.E., vol. 46, 1924, pp. 1095–1128.

8 "The Jendrassik Combustion Turbine," by G. Jendrassik, *Engineering*, vol. 147, 1939, pp. 186–188.

9 "Now Gas Turbines That Work," by S. A. Tucker, *Power*, vol. 83, pp. 316–319.

10 "Why Combustion-Gas Turbines?" by J. T. Rettaliata, *Power*, vol. 83, 1939, pp. 732–734.

Relative "Engine Efficiencies" Realizable From Large Modern Steam-Turbine-Generator Units

By G. B. Warren[1] and P. H. Knowlton,[2] Schenectady, N. Y.

This paper analyzes the results of tests on more than 100 turbines under station operating conditions. The progress in turbine efficiency made over the last 20 years is shown and the analysis of the test results is carried out in such a way as to permit working out a system for predicting relative turbine performance. This method is given in detail and will permit the prediction of relative turbine performance for large condensing and noncondensing machines over a wide range of conditions.

There has been a need in the power industry for publication of the probable relative performance of large steam turbines from the steam-consumption and heat-consumption standpoints. The value of such data will be that potential purchasers and their engineers will be able to make a more complete study of many alternative power-station designs, and so arrive at a final decision as to the conditions for building a new project on the basis of a sounder analysis. Further, it is believed that the power industry will benefit generally by a release of these data.

There are many reasons why this has not been done in the past, the most important being that until the last few years sufficient basic test data had not been accumulated on actual turbine performance in the field, and a sufficiently complete correlation of the data had not been made. Recent tests of numerous turbines have helped this situation markedly and, more recently, intensive analytical work on the part of one of the authors and his associates has permitted a systematization of these results which was not possible before. Consequently, we are now able to present test data and an analysis of these data which will show the probable relative "engine efficiency" of modern condensing and noncondensing turbines over a wide range of pressures, temperatures, exhaust pressures, capacities, and loads ranging from 10,000 kw to 100,000 kw and which covers 3600-rpm turbines and 1800-rpm single-cylinder turbines.

The data so presented also give a good picture of the progress which has been made in turbine efficiencies over the last 20 years.

Figs. 1 and 2 show relative "turbine internal efficiency" for the larger-size condensing turbines (1800 and 3600 rpm, respectively).

These data are based upon actual test-engine efficiencies, obtained on turbines in the owners' plants, with test instruments and procedure as accurate as possible, and with turbines in good condition and clean.

The points are divided into 3 groups as regards dates, viz., group 1, 1919–1926, group 2, 1926–1933, and group 3, 1933–1940. In general the reasons for this segregation are that the first group represents low-pressure low-temperature turbines designed prior to 1925; the second group represents turbines designed during the first period of the trend toward higher pressures and temperatures, larger units, multiple valving for good efficiency over wide load ranges, etc.; and the third group represents modern turbines continuing the trend to high pressures and temperatures, designed since 1932.

There are no large 3600-rpm turbines in group 1. One small 3600-rpm machine has been shown in this group.

In all, there are records of about 70 turbines tested in the group 1 period. These machines commonly had a single "best point," and one point only for each turbine has been plotted.

Groups 2 and 3 are multiple-valved and, for each of these turbines, several points are plotted defining the load range over which the machines have been valved.

The values of "over-all engine efficiency" as obtained from the tests were corrected for calculated generator losses (or test values where available), calculated bearing and mechanical losses, and calculated leaving and exhaust-hood losses, as described later in this paper, so that the resulting relative efficiency values then represent those for turbines having zero bearing and mechanical losses, zero generator losses, and zero leaving and exhaust-hood losses. This resulting value is called "turbine internal efficiency." This is, of course, to eliminate these variable losses from the comparison. Hence, the internal turbine losses and inefficiencies are all included, as are the entrance valve losses and external packing losses.

The values as obtained are also corrected for superheat to a common value of 300 F, and for the effect of initial pressure upon moisture losses and reheat factor.

In Fig. 1, a so-called "1925 mean curve" is drawn. This curve was drawn to represent a certain equation, and was intended to represent the most reliable test values available at the time. In view of the general increase in the average, the "1940 mean curve" was drawn representing the authors' interpretations of the mean value of the efficiencies of the modern 1800-rpm turbine. This latter curve does not follow any definite equation because it is intended to be used only within the range of test data, and it is drawn so as to take into account the varying character of the turbines designed for small- and large volume flows.

Fig. 3 shows an interesting crossplot of the deviation of the tests from the "1925 mean curve" plotted against the date the test was made. It gives an idea of the increase in turbine internal efficiency alone (independent of the heat cycle) over the last 20 years which has resulted from the research work and refinements in design during this period. A rough calculation indicates that this has been worth up to the present time from 5 to 10 times its cost to the industry. Gains in addition to those shown have been made by better valving, thus further reducing the losses on the more recent turbines on either side of the "most economical load," by reduced bearing losses and by more efficient generators.

In 1925, when the first mean curve was developed, a theoretical relationship was worked out between the 1800- and 3600-rpm turbine efficiencies on the basis of the assumption that the ef-

[1] Designing Engineer, Turbine Engineering Department, General Electric Company. Mem. A.S.M.E.

[2] Steam Research and Development, Turbine Engineering Department, General Electric Company. Mem. A.S.M.E.

Contributed by the Power Division, and presented at the Semi-Annual Meeting, Milwaukee, Wis., June 17–20, 1940, of The American Society of Mechanical Engineers.

Note: Statements and opinions advanced in papers are to be understood as individual expressions of their authors and not those of the Society.

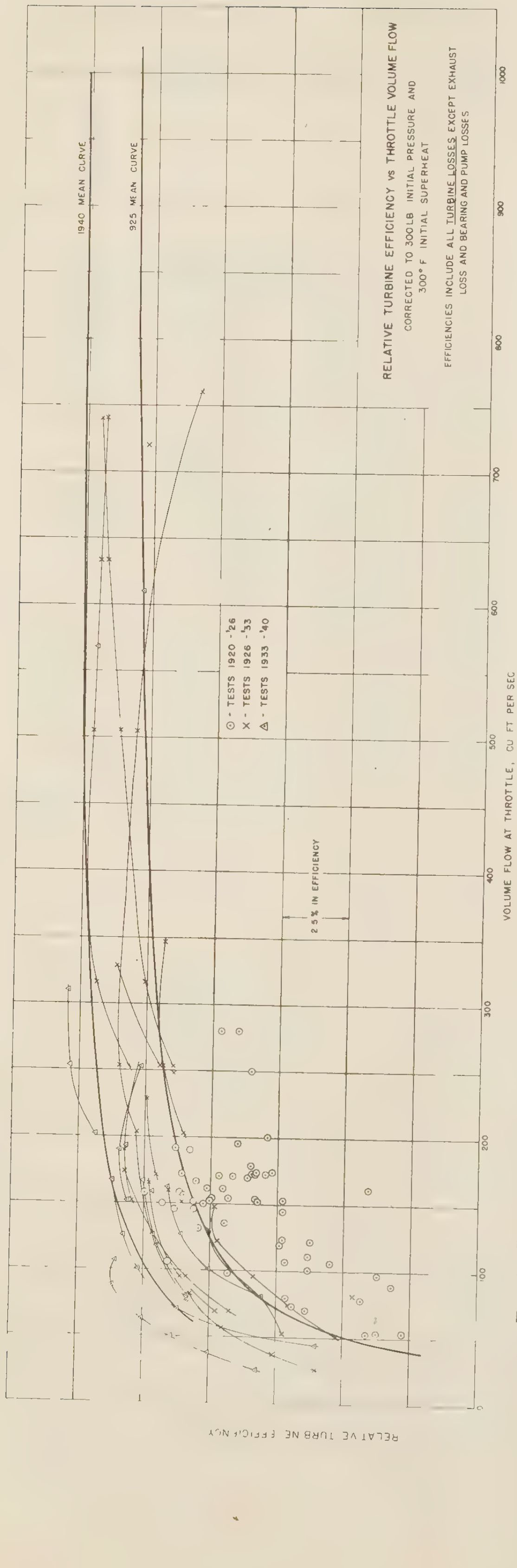

Fig. 1 Comparative Efficiencies of Large General Electric 1800-Rpm Condensing Turbines From Tests Made in the Last 20 Years
(Actual test efficiencies have been credited with generator losses, mechanical losses, and exhaust losses; corrected to 300 F initial superheat.)

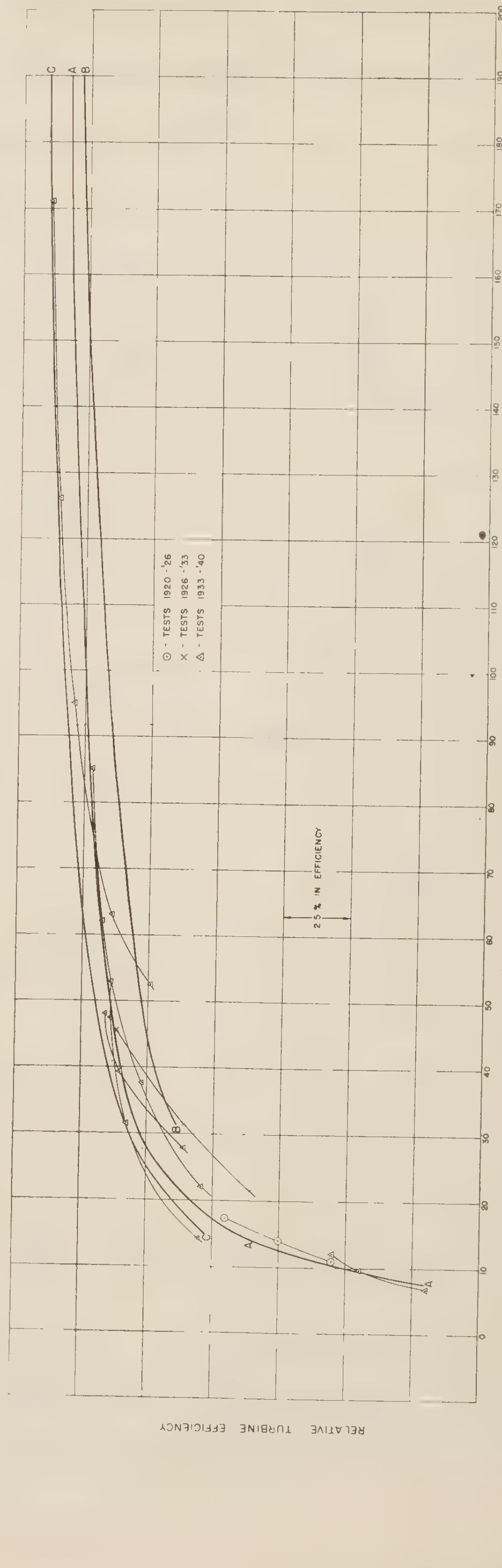

Fig. 2 Comparative Efficiencies of Large General Electric 3600-Rpm Condensing Turbines From Tests Made in the Last 20 Years
(Actual test efficiencies have been credited with generator losses, mechanical losses, and exhaust losses; corrected to 300 F initial superheat.)

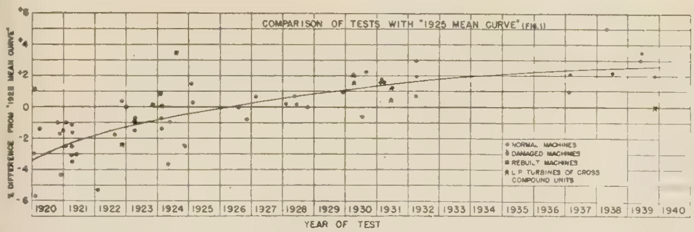

FIG. 3 RELATIVE IMPROVEMENT IN EFFICIENCIES OF LARGE GENERAL ELECTRIC TURBINES IN THE LAST 20 YEARS

(Derived from Fig. 1; 1800 rpm.)

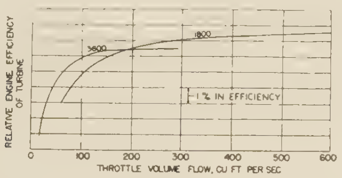

FIG. 4 COMPARISON OF 3600-RPM AND 1800-RPM "1940 MEAN CURVES"

(From Figs. 1 and 2: Vertical scale divisions 1 per cent apart.)

ficiency of geometrically similar turbines at different speeds would be the same and, hence, the capacity of turbines of the same efficiency would vary inversely as the (rpm)^2.

A curve so derived from the "1925 mean curve" in Fig. 1 for 1800-rpm turbines is shown as *A-A* in Fig. 2, for 3600-rpm machines. Knowing, however, that the higher-speed machines would, for various reasons, not come quite up to these values, at that time a "more probable 3600-rpm mean curve" *B-B* was drawn. The various test values show that we have now come higher than this later value, and curve *C-C* has been drawn representing a "1940 3600-rpm mean curve." This again is drawn so as to take into account the changing character of the machines at the various volume flows.

Fig. 4 shows a comparison of the "1940 mean curves" for 1800-rpm and 3600-rpm condensing turbines. Also, some of these 3600-rpm turbines are known not to have been completely clean internally when tested. It is believed that the 3600-rpm turbines on which tests are now available do not represent the state of development represented by the 1800-rpm machines. This is naturally so, since the large 3600-rpm machines are a relatively new development, and certain extra losses are now believed to be related to this higher rotative speed. Continued development may help this situation and result, we believe, in a greater gain in the next few years in 3600-rpm turbine efficiency than in that of 1800-rpm machines. Even so, the 3600-rpm machines show a substantial gain in the lower-volume flows where most of the modern higher-pressure turbines operate.

As can be seen, somewhat higher efficiencies have been obtained (recently) on two 1800-rpm machines; one at low- and the other at medium volume flows. It is not yet certain whether or not these can be duplicated on future turbines and, hence the "mean curve" has not been raised to these values.

The "mean internal-efficiency curves," thus described and shown in Fig. 4, are used as the basis of the following curves, supplemented with calculations to give partial load and overload results, which in turn have been scrupulously compared with test results under these conditions to see that they represent the average of such test results, although this comparison is too lengthy to be presented here.

"ENGINE EFFICIENCIES" AS A MEASURE OF TURBINE PERFORMANCE

Therefore, the turbine engine efficiencies, derived in accordance with the following method, represent, in the authors' opinion, the best reasonably simple exposition of the performance of such turbines as are manufactured by General Electric, in sizes of 10,000 kw and larger, for central-station plants. The design of such turbines has never been exactly standardized, and one has only to look at Figs. 1 and 2 to see that the present system of data correlation does not succeed in bringing all test results into agreement. This need not detract too much from the usefulness of the method, which has been devised to include various factors which directly influence turbine-generator efficiency, aside from what might be called the "internal design."

The results are intended to apply for turbines of conventional-design requirements, and it is expected will have some margin as compared with the probable test results when in good condition.

Condensing and noncondensing turbines are covered in separate sections.

1—CONDENSING TURBINES

Fig. 5 shows the "over-all engine-efficiency ratios," as defined by the turbine test code[3] for condensing turbines from 10,000-kw rating. This over-all engine-efficiency ratio is simply another name for the well-known "Rankine-cycle efficiency ratio," and is equal to the over-all output from the generator terminals divided by the available power input to the turbine.

These curves are so drawn as to show the over-all engine efficiency at rated load, when the set is equipped with an 0.8-power-factor hydrogen-cooled generator, and when the rating and size of the exhaust are such as to give an "exhaust loss" of 4 per cent, and when the superheat is 300 F, and the initial pressure and turbine speed are as shown on the separate curves.

The curves in Fig. 5 are derived from Fig. 4, and from calculations as to the effect of initial pressure on the turbine internal losses, at constant initial superheat. The curves give as accurate a representation as can be achieved by such a simple plot and, together with the superheat-correction curve, Fig. 6, should be useful in presenting a general picture of over-all turbine-generator efficiency for various ratings and steam conditions.

The actual efficiencies of individual turbines as manufactured by General Electric will differ from these curve values at rated load for various reasons; viz., actual exhaust loss different from 4 per cent, different arrangement of controlling valves, and slightly different generator losses or mechanical losses. Also, of course, the efficiency will change at fractional loads or overloads as compared to the rated-load efficiency. Therefore, for more accurate prediction of the performance of a turbine for any given rating and steam conditions, as well as calculation of efficiency at loads other than rated load, corrections for these factors are described in the following paragraphs and figures.

To obtain the over-all efficiency of any given machine under nonextraction conditions, and at all loads, it becomes necessary to apply the following corrections to the values obtained from Fig. 5, preferably in the following order:

1 Superheat correction (Fig. 6), already mentioned in preceding paragraphs.

2 Correction to turbine internal efficiency for fractional and overload conditions, Fig. 7.

3 Correction for generator efficiency change at other than rated load, Fig. 8.

4 Correction for mechanical losses. Actual mechanical losses for specific designs are given in Fig. 9.

[3] "Test Code for Steam Turbines," originally adopted and published in 1928, by THE AMERICAN SOCIETY OF MECHANICAL ENGINEERS, and now competely revised, will be available in pamphlet form from the Society in March, 1941.

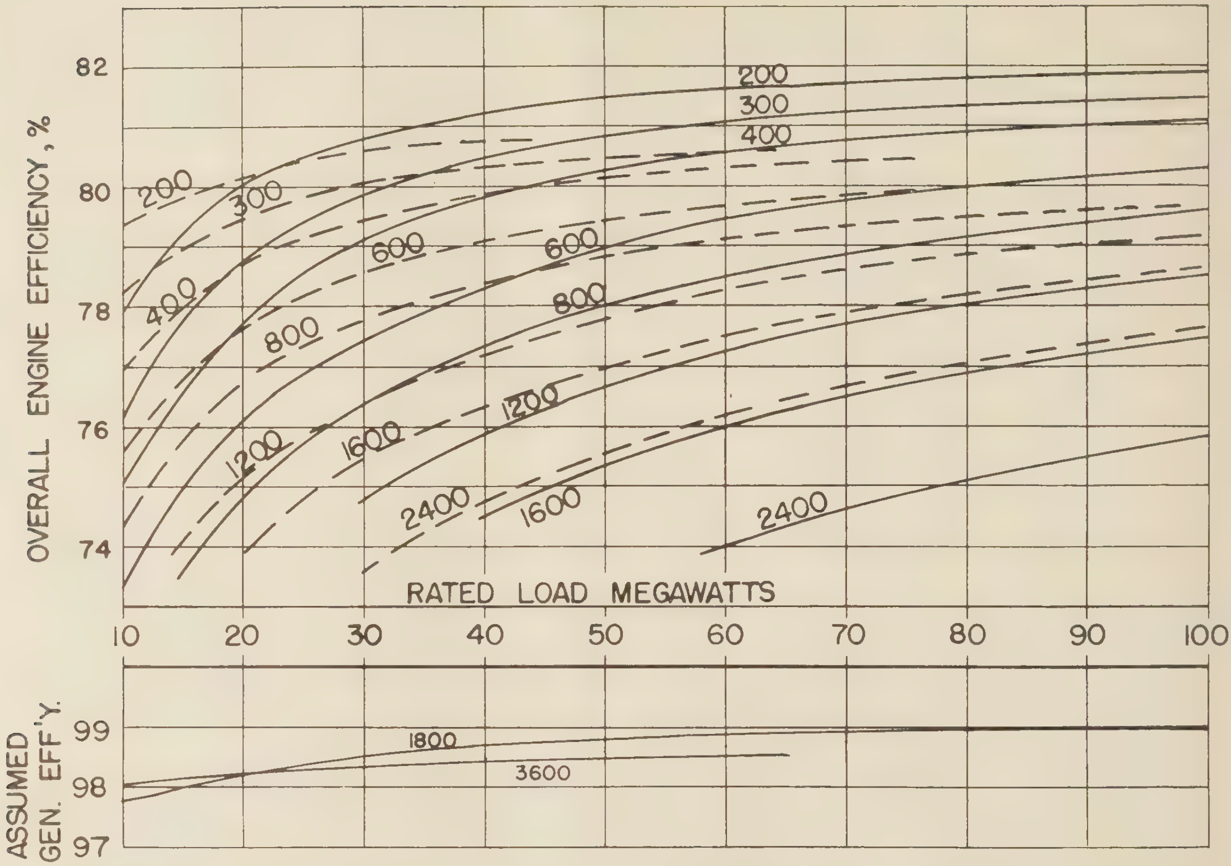

Fig. 5 Over-All Engine Efficiencies of Large General Electric Condensing-Turbine-Generator Units, Versus Rated Load, Megawatts

(Drawn for 300 F initial superheat, with 4 per cent exhaust loss and 1.25 per cent mechanical loss assumed at all ratings. Full lines, 1800 rpm; dash lines, 3600 rpm. Generator efficiencies assumed as shown; hydrogen cooling. Figures on curves are throttle pressure, psi gage.)

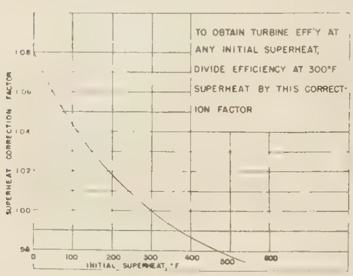

Fig. 6 Throttle-Superheat Correction Factor

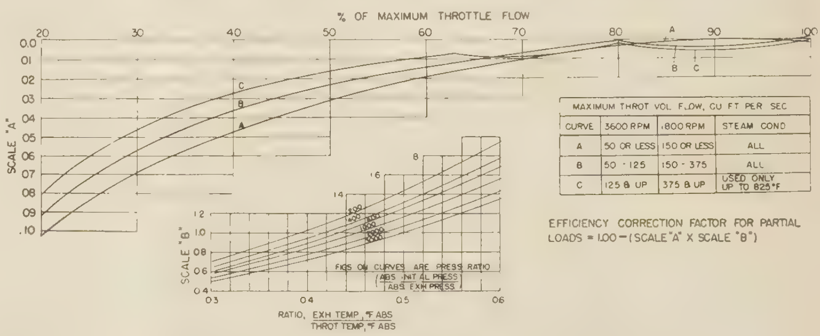

Fig. 7 Partial-Load Correction Factor for Condensing Turbines

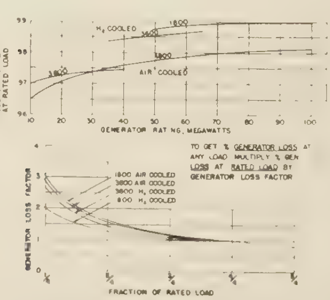

Fig. 8 Approximate Efficiencies of General Electric Turbine Generators, 3600 and 1800 Rpm, Air- and Hydrogen-Cooled

(Curves drawn for 80 per cent power factor; for 90 per cent power factor add 0.15 per cent to rated-load generator efficiency; for 70 per cent power factor subtract 0.25 per cent from rated-load generator efficiency.)

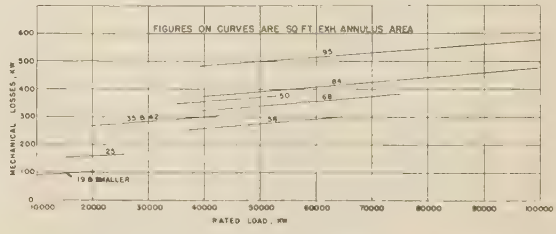

Fig. 9 Approximate Mechanical Losses of Condensing Turbines Versus Rated Load, in Kilowatts

(Mechanical losses are constant at all loads for any given unit; therefore, the per cent mechanical loss varies inversely with unit load.)

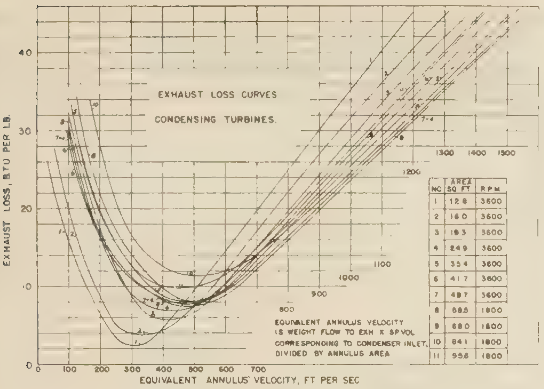

Fig. 10 Exhaust-Loss Curves for Condensing Turbines

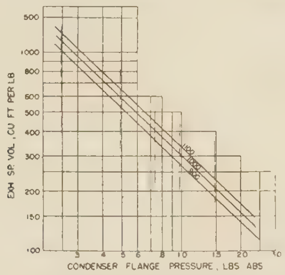

Fig. 11 Exhaust Specific Volume, Cu Ft per Lb Versus Condenser-Flange Pressure, Psi Abs
(Figures on curves are exhaust enthalpy, Btu per lb.)

5 "Exhaust-loss" corrections must be applied at all loads (vacuum corrections are contained in these corrections), Fig. 10 with Fig. 11.

These results will be efficiency values at partial loads and overloads, from which the nonextraction over-all engine efficiency versus generator kilowatt output can be plotted. From this and the "theoretical steam rate" which can be obtained from the steam table[4] or from the steam-rate tables,[5] the nonextracting steam rate can be obtained.

Superheat Corrections

Fig. 6 shows the correction factors to be applied to the curves in Fig. 5, if the initial superheat is different from 300 F. This correction simply shows the change in turbine internal efficiency, occasioned by the changes in reheat factor and moisture losses incident to a change of the initial superheat at any given initial pressure.

Fractional Load and Overload Correction

Fig. 7 shows corrections to be made to efficiencies derived from Figs. 5 and 6, to correct for the change in turbine internal efficiency, due to change in load from rated load. These corrections do not include any correction for change in exhaust loss, mechanical losses or generator losses, which will be treated separately in the following paragraphs.

The corrections are functions of the "inlet-volume-flow" size of the turbine, and the different curves reflect the variation in "governing-stage" efficiency and design which is a function of the inlet-volume flow. In order to use the corrections, it is necessary to make a fairly close approximation to the maximum-weight flow for which the turbine is to be designed, so that the weight flow corresponding to the 100 per cent maximum flow on the abscissa scale in Fig. 7 can be determined, and a weight-flow scale can then be substituted for the "percentage-of-maximum-flow" scale. This is easily done for nonextracting conditions by one or two approximations. Methods for determining the maximum-weight flow for extracting conditions are discussed later.

Corrections for Change in Exhaust Loss[6]

As stated previously, the efficiencies given by Fig. 5 include 4 per cent exhaust loss at all ratings and conditions. Any actual turbine as designed will probably not have exactly this percentage exhaust loss at rated load and, in any case, the exhaust loss will change with changes in exhaust pressure and load. If the calculation of the efficiency of a given turbine is to be made for a range of exhaust pressures or loads, or both, the change in exhaust loss must be carefully taken into account. This requires a determination of the size of exhaust-annulus area which is to be provided on the turbine, and the use of the curves given in Fig. 10.

The table in Fig. 10 shows the sizes of exhaust-annulus area now manufactured by General Electric as standard. The size most suitable for any particular turbine can be determined from the weight steam flow required for the rated output, the particular exhaust pressure being considered, and the amount of exhaust loss which appears economically justifiable. Exhaust-annulus areas usually will lie in the range between 1 and 2 sq ft per 1000-kw rated load, depending upon the condenser pressure, the amount of feed-heating extraction, etc.

For definition and explanation of exhaust loss, the reader is referred to the Robinson paper.[6] Fig. 10 is plotted as exhaust loss in Btu per pound exhaust flow versus equivalent exhaust-annulus velocity. This velocity is the exhaust-weight flow in pounds per second, multiplied by the specific volume of steam at condenser-inlet conditions, cubic feet per pound, and divided by the exhaust-annulus area in square feet. The individual curves of Fig. 10 differ from each other because of different average last-stage-bucket velocities, different bucket shapes, and different exhaust-hood designs. The specific volume can be read from Fig. 11, corresponding to condenser inlet conditions.

In the region of low exhaust-annulus velocities, the exhaust-loss curves of Fig. 10 include the "extra" internal turbine losses which occur on the last few stages of the turbine at low exhaust flows. These losses are not strictly "exhaust losses," but their inclusion as such makes for simplicity in calculation.

The "percentage exhaust loss" might be considered as that percentage by which the output of the turbine would be increased were the exhaust loss to be reduced to zero and the energy so made available to the turbine to be utilized at the "average turbine efficiency," prevailing at the conditions under consideration.

Exhaust loss (kw)

$$= \frac{(\text{Btu per lb loss} \times \text{flow} \times (\text{avg efficiency})}{3412.75} \quad \ldots\ldots [1]$$

$$\text{Exhaust loss, per cent} = \frac{\text{Exhaust loss (kw)} \times 100}{\text{Output (kw)}} \quad \ldots [2]$$

or, for nonextraction operation, when the flow is the same throughout the turbine.

Exhaust loss, per cent

$$= 100 \times \frac{\text{Exhaust loss (Btu per lb, from Fig. 10)}}{\text{Total available energy, line to exhaust}} \quad \ldots [3]$$

[4] "Thermodynamic Properties of Steam," by J. H. Keenan and F. G. Keyes, John Wiley and Sons, Inc., New York, N. Y., 1936.

[5] "Theoretical Steam-Rate Tables," by J. H. Keenan and F. G. Keyes, A.S.M.E., 1938.

[6] "Leaving Velocity and Exhaust Loss in Steam Turbines," by E. L. Robinson, Trans. A.S.M.E., vol. 56, July, 1934, pp. 515–520.

It should be remembered that these factors are percentages and, therefore, not directly additive or subtractive when the efficiency is not 100 per cent.

From the Btu-per-pound exhaust loss so obtained, the percentage exhaust loss at each load may be determined by use of Equation [2] or Equation [3]. As stated, the values of efficiency shown in Fig. 5, are on the basis of a fixed 4 per cent value for all loads. If the true exhaust loss so obtained is above or below this 4 per cent, the final nonextracting efficiency is to be decreased or increased by the difference in percentage of the total efficiency.

In formula form

$$\text{Corrected efficiency} = \text{Efficiency with 4 per cent exhaust loss} \times \frac{(100 - \text{Actual per cent exhaust loss})}{96}$$

This gives the final result for nonextraction operation.

Determination of Maximum Throttle Flow and Efficiency When Steam Is Extracted for Feedwater Heating

It is the general practice to design turbines in the size classification, 10,000-kw to 100,000-kw rating, so that they will develop 5/4 rated load, or full kva generator rating at 1 power factor, whichever is the lower, and with the amount of steam extraction for feedwater heating required by the feed-heating arrangement, as specified by the purchaser.

The maximum-load throttle steam rate must therefore be determined by calculation of the steam-extraction requirements, and this steam rate, multiplied by the maximum load, determines the maximum-weight flow required.

The throttle steam rate with extraction will be higher than without extraction by an amount depending upon the temperature to which the feedwater is to be heated and, to a lesser extent, upon the number and arrangement of feedwater heaters.

Provisions are generally made on these sizes of turbines to extract steam at some 2 to 5 points and, generally, some latitude is available as to where steam may be extracted. In the November 3, 1938, proposed "Preferred Standards for Steam-Turbine Generators,"[7] the following tentative suggestions were made for these extraction points at rated load:

Turbines 10,000 kw to 25,000 kw, inclusive:

First heater terminal temperature, 160 to 180 F
Second heater terminal temperature, 215 to 235 F
Third heater terminal temperature, 280 to 300 F.

Turbines above 25,000 kw to 80,000 kw, inclusive:

The same suggestions were made with respect to the first three heaters and a suggested position for the top heater was 340 to 360 F.

Extraction openings within these ranges can generally be provided. Final decision on any specific proposition will, of course, have to be referred to the manufacturer.

If it is desired to make studies of the extraction performance of turbines based upon the preceding nonextraction information, it may be done quite simply by the following methods:

The efficiency of the turbine, based upon the steam which passes all the way through, will be the same as that given for the nonextracting performance at corresponding fractional flows, except that the exhaust loss will be decreased to correspond to the reduced flow to the condenser under the extracting conditions. The losses in the forward end of the machine due to the governing valves will vary in accordance with Fig. 7 and, hence, these curves are valid for this condition.

[7] "Preferred Standards for Steam-Turbine Generators (10,000-kw rating and above)," Subcommittee on Standardization of the National Defense Power Committee, Washington, D. C., November 3, 1938.

Generally, extraction calculations are carried out on the basis of "state curves," giving the conditions of the steam throughout the turbine at the various conditions of load and from which the enthalpy of the extracted steam can be determined.

Fig. 12 and the following paragraphs show a simplified method of determining such state curves as will be consistent with the previous information given on nonextracting turbines in this paper.

Fig. 13 is an enthalpy-entropy chart. Point A is the initial (throttle) condition for any given machine. Point B_1 is the

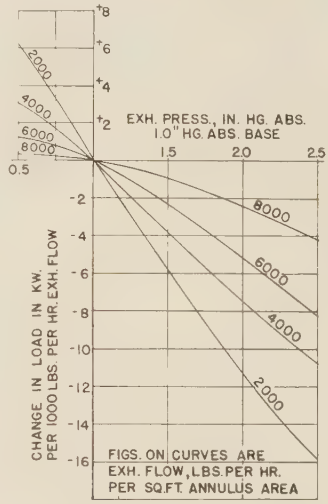

Fig. 12

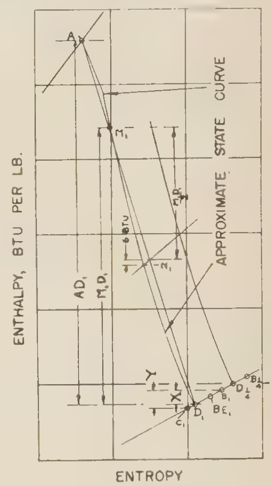

Fig. 13

Fig. 12 Vacuum Correction Curves

(Note that these curves are average for several different turbines. The "change in load" will be slightly larger with the largest exhaust-annulus areas, and smaller with the smallest areas, than is shown by curves.)

Fig. 13 Construction of Approximate "State Curve" for Expansion of Steam Through Turbine

terminal point after the leaving loss has taken place under nonextracting conditions. Point B_1 can be obtained from the over-all nonextraction efficiency as previously explained for the rated conditions, providing only that this is corrected for fixed losses and generator losses.

Fig. 8 shows the percentage generator electrical efficiencies at various fractions of full load for sets with both air- and hydrogen-cooled generators, from $^1/_4$ rated load to full kva generator capacity at unity power factor, and for units from 10,000 kw to 100,000 kw in capacity. These curves include all of the electrical and windage losses in the generators and, when used together with the mechanical losses in Fig. 9, the over-all efficiency previously found can be corrected so as to determine the efficiency of the turbine from the initial conditions to the discharge of the last-stage buckets from which, by means of the well-known methods of finding the available energy and the used energy, point B_1, i.e., the end point, can be determined.

The vertical distance Y between point B_1 and C_1 (Fig. 13) is the nonextraction exhaust loss obtained from Fig. 9 and previously used. The distance X is to Y, from the previously defined way of handling the exhaust loss, approximately as the efficiency of the machine is to 100 per cent; and hence, the point D_1 is what we generally call the end point of the internal efficiency; or the end point of a turbine with "zero exhaust loss."

Once D_1 is determined for the rated load, it becomes possible to determine quite closely the "state line" for the various other stages throughout the turbine.

If a straight line is drawn on such a Mollier diagram from

point A to D_1, the true state curve will generally lie somewhat above this in the upper portion and below it in the lower portion. Generally it will cross about 25 per cent of the way down.

From the standpoint of feedwater-heating calculations, the point above this crossing point may generally be neglected because as a rule steam is not extracted for feedwater heating much above this point. The true state line seems to lie on an average about 6 Btu below this straight line, midway between the crossing point marked M_1 and D_1, as shown at N_1. For all practical purposes, therefore, the state line can be drawn $AM_1N_1D_1$.

The exact shape of the true state curve will depend upon the actual machine, but is not of great importance once the end points are determined.

To find the end point under extracting conditions shown, B_{E1}, it becomes necessary to use the exhaust loss corresponding to the extracting flow. This can be obtained from Fig. 10 quite readily if the exhaust flow under extraction conditions is calculated. This can be done accurately by a complete heat-balance calculation or, for estimating purposes, it may be done by the following approximations:

Generally, the amount of steam extracted is about 1 per cent of the throttle flow for each 10-deg rise in feedwater temperature. At constant load, the throttle flow is increased about as much as the condenser flow is decreased, the average flow remaining constant. Thus, if the feedwater temperature is raised 200 deg through the heaters, the throttle flow will be increased 10 per cent and the condenser flow decreased 10 per cent.

At lower feedwater-temperature rises, the condenser flow tends to be decreased more than the throttle flow is increased, and vice versa at higher feedwater temperatures.

From the foregoing rough rule, it becomes possible to determine an approximate exhaust loss for extraction operation.

From the corrections available from Fig. 7, it becomes possible to determine end points corresponding to D for rated load for various loads within the capacity of the turbine and generator. From the extraction exhaust loss determined similarly for the extracting exhaust flows, it then becomes possible to determine the end point B_E corresponding to these other loads.

In Fig. 12, $B_{E1/4}$, corresponding to the $^1/_4$-load point, is shown as an example. The lower three fourths or so of the state curve will, in general, be substantially parallel to the "rated-load state curve," and can be so drawn.

On the basis thus outlined and the accompanying curves, it is possible to work out approximate state curves for turbines for the sizes and conditions covered and, if the extraction points are picked at the rated-load condition for pressure, etc., it makes available sufficient data upon which a complete heat balance may be secured by one familiar with the usual technique of making such heat balances.

Some regularly used simplifying assumptions for heat-balance calculations are as follows:

The pressure in any extraction stage will vary at loads other than the rated load for which it is determined in direct proportion to the flow below such extraction opening.

The pressure drop from the extraction stage to the extraction opening is assumed to be 5 per cent, and 5 per cent additional from the turbine opening to the heater.

Generally, no terminal temperature difference is assumed in an open or deaerating heater but, in closed heaters, a 5-deg terminal difference is generally used, with the drip from the heater coming out at the saturation temperature corresponding to the pressure in the heater, unless the heater is of the counterflow type with special desuperheating surface or special condensate heat-exchanger surface, under which conditions the feedwater may leave the heater higher in temperature than the saturation temperature of the pressure in the heater, and the condensate may leave closely approaching the feedwater entering the heater. This, of course, will depend upon the specific case encountered and the heater-manufacturer's guarantees.

Exhaust Loss Under Extraction Conditions

It is often worth while to know the true exhaust loss under extracting conditions which may be quite different from the exhaust loss under the nonextracting conditions previously dealt with.

Either the approximate condenser flow under extracting conditions as described, or the final condenser flow which can be determined from the heat-balance setup, may be used to determine the exhaust loss in Btu per pound flow from Fig. 10. If this is then multiplied by the average turbine efficiency and by the exhaust flow, and divided by 3412.75, a figure is obtained in kilowatts and represents the exhaust loss. This, divided by the total turbine output under consideration, gives the fractional relation the exhaust loss bears to the total output. Generally at full rated load this will be in the neighborhood of 60 per cent, more or less, of the percentage exhaust loss at the corresponding load under nonextracting conditions, depending upon the amount of extraction, and the nonextraction exhaust loss. This is because the exhaust loss per pound at rated load varies approximately as the square of the exhaust flow, and the exhaust loss in kilowatts varies as the loss per pound times the flow; hence, at fixed load conditions, and with the exhaust flow changing as a result of extraction, the exhaust loss in kilowatts, and so the percentage exhaust loss, varies about as the cube of the exhaust flow.

Thus, if by virtue of a considerable amount of extraction for feedwater heating, the exhaust flow is dropped 15 per cent at constant load, as compared to what it would be under nonextracting conditions, the percentage exhaust loss would be only about 62 per cent of what it would be with the same nonextracting load.

This, of course, does not hold at the lighter loads, at which, as may be seen from Fig. 10, a reduction of flow may cause an increase in exhaust loss.

Variations in Efficiency and Output With Vacuum

The variations in exhaust loss and available energy for changes in condenser pressure can be worked out accurately according to the preceding discussion to arrive at a family of steam-rate or heat-rate curves at different condenser pressures. A much simpler method, with accuracy high enough for many comparisons, involves the use of Fig. 12. This gives directly the net result of the changes in exhaust loss and available energy which come about with the change in condenser pressure, at constant-weight flow to exhaust.

The curves in Fig. 13 are average curves for a number of different machines on which tests have been made.

2—BACK-PRESSURE OR NONCONDENSING TURBINES

In sizes from 10,000 kw to 60,000 kw, these turbines generally operate at 3600 rpm today, although some 1800-rpm machines are still built to meet certain conditions and many have been built in the immediate past.

Fig. 14 shows the "turbine engine efficiency" of such machines at rated load for both 3600- and 1800-rpm turbines, and as a function of initial volume flow, with correction factors to take account of variations in initial pressure—back-pressure ratio. The shape and relative values of these curves are based on the analysis of tests on turbines. These curves are similar to the curves of Fig. 4 for condensing machines, except that they do include leaving losses.

The generator efficiencies may be used from Fig. 8 to obtain

the "over-all engine-efficiency ratio" at rated load. The mechanical losses on noncondensing machines can be assumed to be 0.75 per cent of the rated-load kilowatts, which will be sufficiently correct for all ratings between 10,000 kw and 100,000 kw.

Noncondensing turbines are usually designed so as to develop sufficient capacity to meet the generator rated kva at 0.9 power factor on an 0.8-power-factor normally rated generator. This

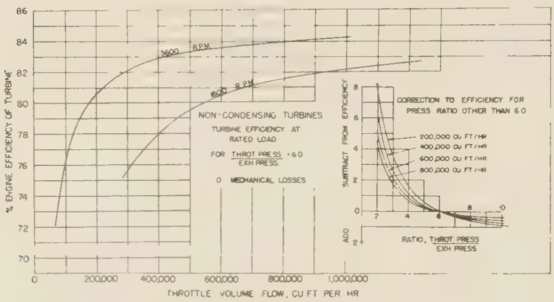

Fig. 14 Efficiency of Large Noncondensing General Electric Turbines, Versus Throttle-Volume Flow, Cu Ft per Hr
(Efficiencies include rated-load exhaust loss, but no mechanical or generator losses.)

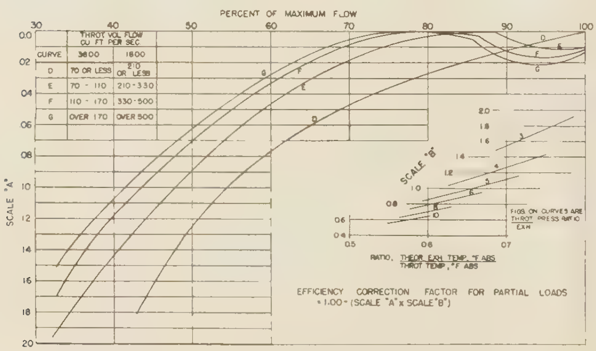

Fig. 15 Partial-Load Correction Factor for Noncondensing Turbines

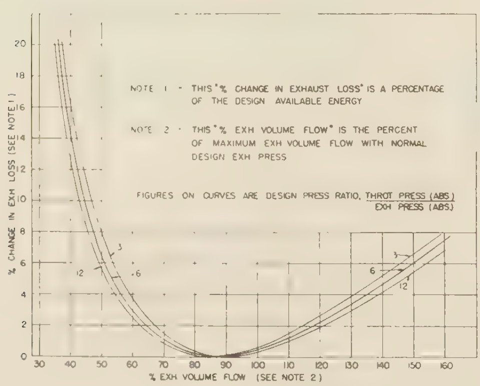

Fig. 16 Change in Exhaust Loss, Noncondensing Turbines

means that the turbine must develop about 1.11 times the rated load. This is ordinarily set as a maximum load limit, because to meet greater capacities than this depreciates the noncondensing turbine a larger amount at lighter loads than it does the condensing turbine. Corrections for such a machine for loads other than rated loads are contained in Figs. 15 and 16, and are applied to the results obtained from Fig. 14 for turbine efficiencies.

Fig. 16 for noncondensing turbines is similar to Fig. 10 for condensing turbines, but more simply drawn. Because of the greater flexibility of design of the exhaust ends of noncondensing turbines, and because of the smaller magnitude of the exhaust losses, it is not necessary to specify particular sizes or exhaust stages. Generally the exhaust is easily made proportional to the volume flow. There is one other point of difference between the exhaust-loss curves of Fig. 10 and those of Fig. 16, i.e., whereas Fig. 10 shows total exhaust losses, Fig. 16 shows only the difference between the exhaust loss at rated flow and the exhaust loss at any other flow. Also, it is possible, by varying the design, to shift the "zero-exhaust-loss" point along the abscissa scale, somewhat, to favor lower or higher loads.

These values are much more dependent upon the available energy or pressure ratio than are the corresponding values in Fig. 7 for condensing turbines and should be applied before the generator and mechanical losses are applied.

Thus, by a method similar to that used for condensing machines, the noncondensing-turbine performance may be calculated at partial loads and overloads. These calculations are based upon constant initial and exhaust pressures over the range of load. Corrections for small changes in exhaust pressure can be made by using the same curves, with proper attention paid to the volume-flow scale.

Cross-Compound Turbines

Generally, it is not possible or economical to make the high-pressure sections of condensing turbines as efficient in the expansion from the initial pressure down to the region between 200 lb and 300 lb as is that of a straight 3600-rpm noncondensing turbine for this pressure range. Hence, an increase in efficiency can be obtained by combining such a noncondensing turbine with a 3600- or 1800-rpm low-pressure turbine into which it exhausts. The performance of such a combination can be obtained by figuring out the performance of each separately from the preceding data and combining them. On resuperheating turbines this process of separating the high- and low-pressure units must be done to get the steam back to the resuperheater.

The method outlined would only give performance figures at a fixed "crossover" pressure between the units, but the data contained herein are sufficient to permit state lines to be drawn for the two combined units for "variable crossover" conditions by one skilled in the art, but space will not permit presenting this case here. This would also apply to resuperheating arrangements.

Conclusions

New designs and the progress of research are continually improving the values of efficiency which can be reached. Turbines are operating today at over-all efficiencies which were scarcely thought possible a few years ago. We do not expect this progress to cease and, hence, these values can only be accepted as tentative. However, the authors do believe them to be relatively correct, and hope they will be of considerable value to those engaged in power-plant design.

Acknowledgment

The authors gratefully acknowledge the cooperation of Messrs. R. Gamache, E. E. Harris, C. M. Gardiner, B. O. Buckland, and others in the preparation of this paper.

Appendix

Example 1—Condensing Turbine

Turbine Data:

Rating, 35,000 kw; 0.8 power factor; 600 psi; 850 F; $1^1/_2$ in. Hg abs; hydrogen-cooled generator; 3600 rpm. Turbine to be able

to carry 43,750 kw at 1 power factor, with extraction for feed-water heating to 322 F.

Section 1. Calculation of approximate maximum required flow to throttle:

From Fig. 5, over-all engine efficiency at 600 psi, 300 F superheat, 35,000 kw for 3600 rpm is 78.8 per cent. 600 psi, 850 F is 361 F superheat.

From Fig. 6, superheat correction for 361 deg is 0.991.

$$\frac{78.8}{0.991} = 79.5 \text{ per cent}$$

Theoretical nonextraction steam rate for 600 psi, 850 F, $1^1/_2$ in. Hg (from tables[5]) is 6.479 lb per kwhr.

Approximate maximum-load nonextraction steam rate =

$$\frac{6.479}{0.795} = 8.15 \text{ lb per kwhr}$$

Expected rise in feed temperature = 322 F — 92 F = 230 F.

From rule given on page 7 of this paper, increase in throttle flow required to hold constant load when extracting is

$$\frac{230}{200} \times 10 = 11.5 \text{ per cent (approximately)}$$

Approximate maximum required throttle flow for 43,750 kw extracting then is

$$43{,}750 \times 8.15 \times 1.115 = 398{,}000 \text{ lb per hr}$$

This is the "100 per cent maximum flow" for use with Fig. 7.

Section 2. Choose actual size of exhaust-annulus area. Enthalpy at throttle conditions, 1435 Btu per lb. Approximate used energy in turbine is

$$\frac{3412.75}{8.15} = 419$$

Approximate enthalpy of exhaust to condenser = 1435 — 419 = 1016.

From Fig. 11, exhaust specific volume = 420 cu ft per lb.

For rated load, the approximate nonextraction flow is 35,000 × 8.15 = 285,000 lb per hr.

At this load, if we choose the 49.7 sq ft exhaust, the equivalent annulus velocity (Fig. 10) is

$$\frac{285{,}000 \times 420}{3600 \times 49.7} = 669 \text{ ft per sec}$$

This would result in exhaust loss (curve 7, Fig. 10) of 11.3 Btu per lb.

$$\text{Theoretical available energy} = \frac{3412.75}{6.479} = 526.7 \text{ Btu per lb.}$$

$$\frac{11.3}{526.7} = 2.15 \text{ per cent exhaust loss at this condition}$$

This percentage loss will be reduced when extracting, and may be lower than is worth while to achieve. If we choose the 41.7-sq-ft size, the annulus velocity at the same condition would be

$$679 \times \frac{49.7}{41.7} = 809 \text{ ft per sec}$$

This would result in exhaust loss (curve 6, Fig. 10) of 18.0 Btu per lb

or $$\frac{18.0}{526} = 3.4 \text{ per cent}$$

This latter case is, in general, more nearly in line with the average choice, and we will assume the 41.7 sq ft exhaust will be used. A still smaller size might be chosen if economically desirable.

Section 3. The calculation of nonextraction steam rate at various loads is given in Table 1. Specific volume of steam to throttle (from tables) = 1.21. Maximum volume flow to throttle $= \frac{1.21 \times 403{,}000}{3600} = 134$ cfs. This volume flow puts the machine in class *C* on Fig. 7, except that initial temperature is too high for this class, so that it becomes class *B*. Choose fractions of maximum flow to reflect shape of curve *B*, Fig. 7.

Section 4. Construction of "state curves" for bleeding performance calculations:

The enthalpy of point *D*, Fig. 12, can be found.

Enthalpy at point *D* for any flow in Table 1 is

$$\left[\text{Enthalpy at throttle} - \left(\frac{\text{item 6}}{100} \times \text{Theoretical available energy}\right)\right]$$

With the various *D* points determined, state curves can be constructed according to Fig. 12, and described in the main text of this paper. Heat-balance calculations, using the particular heater arrangement desired, will give the amounts of steam to be bled from the turbine at the various bleed points at the various throttle flows. At each throttle flow, a table of the steam flows through the turbine can be made, and the power output of each section calculated from the flow through the section and the enthalpy drop through the section according to the state curve. In calculating the power output of the final low-pressure section of the turbine, the true "end point" of the expansion is not at the points *D*. The true enthalpy in the exhaust is the enthalpy

TABLE 1

1	Percentage of maximum throttle flow	20	40	60	80	90	100
2	Throttle flow, lb per hr	79600	159000	239000	318000	358000	398000
3	Base over-all efficiency of turbine (from Section 1) = 79.5 per cent. This includes 4 per cent exhaust loss, 1.25 per cent mechanical loss, and 98.4 per cent generator efficiency						
4	Base value of turbine "internal" efficiency, per cent = $\frac{79.5}{0.96 \times 0.9875 \times 0.984} = 85.1$						
5	Efficiency correction factor (Fig. 7)	0.92	0.968	0.988	1.00	0.996	1.001
6	Actual turbine "internal" efficiency (4 × 5), per cent	78.3	82.4	84.1	85.1	84.8	85.2
7	Equivalent annulus velocity, ft per sec	226	451	677	901	1013	1128
8	Exhaust loss (curve 6, Fig. 10), Btu per lb	14.0	7.0	13.2	22.2	26.6	31.7
9	Exhaust loss (item 8 ÷ available energy), per cent	2.6	1.3	2.5	4.2	5.0	6.0
10	Turbine "wheel" efficiency $\left[\text{Item 6} - \left(\text{item 9} \times \frac{\text{item 6}}{100}\right)\right]$	76.3	81.4	82.0	81.5	80.6	80.1
11	"Turbine wheel" steam rate $\frac{\text{(Theoretical steam rate} \times 100)}{\text{item 10}}$, lb per kwhr	8.49	7.96	7.90	7.95	8.04	8.09
12	Turbine wheel load (item 2 ÷ item 11), kw	9370	19970	30260	40000	44520	49200
13	Mechanical loss (from Fig. 9), kw	290	290	290	290	290	290
14	Generator input (item 12 — item 13), kw	9080	19680	29970	39710	44230	48910
15	Generator loss, per cent (from Fig. 8)	3.60	1.90	1.45	1.2	1.1	1.1
16	Generator loss $\left(\text{item 14} \times \frac{\text{item 15}}{100}\right)$, kw	325	375	435	480	480	480
17	Generator output (item 14 — item 16), kw	8755	19305	29535	39230	43750	48430
18	Over-all nonextraction steam rate (item 2 ÷ item 17), lb per kwhr	9.09	8.24	8.09	8.11	8.18	8.22

at D plus $\left(\frac{\text{item 6}}{100}\right) \times$ exhaust loss (Btu per lb from Fig. 10, corresponding to actual exhaust flow).

When the power outputs of the various sections are summed up, the mechanical losses and generator losses must be deducted to arrive at the generator output.

Example 2—Noncondensing Turbine

Turbine Data:

Rating, 25,000 kw; 0.8 power factor; 3600-rpm air-cooled generator; 1200 psi; 925 F; 250 lb gage exhaust; maximum capacity to be 28,000 kw at improved power factor.

Section 1. Calculation of approximate maximum required flow, and "base" turbine efficiency:

Theoretical steam rate (from tables[5]) = 18.57 lb per kwhr.

Estimated over-all efficiency at 28,000 kw is 77 per cent.

$$\text{Maximum-load steam rate} = \frac{18.57}{0.77} = 24.1 \text{ lb per kwhr.}$$

Maximum flow = 24.1 × 28,000 = 675,000 lb per hr.

Specific volume of steam at throttle (from tables[5]) = 0.63 cu ft per lb.

$$\text{Maximum throttle volume flow} = \frac{675{,}000 \times 0.63}{3600} = 118 \text{ cfs.}$$

This places the machine being considered on curve F, Fig. 15.

Rated-load volume flow to throttle is approximately 25,000 × 24.1 × 0.63 = 379,000 cu ft per hr.

"Base" engine efficiency of turbine (from curve, Fig. 14) is

$$82.7 \text{ per cent at } \frac{P_1}{P_2} = 6$$

$$\text{Actual } \frac{P_1}{P_2} = \frac{1215}{265} = 4.58$$

Pressure-ratio correction (from Fig. 14) = 0.7 per cent.

"Base" engine efficiency $\left(\text{at } \frac{P_1}{P_2} = 4.58\right)$ is 82.7 — 0.7 = 82.0 per cent.

Section 2. The calculation of "steam-rate-versus-load" curve is given in Table 2. Choose fractions of maximum flow to reflect shape of curve F, Fig. 15.

TABLE 2

1	Percentage of maximum throttle flow	40	60	80	86	94	100
2	Throttle flow, lb per hr	270000	405000	540000	581000	635000	675000
3	"Base" turbine efficiency (from Section 1) = 82.0 per cent						
4	Efficiency correction factor (from Fig. 15), per cent	0.86	0.961	1.00	0.996	0.981	0.984
5	Changes in exhaust loss (Fig. 16), per cent	15.2	3.3	0.3	0	0.3	0.6
6	$\frac{100 - \text{item 5}}{100}$	0.848	0.967	0.997	1.00	0.997	0.996
7	Corrected turbine efficiency (3 × 4 × 6), per cent	59.8	76.2	81.8	81.7	80.2	80.4
8	Turbine "wheel" steam rate $\frac{(\text{theoretical steam rate} \times 100)}{\text{item 7}}$, kw	31.06	24.37	22.70	22.73	23.16	23.10
9	Turbine "wheel" load (item 2 ÷ item 8), kw	8695	16620	23800	25550	27420	29220
10	Mechanical losses (0.75 per cent of 25000 kw), kw	190	190	190	190	190	190
11	Generator input, kw = (item 9 — item 10)	8505	16430	23610	25360	27230	29030
12	Generator loss (from Fig. 8), per cent	6.1	3.5	2.8	2.7	2.5	2.4
13	Generator loss $\left(\frac{\text{item 12}}{100} \times \text{item 11}\right)$, kw	520	575	660	685	685	685
14	Generator output (item 11 — item 13), kw	7985	15855	22950	24675	26545	28345
15	Over-all steam rate (item 2 ÷ item 14), lb per kwhr	33.8	25.53	23.52	23.54	23.92	23.82

Addenda

THE purpose of this paper has been to give a working tool to those engineers in public utilities, industries, and consulting groups who are frequently making studies as to the relative performance of turbines at different steam conditions, vacuums, capacities, loads, etc. The authors hope the data will be of value.

It is necessary to point out that this paper gives expected relative efficiencies only. The values obtained for any one particular machine will probably not conform with either guarantees or tests which have been made, since, as stated in the paper: "It is expected (these efficiencies) will have some margin as compared with the probable test results when in good condition." Furthermore, inspection of Figs. 1 and 2 shows quite clearly that the test results of machines within the same time group may frequently vary ± 1 per cent or more, although recently tested machines seem to give more uniform results. Therefore, an analysis such as this must present an average, with some allowance for unfavorable conditions.

Particular attention is directed to Fig. 12 which presents an easy method of making quite accurate vacuum corrections to a turbine guarantee or test, under either extraction or nonextraction conditions and at all loads and over a wide variety of steam conditions.

Discussion

Linn Helander.[8] The authors have presented data on the relative efficiencies of large steam turbines that will be of immeasurable value to teachers and to engineers engaged in designing or operating steam power plants. Not only are the data in a form which should enable engineers to use them conveniently, but they are also of a character which should enable the power-plant designer and operator to evaluate with a greater degree of accuracy than heretofore the economies obtainable from the use of multiple-stage bleeder heaters. For the first time, as far as this writer is aware, data have been presented which should enable power-plant engineers to evaluate conveniently the effects of both the increased throttle flow of steam and the altered leaving losses which accompany the extraction of steam from turbines for use in feedwater heaters.

The data will be of particular help to engineers engaged in making those preliminary studies which usually precede a choice of throttle steam pressure, throttle steam temperature, vacuum, and arrangement of feedwater heaters. They should free the power-plant engineer from the necessity of calling upon turbine manufacturers for numerous data on alternate designs, many of

[8] Professor of Mechanical Engineering, Head of Department, Kansas State College, Manhattan, Kansas. Manager A.S.M.E.

which will prove to be obviously unacceptable during early studies of heat-balance arrangements. The authors' contribution should prove beneficial, therefore, not only to the power-plant designer and operator but also to turbine manufacturers.

The authors have been careful to point out that the data presented by them have been developed from specific designs of General Electric Company turbines and that they are subject to modification, as the art of designing turbines improves. One may assume also that the data should not be used indiscriminately in making final decisions, particularly when those decisions relate to turbines made by manufacturers other than the General Electric Company. Engineers engaged in selecting condensers should no doubt delay their choice of size of condenser until the precise characteristics of the turbine to which the condenser is to be joined are known, and they should then obtain the proper vacuum corrections from the manufacturers of the turbine.

The procedure for making vacuum corrections as proposed by the authors is simple. However, it does not permit evaluating the effect on vacuum corrections of gaging or the mean velocity of the last row of blades. Much remains to be said about vacuum corrections, and we may hope that the authors, or some of their associates, may find a convenient opportunity at some later date to discuss this subject more fully. Engineers engaged in selecting condensers are concerned with the order of accuracy which may be attached to turbine vacuum corrections as they are now being evaluated; an exposition of the methods employed by manufacturers in evaluating vacuum corrections would, therefore, be of general interest.

The term "internal engine efficiency of a turbine" is employed by the authors to denote the ratio obtained by adding the kinetic energy of the leaving steam to the internal shaft work and dividing the result by the isentropic-enthalpy drop. This term is also used to denote the ratio obtained by dividing the internal shaft work, exclusive of the kinetic energy of the leaving steam, by the isentropic-enthalpy drop. These internal efficiencies are obviously not the same, and some means of distinguishing them should perhaps be adopted.

E. H. Krieg.[9] It is most encouraging that the authors have seen the need of operators and designers for the data contained in this paper. For years there has been a feeling that a sort of "no man's land" existed between power-plant designers and turbine designers. The turbine designer, of course, could not know the intricacies of system operation and the myriad complexities of operating details and, at the same time, qualify as a turbine expert. To many power-plant operators and designers, the turbine designer's work was quite mysterious, neither its possibilities nor limitations being clearly understood. When the power-plant designer appreciates some of the problems of the turbine designer, and the turbine designer is confronted by the operating problems raised by his "brain children," then the optimum result is achieved. A common ground of understanding makes it possible to appreciate the issues involved.

There was a time when such data as presented in this paper were considered quite a trade secret, but the truth is that the education of the customer or user in the fundamental characteristics of the equipment will lead to a much more satisfactory application. No longer do we have a plethora of "base-load" single-valve turbines.

May the writer point out that this paper is not quite as comprehensive as would appear to be desirable. However, it is realized that it would be rather a full task to discuss the selection and application of prime movers. Or are we making too much of progressive engineering? It is but a few months ago that a keen longing was expressed in one technical publication for the "good old days" of 250-lb 600 F plants which were quite as efficient as those of 1250 lb 950 F, which we now have. Anyone reading this paper can readily see from Fig. 5 that a 200-lb 50,000-kw turbine has an efficiency of 81.5 per cent against 76.6 per cent for 1200 lb pressure. Obviously this is not the entire story. Perhaps the authors could be induced to explain why, in the face of this fact, it is still possible for high pressure and temperature to show an advantage. But even if they do not, let us keep in mind that governmental statistics indicate that the country's electrical output has doubled for the same coal consumption during the last decade or two. It did not happen by adhering to the pressures, temperatures, and sizes of units of two decades ago. A study of this paper should show some of the reasons.

[9] Engineering Department, American Gas and Electric Service Corporation, New York, N. Y. Mem. A.S.M.E.

Authors' Closure

Professor Helander states that "the procedure for making vacuum corrections as proposed by the authors is simple. However, it does not permit evaluating the effect on vacuum corrections of gaging or the mean velocity of the last row of blades." This apparently refers primarily to the use of Fig. 12. This figure is, as stated in the paper, only an average, and for approximate use only. Accurate vacuum corrections can be calculated by the use of the exhaust-loss curves, Fig. 10, and vacuum corrections so calculated will automatically take care of such variations in "mean velocity" and bucket exit angles as exist with the various last-stage wheels.

There is some justification for Professor Helander's remark regarding confusion of the use of the term "internal engine efficiency." Our own practice, which we believe is consistently followed in the paper, is to reserve the term "internal engine efficiency" for denoting an efficiency of the turbine alone with no exhaust loss, as Professor Helander states.

Mr. Krieg points out that a low-pressure low-temperature turbine is shown to have a better engine efficiency than one for a high pressure and high temperature, and raises the question as to the justification for high pressures and temperatures. Obviously, the power-plant operator is interested in the thermal efficiency of his plant primarily, and this is dependent first of all on the thermal efficiency of his steam cycle. As between the 200-lb and the 1200-lb turbine whose engine efficiencies are compared by Mr. Krieg, there is more than 20 per cent difference in the cycle thermal efficiency which, of course, easily overbalances the change in engine efficiency of 5 per cent. It is expected that a presentation of the theoretical thermal efficiencies of steam cycles can be made in the near future. When the theoretical cycle efficiency differences are thus made available, an evaluation of the net effect of change in cycle efficiency and change in engine efficiency will be comparatively simple.

Experience With Metals at High Temperatures for Power Plants

By A. E. WHITE[1] and C. L. CLARK,[2] ANN ARBOR, MICH.

From wide experience with various metals and applications of different types, in high-pressure, high-temperature power-plant service, the authors have selected piping and bolting materials for detailed discussion. In this field, carbon-molybdenum steel is receiving the greatest amount of attention and so the properties, control of grain size, heat-treating practice, creep rates, and kindred matters for this material are dealt with in the paper. Based on two specifications for bolting material issued by the American Society for Testing Materials, the authors discuss the selection of properties, heat-treatment practice, and causes of failure in this type of material. The conclusion is reached that in so far as suitable alloys for pipes and bolts for high temperature are concerned, the art is yet in its developmental stage.

THE subject of this paper is sufficiently broad so that it could cover experiences with many varying kinds of metals, as well as experiences with the metals in many different types of units which are subject to high-temperature service. For instance, in the power-plant field, experiences with the metals in boilers, heaters, condensers, superheaters, piping, fittings, valves, and turbines might be discussed. Also, the subject could be approached from the standpoint of the relative high-temperature merits of the various brasses and bronzes, monel metal, and, in the ferrous field, plain carbon steels, low-alloyed steels, and stainless steels. The subject is so inclusive, however, that it would appear to be desirable to limit its scope to experiences with piping and bolting materials.

Piping for High-Temperature Service

With respect to piping, numerous alloys have been developed for high-temperature service. Many of these are covered in the specifications of the American Society for Testing Materials, especially in the specification for carbon-molybdenum pipe and in the specification for alloy-steel pipe for service from 750 to 1100 F. In this latter specification, the alloys of molybdenum—low chromium, 4 to 6 per cent chromium, 13 per cent chromium, silicon-molybdenum, and 18-8 chromium-nickel alloys—are the predominant types. Each has its special application and some are used extensively in the petroleum field.

The alloy for pipe in the power-plant field, which today is receiving the greatest amount of attention, is carbon-molybdenum steel. It is used almost exclusively for high-temperature, high-pressure applications. It is by no means the only alloy which is available for this purpose, nor does it have as good high-temperature characteristics as some alloys which might be mentioned. But, for service temperatures up to 950 F and possibly up to 1000 F, it is the least expensive and the most nearly foolproof of all the alloys which are available. For these reasons, it will be the only pipe material which will be discussed.

One of the outstanding needs of those who use carbon-molybdenum steel for high-temperature purposes is a simple test which can be used to determine the high-temperature properties of the metal under examination. The standard creep test is too long, in that it is a test which requires 1000 hr for its completion. Other tests have been proposed, such as Hatfield's time-yield test, varying-rate tensile tests, stress-rupture tests, and others. None of these has proved satisfactory at a temperature of 925 F for this steel, possibly, because this temperature is in the strain-hardening range which introduces, in consequence, an uncontrolled variant. It is possible that some one or more of these tests might prove satisfactory if the temperatures selected were substantially in the plastic rather than in the combined elastic-and-plastic range.

Within the last 2 or 3 years, considerable attention has been focused on the metallographic method of determining acceptable high-temperature properties for plain-carbon and low-alloyed steels. The evidence to date seems to indicate that a steel, the normal tendency of which is to develop coarse grains, is preferable for high-temperature service to one in which the tendency is to develop fine grains. In other words, a steel which will show a grain size of from 3 to 6 seems to have better high-temperature properties than a steel with a grain size of from 7 to 8. Yet, grain size in itself does not appear to be the only determining factor for any given composition. The nature and distribution of the carbides in the carbide-containing grains appears to be of considerable importance. For instance, when the carbide grains assume a Widmanstätten structure, that is, one in which precipitation occurs in cleavage planes, better high-temperature properties appear to be secured than when the carbides are in some other form.

The control of grain size is a function of steel-melting practice and heat-treatment. In order that the steel-melting practice may be of an acceptable type, the steel should be either silicon- or silicon-aluminum-killed. It should not be killed with aluminum exclusively. Of course, any grade of steel can be made to acquire a coarse grain provided it be heated to a sufficiently high temperature, but a properly killed steel of the type desired for high-temperature service should show a 3 to 6 grain size if normalized or annealed from 1700 F. An improperly killed steel, on the other hand, if normalized or annealed from 1700 F, would show a fine grain.

In this connection, in some data which were obtained from an investigation sponsored by The Detroit Edison Company, creep rates at 925 F on various heats of carbon-molybdenum steel of substantially the same composition were found to range from 0.3 to 7.3 per cent per 100,000 hr, under the same stress.

The structures of the steels showing low, medium, and high creep rates are given in Figs. 1, 2, and 3. The creep rate for the steel with the structure shown in Fig. 1 is 0.3 per cent per 100,000 hr. The grain size is from 5 to 7 and the carbide grains are of the Widmanstätten type. The creep rate for the steel shown in Fig. 2 is 2.3 per cent per 100,000 hr. The grain size is from 7 to 8. The creep rate for the steel shown in Fig. 3 is 7.3 per

---

[1] Consulting Engineer, and Director of Engineering Research, University of Michigan. Mem. A.S.M.E.

[2] Research Engineer, Department of Engineering Research, University of Michigan.

Contributed by the Power Division and presented at the Semi-Annual Meeting, Milwaukee, Wis., June 17–20, 1940, of The American Society of Mechanical Engineers.

Note: Statements and opinions advanced in papers are to be understood as individual expressions of their authors and not those of the Society.

Fig. 1 Photomicrograph of Carbon-Molybdenum Steel Showing Low Creep Rate
(Heat 1; N.1650, D.1200 F; ×100.)

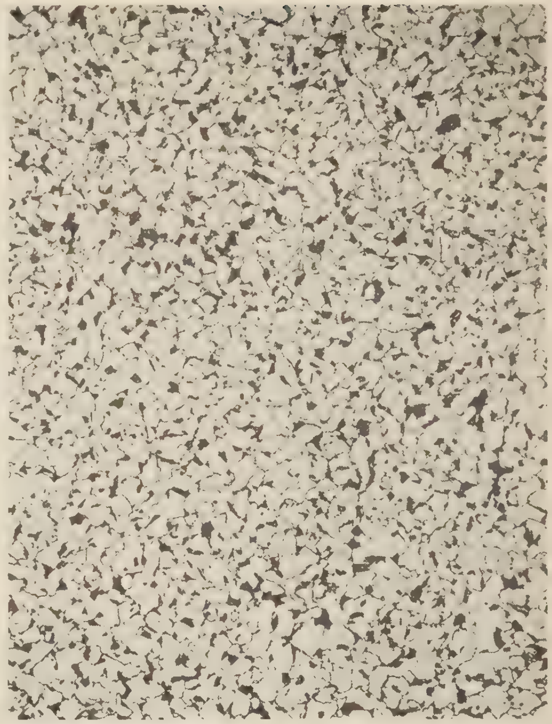

Fig. 2 Photomicrograph of Carbon-Molybdenum Steel Having Medium Creep Rate
(Heat 9; N.1650, D.1200 F; ×100.)

Fig. 3 Photomicrograph of Carbon-Molybdenum Steel Having High Creep Rate
(Heat 10; A.1925–1975 F, 3 hr; ×100.)

cent per 100,000 hr. The grain size in certain sections ranges from 2 to 3 and in other sections from 5 to 7. For the most part, the grain size is large. It is, however, decidedly nonuniform. Its structure is of a type known as duplex. The high creep rate is attributed at least in part to this type of structure.

Too broad generalities must not be drawn from any of these findings. Our knowledge with regard to what causes differences in high-temperature properties and how to interpret the findings of microstructures is still in an experimental stage and, before definite conclusions can be drawn, much further work will be required.[3]

[3] Credit for the emphasis on the high-temperature properties of the metals on the basis of metallographic structure is given to S. H. Weaver, of the General Electric Company, and his associates.

Although it is now possible to get a steel of what is assumed to be the desired type from a steel mill, the grain size and the constitutional characteristics of the crystals may not be of the most suitable type when the metal has been fabricated and installed in the power plant. Constitutional changes may be brought about during fabrication which may adversely affect the type of carbide crystals and grain size, with a resultant change in the high-temperature properties of the metal. For instance, when pipe is bent it is heated, and the temperatures employed for heating may affect grain size and the nature of the carbide crystals. If the temperature of the heating is too low, it may even result in bringing about an agglomeration of the carbides, which is known as spheroidization. Such changes as have occurred during the bending, other than those of spheroidization, can usually be taken care of by a normalizing or annealing of the metal from 1700 F. This operation is not always possible, because it is not always practicable to place a bent section of pipe into a normalizing furnace.

Also, sections of pipe are now being assembled to an increasing degree by welding. This, of course, introduces temperature gradients ranging all the way from the temperature of molten steel to room temperature. The welding operation also introduces changes in chemical composition. Where it is possible to normalize or anneal the material thus welded in a furnace from 1700 F, most of the objections with regard to changes which have been brought about in the grain size and the grain structure are eliminated. Yet, it is not always possible to normalize or anneal the material from 1700 F. In most cases, it is possible only to stress-relieve it from 1200 F. This means, of course, that the grain size and the grain structure may be different from that which is preferred and, therefore, in certain sections, all of the precautions which have been taken to get preferred grain size and a preferred grain structure have gone for naught.

There is yet another matter which should, at least, be mentioned at this time. It relates to the tendency of carbon-molybdenum steel, under certain conditions of time, stress, and temperature, to become practically nonductile. To be sure, most of the known cases to date, in which low ductility has been found, have been under conditions of a high or a relatively high stress. For instance, when a steel was held under a stress of 16,000 psi at 1000 F, fracture occurred in but a few thousand hours, with elongations and reductions of area around 5 per cent for each.[4] This stress value is about 3 times the allowable stress value given by the A.S.M.E. Boiler Code for this kind of steel at this temperature. Some claim that, if the stress values are kept within those recommended by the Boiler Code, no brittleness will develop in the steel. Only time or a systematic investigation of this subject will tell whether or not this kind of steel will maintain normal ductility if conservative stress values are used.

Use of Bolts in High-Temperature, High-Pressure Work

Although the use of bolts in high-temperature, high-pressure lines is rapidly declining, there are still places in which they are extensively used. Bolts are required for the assemblage of certain turbine parts. This use is most important. It is seldom, however, that bolts are used in modern piping systems, as welding has replaced most other types of pipe joints.

From time to time, failures with bolts are reported. These may be due to improper composition of material, improper heat-treatment, faulty material, or abuse in installation.

The American Society for Testing Materials has issued two specifications for high-temperature alloy-steel bolting materials. One merely gives three classifications on the basis of tensile requirements with chemical limits for only sulphur and phosphorus. The other gives eleven types of steels with the full chemical composition of each type. Not all of these eleven types are suitable for all kinds of service. Also there are many classes of steel which are not among the eleven types given but which have a place in this field.

In the selection of bolt stock, care must be exercised to see that the material is of a nonaging type. Further, since all bolt material shows lower impact values at some temperatures than at others, the bolt stock selected should be such as will have a good impact value at the temperature at which bolt is to be used.

Also, care must be exercised to see that the material will not develop low impact values in service. When found, these low values are a manifestation of aging that is produced by strains set up in the quenching operation when followed by a heating for the necessary time at moderately elevated temperatures or by an overstraining, followed, in turn, by a heating cycle.

As a rule, trialloy bolts are superior to dualloy bolts. In this connection, silicon is considered as an alloy when in quantities above 0.3 per cent. Many of the difficulties reported have been with dualloy bolting material.

Improper heat-treatment may be of two types—one a heat-treatment giving improper physical test values, and the other, one in which it is possible for quenching cracks and other defects to develop.

In the matter of heat-treatment, there are two schools of thought—the one wishes high ductility in the finished bolt, even at a sacrifice of strength, while the other seeks high strength, even at a sacrifice of ductility. Personally, the authors favor bolts with high strength characteristics as these resist distortion when they are tightened to a greater extent than the low-strength bolts.

In the realm of poor heat-treatment practice, the mass charging and mass quenching of bolt stock and bolts may yet be found in some plants. To the principle of mass production there is no objection but, when carried out without due regard to each individual piece, there is decided objection. Each piece must be heated and quenched uniformly, otherwise, nonuniformity of stock results. Some of the consequences of nonuniformity in heat-treatment are quenching cracks and too low or too high tensile properties.

Some of the failures which have taken place have been due to faulty material. This may mean an improper choice of material or defective stock. Defective stock may be due to lack of compliance with chemical and physical requirements, stock unduly filled with inclusions, stock with cracks due to faulty quenching or improper machining practice, or other causes of a similar character.

Finally, failures due to abuse in installation must not be forgotten. Less frequently than formerly but, nevertheless still sometimes occurring, undue strains are placed on the bolts during tightening-up operations. These lead to cracks which, in due time, result in bolt failures. Most companies now control the forces used in tightening the bolts so that excessive stresses are not set up, reducing, in consequence, the number of failures from this cause.

The selection of proper bolting material is by no means as simple as may, at first glance, appear to be the case. Due regard must be given to room-temperature tensile properties, proper high-temperature properties, such as adequate creep strength, and acceptable impact values, both at room temperature and at the given elevated temperatures, with little, if any, drop in the values, even after long-continued service.

It is quite apparent from all that has been said that we are yet in the developmental stage so far as suitable alloys for pipes and bolts for high-temperature service are concerned. A master

[4] Courtesy of The Timken Steel and Tube Company.

alloy which will resist oxidation and embrittlement, have high strength at elevated temperatures, irrespective of the nature of its constitutional structure, respond readily to working and welding, and, in addition, be reasonably inexpensive has not as yet been found. Great progress in this direction has already been made and further progress is expected, as many metallurgists are today engaged in bringing forth new and improved alloys for high-temperature service.

Discussion

Hans Dahlstrand.[5] Experience with metals at high temperatures indicates the importance of this subject. Many power plants have been operating at more than 900 F temperature for considerable time and, therefore, experience on the suitability of the materials exposed to such temperatures is being made available. This experience indicates that there is room for much improvement particularly on materials for piping and bolting. Bolts made from certain steels specified by the A.S.M.E. have not in all cases been satisfactory in service whether because of improper heat-treatment of the steel or because the steel would not stand up under the exposed temperatures. It is hoped that we shall have more enlightenment concerning this subject as further increase in operating temperature is contemplated.

F. E. Foster.[6] The conclusion that a coarse-grained steel develops better creep resistance than a fine-grained steel is open to question after a study of the existing data has been made. In particular, a superficial examination of the investigation referred to by the authors indicates that the coarser grain size developed the best creep resistance. However, it is apparent from a study of the results obtained that grain size was coincidental rather than a fundamental factor. For instance, a steel with a 5 to 7 grain size, as shown in the photomicrograph, developed the best creep rate obtained in this investigation. However, two other samples having the same grain size and similar microstructure developed creep rates ranging up to 0.8 per cent per 100,000 hr, or 3 times as much as the example given. The three samples represented three different heats and had received three different treatments prior to testing. Also, steel with a grain size of 7 to 8 is presented as having a creep rate of 2.3 per cent per 100,000 hr.

The original report presents results on six other samples having the same grain size and same type microstructure on which creep rates varied from 1.1 to 2.9 per cent per 100,000 hr. Each of these samples had had the same prior heat-treatment but represented different heats of steel. In addition, a difference in creep rate of only 0.3 per cent was obtained between a 5 to 7 and a 7 to 8 grain size. In regard to photomicrograph Fig. 3, the very high creep rate is attributed to the nonuniform or so-called "duplex" grain. Photomicrographs in the original report show somewhat more uniformity and are in fact classified there as 3 to 6 grain size. It might be noted in passing that a 3 to 6 grain size is required by American Society for Testing Materials, Specifications for Carbon Molybdenum Pipe for High-Temperature Service.

The writer agrees with the authors that the nature and distribution of the carbide appear to be of considerable importance. Miller, Campbell, Aborn, and Wright[7] found that, after tests of 3000 hr duration on carbon-molybdenum steel, the best creep resistance was obtained when the carbide of the pearlite areas was slightly spheroidized and a ground-mass precipitate, probably molybdenum-rich carbide, was finely distributed throughout the ferrite matrix. This, of course, is the direct antithesis of the Widmanstätten type of structure preferred by the authors.

E. H. Krieg.[8] It is most encouraging to have this metallurgical paper made an integral part of the proceedings of the Power Division for it betokens the great importance of metallurgy to the power industry. In acknowledging our indebtedness to the metallurgists, may we at the same time call attention to their large share of responsibility for future progress in the production of power by burning fuel.

Although many metals are being developed for high-temperature piping, the authors call attention to the many factors entering into the selection of piping material. Besides a satisfactory low creep rate, the material must be stable, resistant to oxidation and corrosion, workable, weldable, with a good background of success in minor applications before a major application can be economically justified.

Referring to the photomicrograph Fig. 3, is it possible that a contributing cause of the low creep may be a slight carbide precipitation or spheroidization along the grain boundaries? Would a $\times 500$ magnification more clearly portray such a condition that may not be readily observed at $\times 100$?

Because of the vital importance of the metallographic method of determining acceptable high-temperature properties of steels, would the authors kindly outline the essentials in their closure, because the more engineers who know about it, the more progress will be made in improving the quality of steels available at low price. In other words, we should like to see certain American Society for Testing Materials codes made more rigid as regards quality, because, if everyone demands quality, steels of better quality will be produced as cheaply as former steels of poorer quality. As an illustration, grade B tubing in A.S.T.M. Specification A106-39 is superior to grade A in most respects, yet it now costs no more. Then why retain grade A when it no longer serves any function, although formerly it was considerably cheaper?

Bolting material will continue to occupy a highly important position for some time to come. It is true that valves are being welded into the pipe lines and that in a few cases bonnets are being made, boltless, by welding them on or by using a breech-block design which was adopted for the 2800-lb valves at the Twin Branch plant. But bolting will continue to be used in turbines, and we already have many bolts in service which we shall have to live with for many years to come. We thoroughly agree with the authors that the greatest care should be exercised in their selection and application, if trouble is to be avoided.

G. B. Warren.[9] During the last few years, temperatures adopted by the power industry have jumped from 750 to 825 F, then to 900 and now to 950 F. Much test work has supported these temperature increases but as yet, at the most, only a few years of actual experience. The emphasis placed in this paper, upon the proper manufacture of the steel itself, the heat-treatment of the fabricated pipe, metallographic structural control, and the avoidance of overstress in service, may, if heeded, be conducive to much more satisfactory piping and bolting systems.

Although, as pointed out, the use of bolts is declining in piping and valves, in the turbines themselves bolts are still extensively

[5] Engineer in charge, Steam Turbine Department, Allis-Chalmers Manufacturing Co., Milwaukee, Wis. Mem. A.S.M.E.

[6] Metallurgist, Consolidated Edison Company of New York, Inc., New York, N. Y.

[7] "Influence of Heat-Treatment on Creep of Carbon-Molybdenum and Chromium-Molybdenum-Silicon Steel," by R. F. Miller, R. F. Campbell, R. H. Aborn, and E. C. Wright, Trans. American Society for Metals, vol. 26, 1938, pp. 81–101.

[8] Engineering Department, American Gas and Electric Service Corporation, New York, N. Y. Mem. A.S.M.E.

[9] Designing Engineer, Turbine Engineering Department, General Electric Company, Schenectady, N. Y. Mem. A.S.M.E.

used, therefore, a need for better and more reliable bolts yet exists and probably will continue to exist. The authors indicate the necessity of tightening bolts properly and avoiding over-tightening, particularly for high-temperature service. This is a matter of great importance and appears to the writer to be even more so as we acquire more experience with operation at higher temperatures.

For the last several years, in developing turbine designs at the General Electric Company, efforts have been made to reduce the duty imposed upon bolts of high-temperature machines as much as possible. Working stresses have been drastically lowered, double-shell designs in many cases have permitted equalizing the horizontal-joint bolt load between two rows of bolts, elasticity incorporated in the bolting system has tended to reduce strains due to temperature variations, and designs have been made in such a way as to reduce the temperatures and the temperature variations to which bolted joints have been subjected.

Recently we have been giving more thought to the mechanical design and construction of the bolts themselves, with the idea of reducing stress concentrations.

We have availed ourselves also of the magnetic-powder method of checking bolts at the turbine-inspection period. The bolt threads are first lacquered white and then tested to detect incipient cracks.

It is possible that, until a method of manufacturing better bolts has been developed, a few of the highest stressed and hottest bolts will have to be regarded as "renewable parts." The cost would not be very great.

In the last few years, an increasing number of long-time high-temperature rupture tests have been run both by the authors and by ourselves. We have commenced to learn that grain size and other metallurgical characteristics have an important influence both upon the creep strength and upon the long-time rupture strength at high temperature. It appears probable that there is a relationship between these two values somewhat similar to that existing between elastic limit and tensile strength at ordinary temperatures.

Thus, it is thought that, possibly, heat-treatments which improve the creep strength may not improve the rupture strength a corresponding amount, and may reduce the strain at rupture in much the same manner as certain heat-treatments may increase the elastic limit, without greatly increasing the tensile strength, and reduce the elongation. In many cases, good engineering in the case of low temperatures calls for the use of material heat-treated for the lower elastic limit. We have been considering whether or not good engineering might likewise call for a heat-treatment or grain size which would give a lower creep strength with a better margin between it and the rupture strength, and greater elongation before rupture takes place. Since our own test results are not without exception in this connection, it would be welcome to have the authors' opinion on the general principles outlined.

The writer would also like to ask the authors another question, the answer to which might be of material assistance to operators engaged in utilization of materials under the conditions covered:

Does a heat-treatment which restores the high Charpy impact strength of a bolt, which has lost its high Charpy value as a result of stress, temperature, and time, likewise restore the possible life of the bolt before rupture, providing, of course, the reheat-treatment takes place before rupture has actually developed?

Authors' Closure

The discussion contributed by Messrs. Dahlstrand, Foster, Krieg, and Warren to this paper is much appreciated.

With regard to the discussion by Mr. Foster, possibly creep strength is a better criterion of high-temperature properties than creep rate, although in the paper reference was made only to creep rate. In the case of the steel in which the creep rate was 0.3 per cent per 100,000 hours, the creep strength, on the basis of a stress which would produce an assumed elongation of one per cent in 100,000 hours, was 17,400 psi. In the case of the steel which showed a creep rate of 0.8 per cent, the creep strength was 15,250 psi, and in the case of the steel which showed a creep rate of 2.3 per cent, the creep strength was 12,500 psi. Although it is true that the creep rate is nearly three times as great in the case of the steel which showed a creep rate of 0.8 per cent, as compared with the one which showed 0.3 per cent, the difference in creep strength is by no means of this order as the values are but 15,250 psi as against 17,400 psi.

So many factors which affect the high-temperature properties of steel enter into its manufacture that it is not possible to draw conclusions from merely a few tests. It has been our experience that in general carbon-molybdenum steel possessing a Widmanstätten type of structure shows better high-temperature properties than steels in which the pearlite areas are spheroidized.

With reference to Mr. Krieg's discussion, it is quite possible that a slight carbide precipitation or spheroidization would be found in the steel illustrated by Fig. 3, had it been examined at a magnification of 500 diameters rather than 100 diameters.

Mr. Warren's discussion is timely and interesting. His question as to whether or not it is possible to restore the life of a bolt by reheat-treatment in case rupture has not actually developed is, of course, subject to a number of conditions. Provided the steel is restored to its original ductility and to its original Charpy value by reheat-treatment, there is no reason to assume that it is not in as acceptable condition as it was initially.

Notes on the Measurement of Cylinder Power of High-Speed Steam Passenger Locomotives—Apparatus and Methods

By L. K. BOTTERON,[1] OMAHA, NEB.

The common practice of determining the indicated horsepower of steam locomotives by the use of mechanical indicators driven by a reducing motion attached to the crosshead has limitations for high-speed locomotives. A survey of engineering literature shows that mechanical, optical, and electrical indicators have been developed and are in use primarily for high-speed internal-combustion-engine testing, but it is doubtful if any of these types would be adaptable to locomotive road testing with the exception of the electrical. Due to the limitations of mechanical indicators, the research and mechanical-standards department of the Union Pacific Railroad Company for the last 2 years has used the heat-drop method for the measurement of indicated horsepower.

STEAM locomotives now run for short periods at speeds in excess of 100 mph. Speeds of 90 mph for sustained periods are not unusual. Running over a division at 75 mph, with the exception of the acceleration and deceleration periods in stopping, starting, and observing local speed restrictions, is common practice. At diameter speed, the driving wheel rotates at 336 rpm; high-speed passenger locomotives operate a considerable part of the time at higher than diameter speeds. Considering the size of locomotive cylinders, the rotational speeds are high as compared with other reciprocating engines.

The difficulties encountered in taking indicator cards on high-speed steam locomotives are many and it must be borne in mind that, compared with indicating stationary engines, the problems encountered are far more complex. Reducing motions are a constant source of trouble due to breaking and rapid wear as they must run unprotected from the weather. Due to roadway clearances and interferences of locomotive parts, it is often difficult to apply any sort of a reducing motion. Common to all indicators driven with a reducing motion, the stretching of the indicator cord increases as the speed increases, the indicator-drum spring is hard to adjust correctly, and even the drum is a source for errors due to its inertia. L. Pendred, in an article (1)[2] on high-speed indicators, does not believe any reciprocating reducing motion is reliable above 500 rpm. In the case of steam locomotives, this limit more likely would be 300 rpm. Mechanical indicators of simple and rugged construction for speeds up to 500 rpm are on the market but, if the indicator-drum motion does not proportionally follow the crosshead, the cards are of little or no value.

Since reducing motions, cord stretch, and drum inertia are such a source of error, the thought arises that it might be better to dispense with the reducing motion entirely and drive the drum at constant speed in one direction. In this case it would be necessary to apply an apparatus for marking crosshead dead centers on the card. Also, the drum speeds would have to be high as shown by the following example:

A locomotive with 80-in-diam drivers, at a speed of 100 mph is making 420 rpm, which completes a cycle in $^1/_7$ sec. To obtain cards 3 in. long, paper travel of $1^3/_4$ fps would be required.

The errors common to the mechanical indicator are well covered in technical literature (2). On the steam locomotive, all of the mechanical-indicator errors and troubles common to stationary work are encountered plus some additional ones. The most troublesome of these are the severe rapid vibrations of the front end of the locomotive at high speeds. Front-end vibration will in turn vibrate the entire indicator and especially disturb the pencil motion. Sticking pistons are common, due to highly superheated steam and bits of boiler scale and other foreign matter getting into the indicator cylinder. The operator labors under conditions which are not conducive to good work and, furthermore, there is the hazard of striking obstacles such as vehicles or animals. There is also the possibility of the locomotive meeting with an accident such as knocking out a cylinder head.

Due to clearance limits, indicators usually cannot extend out beyond the width of the cylinders. This means that indicators cannot be connected directly into the cylinders. Instead, relatively long pipes must be used between the cylinder and the indicator in order to locate the instrument so that it is accessible to the operator and within clearance limits. The errors due to long pipes are very serious and at high speeds the events, as shown by the card, lag so far behind the actual events in the cylinder as to make the card valueless both as for the events and the mep (3).

Mechanical indicators, developed primarily for internal-combustion-engine testing, offer possibilities for high-speed steam-locomotive testing, provided the drum is driven at constant speed and not by a reducing motion. However, the errors due to long pipes and locomotive vibration would still be present, and the operator would have to ride the front end. Pressure-time cards instead of pressure-volume cards would be obtained and, to determine the mep, it would be necessary to redraw the cards on a pressure-volume basis unless a special integrator were available.

Optical indicators do not seem to offer any possibilities for locomotive road tests. They are essentially laboratory instruments and are not rugged enough to stand shocks and vibrations.

Electrical-Type Indicator

The indicator which offers possibilities for determining the indicated horsepower of high-speed steam passenger locomotives is the electrical type, such as the Martin and Caris indicator (4), the indicator described by H. T. Sawyer (5), and the indicator advertised by the General Electric Company (6). With the electrical indicator, the only apparatus required on the locomotive are the pressure-measuring heads, an electric dead-center marker, and wiring running back to the test car. The oscillograph, which is the recording instrument, would be carried on the

---

[1] Engineer of Road Tests, Union Pacific Railroad Company. Mem. A.S.M.E.

[2] Numbers in parentheses refer to the Bibliography at the end of the paper.

Contributed by the Railroad Division and presented at the Semi-Annual Meeting, Milwaukee, Wis., June 17–20, 1940, of The American Society of Mechanical Engineers.

test car. The electrical indicator therefore possesses many inherent advantages over other types. The pressure-measuring heads are attached directly to each head of each cylinder, thereby eliminating the error due to piping. Any number of cylinders can be indicated simultaneously. Reducing motion is not used. The operator is not required to ride the front end.

Conditions which might interfere with the accuracy of the electrical indicator are the effects of vibration and temperature differences on the pressure-measuring heads. The electrical indicator makes only pressure-time cards, but with a special integrator the mep of such cards may be directly determined.

Heat-Drop Method of Measuring Indicated Horsepower

Due to the limitations of mechanical indicators and the hazard of men riding the front end, the research and mechanical-standards department of the Union Pacific has used the heat-drop method for determining the steam rates and indicated horsepower of high-speed steam passenger locomotives. The methods of Arthur Williams (7) have been followed and the results obtained for high-speed work have been found to be reasonably accurate.

Briefly, the heat-drop method is based on the first law of thermodynamics. Thus in the case of the steam locomotive, the difference between the total heat in the steam to the cylinders and the steam exhausted from the cylinders is converted into mechanical work regardless of the processes which go on in the cylinder. The question has been raised as to the proper location of thermocouples for measuring exhaust-steam temperatures and it has been pointed out that the state of the steam during the exhaust period is variable (8). The most reasonable location for the exhaust-steam thermocouples is in the exhaust-nozzle stand, since the exhaust pressure at that point has the least pulsation and the steam has had time to mix. The heat content of the exhaust steam cannot change between the valve chamber and the exhaust stand except for the influence of radiation and kinetic energy. If these two items are corrected for and the pressure and the temperature of the exhaust steam are accurately determined in the exhaust stand, it seems that a reasonably accurate determination might be made of the total energy.

The heat-drop method determines the steam rate only. In order to calculate the indicated horsepower, it is necessary to know the steam to the engine as well as the steam rate.

Knowing the pressure and temperature of the steam in the exhaust-nozzle stand, it is a simple matter to calculate the flow through the nozzle, provided the coefficient of discharge is known. Of course, all formulas for steam flow are based upon steady conditions and some doubt will arise as to whether the formulas hold true for locomotive conditions where the flow is pulsating. For low speeds, the pulsations are of such magnitude that the flow computed from the back pressure will be high. However, at high speeds, the exhausts are so frequent and the pressure fluctuations of such small magnitude that the gage will read an average pressure, accurate enough for calculating the flow.

The exhaust-pressure gage should be piped up so as to have a constant hydrostatic head. This can be done by running a pipe vertically from the side of the nozzle stand through the smokebox and terminating the pipe within the clearance limits. At this point, a coil of copper pipe is connected into the vertical pipe and a pipe with a gradual drop is run from the coil to the gage in the cab. The vertical pipe should be 1 in. or larger to be self-draining. Either a mercury manometer or a suitable Bourdon-tube gage may be used for indicating exhaust pressure in the cab.

A potentiometer will be found to work very satisfactorily for the determination of the temperatures, if the galvanometer is removed from the instrument and attached to the data board which is held by the operator when taking readings. Arthur Williams in his paper (7) illustrates and discusses such a mounting. During a test it is imperative to remove all auxiliary exhausts from the exhaust passages, as the exhaust steam from the auxiliaries is in a different state from the exhaust steam from the engines. Of course the exhaust-steam temperature taken in the exhaust stand must be the temperature of the exhaust steam from the engine only. Also by removing the auxiliary exhausts from the exhaust passages, the steam to the engines equals the steam through the nozzle in the case of locomotives equipped with live-steam injectors while, in the case of locomotives equipped with feedwater heaters, the steam to the engines equals the steam through the nozzle plus the steam condensed from the exhaust passages for feedwater heating.

No definite data can be given which will cover the coefficients of discharge of locomotive-exhaust nozzles due to such a wide variety of nozzles being used. Each railroad would have to determine the characteristics of its own nozzle. In general, it will be found that for steady conditions round-hole nozzles without sharp edges or projections and having a smooth approach in the stand have coefficients of about 0.97 to 0.98 for their entire pressure range, while nozzles with complicated shapes and sharp edges have coefficients of 0.8 and lower at low back pressures with the coefficient increasing up to a maximum of about 0.93 at 12 psi pressure.

The author calculated the flow through the plain round-hole exhaust nozzle of Baldwin locomotive No. 60000, considering the flow adiabatic and using a coefficient of discharge of unity, but making no allowance for the velocity of the steam in the exhaust pipe (9). The calculated results, compared with the test-plant measurements, show that, for exhaust-pipe pressures from 9.1 to 19.8 psi, calculated flows are from 3.59 per cent too high to 3.42 per cent too low, with an average of 0.62 per cent too low.

Equipment and Procedure for Heat-Drop Method

The equipment and procedure required for the use of the heat-drop method are simple. It is only necessary to measure steam-pipe and exhaust-stand pressures and temperatures accurately.

The indicating potentiometer is a simple rugged instrument. If any wiring becomes broken, disconnected, or grounded, the potentiometer galvanometer cannot be balanced. Thus there is no possibility of false readings. Only one operator is required and by placing the potentiometer and pressure gages in the cab the operator is removed from the front end to a safer location. The heat-drop method has the advantage over all other methods as it determines both instantaneous steam rate and indicated horsepower. A set of readings can be worked up in about 20 min.

BIBLIOGRAPHY

1 "High-Speed Engine Indicators," by L. Pendred, *Engineering*, vol. 115, January 26, 1939, pp. 119–121.

2 As an example: "Experimental Mechanical Engineering," vol. 1, "Engineering Instruments," by H. Diedrichs and W. C. Andrae, John Wiley and Sons, Inc., New York, N. Y., 1930.

3 "The Effect, Upon the Diagram, of Long Pipe Connections for Steam-Engine Indicators," by W. F. M. Goss, Trans. A.S.M.E., vol. 17, 1896, pp. 398–412.

4 "A New Electrical Engine Indicator," by E. J. Martin and D. F. Caris, *S.A.E. Journal*, vol. 23, July, 1928, pp. 87–97.

5 "An Indicator for High-Speed Engines," by H. T. Sawyer *Mechanical Engineering*, vol. 58, May, 1936, pp. 283–285.

6 "To Measure Pressure Electrically," advertisement of General Electric Company, *Mechanical Engineering*, November, 1939, ad. p. 7.

7 "Measurement of Steam Rate and Indicated Horsepower of Locomotives," by Arthur Williams, Trans. A.S.M.E., vol. 57, 1935, p. 495.

8 "Measurement of Steam Rate and Indicated Horsepower of Locomotives," by Arthur Williams, discussion, Trans. A.S.M.E., vol. 58, 1936, pp. 250–256.

9 "Locomotive Back Pressure," by L. K. Botteron, *Railway Mechanical Engineer*, vol. 104, July, 1930, pp. 400–403.

Discussion

R. M. Ostermann.[3] The author has rendered a distinct service by expounding the advantages of the heat-drop method for determining the water rate of a locomotive. While the paper does not state in detail how the heat-drop method, as recommended by Mr. Arthur Williams, was checked by him in relation to the method of establishing water rates with an indicator, the writer submits that, in his opinion, the value of the heat-drop method, because of its simplicity, is outstanding for comparing the performance of a locomotive with and without certain modifications of design which affect the water rate. Many problems of this sort present themselves constantly to the railroads, and are frequently left unsolved because of the cost and inconvenience of making tests with indicators. To determine the influence of certain modifications in the design of a locomotive upon the drawbar pull and drawbar horsepower of a locomotive, which is only possible with dynamometer cars, is, of course, still more expensive. In this category the writer would include modifications in the setting of the valves, changes in steam pressures and steam temperatures, or other changes in both valve and cylinder designs, steam pipes, and front-end arrangement.

All these are matters which are being continually studied by the mechanical engineers of the railroads. However, many of them have not been given the facilities for testing out such changes, because of the cost and time involved in such tests. The heat-drop method of determining the water rate can be used on any locomotive in regular service. One man in a cab can make all necessary determinations of pressures and temperatures, and take many readings from which averages may be obtained.

In tests of this kind, which can be conveniently carried out on one and the same locomotive, before and after the modification, it is less important that the amount of steam required per indicated horsepower-hour be determined with the utmost accuracy, than to determine correctly the degree of improvement, on a percentage basis, which has been effected by the modification under consideration. Even if it is assumed that the measuring of the temperatures and pressures during the determination of the heat drop involves certain errors, it is altogether probable that errors of the same magnitude will be involved when using the same test equipment and the same observer on the same locomotive after it has been modified.

Arthur Williams.[4] This paper discusses the problems involved in determining the indicated horsepower of steam locomotives in a very complete and concise manner. Since 1935, a number of tests have been run using the heat-drop method for determining cylinder efficiency. Those conducted on the Union Pacific Railroad have been extremely complete. These tests and others all seem to favor the use of the heat-drop method for road tests of locomotives. In the last 5 years, no change has been made in the general method of making these determinations. There have been some refinements, designed to simplify the calculations. The exact formula for determining the steam rate in pounds per indicated horsepower-hour is

$$S = \frac{2545}{(H_1 - H_2) - \left(\dfrac{V_2^2}{50000} + R\right)}$$

where S = steam rate, lb steam per ihp-hr

H_1 = heat content of steam in steam pipe, Btu per lb

H_2 = heat content of exhaust steam, Btu per lb

V_2 = velocity of exhaust steam, fps. (Note that H_2 and V_2 are derived from same readings of pressure and temperature)

R = radiation loss between points of measurement, Btu per lb

The radiation loss can be calculated from the usual heat-transmission formulas for any given cylinder design. An approximate figure for the total radiation loss in Btu per hour can be obtained by multiplying 2400 by the cylinder diameter in inches. Dividing this by the weight of steam to the cylinders will give the radiation loss per pound of steam. The velocity V_2 can be calculated knowing the steam flow, pressure, and temperature of the steam, and the cross-sectional area of the passage.

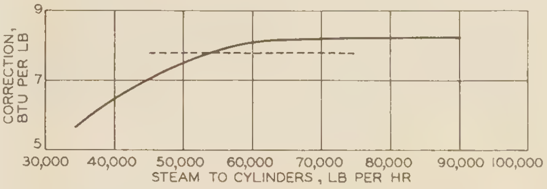

Fig. 1 Correction for Kinetic Energy Change and Radiation

To make these calculations for every reading should not be necessary. Fig. 1 of this discussion shows the correction for both kinetic energy and radiation for various rates of steam flow. These calculations were made for a modern steam locomotive which was tested by the heat-drop method. Nearly all of the tests conducted were in the range of 45,000 to 70,000 lb of steam per hr to the cylinders. By using an average correction of 7.8 Btu per lb, the maximum error introduced was only 0.8 Btu and the average error practically negligible. To calculate the results in this manner was then simple. The heat content of the steam for the conditions observed at the exhaust was subtracted from the heat content in the steam pipe and the correction of 7.8 Btu subtracted from this figure. This gave the corrected heat drop, and dividing into 2545 gave the steam rate in pounds of steam per indicated horsepower-hour.

This figure of 7.8 Btu per lb applies only to this particular case and is higher than would usually be found. This was due to measurement of the exhaust pressure and temperature at a point in the exhaust stand with relatively small area.

To save time in interpolating the values in steam tables, it is convenient to plot heat content against steam temperature for various lines of constant steam pressure on a large scale for the range in which the tests are being conducted.

In using the exhaust nozzle as a flow meter, it is important that accurate observations of exhaust pressure be made. The method described in the paper appears to be accurate and practical for locomotive use. The principle of using a condensing coil or reservoir to obtain a constant hydrostatic head on a gage or manometer is used for industrial steam-flow meters, and is particularly important where low pressure drops are being observed.

The statement is made that no definite data can be given which will cover the coefficients of discharge of locomotive-exhaust nozzles. No doubt with proper publication of results the information on this will be increased as time goes on, and in the future it should be possible to have accessible sufficient data on this subject to cover a wide range of conditions.

While the heat-drop method is convenient for observations of over-all cylinder efficiency, studies of valve events and pressure conditions in the cylinder require some form of indicator. Therefore, it is important that improvement be made in indicating equipment so that accurate readings can be obtained at high speeds.

[3] Vice-President, Western Territory, The Superheater Company, Chicago, Ill. Mem. A.S.M.E.

[4] Manager, Production Engineering Division, The Superheater Company, East Chicago, Ind. Mem. A.S.M.E.

Train Acceleration and Braking

By R. Clark Jones,[1] Cambridge, Mass.

This paper presents a direct analytical method for determining the equations of the motion of a steam train, either when it is being accelerated or when it is being braked. The following important relations are found: The relation between (*a*) speed and acceleration or deceleration; (*b*) speed and time; and (*c*) distance traveled and speed or time. The results obtained are compared with actual performance records. The author feels that, in some cases, an analytical method of the type presented in the paper compares favorably with numerical or graphical integration.

The method is based in part upon the well-known Davis formula, which states that the resistance encountered by a moving train may be represented quite accurately by means of an expression of the general form $a + bV + cV^2$, that is, by a form quadratic in the velocity V. Detailed information and data for calculating the coefficients a, b, and c for modern types of passenger trains, in a form conveniently usable, is to be found in a paper by A. I. Totten (1).[2] The gross tractive-effort-versus-speed curve of a steam locomotive can also be approximated quite closely by a similar quadratic form in the velocity, with the following difference, however: The typical tractive-effort curve consists of a flat portion at low speeds, where the tractive effort is limited only by slipping or maximum boiler pressure, and of a falling curve at higher speeds, as in Fig. 1; the falling part of the curve can be represented quite well by a quadratic form.

G. E. Terwilliger (2) and A. C. Barrow (3) are among those who have previously discussed the subject treated in this paper.

The gross tractive effort may be calculated by the highly developed methods of E. G. Young and C. P. Pei (4), or it may be estimated by other methods, such as Cole's factors. It will usually be known, in any event.

The decelerating force of a constant brake-shoe pressure also varies with the speed in such a way that it can be expressed fairly well by a quadratic form.

We see, therefore, that it is always possible under the given conditions to represent the net accelerating force (positive or negative) on a train by an expression of the form $a' + b'V + c'V^2$, where a', b', and c' are constants. By Newton's third law, we then have

$$A = \frac{dV}{dt} = a + bV + cV^2$$

$$\frac{dV}{dt} = \frac{0.01090}{M}(a + b'V + c'V^2) \ldots [1]$$

where

A = acceleration, mph per sec
V = velocity, mph
t = time, sec
M = total weight of train, short tons

[1] Research Laboratory of Physics, Harvard University.

[2] Numbers in parentheses refer to the Bibliography at the end of the paper.

Contributed by the Railroad Division and presented at the Semi-Annual Meeting, Milwaukee, Wis., June 17–21, 1940, of The American Society of Mechanical Engineers.

and where $a' + b'V + c'V^2$ is the net accelerating force in pounds.

We shall suppose then, that we have a way of obtaining the coefficients a, b, and c in Equation [1]. To obtain the desired equations of motion from Equation [1], it is necessary to integrate twice an equation of the form

$$\frac{dV}{dt} = a + bV + cV^2 \ldots\ldots\ldots\ldots\ldots [2]$$

where V itself is the first derivative of the distance in respect to the time. The problem before us, therefore, is the integration of Equation [2].

We shall assume that the speed and the distance x from some fixed point are given at the time $t = t_0$. Thus the initial conditions are

$$\left.\begin{aligned} V &= V_0 \text{ at } t = t_0 \\ x &= x_0 \text{ at } t = t_0 \end{aligned}\right\} \ldots\ldots\ldots\ldots\ldots [3]$$

The integration of Equation [2] is now straightforward, but is complicated by the fact that there are three distinct mathematical cases (unless one uses a complex number representation). The three mutually exclusive cases are distinguished by the following criteria:

$$\begin{array}{lll} \text{Case 1} & \left|\dfrac{2cV_0 + b}{(b^2 - 4ac)^{1/2}}\right| > 1 & \text{The roots of} \\ & & a + bV + cV^2 = 0 \\ \text{Case 2} & \left|\dfrac{2cV_0 + b}{(b^2 - 4ac)^{1/2}}\right| < 1 & \text{are real.} \end{array}$$

Case 3 The roots of $a + bV + cV^2 = 0$ are not real.

In the acceleration of trains, we always have to do with cases 1 or 2; in fact, it will always be case 1 if the tractive effort versus speed curve is concave upward, as is usually the case. In the braking of trains, however, we may encounter all three cases. One should remember, of course, that our equations correspond to physical reality only for positive values of V; if we try to extend our solutions of Equation [2] into a range of A, t, or x, where V would be negative, the solution has no physical interpretation in this range.

It is clear from Equation [2] that, if a limiting speed exists, it must be given by the condition $dV/dt = 0$. Indeed, the limiting speed is always the root

$$V_\infty = -(b + q)/(2c) \ldots\ldots\ldots\ldots\ldots [4]$$

where

$$q = (b^2 - 4ac)^{1/2}$$

The converse of this proposition is not always true, because V_∞ as defined by Equation [4] may be negative, or q may be an imaginary number.

The actual integration of Equation [2] for each of the three cases is carried out in the Appendix. We shall refer to the results there obtained in the next section.

Application to the "Hiawatha"

In order to exemplify the use of these considerations, we shall apply them to a discussion of the acceleration of the *Hiawatha*, crack train of the Chicago, Milwaukee, St. Paul & Pacific Railroad. This train runs daily between Chicago and St. Paul, a distance of 410 miles, in an average time of $6^1/_2$ hr. The regular

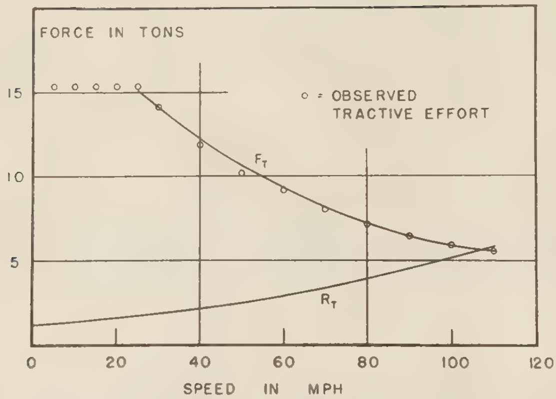

FIG. 1 SHOWING HOW TRACTIVE EFFORT AND TRAIN RESISTANCE OF THE "HIAWATHA" DEPEND UPON SPEED

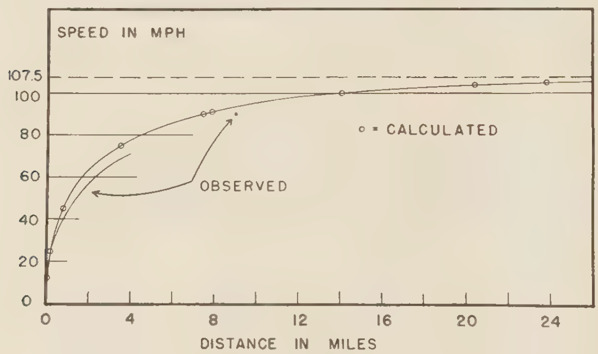

FIG. 2 COMPUTED AND OBSERVED SPEED-DISTANCE RELATION OF THE "HIAWATHA"

train consists of 9 cars, engine, and tender, with a total weight of 1,409,400 lb.[3]

Through information courteously supplied to the author by the Milwaukee Railroad, and by reference to the paper (3) by A. I. Totten, a theoretical expression for the resistance of this train has been obtained. This expression for the train resistance is

$$R_t = 2610 + 21V + 0.56V^2 \qquad [5]$$

The cylinder tractive effort was also supplied by the railroad, and is expressed graphically by the open circles in Fig. 1, whereas the solid line F_t is the author's quadratic approximation to these data. The equation for F_t

$$F_t = 41{,}530 - 503V + 2.07V^2 \qquad [6]$$

was obtained by requiring that it have the correct value at 30 mph and 100 mph, and that it have the correct slope at 100 mph. The quantity $F_t - R_t$ is the net accelerating force on the train, and then Equation [1] becomes

$$\frac{dV}{dt} = 0.601 - 0.00810\,V + 0.00002335V^2 \qquad [7]$$

whence

$$\begin{aligned} a &= 0.601 \\ b &= -0.00810 \\ c &= 0.00002335 \\ q &= 0.00308 \\ V_\infty &= 107.5 \text{ mph} \end{aligned}$$

[3] Reference is to the 1936 *Hiawatha* train, and not to that placed in service in 1938

Equation [7] holds approximately for the range of speed from 25 to 120 mph. For the range from zero to 25 mph, however, as we see by Fig. 1, the tractive effort is constant at the large value of 30,600 lb. The resistance changes but little in this range, and so the net force is practically constant at 27,600 lb. Since the mass of the train is 705 tons, the acceleration is 0.426 mph per sec, if the net force is treated as constant. Then we have

$$V = 0.426\,t \qquad [9]$$

$$x = 0.000591\,t^2 \qquad [10]$$

for V less than 25 mph, by the ordinary laws of uniformly accelerated motion. From Equation [9], the time to reach 25 mph is 59 sec, in which time the train goes 0.204 mile, by Equation [10]. Thus at V_0 = 25 mph, we have

$$\begin{aligned} t_0 &= 59 \text{ sec} \\ x_0 &= 0.204 \text{ mile} \end{aligned}$$

These are the initial conditions for the range in which Equation [7] holds.

For the latter range, we have $(2cV_0 + b)/q = -2.251$; therefore, we are concerned with case 1. With the use of the values given with Equation [7], we obtain from Equations [C1*a*], [C1*b*], and [C1*c*] of the Appendix

$$t = 649 \operatorname{ctnh}^{-1} (2.63 - 0.01516\,V) - 251 \qquad [11a]$$

$$V = 173.4 - 66.0 \operatorname{ctnh} (0.00154\,t + 0.386) \qquad [11b]$$

$$x = 0.0482\,t - 10.98 - 11.90 \log_e \sinh (0.00154t + 0.386) \qquad [11c]$$

These equations, together with Equations [9] and [10], give all the essential information about the motion of the train. Part of this information is expressed graphically in Fig. 2, in which we find the speed-distance curve calculated from Equations [11]. In the same figure are plotted some actual performance data; the solid experimental curve was plotted through 50 closely spaced empirical points, whereas the single point represents a statement in a letter from C. H. Bilty, of the Milwaukee road: "I recall that while riding one of the *Hiawatha* engines, I observed the acceleration from rest was 90 mph in 9 min within a distance of 9 miles." It would appear that the locomotive was being used at nearly its maximum capacity on this occasion.

The fact that the maximum tractive effort is not used in practice probably accounts for most of the discrepancy between the computed and observed behavior. A calculation of the type presented in this section should be performed on the basis of the tractive effort used in practice, rather than upon the basis of the maximum tractive effort. It is possible that the use of a constant fraction of the maximum tractive effort would be sufficiently accurate for this purpose. Equations [11] really represent what the motion of the *Hiawatha* would be if the engine were used at its maximum capacity during the entire acceleration.

We find in Table 1 a more complete presentation of the computations the writer has performed on the basis of Equations [11]. Most of the columns are self-explanatory. The stopping distance and time have been computed on the basis of a constant deceleration of 0.8 mph per sec, a deceleration which checks very well with actual performance data which the writer has received from the Milwaukee road. The "time lost in stopping" column gives the difference between the time t_t and the time that would be required to go the distance x_t at the velocity V. The last column shows the maximum average speed of which the *Hiawatha* would be capable if it were used as a local train between stations x_t miles apart, and remained 90 sec at each station.

It may be shown that the quantity "time lost in stopping" does not increase indefinitely as the train approaches its limiting

TABLE 1 COMPUTED OPERATING DATA OF THE "HIAWATHA"

Speed, V mph	Time to reach V, t, min:sec	Distance, x, miles	Stopping distance, x_s, miles	Stopping time, t_s, min:sec	Total distance, $x_t = x + x_s$, miles	Total time, $t_t = t + t_s$, min:sec	Time[a] lost in stopping, t_l, min:sec	Local[b] train average speed, V_{avg}, mph
12.5	0:30	0.05	0.03	0:16	0.08	0:46	0:17	2.06
25	0:59	0.20	0.11	0:31	0.31	1:30	0:46	6.19
45	1:56	0.79	0.35	0:56	1.14	2:52	1:21	15.7
75	4:34	3.50	0.98	1:34	4.48	6:08	2:33	43.8
90	7:24	7.43	1.41	1:52	8.84	9:16	3:22	49.2
91	7:42	7.85	1.44	1:54	9.29	9:36	3:28	50.1
100	11:37	14.11	1.74	2:05	15.85	13:42	4:12	62.5
104	15:18	20.43	1.88	2:10	22.31	17:28	4:36	70.6
105	17:16	23.87	1.91	2:11	25.78	19:27	4:43	73.9

[a] This is simply the quantity $t_t - 3600x_t/V$.
[b] Length of stop assumed to be 90 sec, with stations x_t miles apart.

speed V_∞, but instead approaches a limiting value. The time lost may be broken into two parts, namely, that lost t_1, during the time the train is being brought to rest, and that lost t_2, during the acceleration. The limiting values of t_1 and t_2 are

$$t_1 = V_\infty/(2A_d)$$

$$t_2 = (V_0/A_a) - V_0^2/(2A_aV_\infty) + 2\Big[Q + \log_e 2 \sinh |Q|\Big]/(b + q)$$

where A_d is the constant deceleration used in stopping the train, and A_a is the constant acceleration obtained until the train reaches the intermediate speed V_0. For the case we have discussed $t_1 = 67$ sec, $t_2 = 246$ sec, or the limiting "time lost in stopping" is 313 sec = 5 min 13 sec. The author feels it to be of some interest that it is possible to express in so simple a manner the maximum time that a train can lose because it makes a stop instead of proceeding at full speed. Suppose, for example, that the train under discussion were required to make a stop on a part of the line which was usually traversed at 100 mph. By inspection of Table 1 we see at once that the extra time required for this stop would be 4 min 12 sec, plus whatever length of time the train might remain in the station. But even if the table had not been computed, we know merely from the computation of $t_1 + t_2$ that the maximum time which the train could lose because of any stop is 5 min 13 sec, plus the length of the stop itself.

For case 2, the square bracket in t_2 should be replaced by $[P + \log 2 \cosh P]$.

The weakness of the method herein presented lies in the fact that the constants a, b, and c are constants, and cannot vary with the time. It will not in general be possible, therefore, to apply our method to the braking of passenger trains, since the brake-shoe pressure is usually varied as the train loses speed and, indeed, in some of the recent trains, the brake-shoe pressure is automatically adjusted so as to secure a uniform deceleration. The method should be valuable in the case of freight-train braking, where the coefficient of friction between shoe and wheel varies considerably as the speed changes. Even in this case, however, the necessarily gradual application of the brakes cannot be taken into consideration; in many cases the time required for the application of brakes will be small compared with the stopping time, so that the method may still give fairly accurate results.

The writer wishes to express his appreciation to C. H. Bilty of the Chicago, Milwaukee, St. Paul & Pacific Railroad for data on the *Hiawatha*, and to Professor J. H. Van Vleck of the department of physics at Harvard University for his constant interest and valuable advice in the preparation of this paper.

Appendix

The following will be devoted to the task of integrating Equation [2], with the boundary conditions of Equation [3], for each of the three cases. We shall discuss case 1 in some detail, and then merely state the result for cases 2 and 3; the latter cases are exactly analogous.

We shall integrate Equation [2] in two steps; by first integrating that equation as it stands, and then substituting dx/dt for V and integrating again. Thus we must first integrate

$$\frac{dV}{dt} = a + bV + cV^2 \quad \ldots\ldots [2]$$

There are three distinct integrals

$$t = -\frac{2}{q} \operatorname{ctnh}^{-1} \frac{2cV + b}{q} + \text{constant} \quad \ldots\ldots [12a]$$

$$t = -\frac{2}{q} \tanh^{-1} \frac{2cV + b}{q} + \text{constant} \quad \ldots\ldots [12b]$$

$$t = \frac{2}{p} \tan^{-1} \frac{2cV + b}{p} + \text{constant} \quad \ldots\ldots [12c]$$

where

$$q = (b^2 - 4ac)^{1/2}$$

$$p = (4ac - b^2)^{1/2}$$

Each of these expressions for t is a solution of the differential Equation [2] and corresponds, respectively, to the three cases previously distinguished.

We continue with case 1 only, that is, with Equation [12a]. Under the condition $V = V_0$ when $t = t_0$, Equation [12a] becomes

$$t = t_0 + \frac{2}{q}\left[\operatorname{ctnh}^{-1} \frac{2cV_0 + b}{q} - \operatorname{ctnh}^{-1} \frac{2cV + b}{q}\right] \quad \ldots [C1a]$$

Solved for V, Equation [C1a] becomes

$$V = \frac{1}{2c}\left[-b - q \operatorname{ctnh}\left(\frac{(t - t_0)q}{2} - Q\right)\right] \quad \ldots [C1b]$$

where

$$Q = \operatorname{ctnh}^{-1} \frac{2cV_0 + b}{q} = \tanh^{-1} \frac{q}{2cV_0 + b}$$

We note as a check that since

$$\lim_{x \to \infty} \operatorname{ctnh} x = 1$$

we have

$$\lim_{t \to \infty} V = -\frac{b + q}{2c}$$

The second step consists in substituting

$$3600 \frac{dx}{dt} = V$$

where

x = distance traveled, miles
t = time, sec
V = speed, mph

in Equation [C1b]. The factor 3600 is inserted because dx/dt is the velocity in miles per sec, whereas V is in mph. With this substitution, Equation [C1b] integrates to

$$x = x_0 + \frac{1}{3600}\left[-\frac{b(t-t_0)}{2c} - \frac{1}{c}\log_e \sinh\left|\frac{(t-t_0)q}{2} - Q\right| + \frac{1}{c}\log_e \sinh|Q|\right] \ldots\ldots [\mathrm{C}1c]$$

where we have used the condition $x = x_0$ when $t = t_0$.

The explicit relation between x and V may be obtained by substituting Equation [C1a] in Equation [C1c]. The relation is cumbersome, however.

By using the other expressions for t, namely, Equations [12b] and [12c], we may obtain the corresponding relations for cases 2 and 3:

$$t = t_0 + \frac{2}{q}\left[\tanh^{-1}\frac{2cV_0+b}{q} - \tanh^{-1}\frac{2cV+b}{q}\right] \ldots [\mathrm{C}2a]$$

$$V = \frac{1}{2c}\left[-b - q\tanh\left(\frac{(t-t_0)q}{2} - P\right)\right] \ldots . [\mathrm{C}2b]$$

$$P = \tanh^{-1}\frac{2cV_0+b}{q}$$

$$x = x_0 + \frac{1}{3600}\left[-\frac{b(t-t_0)}{2c} - \frac{1}{c}\log_e \cosh\left(\frac{(t-t_0)q}{2} - P\right) + \frac{1}{c}\log_e \cosh P\right] \ldots [\mathrm{C}2c]$$

$$t = t_0 + \frac{2}{p}\left[\tan^{-1}\frac{2cV+b}{p} - \tan^{-1}\frac{2cV_0+b}{p}\right] \ldots [\mathrm{C}3a]$$

$$V = \frac{1}{2c}\left[-b + p\tan\left(\frac{(t-t_0)p}{2} + B\right)\right] \ldots . [\mathrm{C}3b]$$

$$B = \tan^{-1}\frac{2cV_0+b}{p}$$

$$x = x_0 + \frac{1}{3600}\left[-\frac{b(t-t_0)}{2c} - \frac{1}{c}\log_e \cos\left(\frac{(t-t_0)p}{2} + B\right) + \frac{1}{c}\log_e \cos B\right] \ldots . [\mathrm{C}3c]$$

BIBLIOGRAPHY

1 "Resistance of Lightweight Passenger Trains," by A. I. Totten, *Railway Age*, vol. 103, 1937, pp. 75–80.

2 "Calculating the Stopping Distance of Trains," by G E. Terwilliger, *Railway Mechanical Engineer*, vol. 102, 1928, pp. 259–261.

3 "Problems in Locomotive Acceleration," by A. C. Barrow, *Civil Engineering*, vol. 4, 1934, pp. 202–204.

4 "Locomotive Tractive Effort in Relation to Speed and Steam Supply," by E. G. Young and C. P. Pei, Trans. A.S.M.E., vol. 57, 1935, pp. 335–341.

Discussion

B. S. Cain.[4] The author's method is based on acceleration and braking curves given by the formula

$$\frac{dV}{dt} = a + bV + cV^2 \ldots\ldots\ldots\ldots\ldots . [2]$$

This method can be extended to have a power and practical convenience beyond that mentioned in the paper. It can be shown that one set of speed-time curves can be drawn, applicable to all motion covered by the author's formula. This enables approximate calculations or checks to be made almost at a glance. These curves are particularly suitable for calculating motion over a profile containing variable grades and curvature.

Then too, the author's Equation [2] can be fitted to any tractive effort or braking curve by a particularly easy method which provides a graphic check on the accuracy of the fit. This is important because the fit determines whether or not the method is applicable. The writer has found some tractive-effort curves to which the formula is applicable and others to which it is not.

To show that all curves covered by the formula are included in one set, multiply both sides of Equation [2] by c/b^2 and arrange the terms to give

$$\frac{d(cV/b)}{d(bt)} = \left(\frac{ac}{b^2}\right) + \left(\frac{cV}{b}\right) + \left(\frac{cV}{b}\right)^2 \ldots\ldots\ldots [13]$$

Then we can treat cV/b and bt as the variables and the equation contains only one parameter, ac/b^2.

By plotting cV/b against bt for different values of ac/b^2 we obtain, on one sheet, the complete graphical solution of the author's equation. Similarly, if we use cx as a variable in place of x, we can plot cV/b against cx or bt against cx and ac/b^2 will be the only other parameter involved.

As an example, Fig. 3 of this discussion shows a number of the curves satisfying Equation [13] of this discussion for various values of ac/b^2 which give different kinds of solutions. The application of these curves to motion over a variable profile

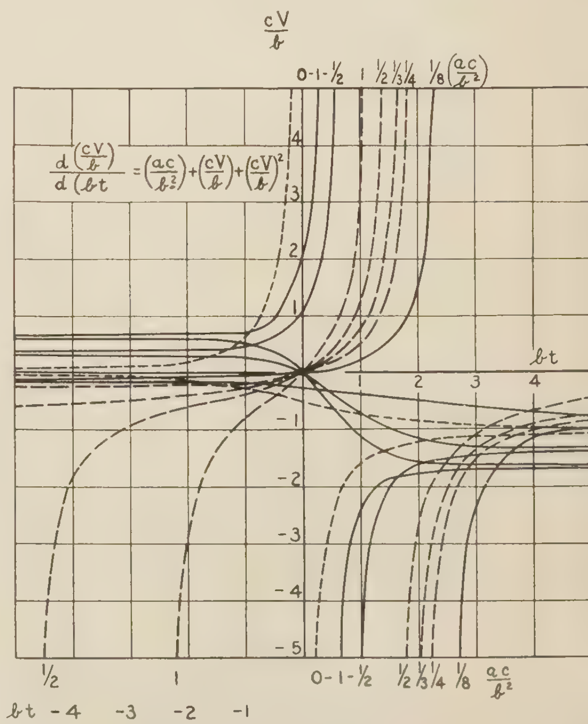

Fig. 3 Graphical Solution of Author's Equation [2]

[4] Assistant Engineer, Locomotive Division, General Electric Company, Erie, Pa. Mem. A.S.M.E.

ll be obvious, when it is considered that the effect of grade and rvature is to modify the constant term in the train-resistance rmula, that is, they only modify the constant a.

Thus, to calculate motion through a change in grade, we callate ac/b^2 for each grade and, when the grade changes, we ove from one master curve to another, keeping the same lue of cV/b. Obviously, only differences in cx or bt are imrtant, the absolute values being arbitrary.

Even where calculation is used in place of a master-curve eet, there is often advantage in using the dimensionless quanties

$$cV/b,\ bt,\ cx, \text{ and } ac/b^2$$

hey facilitate checking and comparison if nothing else. The uthor's formula [12a], for example, becomes

$$bt = -\frac{2}{r}\,\mathrm{ctnh}^{-1}\,\frac{2\,(cV/b) + 1}{r} + \text{constant} \ldots\ldots [14]$$

$$\text{where } r = \pm\left(1 - 4\,\frac{ac}{b^2}\right)^{1/2}$$

o doubt the author has considered it unnecessary to explain ow to fit his formula to a tractive-effort curve, but it may be orth noting one useful method. In Fig. 4 of this discussion, he dotted curve 1 represents the tractive effort of a certain ocomotive plotted against speed. To fit a curve which has the ame values at A and B and the same slope at A, draw the angent AC, the vertical line BE, and the horizontal line AD.

Then, for the fitted curve, having the form

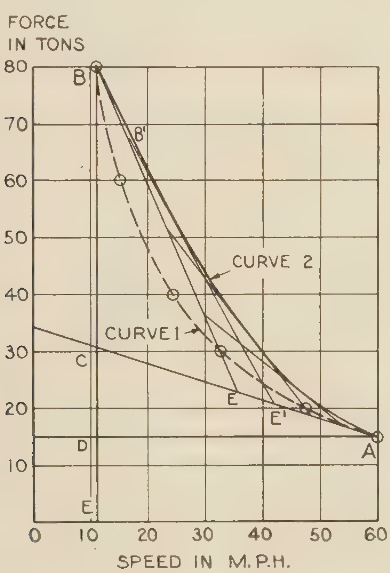

FIG. 4 METHOD OF FITTING EQUATION [2] TO TRACTIVE-EFFORT CURVE

$$\text{Force} = a + bB + cV^2$$

$$\text{Force} = ED - \frac{DC}{DA}\,(V - V_A) + \frac{CB}{DA^2}\,(V - V_A)^2$$

In Fig. 4

$$\text{Force} = 15 - \frac{15.5}{49}\,(V - 60) + \frac{49.5}{49^2}\,(V - 60)^2$$

$$= 108 - 2.796V + 0.0206V^2$$

As a check, bisect the tangent AC at E and join BE. Then, from the properties of a parabola, BE is a tangent at B and the curve can be readily drawn by dividing BE and EA into the same number of equal parts, and joining corresponding parts, such as $B'E'$. These lines are all tangent to the curve. This gives curve 2 for the fitted curve and it is apparent that the author's method of fitting will not apply to the particular curve in Fig. 4. This illustrates the importance of checking the fit in each case as it arises in practice.

It may be worth noting that tractive-effort or braking curves which are not readily represented by expressions of the form $a + bV + cV^2$ can usually be represented very accurately by the form

$$\frac{k}{V} + a + bV + cV^2$$

The resulting equations can be integrated without difficulty and calculations made on similar lines to those in the paper. The integrals involve the roots of the equation

$$k + aV + bV^2 + cV^3 = 0$$

which can be reduced to the form

$$Z^3 + C(Z + 1) = 0$$

the roots of which are obtainable from a master curve of C plotted against Z.

The writer has also examined tractive-effort and braking curves of the form

$$\frac{k}{V} + a + bV$$

This expression fits many curves very well and it can also be fitted to the Davis train-resistance curves very closely except at low speeds. The curve is fitted by plotting the product of speed and acceleration against speed and then fitting the curve

$$k + aV + bV^2$$

to it by the simple method previously given.

The dimensionless coordinates to use are bV/a, bt and b^2x/a and the single parameter is bk/a^2.

In this way there is only one set of curves to draw, but the coordinates are affected by the profile so that calculations on a variable profile are more laborious.

E. E. KIMBALL.[5] Many attempts have been made to develop direct analytical methods for determining train performance but this is the first time to the writer's knowledge that anyone has succeeded in obtaining a mathematical solution.

Unfortunately, the solution is not a simple one and for this reason the analytical method may not receive widespread attention, but it has possibilities which should not be overlooked. A few comments regarding its practicability may, therefore, be in order.

In some respects, it is much shorter than the usual step-by-step method; when applied to the same data, both methods give practically the same results.

The final equations are not difficult to handle, but considerable difficulty is experienced in substituting numerical values in the basic formulas from which they are derived. Undoubtedly the author has some helpful hints for arranging the calculations so as to save time and avoid errors. Facsimiles of his forms or

[5] Chairman Subcommittee 1, Committee on Economics of Railway Location and Operation, American Railway Engineering Association, Schenectady, N. Y.

TABLE 2 DATA FOR OBTAINING NORMAL HORSEPOWER CAPACITIES OF TYPICAL STEAM LOCOMOTIVES FROM WEIGHT OF ENGINE AND WEIGHT ON DRIVERS BASED ON COAL-FIRED LOCOMOTIVES

Weight on Drivers Per cent		HP Per Ton on Drivers	Types of Locomotives Available			Weight on Drivers Per cent		HP Per Ton on Drivers	Types of Locomotives Available		
Wt. of Eng.	Wt. of Eng. & Tender					Wt. of Eng.	Wt. of Eng. & Tender				
41						71	40.8	28.2	2-10-4	2-8-2	
42						72	41.4	27.8	2-10-4	2-8-2	
43	24.0	40.0	4-4-4			73	42.0	27.4		2-8-2	
44	24.6	39.6	4-4-4			74	42.6	26.9	2-10-2	2-8-2	
45	25.2	39.2	4-4-4			75	43.2	26.5	2-10-2	2-8-2	
46	25.8	38.7	4-4-4			76	43.8	26.1	2-10-2	2-8-2	
47	26.4	38.3	4-4-4			77	44.4	25.7	2-10-2	2-8-2	
48	27.0	37.9				78	45.0	25.3	2-10-2	2-8-2	
49	27.6	37.5				79	45.6	24.8	2-10-2	2-8-2	
50	28.2	37.1	4-4-2			80	46.2	24.4	2-10-2		
51	28.8	36.6	4-4-2			81	46.8	24.0	2-10-2		
52	29.4	36.2	4-4-2	4-6-4		82	47.4	23.6	2-10-2		
53	30.0	35.8	4-4-2	4-6-4		83	48.0	23.2	2-10-2		
54	30.6	35.4	4-4-2	4-6-4		84	48.6	22.7	2-10-2		
55	31.2	34.9	4-4-2	4-6-4		85	49.2	22.3			0-10-2
56	31.8	34.5	4-4-2	4-6-4		86	49.8	21.9			
57	32.4	34.1	4-4-2	4-6-4	4-8-4	87	50.4	21.5		2-8-0	
58	33.0	33.7	4-6-2		4-8-4	88	51.0	21.1		2-8-0	
59	33.6	33.3	4-6-2		4-8-4	89	51.6	20.6		2-8-0	
60	34.2	32.8	4-6-2	2-8-4	4-8-4	90	52.2	20.2	2-10-0	2-8-0	
61	34.8	32.4	4-6-2	2-8-4	4-8-4	91	52.8	19.8	2-10-0	2-8-0	
62	35.4	32.0	4-6-2	2-8-4	4-8-4	92	53.4	19.4	2-10-0	2-8-0	
63	36.0	31.6	4-6-2	2-8-4	4-8-4	93	54.0	18.9	2-10-0	2-8-0	
64	36.6	31.2	4-6-2	2-8-4	4-8-4	94	54.6	18.5			
65	37.2	30.7	4-6-2	2-8-4	4-8-2	95	55.2	18.1			
66	37.8	30.3	2-10-4	2-8-4	4-8-2	96	55.8	17.7			
67	38.4	29.9	2-10-4	2-8-4	4-8-2	97	56.4	17.2			
68	39.0	29.5	2-10-4		4-8-2	98	57.0	16.8			
69	39.6	29.1	2-10-4	2-8-2	4-8-2	99	57.6	16.4			
70	40.2	28.6	2-10-4	2-8-2	4-8-2	100	58.2	16.0			

4 Cylinder Articulated Locomotives

67					79	49.2	22.3	2-8+8-4	
68	44.6	25.6	4-6+6-4		80	49.7	22.0	2-8+8-4	
69	45.0	25.3	4-6+6-4	2-6+6-4	81	50.1	21.7	2-8+8-4	
70	45.4	25.0	4-6+6-4	2-6+6-4	82	50.5	21.4	2-8+8-4	
71	45.8	24.7		2-6+6-4	83	51.0	21.1	2-8+8-4	2-6+6-2
72	46.2	24.4		2-6+6-4	84	51.4	20.8	2-8+8-4	
73	46.7	24.1		2-6+6-4	85	51.8	20.5	2-8+8-4	
74	47.1	23.8		2-6+6-4	86	52.2	20.2	2-8+8-4	2-8+8-2
75	47.5	23.5		2-6+6-4	87	52.6	19.9		2-8+8-2
76	48.0	23.2		2-6+6-4	88	53.0	19.6		2-8+8-2
77	48.4	22.9	2-8+8-4		89	53.4	19.3		2-8+8-2
78	48.8	22.6	2-8+8-4		90	53.9	19.0		2-8+8-2

Compiled 1937 by AREA Committees XVI and XXI

work sheets would largely remove one of the chief handicaps of the method.

In regard to the characteristics of steam locomotives, the author may be interested to note that the empirical formula,[6] developed by the Committee on Economics of Railway Location and Operation, can be closely approximated by the quadratic equation

$$\text{Cylinder tractive effort} = W(642 - 136U + 9.07U^2)$$

Where W = weight on drivers in tons (2000 lb)
$U = V/V_1$
V = miles per hour
$V_1 = 0.396\ K$
K = Normal horsepower per ton on drivers obtained from Table 2 or from design
$V_0 = 1.125\ V_1$

Thus for a typical *Hiawatha* locomotive, type 4-4-2 (140/280/530)[7]

$W = 70$
$K = 37.1$ (from table)
$V_1 = 14.7$
$\text{Cyl TE} = 44940 - 648\ V + 2.94\ V^2$
Max TE = 25 per cent weight on drivers = 35000 lb, corresponding to V_0 = 16.6 mph

Table 2 of this discussion shows the performance or normal horsepower capacities of typical steam locomotives of modern design. It is assumed theoretically that the maximum capacities are $33^1/_3$ per cent greater than the normal capacities but, in practice, the percentage will vary depending upon the boiler capacity. For this reason no attempt has been made to derive quadratic equations based upon the maximum capacity of steam locomotives.

As a matter of record, attention should be called to the fact that the paper makes no allowance for the force required to accelerate the revolving parts in addition to that required for the train. It is customary to add about 5 per cent for this purpose; hence the constant 0.0109 in Equation [1] should be 0.0104.

Likewise an allowance of 20 lb per ton on drivers for the losses in the engine between the cylinders and driving axles should be added to the train resistance when the calculations are based on cylinder tractive effort.

If these adjustments are made in the example used in the paper, it will be found that the agreements between the calculated and observed performances are closer than claimed by the author.

A. W. Laird.[8] So many variables are met with in dealing with all subjects pertaining to railway-train operation that it is seldom possible to group the effect of all these variables and write a single expression which will reasonably describe train movement on a time or distance basis. The author has attempted such a process and his analyses of train-acceleration factors, knowing train consist and locomotive capacity, can be credited as much more than a classroom exercise in the mathematical treatment of a very real railway problem, based upon the road performance of a single locomotive class. The author assumes that the decrease in tractive effort of a locomotive with increasing speed can be expressed in definite quadratic form. Similarly, employing the Totten modifications of the Davis train-resistance formula, the inherent train resistances also can be expressed in quadratic form, the difference between tractive effort and train resistance at any point representing net accelerating force. The composite expression is then capable of being integrated on either a time or distance basis. In fact, all time and distance calculations are constituted of some application of this process, but generally take the form of a step-by-step procedure which, although less direct, once the more complex equations of the author have been written and solved for the specific case, offers the advantage of progressive determination through intermediate phases of the analyzed performance.

Whether or not the author's procedure is accurate and appropriate resides in the ability to write a true quadratic expression for locomotive tractive effort as a function of speed. This has been checked by attempting to write similar expressions for three

[6] "Economics of Railway Location and Operation," Report of Committee 16, Appendix A, Proceedings American Railway Engineering Association, vol. 39, 1938, pp. 440–472; vol. 40, 1939, pp. 84–122.

[7] Figures in parentheses indicate weight on drivers/weight of engine/weight of engine and tender, in 1000-lb units.

[8] General Mechanical Engineer, Research, The New York Air Brake Company, Watertown, N. Y. Mem. A.S.M.E.

additional locomotives for which dynamometer or testing-plant performance data are available. This has verified the propriety of the author's assumption; the quadratic expressions follow closely the test results in every case, with locomotive tractive effort holding up somewhat better than the quadratic expression indicates at high speeds beyond the point of horsepower peak.

Despite the author's statement of conditions and exceptions, the application of the method to train braking seems to be in nowise justified. This is for the reason that it is impossible to write the necessary quadratic expression which properly will describe the change in braking force as a function of speed. During stops from high speed with cold brake shoes bearing upon cold wheel treads a high initial retarding force ordinarily is obtained which decreases slightly as the stop progresses. There follows a relatively constant retarding force which continues until a speed of 25 to 35 mph is attained; the net retarding force then increasing without interruption to the stop if a constant brake-shoe pressure is maintained. No single quadratic expression can be written for a curve of this character and the curve is characteristic of all which are witnessed in conventional brake performance.

I. Opatowski.[9] The author has successfully applied analytical methods where graphical methods have generally been preferred. The writer has been interested in problems closely related to that solved by the author.[10] In practical calculations, it often happens that during short intervals of time the coefficients a, b, c in Equation [2] have special values due to short changes of gradients, to curves, or to changes of the course of the train. If the time intervals here involved are sufficiently small, the formulas for speed and distance may be simplified to a great extent. If $V = V_0$, $x = x_0$ when $t = 0$, the integral of Equation [2] may be written in the form

$$V = (V_0 + AT)/(1 - BT) \qquad [15]$$

where

$$A = a + \frac{1}{2}bV_0, \quad B = \frac{1}{2}b + cV_0 \qquad [16]$$

and $T = 2p^{-1}\tan(pt/2)$ or $T = 2q^{-1}\tanh(qt/2)$ according to whether p or q is real. If t is small, $\tan(pt/2) \approx pt/2$ and $\tanh(qt/2) \approx qt/2$, so that $T \approx t$ and Equation [15] becomes

$$V \approx (V_0 + At)/(1 - Bt) \qquad [17]$$

From Equation [17] we have by integration

$$x \approx x_0 - [At + (AB^{-1} + V_0)\log_e(1 - Bt)]/B \qquad [18]$$

Here again for small values of t the formula $\log_e(1 + z) \approx 2z/(2 + z)$ may be used, so that Equation [18] becomes

$$x \approx x_0 + t(2V_0 + At)/(2 - Bt) \qquad [19]$$

The speed-distance relation plotted in the upper curve Fig. 2 of the paper may be expressed by a formula. In fact, Equation [2] is equivalent to

$$V.dV/dx = a + bV + cV^2 \qquad [20]$$

and the integral of this is

$$x = x_0 + \frac{1}{2c}\log_e\frac{a + bV + cV^2}{a + bV_0 + cV_0^2} - \frac{b}{c}(\tau - \tau_0) \qquad [21]$$

where $\tau = p^{-1}.\tan^{-1}(b + 2cV)/p$ or $\tau = -q^{-1}.\tanh^{-1}(b + 2cV)/q$, according to whether p or q is real, and τ_0 is the value of τ for $V = V_0$. Equation [21] is an exact formula which could also be obtained by eliminating t in Equation [15] and in (Cc). For small values of t an approximate relation between V and x is deduced from Equations [17] and [19]

$$x = x_0 + \frac{A(V_0 + V) + 2BV_0V}{B(V_0 + V) + 2A} \times \frac{V - V_0}{A + VB} \qquad [22]$$

To illustrate the use of these formulas refer to the data of Table 1 of the paper for $V_0 = 25$ and $V = 45$ mph. The coefficients of Equation [7] give $q = 11.082\ h^{-1}$. The time is here $t = 1$ min 56 sec — 59 sec — 57/3600 h, so that $qt/2 = 0.08773$. Since $\tanh 0.09 = 0.0898$, the approximation $\tanh(^1/_2qt) \approx {^1/_2}qt$ is here permissible and Equation [17] gives $V = 44.7$ against the round value of 45 mph in Table 1. Here, $Bt = -0.19712$ and since $\log_e 1.2 = 0.1823$, whereas $2 \times 1.2/(2 + 1.2) = 0.1818$, the approximation introduced in Equation [18] is also permissible. Since $x_0 = 0.2\ m$, either Equation [19] or [22] gives $x = 0.77$ against $0.79\ m$ of Table 1. If we try to go further with our approximations by neglecting Bt in Equations [17] and [19] against 1 and 2, we obtain: $V - V_0 = At$, $x = x_0 + t(V_0 + At/2)$. Combining these two equations we get $x = x_0 + t(V + V_0)/2$, e.g., the same x as if the motion were uniform during t with a velocity equal to the arithmetical mean of its initial and final value. Equations [17], [19], and [22] may be also looked upon as involving during t a substitution of the acceleration law Equation [2] by a simpler one

$$dV/dt = a_1 + b_1V, \quad \text{or } dV/dt = a_2 + c_2V^2 \qquad [23]$$

where $a_1 = a - cV_0^2$, $b_1 = b + 2cV_0$; $a_2 = a + {^1/_2}bV_0$, $c_2 = c + {^1/_2}\dfrac{b}{V_0}$. In fact, by Equations [16] A and B have for Equation [20] the same values as for Equations [23], so that by Equations [17], [19], and [22] the motion is the same during t in all three cases.

As the author pointed out, the applicability of his method is dependent upon the possibility of expressing the acceleration in a form Equation [2], where a, b, c are constant coefficients, at least for sufficiently large intervals of time. Therefore, it is important to be able to ascertain for a given train that this acceleration law Equation [2] holds and to determine the coefficients a, b, c from test runs. Such runs usually provide a set of values (x, V, t) and either Equation [17] or [19] enables one to evaluate a, b, c. The calculations are particularly simple if Equation [17] is used which leads to the formulas

$$c = (s_1 - s_2)/(21),\ b = -2(V_1c + s_1),\ a = (10)/t_1 - (V_0 + V_1)b/2 - V_0V_1c \qquad [24]$$

where $(20)s_1 = (10)/t_1 - (21)/t_2$, $(31)s_2 = (21)/t_2 - (32)/t_3$.

In these equations V_0, V_1, V_2, V_3 are four values of the velocity, t_i is the time elapsed between V_i and V_{i-1}, $(ij) = V_i - V_j$. The application of Equation [24] does not require any measurement of distance x. It is important however that the time intervals t_i be not too small, otherwise the errors in calculating a, b, c may be so large as to deprive Equation [24] of any practical value. According to data kindly submitted to the writer by the author and by C. H. Bilty, during the test represented by the lower graph Fig. 2 of the paper, the speed increment $V - V_0$ over a distance of 500 ft varied from ≈ 3 to $^1/_2$ mph, whereas, the corresponding time t was decreasing from ≈ 0.2 to 0.1 min, respectively. Assuming as an approximate value of c that of Equation [7] $\approx 0.1\ h^{-1}$ it is easy to cal-

[9] Instructor in Mathematics and Mechanics, University of Minnesota, Minneapolis, Minn. Mem. A.S.M.E.

[10] "La perdita di velocita' delle automotrici ferroviarie," by I. Opatowski, *Politecnico*, 1936, pp. 22–25.

culate from the first Equation [24] the error δc of c involved by errors[11] δt_i of t_i

$$\delta c/c \approx 2D.\delta t_2/t_2 - D.\delta t_1/t_1 - D.\delta t_3/t_3$$

where, for the foregoing values of $V - V_0$ and t, D varies between ≈ 1000 and $\approx 12{,}000$. This means a prohibitive value of the error due to an inexact knowledge of the time. The situation is entirely different for larger values of t. For instance for $t \approx 2$ min, which is approximately one third of the total time elapsed during the test Fig. 2, we have $V_0 = 0$, $V_1 \approx 40$, $V_2 \approx 60$, $V_3 \approx 70$ mph, so that

$$\delta c/c \approx 15.\delta t_2/t_2 - 10.\delta t_1/t_1 - 5.\delta t_3/t_3 \quad [25]$$

The approximation $\tanh(qt/2) \approx qt/2$, which is implicitly contained in Equation [24], is equivalent, by Equations [15] and [17], to the use of slightly higher values of t than the actual ones, because $\tanh x < x$. For $t = 2$ min, $qt/2 \approx 0.18$ and the approximation $\tanh 0.18 \approx 0.18$ instead of its exact value 0.1781 is still very good. But even if this difference were larger it could not give an appreciable error δc of c, because in Equation [25] all δt are here of the same order of magnitude and all have the same sign.

This method was applied by the writer, some years ago, for the determination of automobile resistance, which is assumed usually in the form $a + cV^2$. Obviously, the calculations must be carried out for a certain number of different sets of (V_0, V_1, V_2, V_3) and (t_1, t_2, t_3) in order to obtain sufficiently exact values of the coefficients.

Another method for the determination of a, b, c in the acceleration formula is obtained as a generalization of a method applied by S. Hoerner[12] for the determination of automobile resistance. The differentiation of Equation [20] with respect to V gives $d(VV')/dV = b + 2cV$, where $V' = dV/dx$. From the speed-distance curve Fig. 2, $d(VV')/dV$ may be numerically or graphically evaluated; plotted against V it gives a straight line, whose slope and point of intersection with the V-axis give c and b. If the acceleration law Equation [20] is correct, the difference $VV' - bV - cV^2$ is a constant $= a$. The writer applied this method to the lower graph Fig. 2 with a negative result, which proves, in agreement with a remark of the author, that the tractive force actually used was different from the maximum available.

Author's Closure

At the request of the editor the paper which the author originally submitted on this subject was revised and condensed considerably. In so doing, it was necessary to omit such material as discussion of the methods of fitting quadratic forms to empirical curves; discussion of the various singular cases; an explanation of how the method is to be applied to the braking of trains; and certain asymptotic approximations.

The extension proposed by Mr. Cain, involving the use of dimensionless variables, is an important one, and the author agrees that the utility of the method is thereby greatly increased, once the necessary curves have been plotted or tabulated.

Let us examine the procedure suggested by Mr. Cain in greater detail. We introduce the dimensionless quantities

$$\left.\begin{aligned} x' &= 3600cx \\ t' &= bt \\ V' &= cV/b \end{aligned}\right\} \quad [26]$$

[11] For the method of calculating errors here applied see, for instance, "Calculus," by H. H. Dalaker, third edition, McGraw-Hill Book Co., Inc., New York, N. Y., 1935, p. 195.

[12] "Bestimmung des Luftwiderstandes von Kraftfahrzeugen im Auslaufverfahren," by S. Hoerner, *Zeit. V.D.I.*, vol. 79, 1935, pp. 1028–1033.

For any given case, the primed quantities are simply constant multiples of the unprimed quantities. In terms of the primed quantities, the fundamental Equation [2] may now be written

$$\frac{dV'}{dt'} = V'\frac{dV'}{dx'} = \alpha + V' + V'^2 \quad [27]$$

where α is an abbreviation for ac/b^2.

For the four cases distinguished by

Case 1	$4\alpha < 1$	$\lvert(2V_0' + 1)/r\rvert > 1$
Case 2	$4\alpha < 1$	$\lvert(2V_0' + 1)/r\rvert < 1$
Case 3	$4\alpha > 1$	
Case 4	$4\alpha = 1$	

of which the first three correspond to those already distinguished, we find upon integrating Equation [27] with respect to t'

$$t' = -\frac{2}{r}\,\mathrm{ctnh}^{-1}\frac{2V' + 1}{r} + \text{constant} \quad [28a]$$

$$t' = -\frac{2}{r}\tanh^{-1}\frac{2V' + 1}{r} + \text{constant} \quad [28b]$$

$$t' = \frac{2}{s}\tan^{-1}\frac{2V' + 1}{s} + \text{constant} \quad [28c]$$

$$t' = -\frac{2}{2V' + 1} + \text{constant} \quad [28d]$$

where

$$\left.\begin{aligned} r &= q/b = (1 - 4\alpha)^{1/2} \\ \text{and} \quad s &= p/b = (4\alpha - 1)^{1/2} \end{aligned}\right\} \quad [29]$$

Similarly the integration with respect to x' yields

$$x' = \frac{1}{2}\log_e\lvert\alpha + V' + V'^2\rvert + \frac{1}{r}\,\mathrm{ctnh}^{-1}\frac{2V' + 1}{r} + \text{constant} \quad [30a]$$

$$x' = \frac{1}{2}\log_e\lvert\alpha + V' + V'^2\rvert + \frac{1}{r}\tanh^{-1}\frac{2V' + 1}{r} + \text{constant} \quad [30b]$$

$$x' = \frac{1}{2}\log_e\lvert\alpha + V' + V'^2\rvert - \frac{1}{s}\tan^{-1}\frac{2V' + 1}{s} + \text{constant} \quad [30c]$$

$$x' = \log_e\lvert 2V' + 1\rvert + \frac{1}{2V' + 1} + \text{constant} \quad [30d]$$

Mr. Cain proposes that Equations [28] be plotted for a large number of values of α, similarly for Equations [30]. One would then be able to solve any acceleration or braking problem which could be formulated in terms of Equation [2], without further recourse to the analytical expressions. Fig. 3 is, of course, offered only as an illustration; it does not contain sufficient curves, neither is it drawn on a sufficiently large scale to be extremely useful in practice.

Before undertaking a comprehensive construction of the curves contained in Equations [28] and [30], it would be best to make a study of what range of values of α is of practical interest, and also what corresponding ranges of x', t', and V' are of interest. It is improbable that it would be desirable to construct all of the curves on the same scale, and it is also improbable that it would be advisable to choose the constants of integration so that nearly all of the curves pass through the origin, because of the consequent confusion of curves near the origin.

It is evident that, since only positive values of V have physical significance, only the upper half, or only the lower half of Fig. 3 will be useful, depending upon whether c/b is positive or negative. Similarly, time will increase to the right when b is positive, and to the left when b is negative. For example, in the case

represented by Equation [7], where both c/b and b are negative, it is necessary to turn Fig. 3 upside down in order to obtain an ordinary plot of the speed versus time.

In using Fig. 3, or the corresponding plot of V' versus x', it is necessary to remember that the origin of x' and t' is arbitrary, whereas, the origin of V' is not. In practice, this means that only changes in the values of x' and t' are significant, and that the actual values of x' and t' obtained from the plots are without significance. An illustration in the form of a hypothetical example may serve to clarify this situation.

Let us assume that in a given case the constants a, b, and c have been evaluated, and that they are all positive, with $ac/b^2 = 1/8$. Suppose further that the initial value of the velocity V_0 corresponds to $V_0' = 0.25$. By inspection of the upper half of Fig. 3, we see that with $\alpha = 1/8$ this value of V' corresponds to $t' = 1.1$. We shall now assume that the grade remains the same until a time has elapsed corresponding to an increase of 0.6 in t'. From the plot we see that $t' = 1.7$ corresponds to $V' = 0.8$. At this point, we shall suppose that the train encounters a descending grade which doubles the value of a, so that α changes from 1/8 to 1/4. This change does not affect the relations in Equation [26] but it does mean that the change must be made from one curve to another. The new initial value $V' = 0.8$ corresponds on the $\alpha = 1/4$ curve to $t' = 1.2$ and times which elapse after the change of grade should be reckoned with $t' = 1.2$ as the zero of elapsed time.

It will be noted that the graphical method automatically takes care of the constant of integration. The constant is effectively evaluated by measuring t' in each case from the point on the curve corresponding to the initial value of V'.

The plot of V' versus x' would be used in an exactly similar manner. Used together, the two plots can be made to yield a complete description of the motion of the train. As Mr. Cain suggests, it would be possible to replace both Fig. 3 and the plot of V' versus x' by a single family of curves of x' versus t'. Such a family of curves would be more difficult to use, however, since the velocity would appear in the curves only through the fact that it would be proportional to the slope. The slope would thus have to be marked at frequent intervals on the curve in order that one might be able to introduce the initial conditions.

The singular cases $b = 0$ and $c = 0$ cannot be treated in the foregoing manner, because Equations [26] become meaningless. When $b = 0$ new dimensionless quantities may be introduced, and two curves will suffice to treat every case. Correspondingly, when $c = 0$ one curve will suffice.

The particular method of fitting by which Equation [6] was obtained was employed not because it afforded the most accurate fit (it does not), but because at the time the writer was primarily interested in obtaining analytical expressions for the maximum time which could be lost in making a stop. For this purpose, it is important that the slope be accurate for values of V near the limiting velocity. The task of fitting quadratic forms to empirical curves is largely a matter of trial and error and, as Messrs. B. S. Cain and A. S. Laird remark, it may sometimes be impossible to find a good fit. In this case, it is necessary either to use a different type of approximation, such as the one suggested involving cube roots, or to split the range of V into several parts, with a different quadratic form for each part. The latter is often the easier procedure.

As remarked by Mr. Laird, it is usually not possible to fit a braking curve by a single quadratic form. It is frequently possible, however, to find a good fit except at very low frequencies with two quadratic forms, each holding in a different range of velocities.

The use of a quadratic form as an approximation to the accelerating force may be looked upon as a generalization of the step-by-step method. In the step-by-step method, the range of velocity is divided into a large number of subintervals, in each of which the acceleration is regarded as constant. The next approximation would consist in assuming that the acceleration was given by an expression of the form $a + bV$. The third approximation, from this point of view, consists in approximating the accelerating force by a quadratic form. The advantage of the third approximation is that a single quadratic form will often suffice for the entire range of velocities in question, and the subdivision of the total interval into two parts is nearly always sufficient.

The ideal method of computing the behavior of trains running over a variable profile is probably the use of a differential analyzer, which performs the integration of the acceleration equation mechanically, as described by F. Cuypers,[13] T. F. Perkinson,[14] D. R. Hartree and J. Ingham,[15] and others. The advantages of this method are several:

(*a*) The exact experimental data on the resistance and tractive effort may be used without approximation.

(*b*) The entire run of a train may usually be computed in a time approximately equal to that required by the train to make the run. In the paper[15] by Hartree and Ingham, which may have escaped the notice it deserved because of its obscure place of publication (from an engineer's point of view), the authors describe a remarkable run of the *Macunian*, in which the train required 67.5 min to make the run of 82.5 miles from Rugby to London, whereas, the machine required 75 min to obtain the speed-distance curve.

(*c*) Speed restrictions are more easily taken into account than with the analytical method.

Unfortunately, differential analyzers are rarely available and are costly instruments. They are usually in demand for other problems which cannot be treated at all by analytical methods. It would therefore seem that analytical methods of the type suggested here are of some practical use.

The work reported in this paper was performed 4 years ago while the author was an undergraduate in Harvard College. Since that time, his interest has shifted to other fields and the pressure of these interests will prevent his carrying out the implications of the material presented in the discussion. He therefore hopes that the possibilities of the analytical methods will be explored further by those in a position to do so.

The author wishes again to express his gratitude to Professor J. H. Van Vleck for his interest and helpful advice.

---

[13] "Machine for Calculating Running Times," by F. Cuypers, Bulletin of the International Railway Congress Association, July, 1936, pp. 699–705.

[14] "A Machine for the Calculation of Train Performance Data," by T. F. Perkinson, *General Electric Review*, vol. 40, 1937, pp. 574–583.

[15] "Note on the Application of the Differential Analyzer to the Calculation of Train Running Times," by D. R. Hartree and J. Ingham, Memoirs and Proceedings of the Manchester Literary and Philosophical Society, Manchester, England, November, 1938, pp. 1–15.

Thermodynamic Properties of Vapors[1]

By ERICH F. LEIB,[2] NEW YORK, N. Y.

By introducing new properties of state and an ideal system, that is, a perfect vapor, the representation of the thermodynamic properties of vapors is simplified. The field of state reduces to one curve of state which requires in the experimental investigation of vapors only as many measurements as are necessary for the determination of this curve. The equations of state are found more easily, the calculations required to determine the vapor tables are reduced, and a simple formula for the external work is found. An analytic investigation of the equilibrium of a liquid with its vapor shows how the vapor-pressure curve can be found from the equation of state.

THERE are essentially three ways to investigate the properties of thermodynamic systems. In the first case, the properties are derived from experiments made with real substances. In the second case, the properties are determined from a molecular theory, on which the system is based. In the third case, the properties are deducted from a definition, by which an ideal system is created. This paper will use the latter way to introduce an ideal system, the qualities of which are in good agreement with the qualities of actual vapors. Reliable tables and equations of state for vapors can be established on the basis of such a system even if only a few experimental data are available. The application of this method to several substances will be demonstrated by examples.

Nomenclature

The following symbols are used in this paper:

- p = pressure
- v = volume
- u = internal energy
- h = enthalpy
- s = entropy
- T = absolute temperature
- $\theta, \pi, \varphi, \epsilon$ = elementary properties of state
- f = number of degrees of freedom
- c_v = specific heat at constant volume
- c_p = specific heat at constant pressure
- A = isothermal work
- L = adiabatic work
- R = gas constant
- Ψ = characteristic function
- Θ = characteristic temperature
- G = thermodynamic potential
- g, Φ, ϕ = functions of equilibrium
- a, b = constants of equation of state
- x, y, z = functions of state
- α, β, w = auxiliary functions
- sub. 0 = zero pressure
- sub. k = critical properties
- sub. r = reduced properties
- sub. l = liquid state
- sub. v = vaporous state

1—The Elementary Properties of State†

To investigate a thermodynamic system, start with the Second Law in the form

$$ds = \frac{du + pdv}{T} \qquad [1]$$

The internal energy of a vapor is composed of four components: translation, rotation, oscillation, and intermolecular forces. In the gaseous or vaporous state, translation and rotation may assume their full activity, while oscillation may not reach its full activity. Thus, the internal energy u is represented as the sum of three terms: the classic contribution of translation and rotation, the contribution of oscillation, and the contribution of intermolecular forces. For the latter an empirical formula will be established in order to derive the properties of vapors.

If f denotes the total sum of degrees of freedom of translation and rotation, we can write

$$u = (f/2)RT + u_{\text{osc}} + u_{\text{mol}}$$

or

$$u = (f/2)pv + u_{\text{osc}} + u_{\text{mol}} + (f/2)(RT - pv) \qquad [2]$$

Writing $\alpha = 2/f$

$$\left.\begin{array}{lll} \text{we have for monatomic molecules} & f = 3 + 0 = 3, & \alpha = 2/3 \\ \text{for linear molecules} & f = 3 + 2 = 5, & \alpha = 2/5 \\ \text{for polyatomic molecules} & f = 3 + 3 = 6, & \alpha = 1/3 \end{array}\right\} [3]^*$$

Introducing

$$pv = \alpha u - p^*v \qquad [4]$$

into Equation [1], it follows that

$$ds = \frac{du + (\alpha u - p^*v)(dv/v)}{T}$$

$$= \frac{v^\alpha du + \alpha u v^{\alpha-1} dv}{Tv^\alpha} - \frac{p^*v^{\alpha+1}}{Tv^\alpha}\frac{dv}{v}$$

$$ds = \frac{d(uv^\alpha)}{Tv^\alpha} - \frac{p^*v^{\alpha+1}}{Tv^\alpha}\frac{dv}{v}$$

So far we have used only the properties of state—temperature, volume, pressure, and energy—which can be represented from direct measurements. Therefore, we can refer to these as *the natural properties of state.* To represent the laws of change of state in a more elementary form, we introduce the following quantities as *the elementary properties of state:*

Independent variables

$$\theta = Tv^\alpha; \qquad \varphi = \log_e v$$

Dependent variable (derived calorific property of state)

$$\epsilon = uv^\alpha$$

Dependent variable (derived thermal property of state)

$$\pi = pv^{\alpha+1} \qquad [5]$$

† New derivation in author's closure.
* Superseded by Equation [104].

[1] Thesis presented before the faculty of mechanical engineering of the Swiss Federal Institute of Technology, Zurich, Switzerland, in partial fulfillment of the requirements for the degree of Doctor of Engineering. Sponsored by Professor G. Eichelberg.

[2] Engineer, Combustion Engineering Company.

Contributed by the Heat Transfer Professional Group and presented at the Spring Meeting, Worcester, Mass., May 1–3, 1940, of The American Society of Mechanical Engineers.

If we substitute

$$\pi^* = p^* v^{\alpha+1}$$

it follows that

$$ds = \frac{d\epsilon - \pi^* d\varphi}{\theta} \quad [6]$$

If ds is a total differential, the following equation must be satisfied

$$\frac{\partial}{\partial\varphi}\left(\frac{\partial s}{\partial\theta}\right) = \frac{\partial}{\partial\theta}\left(\frac{\partial s}{\partial\varphi}\right)$$

From Equation [6]

$$\frac{\partial\epsilon}{\partial\varphi} = \pi^* - \theta\frac{\partial\pi^*}{\partial\theta} \quad [7]$$

and from Equation [4]

$$\epsilon = (1/\alpha)(\pi + \pi^*) \quad [8]$$

Substituting Equation [8] into Equation [7] yields

$$\frac{1}{\alpha}\left(\frac{\partial\pi}{\partial\varphi} + \frac{\partial\pi^*}{\partial\varphi}\right) = \pi^* - \theta\frac{\partial\pi^*}{\partial\theta} \quad [9]$$

2—The Perfect Vapor

Equation [9] is a general relation between two dependent variables which holds for every thermodynamic system, but is not sufficient to recognize its condition. For an ideal system with a limiting condition in which Equation [9] contains only one dependent variable, this modified equation yields a relation for the condition of the system. The limiting condition is

$$\left(\frac{\partial\pi}{\partial\varphi}\right)_\theta = 0 \quad [10]$$

The *perfect vapor* defined by Equation [10] has the characteristic that one of the elementary properties of state depends only on *one* independent variable. This is in remarkable agreement with the behavior of actual vapors. Simple laws will also be found for the other properties. By substituting Equation [10] into Equation [9]

$$\theta\frac{\partial\pi^*}{\partial\theta} + \frac{1}{\alpha}\frac{\partial\pi^*}{\partial\varphi} = \pi^*$$

Integration gives

$$\pi^* = \theta f\left(\frac{\theta}{e^{\alpha\varphi}}\right)$$

Using Equation [5] gives

$$\pi^* = \theta f(T) \quad [11]$$

where $f(T)$ is an arbitrary function of the temperature. The relations between the thermal and calorific properties of the perfect vapor are, according to Equation [8]

$$\epsilon = \frac{1}{\alpha}\left[\pi + \theta f(T)\right]$$

and

$$u = \frac{1}{\alpha}\left[pv + Tf(T)\right] \quad [12]$$

Being a function of temperature only, $f(T)$ can be determined for an arbitrary pressure. If we choose the pressure zero, the intermolecular forces will disappear and the perfect gas law will be fulfilled, whence $pv = RT$.

Then the internal energy at $p = 0$ is given as

$$u = (1/\alpha)\,RT + (1/\alpha)Tf(T)$$

According to the previous assumption that the translation and rotation is fully activated and that the oscillation is partially activated, $(1/\alpha)RT$ is the contribution by the translation and rotation to the internal energy of the perfect vapor. Thus, $(1/\alpha)Tf(T)$ is the contribution due to the oscillation.

Since the variation of the energy of oscillation with pressure is negligible, the quantity $(1/\alpha)Tf(T)$ represents the energy of oscillation at arbitrary pressures.

Then from Equation [11]

$$\pi^* = \alpha v^\alpha u_{osc} \quad [13]$$

from Equation [12]

$$u = (1/\alpha)pv + u_{osc} \quad [14]$$

and from Equation [2]

$$u_{mol} = (1/\alpha)(pv - RT) \quad [15]$$

Equation [15] can be considered as characteristic for the perfect vapor.

Making simplifying assumptions which are exact enough for technical applications, the specific heat of oscillation for every degree of freedom can be written as

$$c_{osc} = R\,\frac{\left(\frac{\Theta}{T}\right)^2 e^{\Theta/T}}{(e^{\Theta/T} - 1)^2}$$

where Θ represents the "characteristic temperature" of the oscillation. By integration and addition over the f_0 degrees of freedom, the contribution of the oscillation to the internal energy is

$$u_{osc} = R\sum_{\iota=1}^{f_0}\frac{\Theta_\iota}{e^{\Theta_\iota/T} - 1}$$

where ι represents the individual terms in the summation. Therefore from Equation [14]

$$u = \frac{1}{\alpha}\,pv + R\sum_{\iota=1}^{f_0}\frac{\Theta_\iota}{e^{\Theta_\iota/T} - 1} \quad [16]^*$$

Introducing the enthalpy $h = u + pv$, we obtain

$$h = \frac{\alpha+1}{\alpha}\,pv + R\sum_{\iota=1}^{f_0}\frac{\Theta_\iota}{e^{\Theta_\iota/T} - 1} \quad [17]\dagger$$

The characteristic function $\Psi = s - (u/T)$ has the differential

$$d\Psi = ds - \frac{Tdu - udT}{T^2}$$

Substituting Equation [1] gives

$$d\Psi = \frac{u}{T^2}\,dT + \frac{p}{T}\,dv \quad [18]$$

In Equation [18] the coefficient of dT is $(\partial\Psi/\partial T)_v$ and the coefficient of dv is $(\partial\Psi/\partial v)_T$, which yields the relations

$$u = T^2\frac{\partial\Psi}{\partial T} \quad \text{and} \quad p = T\frac{\partial\Psi}{\partial v} \quad [19]$$

* Superseded by Equation [105].
† Superseded by Equation [106].

By substitution of Equation [19] into Equation [16], the following differential equation for Ψ is obtained

$$T\frac{\partial\Psi}{\partial T} = \frac{1}{\alpha}v\frac{\partial\Psi}{\partial v} + R\sum_{1}^{f_0}\frac{\Theta_\iota/T}{e^{\Theta_\iota/T}-1}$$

which has the integral

$$\Psi = F(Tv^\alpha) + R\sum_{1}^{f_0}\log_e\frac{e^{\Theta_\iota/T}}{e^{\Theta_\iota/T}-1}$$

The function Ψ determines the entire behavior of the system. $F(Tv^\alpha)$ is an arbitrary function of the elementary property θ only, while the second term is a function of the temperature only; F must be determined for each substance by experiment or individual theory. The definition of the perfect vapor does not include any limitation whatsoever regarding the character of the function $F(\theta)$. Its significance results from the following derivations:

Equation [19] gives

$$p = \alpha T^2 v^{\alpha-1}F'(Tv^\alpha)$$

which yields

$$\frac{\pi}{\theta} = \frac{pv^{\alpha+1}}{Tv^\alpha} = \alpha\theta F'(\theta)$$

when integrated

$$F(\theta) = \frac{1}{\alpha}\int\frac{\pi}{\theta^2}d\theta$$

therefore

$$\Psi = \frac{1}{\alpha}\int\frac{\pi}{\theta^2}d\theta + R\sum_{1}^{f_0}\log_e\frac{e^{\Theta_\iota/T}}{e^{\Theta_\iota/T}-1} \quad \text{[20]}$$

As soon as $\pi(\theta)$ and the Θ_ι are given, the function Ψ is entirely determined.

The further characteristic qualities of the perfect vapor can be found:

(a) The specific heats can be written as

$$c_v = \left(\frac{\partial u}{\partial T}\right)_v = \frac{1}{\alpha}v\frac{\partial p}{\partial T} + c_{osc} \quad \text{[21]*}$$

from Equation [16], and

$$c_p = \left(\frac{\partial h}{\partial T}\right)_p = \frac{\alpha+1}{\alpha}p\frac{\partial v}{\partial T} + c_{osc} \quad \text{[22]†}$$

from Equation [17].

(b) The derivatives of the natural properties of state are

$$\alpha\frac{\partial u}{\partial v} = \frac{\partial(pv)}{\partial v} \quad \text{[23]}$$

from Equation [16], and

$$\frac{\alpha}{\alpha+1}\frac{\partial h}{\partial p} = \frac{\partial(pv)}{\partial p} \quad \text{[24]}$$

from Equation [17].

With $(\partial u/\partial v) = T(\partial p/\partial T) - p$, which follows from the Second Law, we obtain from Equation [12]

$$p + v\frac{\partial p}{\partial v} = \alpha\left(T\frac{\partial p}{\partial T} - p\right)$$

or

$$T\frac{\partial(pv/T)}{\partial T} = \frac{v}{\alpha}\frac{\partial(pv/T)}{\partial v} \quad \text{[25]}$$

From Equation [21]

$$\frac{\partial c_v}{\partial T} = \frac{v}{\alpha}\frac{\partial^2 p}{\partial T^2} + \frac{dc_{osc}}{dT} \quad \text{[26]}$$

With $\partial c_v/\partial v = T(\partial^2 p/\partial T^2)$, which follows from the Second Law Equation [26] yields

$$\frac{\partial(c_v - c_{osc})}{\partial T} = \frac{1}{\alpha}\frac{v}{T}\frac{\partial c_v}{\partial v}$$

or, since c_{osc} does not depend on v

$$T\frac{\partial(c_v - c_{osc})}{\partial T} = \frac{v}{\alpha}\frac{\partial(c_v - c_{osc})}{\partial v} \quad \text{[27]}$$

For the perfect vapor

$$c_v - c_{osc} = c_{tr} + c_{rot} + c_{mol} = (R/\alpha) + c_{mol}$$

Accordingly

$$T\frac{\partial c_{mol}}{\partial T} = \frac{v}{\alpha}\frac{\partial c_{mol}}{\partial v} \quad \text{[28]}$$

As a consequence of the fundamental condition of the perfect vapor Equation [10], there exist relations of Equations [21] to [28], inclusive, between the natural properties of state. These equations are the only limitations for the properties of that system. No limitations are made of the value of these properties or their derivatives. In this manner, the perfect vapor differs from the perfect gas, which has, in addition to Equation [10], the limiting condition $(\partial u/\partial v)_T = 0$ for the value of a certain derivative. The fundamental property of the perfect vapor, from which all other properties derive, is that the elementary property of state π is a function of θ only.

3—Technical Vapors Described as Perfect Vapors

The agreement of the thermodynamic properties of vapors used in technical processes with those derived in Section 2 for the perfect vapor can easily be checked by the results of Equations [10] and [17]. This means (a) if we represent the thermal properties on a π, θ chart, all points of the vapor state will coincide on one curve, since π depends on θ only; and (b) the quantity $h - [(\alpha + 1)/\alpha]pv$ is a function of temperature only, which has the value given in Equation [17]. We proceed now with a verification of the properties in (a) and (b) for several substances.

Steam: $\alpha = 1/3$. The calculations are based on the skeleton table (1)[3] of 1935 for the tolerance ± 0. From this table, we obtain the well-known pv/RT, t chart, shown in Fig. 1, from which those points for saturated and superheated steam which are indicated by circles were selected to be represented in a π, θ chart, shown in Fig. 2. These points cover a range from an approximately gaseous condition to a condition which deviates 75 per cent from the gas law. These points coincide almost exactly into a single curve, which for great values of θ approximates the straight line $\pi = R\theta$, the latter characterizing the perfect gas law. The values for the critical point are

$$\theta_k = 97.123 \text{ m deg C/kg}^{1/3}; \quad \pi_k = 1142.8 \text{ m}^2/\text{kg}^{1/3}$$

The points for saturated water are marked as a supplement to the vapor. We see that only for very small volumes—about $v < 2v_k$—the points will not coincide into one curve. The tangent

* Superseded by Equation [107].
† Superseded by Equation [108].

[3] Numbers in parentheses refer to the Bibliography at the end of the paper.

TABLE 1 VALUES OF $h - 4pv$ FOR STEAM

Pressure, kg/cm²	Temperature, C: 0	50	100	150	200	250	300	350	400	450	500	550
	Values of $h - 4pv$											
p_s	203654	203713	203709	203912	204129	204447	204312	203015	...	...	...	...
1	...	...	203738	204186	204496	205053	205778	206546	207525	208674	209952	211401
10	...	...	...	...	204108	204757	205536	206465	207510	208722	210013	211429
25	...	...	...	...	...	204691	205486	206570	207600	208900	210216	211460
50	...	...	...	...	...	...	205397	206708	207744	208813	210257	211597
75	...	...	...	...	...	...	204760	206755	207807	208936	210334	211700
100	...	...	...	...	...	...	...	206567	207780	209072	210362	211735
200	...	...	...	...	...	...	...	...	206386	208762	210472	211764
300	...	...	...	...	...	...	...	...	...	205533	209052	211422

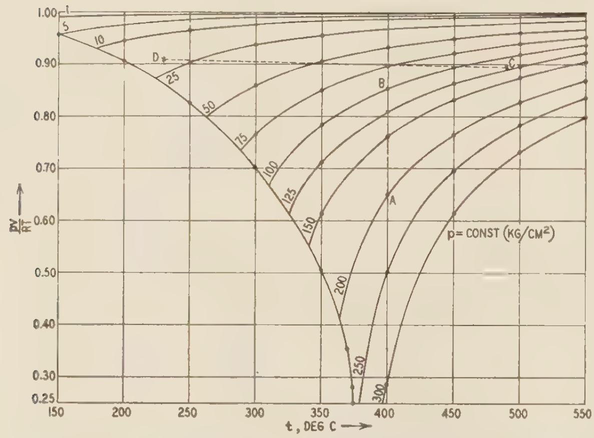

Fig. 1 Deviation of a Water Vapor From the Perfect Gas

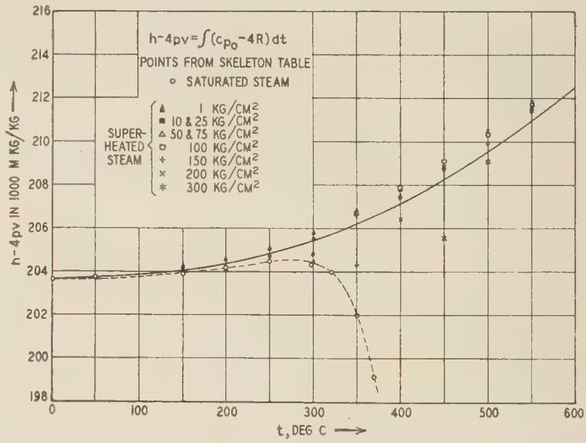

Fig. 4 Enthalpy of Steam Compared With That of a Perfect Vapor

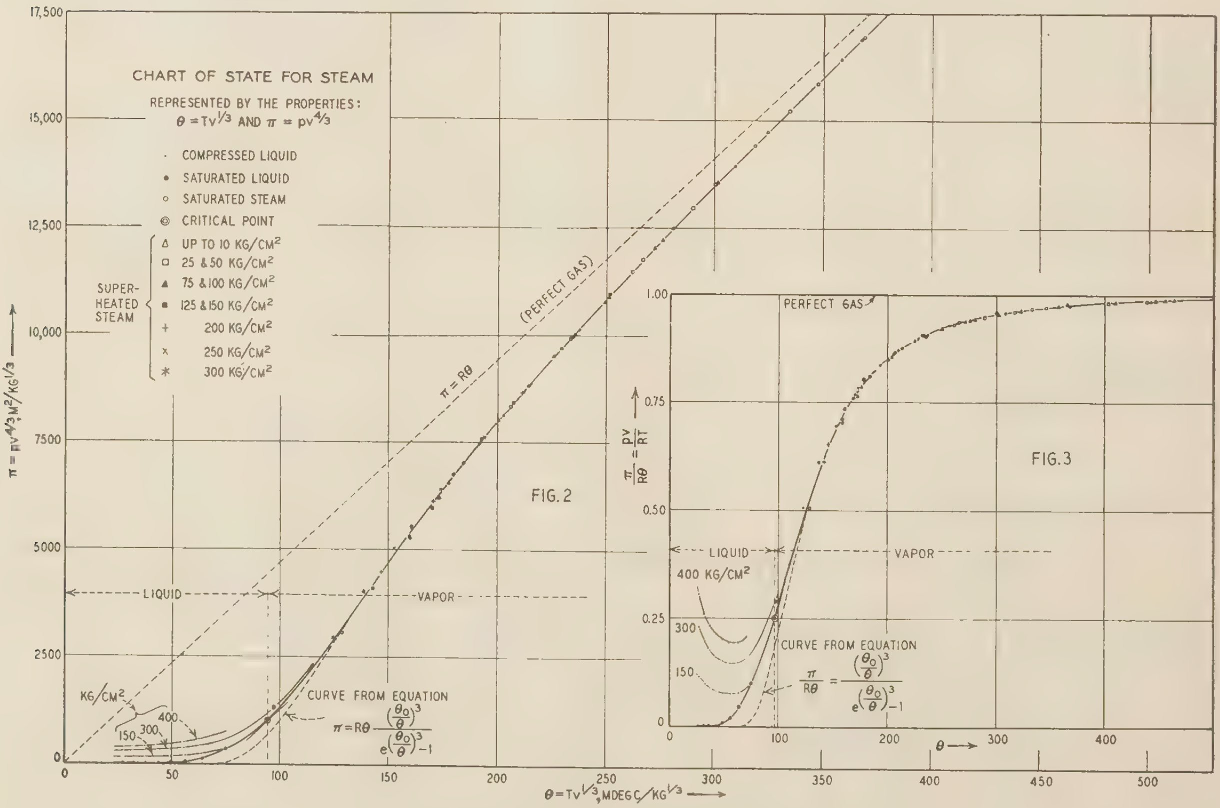

Figs. 2 and 3 Elementary Properties of State of Steam

of the π, θ curve at the critical point has the same slope as the gas line $\pi = R\theta$.

From Fig. 2, the curve $\pi/R\theta = f(\theta)$ can be derived. This curve is shown in Fig. 3 and can be used to establish an empirical equation of state. It indicates how the points in Fig. 1 coincide into a single curve, if one chooses θ instead of T as abcissas; the ordinate is the same, since according to Equation [5] $\pi/R\theta = pv/RT$.

The quantity $h - 4pv$ has the values given in Table 1, which are derived from the skeleton tables (1) and expressed in m kg/kg.

In the large range covered by these tables, $h - 4pv$ is, at constant temperature, almost independent of pressure except the values at very high pressures. Most points from the table are marked in Fig. 4 together with the curve $\int(c_{p0} - 4R)dT$ according to the c_{p0} data by Justi and Lüder (2). The constant of integration is fixed to make the saturation curve pass through the 0 C point of Table 1.

We recognize from the figure that the deviation of the observed values from the curve is very small. Even the variation of $h - 4pv$ with the temperature amounts only to a few per cent. The reason is the small variation of $\int(c_{p0} - 4R)dT$ compared with the great value of the constant of integration. Thus, we obtain as an approximation $h = a_0 + a_1pv$ which relation had already been found in an empirical manner (3). Thus we see that steam is in close agreement with the condition of the perfect vapor.

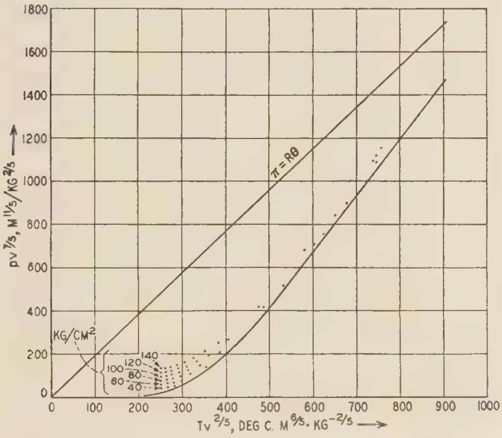

FIG. 5 ELEMENTARY PROPERTIES OF STATE OF CARBON DIOXIDE

*Carbon Dioxide:** $\alpha = {}^2/_5$. Fig. 5 shows the π, θ chart, calculated from Amagat's values. For this substance also the points of state coincide, in general, into one curve when the volume is not too small. Since the volume of carbon dioxide is not measured as accurately as that of steam, the points scatter a little more than those on the steam chart. The chart covers the range from 40 to 140 kg/cm² and from —20 C to +50 C. In the whole range, the deviation from the gas law is very considerable as shown by the straight line $\pi = R\theta$. An empirical equation of state, which holds for pressures up to 40 kg/cm² (4) is

$$v = \frac{RT}{p} - \frac{0.0825 + (1.225 \times 10^{-7})\,p}{(T/100)^{10/3}}$$

$R = 19.273$ m kg/kg deg C; $[v] = \mathrm{m^3/kg}$; $[p] = \mathrm{kg/m^2}$.

According to the Second Law, we obtain the enthalpy by integrating the equation

$$\frac{\partial h}{\partial p} = v - T\frac{\partial v}{\partial T}$$

which gives

$$h = \int c_{p0}dT - \frac{8.3724p + 0.06216p^2}{(T/100)^{10/3}}$$

where p is to be substituted in kg/cm² and $\int c_{p0}dT$ is the temperature function to be introduced by the integration. Then we obtain from Equation [17]

$$h - \frac{7}{2}pv = \int\left(c_{p0} - \frac{7}{2}R\right)dT - \frac{1.61p - 0.03826p^2}{(T/100)^{10/3}}$$

The first term on the right-hand side corresponds to the value of $h - (7/2)pv$ for the perfect vapor, according to Equation [17]. The second term on the right-hand side denotes the deviation of the actual CO_2 vapor from the perfect vapor. The constants used in the calculation of c_{p0} are

$$\Theta_1 = \Theta_2 = 960 \text{ C}; \qquad \Theta_3 = 1830 \text{ C}; \qquad \Theta_4 = 3280 \text{ C}$$

Fig. 6 represents this equation where the constant of integration is so fixed that $\int[c_{p0} - (7/2)R]dT = 0$ at the freezing point $T = 216.8$ C_{abs}. The addition of the second term of the equation results in the scattering of the actual points of state about the theoretical curve. The figure shows that the scattering is very slight and that the CO_2 vapor can be represented with sufficient accuracy as a perfect vapor.

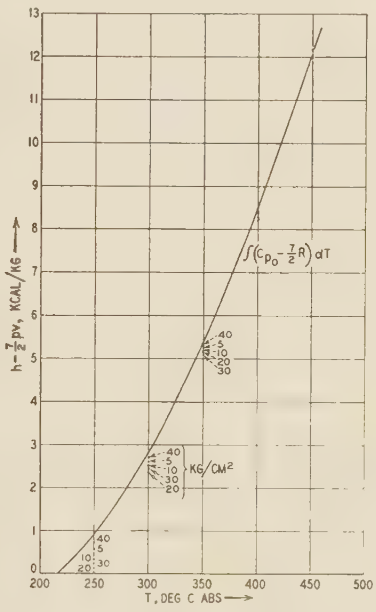

FIG. 6 ENTHALPY OF CO_2 VAPOR COMPARED WITH THAT OF A PERFECT VAPOR

Hydrocarbons: $\alpha = {}^1/_3$. Edmister has succeeded (5) in representing 17 hydrocarbons with close approximation by a joint equation in *reduced* properties of the type

$$v = (RT/p) - b$$

Dividing the quantities T, p, b by their respective values T_k, p_k, b_k for the critical point, yields

$$\frac{v}{b_k} = \frac{RT_k}{p_kb_k}\frac{T_r}{p_r} - b_r$$

* This example superseded by Fig. 16; text obsolete.

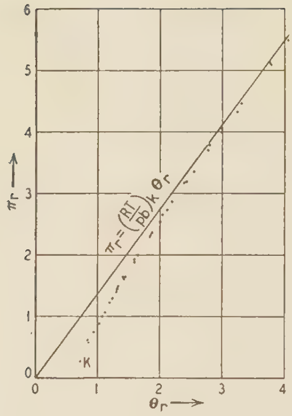

Fig. 7 Elementary Properties of State of Propane

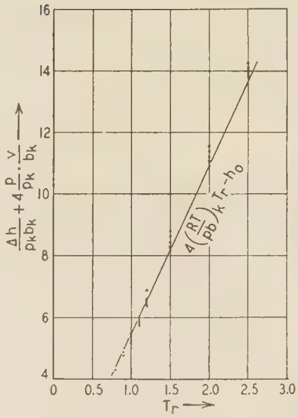

Fig. 8 Enthalpy of C_3H_8 Vapor Compared With That of a Perfect Vapor

where b_r is the same function of both T_r and p_r for the 17 substances examined, and the average value of RT_k/p_kb_k is 1.368, which happens to be the correct value of propane (C_3H_8).

We apply the laws of the perfect vapor to this substance. For this case, let

$$\theta_r = T_r\left(\frac{v}{b_k}\right)^{1/3} \quad \text{and} \quad \pi_r = p_r\left(\frac{v}{b_k}\right)^{4/3}$$

The experimental data determine the π_r, θ_r chart of Fig. 7 where the gas condition is represented by the straight line, $\pi_r = (RT/pb)_k\theta_r$. The figure contains the range of $0.2 < p_r < 2.5$ and $0.8 < T_r < 2.5$ and shows that within these limits, the points of state are approximately located on a single curve.

By means of the statements made in the reported paper (5), we can write Equation [17] as shown in the following paragraph.

The specific heat of propane in the gas condition is

$$c_{p0} = 4.09 + 0.0432T \text{ Kcal/mol deg C}$$

from which the enthalpy in the gas condition can be obtained by integration as

$$h_0 = 4.09T + 0.0216T^2 + h' \text{ Kcal/mol}$$

or

$$h_0 = 1513T_r + 2955T_r^2 + h' \text{ Kcal/mol}$$

If Δh denotes the difference in enthalpy between the gas condition and the condition at any pressure, Equation [17] is written as

$$h_0 - p_kb_k\left(\frac{\Delta h}{p_kb_k} + 4\frac{p}{p_k}\ \frac{v}{b_k}\right) = h_0 - 4RT + h'$$

where $\Delta h/p_kb_k$ is again the same function of both p_r and T_r for the 17 hydrocarbons.

If we suppress h_0

$$\frac{\Delta h}{p_kb_k} + 4\frac{p}{p_k}\ \frac{v}{b_k} = 4\left(\frac{RT}{pb}\right)_k T_r - h'$$

This equation is represented in Fig. 8 for propane where the constant of integration is so fixed that $h' = 0$ at the critical point. The critical data of propane are $T_k = 369.9\ C_{abs}$; $p_k = 43.4$ kg/cm²; $v_k = 0.195$ m³/mol; $b_k = 0.528$ m³/mol. Furthermore, the molecular weight $M = 44.06$ kg/mol, and the gas constant $R = 848$ m kg/mol deg C.

Fig. 8 shows also that the observed values scatter only slightly about the straight line calculated from the foregoing equation for the perfect vapor. Due to the rough approximation in representing the 17 substances by the same law, we cannot expect the points to coincide better on the straight line. We recognize from Figs. 7 and 8 that hydrocarbon vapors in general follow the laws of the perfect vapor.

The advantages which result from the possibility of representing technical vapors as perfect vapors consist in great simplification of the preparatory work required to establish equations of state and tables.

Since the whole field of natural properties reduces to one curve of elementary properties, it is necessary to determine by experiments only as many points as are needed to determine this curve. Then, all other states can be calculated from this curve. By this method we can avoid part of the measurements at high pressures.

The calculation of the calorific properties from the thermal properties will also be simple. From Equation [17] it follows, that an additional temperature function only must be given to calculate the enthalpy for given values of p and v. This function can either be given empirically or can be calculated from the Θ values, which are known by spectroscopic measurements for many substances.

4—Empirical Equation of State for Vapors

The possibility of representing the state of vapors by one curve

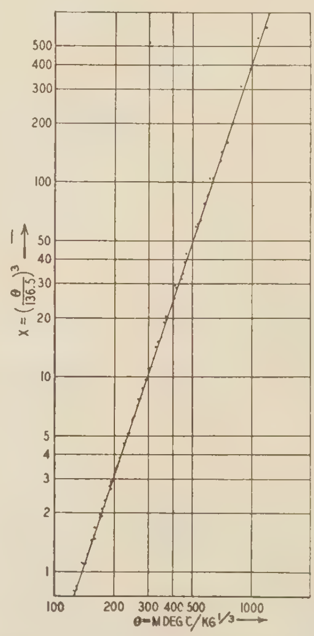

Fig. 9 Representation of the Curve of State of Steam by Equation [30]

facilitates the formation of an empirical equation of state. Due to its characteristic form, the function $\pi/R\theta = f(\theta)$ is most suitable for the analytic representation. The curve of this function belongs to the type

$$y = \frac{1/x}{e^{1/x} - 1} \quad \text{[29]}$$

where x must be represented as such a function of θ that y from Equation [29] gives the same value as $y = \pi/R\theta$ from the curve of state, shown in Fig. 3, for the same value of θ.

To find this function $x = f(\theta)$ we plot the values x in Equation [29] against those values θ of the curve of state, shown in Fig. 3, which belong to the same ordinate. Fig. 9 shows the curve $x = f(\theta)$ for steam which can be represented with great exactness by

$$x = \left(\frac{\theta}{\theta_0}\right)^3 \qquad [30]$$

The points of state in the figure are the same as in Fig. 1. They scatter very slightly about the straight line which is for two thirds of all points within the tolerance of the skeleton table if θ_0 is taken equal to 136.5 m deg C/kg$^{1/3}$. For the other points the deviation also amounts, in the most unfavorable case, to a small percentage. Since the measurements of volume of most vapors have small errors we can expect that the method described here for steam can be applied to the equations of state of other substances.

From Equations [29] and [30] we obtain

$$\frac{\pi}{R\theta} = \frac{(\theta_0/\theta)^3}{e^{(\theta_0/\theta)^3} - 1} \qquad [31]$$

The empirical equation of state then is expressed in natural properties by

$$\frac{pv}{RT} = \frac{\theta_0{}^3/T^3v}{e^{(\theta_0{}^3/T^3v)} - 1} \qquad [32]$$

Equation [32] holds for the entire range of vapor when $v > 2v_k$. With the exception of the gas constant, this equation contains only one other constant, θ_0. It follows from Equation [20] that we must determine $\int (\pi/\theta^2)d\theta$ in order to know the value of the characteristic function. It follows from Equation [31] that

$$\frac{\pi}{\theta^2}\,d\theta = R\,\frac{(\theta_0/\theta)^4}{e^{(\theta_0/\theta)^3} - 1}\,d\left(\frac{\theta}{\theta_0}\right) = -\frac{R}{3}\,\frac{d(\theta_0/\theta)^3}{e^{(\theta_0/\theta)^3} - 1}$$

the integral of which is $\displaystyle\int \frac{\pi}{\theta^2}\,d\theta = \frac{R}{3}\log_e \frac{e^{(\theta_0/\theta)^3}}{e^{(\theta_0/\theta)^3} - 1}$

Thus, we obtain

$$\Psi = R\log_e \frac{e^{(\theta_0/\theta)^3}}{e^{(\theta_0/\theta)^3} - 1} + R\sum_1^{f_0}{}_{\iota} \log_e \frac{e^{\Theta_\iota/T}}{e^{\Theta_\iota/T} - 1} \qquad [33]^*$$

as the characteristic function.

Hence, from Equation [19], the energy of the perfect vapor is obtained as the empirical equation

$$u = 3RT\,\frac{\theta_0{}^3/T^3v}{e^{(\theta_0{}^3/T^3v)} - 1} + R\sum_1^{f_0}{}_{\iota} \frac{\Theta_\iota}{e^{\Theta_\iota/T} - 1} \qquad [34]^*$$

Finally, the entropy results from the Second Law as

$$s = \Psi + (u/T)$$

From Equations [33] and [34]

$$s = R\log_e \frac{e^{(\theta_0/\theta)^3}}{e^{(\theta_0/\theta)^3} - 1} + 3R\,\frac{(\theta_0/\theta)^3}{e^{(\theta_0/\theta)^3} - 1}$$
$$+ R\sum_1^{f_0}{}_{\iota} \log_e \frac{e^{\Theta_\iota/T}}{e^{\Theta_\iota/T} - 1} + R\sum_1^{f_0}{}_{\iota} \frac{\Theta_\iota/T}{e^{\Theta_\iota/T} - 1} \qquad [35]^*$$

Equations [31] to [35] involve Equation [30].

5—Establishment of the Vapor Table

If we start from the characteristic function to describe the thermodynamic properties of a vapor, it follows from Equation [19] that pressure is the only thermal property which can be represented as an explicit function of temperature and volume. It is not possible to obtain volume or temperature as an explicit function of the other two properties of state. In vapor tables, the volume is to be represented as a function of pressure and temperature. A solution of this problem by an empirical method results in an analytic expression, which becomes more complicated for greater validity and exactness of the formula. However, the problem presents a simple solution for a system of the type of Equation [33].

The equation $p = f(T, v)$, belonging to Equation [33], is represented in Equation [32]. Multiplying both sides of Equation [32] with $\theta_0{}^3/T^3v$, we obtain, with the aid of Equation [30]

$$\left(\frac{\theta_0}{T}\right)^3 \frac{p}{RT} = \frac{1/x^2}{e^{1/x} - 1} \qquad [36]$$

Moreover, from Equations [30] and [5]

$$v = x(\theta_0/T)^3 \qquad [37]$$

Thus, it is only necessary to establish a table of the function

$$z = \frac{1/x^2}{e^{1/x} - 1}$$

to determine the volume for the given pressure and temperature.

First, calculate the left side of Equation [36] to obtain $z(x)$. Taking the value x from the table, calculate v according to Equation [37]. After finding the p, v, T values, the temperature function of Equation [17] must be obtained from experimental data, from which equation the enthalpy can be calculated. The entropy is obtained from Equation [35].

In the equations used for the calculation of v, h, and s, the same functions which belong to the following types, are used

$$\frac{1/x}{e^{1/x} - 1}, \qquad \frac{1/x^2}{e^{1/x} - 1}, \qquad \log_e \frac{e^{1/x}}{e^{1/x} - 1}$$

Once tables for these functions are made, the calculation of vapor tables presents no difficulty. An assumption similar to that of Equation [30] will be sufficient, in general, if the neighborhood of the critical point is avoided. By modification of θ_0 in the neighborhood of the saturation line, the accuracy required by the International Steam Tables can be maintained.

6—Isothermal Work of Vapors

For a vapor which satisfies Equation [33], the following is obtained

$$p = \frac{RT}{v}\,\frac{\theta_0{}^3/T^3v}{e^{\theta_0{}^3/T^3v} - 1} \qquad [38]$$

or

$$p = \frac{RT^4}{\theta_0{}^3}\,\frac{(\theta_0/\theta)^6}{e^{(\theta_0/\theta)^3} - 1}$$

The isothermal work of expansion can be found from

$$dA = pdv = \frac{RT^4}{\theta_0{}^3}\,\frac{(\theta_0/\theta)^6}{e^{(\theta_0/\theta)^3} - 1}\,dv$$

By substituting Equation [30] for T = constant

$$dA = RT\,\frac{1/x^2}{e^{1/x} - 1}\,dx$$

* See amendment in author's closure.

the integral of which for the work of expansion, from the initial state to the final state, is

$$A = RT \log_e \frac{1 - e^{-1/x_1}}{1 - e^{-1/x_2}}$$

Substituting the original variables, the isothermal work of expansion is found as

$$A = RT \log_e \frac{1 - e^{-(\theta_0/T)^3(1/v_1)}}{1 - e^{-(\theta_0/T)^3(1/v_2)}} \qquad [39]$$

In the limiting case, where the vapor condition approximates the gas condition—large values of T or v—the exponential function can be developed in a series which can be terminated after the linear term, thus obtaining the approximation

$$e^{-(\theta_0/T)^3(1/v)} = 1 - \left(\frac{\theta_0}{T}\right)^3 \frac{1}{v}$$

In this case

$$A = RT \log_e (v_2/v_1) \qquad [40]$$

which is the well-known law for the work of expansion of a perfect gas. It is of interest to examine the manner in which the external work of Equation [39] varies if the volumes v_1 and v_2 remain the same, but the temperature T is changed by dT and then T is allowed to approach zero.

By differentiation at constant volume, from Equation [39]

$$\left(\frac{\partial A}{\partial T}\right)_v = R \log_e \frac{1 - e^{-(\theta_0/T)^3(1/v_1)}}{1 - e^{-(\theta_0/T)^3(1/v_2)}} + 3R\left(\frac{(\theta_0/T)^3(1/v_2)}{e^{(\theta_0/T)^3(1/v_2)} - 1} - \frac{(\theta_0/T)^3(1/v_1)}{e^{(\theta_0/T)^3(1/v_1)} - 1}\right) \qquad [41]$$

The first term in Equation [41] is

$$R \log_e \frac{e^{(\theta_0/T)^3(1/v_2)}}{e^{(\theta_0/T)^3(1/v_2)} - 1} - R \log_e \frac{e^{(\theta_0/T)^3(1/v_1)}}{e^{(\theta_0/T)^3(1/v_1)} - 1}$$

Then, if T approaches zero, each term in Equation [41] approaches zero. Accordingly

$$\lim_{T \to 0} \left(\frac{\partial A}{\partial T}\right)_v = 0 \qquad [42]$$

To show the application of Equation [39], calculate the work of isothermal expansion for steam at 400 C from 200 kg/cm² to 100 kg/cm² (A-B in Fig. 1), which is a range where the deviation from the gas law is very large.

For a check, first calculate the amount of the work from the V.D.I. steam tables.

In the initial state:	In the final state:
$v_1 = 0.01031$ m³/kg	$v_2 = 0.02710$ m³/kg
$h_1 = 676.6$ Kcal/kg	$h_2 = 740.4$ Kcal/kg
$s_1 = 1.3327$ Kcal/kg deg C	$s_2 = 1.4865$ Kcal/kg deg C
$u_1 = 628.3$ Kcal/kg	$u_2 = 676.9$ Kcal/kg

According to the Second Law, the work of isothermal expansion is

$$A = T(s_2 - s_1) - (u_2 - u_1)$$

With these values, it follows that

$$A = 54.9 \text{ Kcal/kg}$$

According to Equation [39], taking $\theta_0 = 136.5$ m deg C/kg$^{1/3}$ and v_1, v_2 from the V.D.I. steam tables

$$A = 74.2 \log_e \frac{1 - e^{-\frac{0.008337}{0.01031}}}{1 - e^{-\frac{0.008337}{0.02710}}} = 74.2 \log_e 2.0940 = 54.8 \text{ Kcal/kg}$$

which is in close agreement with the steam tables.

The perfect gas law gives

$$A = RT \log_e (p_1/p_2) = 74.2 \log_e 2 = 51.4 \text{ Kcal/kg}$$

which is in error 6.8 per cent. If the work is calculated from Equation [40] which is an equivalent form for gases, we obtain

$$A = RT \log_e (v_2/v_1) = 74.2 \log_e 2.6285 = 71.7 \text{ Kcal/kg}$$

which is in error 30.6 per cent.

7—The Adiabatic Curve*

The differential equation for the adiabatic curve of the perfect vapor can be derived from Equation [6] where $ds = 0$. Using Equation [8], the following can be written

$$(1/\alpha)(d\pi + d\pi^*) = \pi^* d\varphi$$

or

$$d\pi = \alpha\pi^* d\varphi - d\pi^* \qquad [43]$$

From Equation [13] it follows that

$$d\pi^* = \alpha^2 v^{\alpha-1} u_{osc}\, dv + \alpha v^\alpha du_{osc}$$

which when substituted with Equation [13] in Equation [43] yields

$$d\pi = -\alpha v^\alpha du_{osc}$$

Hence, making use of Equation [5], the differential equation for the adiabatic curve is

$$\frac{d\pi}{\theta} = -\alpha \frac{du_{osc}}{T} \qquad [44]$$

In Equation [44], π is a function of θ only, while u_{osc} is a function of T only. Thus, the integration is possible as soon as these functions are known.

Since monatomic vapors have no energy of oscillation and, for diatomic vapors, the energy of oscillation is not activated at low temperatures, in these particular cases, $u_{osc} = 0$. Consequently $d\pi = 0$ and $\pi = $ const which can be written as

$$pv^{\alpha+1} = \text{const} \qquad [45]$$

in the natural properties of state.

It follows from Equation [45] that for monatomic vapors and for diatomic vapors at low temperatures each point on the curve of state in the π, θ diagram represents an entire adiabatic curve. Thus, all states which coincide into one point in the π, θ diagram are connected between each other by an adiabatic change of state.

As an approximation, the energy of oscillation of polyatomic vapors can be considered constant over limited ranges of an adiabatic change of state. Then in Equation [44] du_{osc} again equals zero, and Equation [45] may be used for polyatomic vapors also.

Using the α values in Equation [3], the equation of the adiabatic curve is

$$\left.\begin{array}{ll} \text{for monatomic vapors} & pv^{5/3} = \text{const} \\ \text{for diatomic vapors} & pv^{7/5} = \text{const} \\ \text{for polyatomic vapors} & pv^{4/3} = \text{const} \end{array}\right\} \qquad [46]$$

* This section superseded by Equations [110–113].

The last equation has been introduced by Zeuner for the adiabatic curve of superheated steam.

Equations [46] do not involve the fact that the perfect gas law be fulfilled, or that u_{mol} equals zero.

8—Establishment of the Mollier Chart

To represent adiabatic changes of state, the Mollier chart must be used which, for the perfect vapor, is developed as follows:

Equation [35] can be written in the dimensionless form

$$\frac{s}{R} = f\left(\frac{\theta}{\theta_0}\right) + g\left(\frac{T}{\Theta}\right) \qquad [47]$$

where the functions f and g are given by Equation [35]. Determine the isothermals in the h, s diagram. In this case, $g(T/\Theta)$ is constant. Then, choose an arbitrary pressure, calculate v from Equations [36] and [37]. This allows us to calculate h from Equation [17], and $\theta, f(\theta/\theta_0)$, and s/R from Equation [47]. Thus, h can be plotted against s/R for given values of p and T. This may be done for any pressure desired. Finally, the isobars can be traced through the points of constant pressure on different isothermals.

To show the reliability of a Mollier chart thus established, we consider an adiabatic expansion of steam where the results can be compared with the V.D.I. Mollier chart. Take the initial state as

$$p_1 = 120 \text{ kg/cm}^2, \qquad t_1 = 490 \text{ C}$$

In the final state, the temperature be given as

$$t_2 = 230 \text{ C}$$

while the final pressure is obtained from the condition for the adiabatic change of state

$$s/R = \text{const}$$

This process is marked by the line C-D in Fig. 1.

First determine $g(T/\Theta)$ for the initial condition. The three characteristic temperatures of H_2O are

$$\Theta_1 = 2342 \text{ C}, \qquad \Theta_2 = 5357 \text{ C}, \qquad \Theta_3 = 5492 \text{ C}$$

With these constants, the first term in the function $g(T/\Theta)$ in Equation [47] reads

$$\Sigma L\left(\frac{T}{\Theta_i}\right) = \log_e \frac{e^{2342/T}}{e^{2342/T}-1} + \log_e \frac{e^{5357/T}}{e^{5357/T}-1} + \log_e \frac{e^{5492/T}}{e^{5492/T}-1}$$

Substituting the initial temperature $T_1 = 490 + 273.16 = 763.16$ C_{abs} gives

$$\Sigma L(T/\Theta_i) = 0.04765 + 0.00090 + 0.00075 = 0.04930$$

With the same constants, the second term in the function $g(T/\Theta)$ in Equation [47] reads

$$\Sigma y(T/\Theta_i) = \frac{2342/T}{e^{2342/T}-1} + \frac{5357/T}{e^{5357/T}-1} + \frac{5492/T}{e^{5492/T}-1}$$

Substituting the initial temperature $T_1 = 763.16$, we have

$$\Sigma y(T/\Theta_i) = 0.1496 + 0.0063 + 0.0054 = 0.1613$$

Thus

$$g(T/\Theta) = 0.1613 + 0.0493 = 0.2106$$

The initial volume is calculated from the method developed in Section 5, using Equations [36] and [37]. For steam, $\theta_0 = 136.5$ m deg C/kg$^{1/3}$.

Thus we have

$$\frac{p}{RT} = \frac{120 \times 10^4}{47.064 \times 763.16} = 33.410 \text{ kg/m}^3$$

and

$$\left(\frac{T}{\theta_0}\right)^3 = \left(\frac{763.16}{136.50}\right)^3 = 174.76 \text{ kg/m}^3$$

Equation [36] gives

$$z(x) = \frac{p/RT}{(T/\theta_0)^3} = \frac{33.410}{174.76} = 0.191176$$

From a table of the function $z(x) = \dfrac{1/x^2}{e^{1/x}-1}$

it is found that

$$x = 4.6933$$

From Equation [37] it follows that

$$v_1 = \frac{x}{(T/\theta_0)^3} = \frac{4.6933}{174.76} = 0.02686 \text{ m}^3/\text{kg}$$

This value agrees with 0.02687 m³/kg from the V.D.I. steam table within the tolerance.

Then, from Equation [17] the enthalpy in the initial state is

$$h_1 = 4pv + RT\Sigma y\left(\frac{T}{\Theta_i}\right) = \frac{4 \times 120 \times 10^4 \times 0.02686}{427} + 0.11023 \times 763.2 \times 0.1613$$

which gives

$$h_1 = 315.5 + h_0 \text{ Kcal/kg}$$

where the constant h_0 is introduced to provide the conventional zero point of enthalpy.

To calculate the function $f(\theta/\theta_0)$, we find from the initial data

$$\theta = Tv^{1/3} = 763.16 \times 0.02686^{1/3} = 228.58 \text{ m deg C/kg}^{1/3}$$

and

$$\frac{\theta}{\theta_0} = \frac{228.58}{136.50} = 1.6746$$

Then, the two functions constituting $f(\theta/\theta_0)$ are

$$\frac{(\theta_0/\theta)^3}{e^{(\theta_0/\theta)^3}-1} = 0.89731$$

and

$$\log_e \frac{e^{(\theta_0/\theta)^3}}{e^{(\theta_0/\theta)^3}-1} = 1.6513$$

Thus

$$f(\theta/\theta_0) = 1.6513 + 3 \times 0.89731 = 4.3432$$

Furthermore, from Equation [47]

$$s/R = 4.3432 + 0.2106 = 4.5538$$

The final temperature is

$$T_2 = 230 + 273.16 = 503.16 \text{ C}_{abs}$$

For this temperature, the two terms in the function $g(T/\Theta)$ are

$$\Sigma y\left(\frac{T}{\Theta_i}\right) = 0.04518$$

and

$$\Sigma L\left(\frac{T}{\Theta_\iota}\right) = 0.00960$$

Hence

$$g\left(\frac{T}{\Theta}\right) = 0.05478$$

For an adiabatic change of state

$$s/R = \text{const}$$

Substituting the previously obtained value of s/R, Equation [47] yields

$$f(\theta/\theta_0) = 4.5538 - 0.05478 = 4.4990$$

From a table of this function

$$\theta/\theta_0 = 1.7498$$

Hence

$$\theta = 238.85 \text{ m deg C/kg}^{1/3}$$

and for the final volume

$$v_2 = (\theta/T)^3 = 0.1070 \text{ m}^3/\text{kg}$$

The final pressure is obtained from Equation [38] as

$$p_2 = 20.13 \text{ kg/cm}^2$$

For these values T_2 and p_2, the V.D.I. steam table gives $v_2 = 0.1071$ m³/kg, which agrees with our calculated value within the tolerance.

From these properties the enthalpy in the final state is obtained as

$$h_2 = 204.3 + h_0 \text{ Kcal/kg}$$

The net adiabatic work follows from the Second Law as

$$L = h_1 - h_2 = 111.2 \text{ Kcal/kg}$$

The V.D.I. Mollier chart gives for adiabatic expansion between the considered limits

$$L = 112.4 \text{ Kcal/kg}$$

The deviation is within the tolerance. The example shows that the described method permits establishing a Mollier chart of satisfactory exactness.

9—Extension of the Equation of State to High Densities

The characteristic function of the perfect vapor is composed of the following four terms:

(*a*) Translation, according to classic theory

$$\Psi_{tr} = \left(\frac{3}{2}\right) R \log_e (2\pi mkT) + R \log_e (v/h^3)$$

(*b*) Rotation, according to classic theory

$$\Psi_{rot} = \left(\frac{1}{\alpha} - \frac{3}{2}\right) R \log_e \left(\frac{8\pi^3 kT}{h^2}\right) + R \log_e \frac{\sqrt{(JKL)}}{\pi}$$

(*c*) Oscillation, according to theory of quanta

$$\Psi_{osc} = R \sum_1^{f_0} \log_e \frac{1}{1 - e^{-\Theta_\iota/T}}$$

(*d*) Molecular forces, according to empirical formula Equation [33]

$$\Psi_{mol} = R \log_e \frac{(\theta_0/\theta)^{1/\alpha}}{1 - e^{-(\theta_0/\theta)^{1/\alpha}}} \quad [48]$$

where h, J, K, L, m are constants. Then,

$$\Psi = \Psi_{tr} + \Psi_{rot} + \Psi_{osc} + \Psi_{mol}$$

By differentiation according to Equation [19] the relations for the perfect vapor are obtained.

At high densities, the space occupied by the molecules has to be taken into account, whence

$$\Psi_{tr} = (3/2)R \log_e (2\pi mkT) + R \log_e (v - b)/h^3 \quad [49]$$

Thus, Equation [19] yields the thermal equation of state

$$p = \frac{RT}{v-b} - \frac{RT}{v}\left(1 - \frac{(\theta_0/\theta)^{1/\alpha}}{e^{(\theta_0/\theta)^{1/\alpha}} - 1}\right)$$

The second term represents the internal pressure resulting from the molecular forces. After rewriting this equation, for $\alpha = 1/3$ the following is obtained

$$\frac{pv}{RT} = \frac{(\theta_0/\theta)^3}{e^{(\theta_0/\theta)^3} - 1} + \frac{b}{v-b} \quad [50]$$

and

$$p = \frac{RTb}{v(v-b)} + \frac{R\theta_0^3/T^2v^2}{e^{\theta_0^3/T^3v} - 1} \quad [51]$$

Equations [50] and [51] represent an empirical equation for both the liquid and the vapor state. It is evident that, in the range of high densities, the points of state do not coincide on one curve. The relations derived for the perfect vapor do not hold, but they are obtained for the limiting case $v \gg b$.

Superimposing the curves which are represented by the two terms in Equation [51] yields p, v isothermals similar to those in van der Waals' equation of state, with the distinction that the difference between the maxima and minima approaches zero for very low temperatures as well as for very high temperatures, so that p is unable to assume negative values.

It is not possible by means of the simple assumptions of Equations [48] and [49] to obtain more than a qualitative representation of the equation of state of a liquid, because in the range of very high densities more complicated laws hold for the molecular forces.

10—Deduction of the Vapor-Pressure Curve From the Equation of State

If the equation of state of a system

$$F(p, v, T) = 0 \quad [52]$$

which includes both the liquid and vapor state, be known, it is possible to deduce the vapor-pressure curve

$$f(p, T) = 0 \quad [53]$$

from this equation. The knowledge of such energy quantities as heat of evaporation is not necessary for the solution of this problem.

First, set up the mathematical relation, which must be satisfied by the corresponding points of state of the liquid and vapor phase. This relation is obtained by representing the system by the three properties of state which have the same value for both phases in the thermodynamic equilibrium, i.e., pressure, temperature, and thermodynamic potential. The thermodynamic potential

$$G = u + pv - Ts$$

may be considered as a function of the two other properties and is connected with them by the relation

$$\left(\frac{\partial G}{\partial p}\right)_T = v \qquad [54]$$

from which

$$G = \int v dp + \psi(T) \qquad [55]$$

The condition of equilibrium to be satisfied for the vapor-pressure curve is that G has the same value for both the liquid and for the vapor phases. Therefore

$$G_l = G_v \qquad [56]$$

Since the temperature is identical in both phases, the temperature function in Equation [55], resulting from the integration of Equation [54] can be deleted in Equation [56]. Then, the condition of equilibrium can be formulated as follows. The function

$$g = \int v dp$$

has the same value in both phases; a fact which gives

$$g_l = g_v \qquad [57]$$

and, instead of Equation [54]

$$v = dg/dp \qquad [58]$$

Introduce this expression into Equation [52] to obtain the differential equation

$$F\left(\frac{dg}{dp}, p, T\right) = 0 \qquad [59]$$

which when integrated at constant T gives the state of the system represented by a family of isothermals on a g, p diagram, namely

$$\Phi(g, p, T) = 0 \qquad [60]$$

To recognize the character of the vapor-pressure curve, examine the isothermals in Equation [60] for a given equation of state.

Since an analytic determination of the function in Equation [60] is not possible for the Equation of State [51], we choose as an example Berthelot's equation of state

$$p = \frac{RT}{v - b} - \frac{a/T}{v^2} \qquad [61]$$

The constants are found from the condition that in the critical point both $\partial p/\partial v = 0$ and $\partial^2 p/\partial v^2 = 0$, namely

$$a = (9/8)RT_k^2\ v_k \quad \text{and} \quad b = (1/3)v_k \qquad [62]$$

These results give the p, v isothermal of Fig. 10. According to Equation [58], by integration of the p, v isothermals

$$g = \int v dp = pv - \int p dv$$

which gives the g, v isothermals.

Plot p against the values of g, which belong to the same v, to obtain the isothermals of the g, p diagram. These isothermals represent the integral curves of Equation [60] which belong to the Differential Equation [59]. These integral curves have one double point located between two cusps. On the branch of the curve between the cusps, $d^2g/dp^2 > 0$, or according to Equation [58] $dv/dp > 0$. This portion of the curve corresponds to the unstable space between the two phases. The double point represents the state in which the thermodynamic potentials of both phases have the same value; it is a point on the vapor-pressure curve. Thus, the two portions of the curve between the double point and the cusps represent the metastable range. The parts of the curve outside of the double point represent the ranges of stable liquid and stable vapor. Therefore, the boundary curves between the unstable and the metastable state are the locus of the cusps and the vapor-pressure curve is the locus of the double points of the family of isothermals. *Thus the curves of equilibrium are represented as the curves of singularities of the integral curves in Equation [60].* The curves of singularities, however, are not singular solutions of the Differential Equation [59], because their tangents do not coincide with those of the regular integral curves, which is evident from Fig. 10.

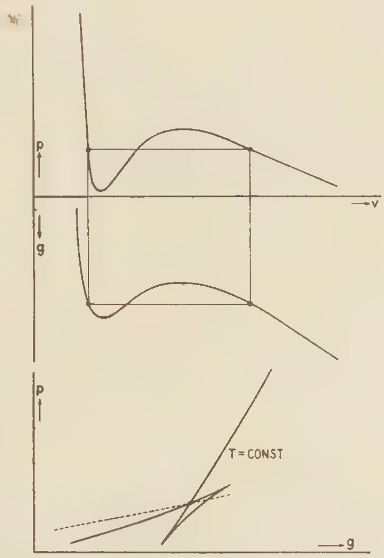

FIG. 10 DETERMINATION OF THE PHASE EQUILIBRIUM FROM THE EQUATION OF STATE

The problem to calculate the vapor-pressure curve for a given equation of state requires the determination of the curve of the double points in Equation [60], that is, the determination of that point of the integral curves in Equation [60], for which the condition

$$\frac{dg}{dp} = -\frac{\partial\Phi/\partial p}{\partial\Phi/\partial g} = \frac{0}{0} \qquad [63]$$

is satisfied by two real and different solutions. Although the graphic solution of this problem is not difficult, the analytic solution will be practicable in particular cases and then only in the implicit form of Equation [53].

To explain the method developed, first calculate the vapor-pressure curve belonging to the Equation of State [61]. By substituting Equation [58] into Equation [61], the particular form of the Differential Equation [59] is

$$p = \frac{RT}{(dg/dp) - b} - \frac{a}{T(dg/dp)^2}$$

Writing

$$w = b\frac{dp}{dg} = \frac{b}{v} \qquad [64]$$

where

$$0 < w < 1$$

$$p = \frac{RT}{b}\frac{w}{1-w} - \frac{a}{b^2T}w^2 \ldots\ldots\ldots\ldots [65]$$

is obtained. Differentiation with respect to g gives

$$w = RT\frac{dw/dg}{(1-w)^2} - \frac{2a}{bT}w\frac{dw}{dg}$$

In this latter equation, a separation of variables is possible, so that

$$dg = RT\frac{dw}{w(1-w)^2} - \frac{2a}{bT}dw$$

and the integration gives

$$g = RT\log_e\frac{w}{1-w} + \frac{RT}{1-w} - \frac{2a}{bT}w + C \ldots\ldots [66]$$

Let the constant of integration be zero. Now, eliminate w in Equation [66] by using the Equation of State [65]. Equation [65] then gives an equation of third degree in w

$$w^3 - w^2 + w\left(\frac{RT^2b}{a} + \frac{b^2T}{a}p\right) - \frac{b^2T}{a}p = 0$$

If the quantities

$$\alpha = \frac{RT^2b}{a} \qquad \text{and} \qquad \beta = \frac{b^2T}{a}p \ldots\ldots\ldots [67]$$

are introduced

$$w^3 - w^2 + w(\alpha + \beta) - \beta = 0 \ldots\ldots\ldots\ldots [68]$$

If w_1, w_2, w_3 denote the three roots in Equation [68]

$$(w - w_1)\,(w - w_2)\,(w - w_3) = 0$$

or

$$w^3 - (w_1 + w_2 + w_3)w^2 + (w_1w_2 + w_1w_3 + w_2w_3)\,w - w_1w_2w_3 = 0$$

By comparison of the coefficients with Equation [68]

$$\left.\begin{aligned} w_1 + w_2 + w_3 &= 1 \\ w_1 \times w_2 \times w_3 &= \beta \end{aligned}\right\} \ldots\ldots\ldots\ldots\ldots [69]$$

Using Equation [65], β can be replaced by α so that

$$\frac{\beta}{w} = \frac{\alpha}{1-w} - w \ldots\ldots\ldots\ldots\ldots\ldots [70]$$

Thus, the second of Equations [69] reads

$$w_2 \times w_3 = \frac{\alpha}{1-w_1} - w_1$$

The roots w_2 and w_3 can be expressed by w_1 with the aid of Equations [69]. Let

$$W = \sqrt{(1+w)^2 - 4\alpha/(1-w)}$$

Then by omission of the subscript of w_1

$$\left.\begin{aligned} w_2 &= {}^1/_2(1 - w + W) \\ w_3 &= {}^1/_2(1 - w - W) \end{aligned}\right\} \ldots\ldots\ldots\ldots\ldots [71]$$

Equation [68] gives w, according to the Cardan formula, as

$$w = \frac{1}{3} + \sqrt[3]{\frac{1}{3}\left(\beta - \frac{\alpha}{2} + \frac{1}{9}\right) + \frac{1}{3}\sqrt{\left[\frac{1}{3}\left(\alpha + \beta - \frac{1}{3}\right)^3 + \left(\frac{\alpha}{2} - \beta - \frac{1}{9}\right)^2\right]}}$$
$$+ \sqrt[3]{\frac{1}{3}\left(\beta - \frac{\alpha}{2} + \frac{1}{9}\right) - \frac{1}{3}\sqrt{\left[\frac{1}{3}\left(\alpha + \beta - \frac{1}{3}\right)^3 + \left(\frac{\alpha}{2} - \beta - \frac{1}{9}\right)^2\right]}} \ldots\ldots [72]$$

Introduce the function

$$\phi = g/RT$$

which can also be considered as a function of equilibrium, because T has the same value in both phases. The three roots of ϕ can be found from Equation [66] as

$$\left.\begin{aligned} \phi_1 &= \log_e\frac{w}{1-w} + \frac{1}{1-w} - \frac{2w}{\alpha} \\ \phi_2 &= \log_e\frac{1-w+W}{1+w-W} + \frac{2}{1+w-W} - \frac{1}{\alpha}(1 - w + W) \\ \phi_3 &= \log_e\frac{1-w-W}{1+w+W} + \frac{2}{1+w+W} - \frac{1}{\alpha}(1 - w - W) \end{aligned}\right\} [73]$$

Then, the complete integral function is

$$\Phi = (\phi - \phi_1)(\phi - \phi_2)(\phi - \phi_3) \ldots\ldots\ldots\ldots [74]$$

in which the values above are to be substituted for ϕ_1, ϕ_2, ϕ_3. The locus of the double points of this function is the vapor-pressure curve.

Equation [74] is too complicated to calculate the curve of the double points from the condition expressed by Equation [63]. But since, in the foregoing example, the equations of each of the three branches of the equilibrium function are given, only the point of intersection of two branches need be calculated.

The problem can be solved easily by first determining which of the three roots of w belongs to the liquid, the unstable, and the vapor phase. By calculating these values for one isothermal we find that w_1 corresponds to the liquid state, w_2 to the unstable state, and w_3 to the vapor state. The same holds for the functions ϕ_1, ϕ_2, ϕ_3. Thus, the vapor-pressure curve is the locus of the points of intersection of ϕ_1 with ϕ_3 on the different isothermals, so the condition is

$$\phi_1 = \phi_3 \ldots\ldots\ldots\ldots\ldots\ldots\ldots\ldots [75]$$

Thus, it follows, after rewriting Equation [73] that

$$\log_e\left[\left(\frac{2}{1+w+W} - 1\right)\left(\frac{1-w}{w}\right)\right] = \frac{1}{\alpha}(1 - 3w - W) + \frac{1}{1-w} - \frac{2}{1+w+W} \ldots\ldots [76]$$

If, for w in Equation [76] is substituted its value from Equation [72] and the α and β are replaced according to Equation [67] by functions of p and T, Equation [53] is obtained. This is the implicit vapor-pressure curve of the Equation of State [61]. Also, p as a function of T is obtained by graphic solution of the

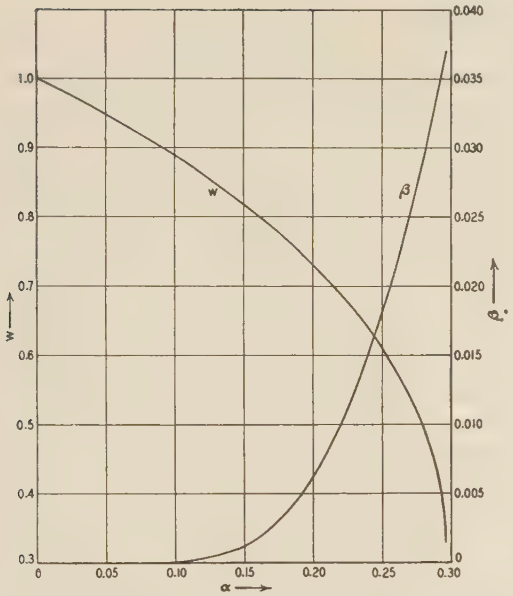

Fig. 11 Determination of the Vapor-Pressure Curve of Equation [61]

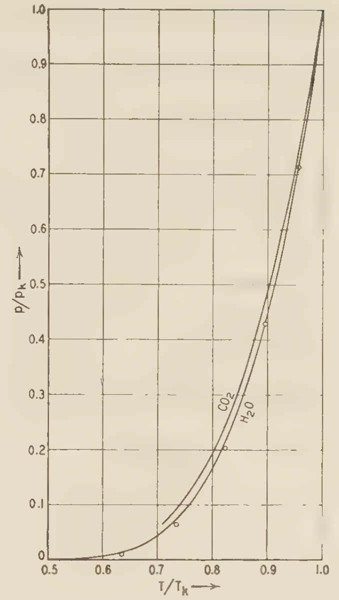

Fig. 12 Vapor-Pressure Curve of Equation [61] Compared With Actual Substances

transcendental Equation [76] giving $w = f(\alpha)$, as shown in Fig. 11. This curve in conjunction with Equation [70] gives

$$\beta = \alpha \frac{w}{1 - w} - w^2$$

which is the curve $\beta = f(\alpha)$ in Fig. 11. Replacing α and β by Equation [67] gives with the aid of Equation [62]

$$\frac{T}{T_k} = \sqrt{\left(\frac{27}{8}\alpha\right)} \quad \text{and} \quad \frac{p}{p_k} = \frac{27\beta}{\frac{T}{T_k}}$$

The vapor-pressure curve of Berthelot's Equation of State [61] in reduced properties can now be found from Fig. 11. The location of this curve is marked by circles in Fig. 12. The figure shows that the vapor-pressure curves of H_2O and CO_2 are very close to this curve.

Acknowledgment

The author wishes to express his indebtedness to M. J. Fish of the Combustion Engineering Company for his aid in the translation of this paper.

BIBLIOGRAPHY

1 "Third International Conference on Steam Tables," *Mechanical Engineering*, vol. 57, 1935, p. 710.

2 "Spezifische Wärme, Entropie und Dissoziation technischer Gase und Dämpfe," by E. Justi and H. Lüder, *Forschung auf dem Gebiete des Ingenieurwesens*, vol. 6, no. 5, 1935, p. 210.

3 "Empirische Kontrolle einer einfachen Gleichung für reale Gase," by E. J. M. Honigmann, *Forschung auf dem Gebiete des Ingenieurwesens*, vol. 2, no. 7, 1931, p. 261.

4 "Die thermischen Eigenschaften der Kohlensäure im gasförmigen, flüssigen und festen Zustand," by R. Plank and J. Kuprianoff, *Zeitschrift gesamte Kälteindustrie*, vol. 36, March, 1929, p. 41.

5 "Thermodynamic Properties of Hydrocarbons," by W. C. Edmister, *Industrial and Engineering Chemistry*, vol. 30, 1938, p. 352.

Discussion

H. D. Baker.[4] The author has undertaken to establish a method of computing tables for the thermodynamic properties of substances when only a few experimental data are available—less than have previously been considered necessary.

In order to do this he has assumed that the internal energy of a gas is given by his Equation [2], which takes account of energy due to translation, rotation, oscillation, and intermolecular forces. He neglects other forms of energy, such as electronic, nuclear, and chemical energy in the molecule. There is little if any evidence that these last undergo appreciable changes in thermal processes at ordinary temperatures. Hence, they are of no practical importance here.

Translational and rotational energies are computed by means of the Boltzmann "equipartition theorem." It is to be noted, however, that this is not a rigid law, but rather a rough generalization. The term α is usually a function of temperature, decreasing in the case of hydrogen almost linearly from approximately $^2/_3$ at —350 F to approximately $^2/_5$ at 100 F (6).[5]

The author has obtained an expression from the quantum theory for the energy due to oscillation. This method has been used with success in computing specific heats and radiation exchange (7). It is, however, somewhat laborious. To determine the energy due to intermolecular forces he has, in effect, assumed an equation of state

$$pv^{\alpha+1} = F(Tv^{\alpha})$$

where F is an undetermined function, but which is later limited by the condition that pv approach RT at very low pressures. This implies an assumption that when Tv^{α} is constant, $pv^{\alpha+1}$ is also constant. This is true for an ideal gas, for which

$$\frac{C_p}{C_v} = \alpha + 1$$

[4] Department of Mechanical Engineering, Columbia University, New York, N. Y.

[5] Numbers in parentheses (6) to (15) refer to the Bibliography at the end of this discussion.

The latter condition imposed is justified by experience with actual gases (8).

The expression which the author has obtained for the contribution to the internal energy by intermolecular forces is

$$u_{\text{mol}} = \frac{1}{\alpha}(pv - RT)$$

The accuracy of this expression must be tested.

Differentiating at constant temperature, we obtain

$$\left[\frac{du_{\text{mol}}}{dv}\right]_T = \frac{1}{\alpha}\left[\frac{d(pv)}{dv}\right]_T$$

It is assumed that the internal pressure $\left(\frac{du}{dv}\right)_T$, denoted by λ, is due to intermolecular forces (9, 13). Then $\left(\frac{du}{dv}\right)_T$ should equal $\left[\frac{du_{\text{mol}}}{dv}\right]_T$; or λ should equal $\frac{1}{\alpha}\left[\frac{d(pv)}{dv}\right]_T$.

Reliable experimental data exist for both λ and pv. The degree to which values of $\frac{1}{\alpha}\left[\frac{d(pv)}{dv}\right]_T$, as calculated from these data, approximate the experimental values of λ will then be a test of the accuracy of the author's Equation [15], $u_{\text{mol}} = \frac{1}{\alpha}(pv - RT)$.

The writer has made such a test and for it has chosen nitrogen as being a substance of normal behavior. He has obtained $\frac{1}{\alpha}\left[\frac{d(pv)}{dv}\right]_T$ by scaling isothermal pv versus p curves (8), and has scaled values for λ from Clark's curves (10, 11, 12, 13, 14).[6] α is assumed to be $^2/_5$. The results are shown in Fig. 13 of this discussion.

[6] Dr. Roebuck has communicated to the writer the fact that Ward Murrell and Vance have recently computed λ for nitrogen from data previously published (14). They find λ = 0.00297 at 1; 1.186 at 20; 10.56 at 60; 28.47 at 100; 53.25 at 140; and 101.83 at 200, all in atmospheres at 32 F.

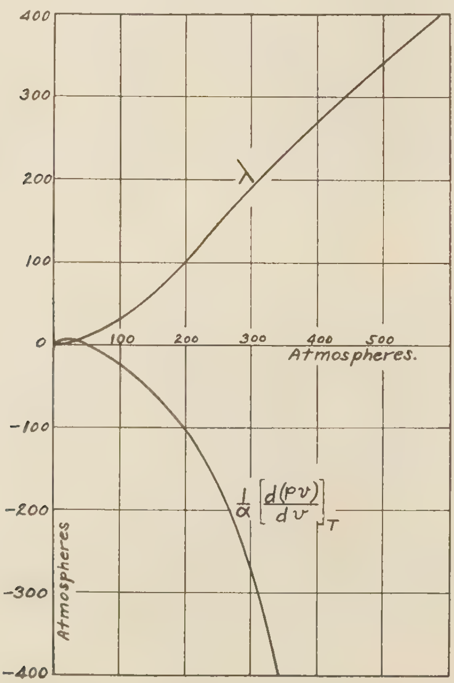

Fig. 13 Results of Tests to Check Accuracy of Author's Equation [15] for Nitrogen at 32 F

It is clear that values for $\frac{1}{\alpha}\left[\frac{d(pv)}{dv}\right]_T$ do not at all agree with those for λ. Hence, the validity of the author's expression $u_{\text{mol}} = \frac{1}{\alpha}(pv - RT)$ is not sustained in this test. The fair degree of agreement with experiment which he demonstrates in his section 3 may be accounted for by the fact that there the energy changes, due to intermolecular forces, are lumped together with much larger quantities (11, 13). Hence, his check is not a reliable test of the accuracy of his expression $u_{\text{mol}} = \frac{1}{\alpha}(pv - RT)$.

Most of the relations in section 2 of the paper depend upon those assumptions which gave rise to the foregoing relation. Also many equations and calculations in subsequent parts of the paper depend upon the equations in section 2. The results of the test, shown in Fig. 13, indicate that such equations and calculations cannot be relied upon implicitly. If used, they must be used with due discretion.

In the writer's opinion, expressing isolated experimental observations in general formulas is useful in proportion to the accuracy with which these formulas represent the facts, to the simplicity of these formulas, and to the degree to which they may reasonably be used for extrapolation to cases for which no experimental data exist. Such a form as a power series, for example, is simple, and the accuracy of the "fit" to the experimental data will be in proportion to the number of empirically determined constants (15). However, extrapolation is resorted to with confidence only when the formulas have thoroughly sound rational bases.

It is the writer's opinion that the author has succeeded in satisfying the first of these three requirements but there is lack of evidence of success in regard to the other two.

BIBLIOGRAPHY

6 "Introduction to Modern Physics," by F. K. Richtmyer, McGraw-Hill Book Company, Inc., New York, N. Y., 1934, p. 297.

7 Ibid., p. 280.

8 "Relations Between the Temperatures, Pressures, and Densities of Gases," U. S. Bureau of Standards, Circular No. 279, 1926, p. 40.

9 "The Thermodynamic Properties of Helium Gas," by J. R. Roebuck and H. Osterberg, *Physical Review*, vol. 45, 1934, p. 337.

10 "A Study of the Joule and Joule-Thomson Effects," by A. L. Clark and L. Katz, *Canadian Journal of Research*, vol. 16, sec. A., 1938, p. 53.

11 "The Calorimetric Determination of the Intrinsic Energy of Gases as a Function of the Pressure," by F. D. Rossini and M. Frandsen, U. S. Bureau of Standards, *Journal of Research*, Research Paper 503, vol. 9, 1932, p. 746.

12 "The Joule-Thomson Effect in Air," by J. R. Roebuck, Proceedings of the American Academy of Arts and Sciences, vol. 64, no. 9, August, 1930, p. 334.

13 "The Joule Effect in Air," by H. D. Baker, Summaries of Doctoral Dissertations, University of Wisconsin Press, vol. 4, 1938, p. 125.

14 "The Joule-Thomson Effect in Nitrogen," by J. R. Roebuck and H. Osterberg, *Physical Review*, vol. 48, 1935, pp. 450–457.

15 "Higher Mathematics for Engineers and Physicists," by I. S. Sokolnikoff, McGraw-Hill Book Company, Inc., New York, N. Y., 1934, p. 396.

Fr. Bosnjakovic.[7] The attempt to characterize a perfect vapor by the property, that π is a function of θ only, is very interesting. The possibility of establishing an exact equation of state with the aid of only a few experiments is quite valuable. The disadvantage of this method is that the physical significance of the "elementary properties of state" π and θ is not evident.

[7] University of Zagrab, Jugoslavia.

The neighborhood of the critical point is described incompletely, even by means of these complicated considerations. The reason probably is the extraordinary variety and variability of the molecular clusters in this region, where any assumption of a roughly uniform substance cannot even lead to approximate solutions. Such an assumption is introduced by the calculation of the internal energy u from Equation [16].

It is desirable to extend the considerations to vapor mixtures where experimental data are even more scarce. Here, the knowledge of the enthalpy and entropy is particularly valuable for many purposes. It may be that the definition of a "perfect-vapor mixture" in the described manner would be useful.

The same may be said of gas mixtures at high pressures, as used in process industries, but here the prospect looks less hopeful.

J. H. Keenan.[8] This paper is an interesting addition to the literature of the equation of state. The author provides a means of control in the development of an equation of state which will doubtless be frequently employed in future work.

Perhaps it is worth-while to point out that the author's method is based on the assumption that along a line for which pv^k is constant Tv^{k-1} is nearly constant, where k denotes the author's $(\alpha + 1)$. The value of k is 5/3 for a monatomic gas, 7/5 for a diatomic gas, and so forth. It is well known that for most engineering gases a line for which pv^k is constant is, very closely, a line of constant entropy over most of the vapor region; and the same may be said of a line for which Tv^{k-1} is constant. Therefore, each point on the empirical curves of Figs. 2 and 3 of the paper represents, approximately, a line of constant entropy, at least in the vapor region. From this point of view it is not astonishing that the relation between π and Θ is not unique at high pressures relative to the critical pressure or in the liquid region.

The curves of Figs. 2, 3, and 4 are to such a small scale that it is not possible to determine the precision to which properties of steam can be represented by a single curve. A table of differences from the International Skeleton Table values would be illuminating.

The author might well have shown more consideration for his readers, one of whom encountered the following difficulties: The derivation of Equation [7] is not adequately indicated. The independent variables change so often in the course of the analysis that it is only by great effort that one can determine which variable is held constant in differentiation. Perhaps it is not too late to add subscripts to the derivatives. The introduction of the expression for c_{osc} and the consequent summations in Equations [16] and [17] appear to serve only to complicate the mathematical relations; symbols for pure temperature functions would have served as well. In the applications made by the author, empirical data take the place of these involved expressions. Equation [63] is not enlightening. The symbol α appears with two different connotations. Section 10 seems to bear little or no relation to the previous sections; moreover, there is nothing in it which tells just what new material it contains.

F. G. Keyes.[9] The author states that three ways are available for investigating the properties of thermodynamic systems: (1) The "properties are derived from experiments with real substances." Experience has shown without exception the soundness of this method, and one might well add, the absolute necessity of carrying out controlled measurements if real knowledge is desired about any substance. (2) The author states that the properties are determined from a theory. It is, however, self-evident that a "theory" is bounded strictly by the experimental basis upon which it is established. For example, Maxwell's theory of electricity and magnetism based on Faraday's experimental results at ordinary temperatures has been so satisfactory that anyone questioning its inclusiveness would be considered suffering from an aberration. The electromagnetic behavior of some metals and many semiconductors at low temperatures is now known however to be at variance with Maxwell's theory, so much so that we must regard the theory (as finally all human effort must be regarded) as bounded. (3) The author states, "the properties are deduced from a definition, by which an ideal system is created." It is difficult to perceive how positive knowledge can evolve out of definitions, and moreover the number of possible definitions is about infinite at least.

The author's procedure rests essentially on the introduction of a number of new variables which are functions of physically measurable quantities, "observables" for example, pressure, volume, and temperature. The new variables are therefore not observables but must be deduced from them.

Thus, $\Theta = Tv^\alpha$, $\varphi = \ln v$, $\epsilon = uv^\alpha$ (u is intrinsic energy)

$\pi = pv^{\alpha+1}$ (α is twice the reciprocal of the number of degrees of freedom of the molecule regarded as a mechanical model)

are called by the author "elementary properties of state." The author does not show that Θ, φ, ϵ, and π are unique, and it will be observed that they are not independent. That is, the thermodynamic state of a body may be specified by its energy, entropy, or the functions enthalpy or free energy, and each of these is expressible in terms of two variables, p, T; v, T; or p, v provided gravitational and electrical effects are absent and the body is isotropic. The observables u, p, v, T in terms of Θ, φ, ϵ, π, and α are

$$T = \Theta e^{-\alpha\varphi}; \quad p = \pi e^{-\varphi(\alpha+1)}; \quad v = e^\varphi; \quad u = \epsilon e^{-\alpha\varphi} \ldots [77]$$

Thus it is seen that except for v three of the new variables are required to specify each observable T, p, or u. Of course α is a constant for any specified pure substance but in the general case α would vary from one equilibrium state to another (chemical-reactive gas mixture).

The quantity intrinsic energy u is expressed in three ways

$$u = \frac{RT}{\alpha} + u_{osc} + u_{mol} \ldots\ldots [78a]$$

$$u = \frac{pv}{\alpha} + p^*v \ldots\ldots [78b]$$

$$u = \epsilon e^{-\alpha\varphi} \ldots\ldots [78c]$$

In these equations u_{osc} is the energy due to the vibrational energy of the separate atoms comprising the molecule; u_{mol} is the intramolecular energy while p^* from Equation [11] and that following Equation [5] is given by the following equation

$$p^* = \Theta e^{-\varphi(1+\alpha)} f(\Theta e^{-\alpha\varphi}) = v^{-(\alpha+1)} [\Theta f(T)]^{-1}$$

The term for the rotational energy is taken to have its classical value and incorporated in the first member with the translational in the factor α^{-1}. This is not a valid assumption except at high temperatures. The Equation [78c], however, admits of no restriction unless it is equated to [78a] as a means of defining ϵ. Thus, something is left to be desired with respect to just how u is to be regarded. Of course the unambiguous method would be to

---

[8] Associate Professor of Mechanical Engineering, The Massachusetts Institute of Technology, Cambridge, Mass. Mem. A.S.M.E.

[9] Department of Chemistry, The Massachusetts Institute of Technology, Cambridge, Mass.

integrate a general relation for u without making any hypothesis about new composite variables.

Using the author's variables one may integrate the following equation

$$\left(\frac{\partial u}{\partial v}\right)_T = T\left(\frac{\partial p}{\partial T}\right)_v - p$$

Introducing the variables and letting α remain constant[10] we find the equation for energy becomes

$$u - u_0 = f(T)_{p\to 0} + \int_{\varphi=\varphi_0}^{\varphi} e^{-\alpha\varphi}\frac{\partial\pi}{\partial\Theta}d\varphi - \int_{\varphi=\varphi_0}^{\varphi} e^{-\alpha\varphi}\pi d\varphi. \quad [79]$$

where $f(T)$ is a function of temperature alone and u_0 a constant corresponding to selected values of T and φ. To evaluate the energy in these variables does not appear to offer special advantages even if the integrands of the second and third terms of the right-hand member of Equation [79] can be integrated in terms of known functions. Of course, in the end, for practical purposes, the energy must be expressed in terms of observables, i.e., p, T; v, T.

The author's real objective is, however, to suggest a relation connecting the variables p, v, and T for a unit of a pure substance and this he comes to in Equation [32]. The value of the paper is in the main to be judged on the basis of whether this two-constant equation, in the case of any pure substance of interest, will suffice to represent the available experimental data with satisfactory fidelity. The "perfect vapor" is one that follows the relation $(\partial\pi/\partial\varphi)_\Theta = 0$ or $\pi = f(\Theta)$, or again, $pv^{(1+\alpha)} = f(Tv^\alpha)$ and the author finds that, in the case of steam, $pv^{4/3}$ versus $Tv^{1/3}$ does bring the p, v, T data into a single line except at the higher densities in the vapor phase. The line in these variables is linear at low densities but the curvature is pronounced as high densities are approached. It is Equation [32] of the paper which is offered as the best empirical expression of the "perfect vapor."

A small transformation of Equation [32] with expansion of the transcendental term leads to

$$\left.\begin{aligned} pv &= RT - \frac{R}{2!}\frac{\theta^3}{T^2v} - \frac{R}{3!}\frac{\theta^6}{T^5v^2} - \ldots \\ \text{or}\quad pv &= RT - \frac{A_1}{T^2v} - \frac{A_2}{T^5v^2} - \ldots \end{aligned}\right\} \ldots\ldots [32a]$$

where A_1, A_2, etc., are constants characteristic of each substance.

Forming the expression for the Joule-Thomson coefficient μ, we find

$$\mu c_p = \frac{2A}{R}\cdot\frac{1}{T^3} + \frac{6A_2}{R}\cdot\frac{1}{T^3}\cdot\frac{1}{v} \ldots\ldots [80]$$

where pv has been eliminated by using Equation [32a]. Thus, it is seen that the latter equation suggests the original treatment of Joule and Thomson whereby their results were found to follow the form[11] $\mu c_p = \frac{c}{T^n}$ where c is a constant and n is taken to be 2. Callendar chose an equation of state which may be regarded as a special form of Equation [32a] where the higher terms are dropped.

It is now well known, however, that the Joule-Thomson coefficient is positive, zero, or negative for pure substances, depending upon the temperature even at very low pressures. Thus, it is perceived that any equation of state leading to a Joule-Thomson representation which is invariably a positive quantity is greatly restricted in generality.

The author has not shown by actual comparisons the degree of fidelity with which the p, v, T data for steam may be represented by his Equation [32] but, if it is not better than the approximation shown in Table 1 for (h — 4 pv), considerable is left to be desired in point of precision. It is also worth stating that there is no a priori theoretical justification for believing that the author's Equations [32] or Equation [80] of this discussion offer any prospect of finality. The graphical representations of the properties of steam, carbon dioxide, and propane are however astonishingly good.

Section 10 contains nothing new[12] and it is well known that one uses the devices of the section only as a last resort in the absence of experimental information.

B. H. Sage.[13] The author has suggested the use of certain derived properties of state which are related to the ordinary thermodynamic properties in an arbitrary fashion. The behavior of a "perfect vapor" is derived by employing these "elementary properties of state," so restricted that for a single substance each such property is a single-valued function of one individual variable. In so far as the assumptions are in agreement with experimentally determined behavior, this procedure reduces materially the experimental information required to establish the thermodynamic behavior of a pure substance. Comparisons with experimental data are given and indicate that digressions from this relatively simple correlation become appreciable at the higher densities. Apparently, the relationships are no more than qualitatively applicable to liquids. The general approach to the evaluation of the constants in the "elementary" equation of state is based upon kinetic hypotheses and the values vary with the molecular nature of the gas.

Thermodynamic relations, based upon the equation of state for a perfect vapor, are employed to calculate a number of properties such as enthalpy and free energy. Several comparisons between predicted values for the work associated with changes in state under arbitrary conditions of restraint with those obtained from experimental information are given. In general, reasonable agreement is obtained but it should be realized that the equation of state is based upon experimental information concerning the behavior of the material. It is the writer's belief that the agreement with experiment is not as good as has been obtained in some other cases, notably in the application of the Beattie-Bridgeman equation of state to the behavior of hydrocarbon gases. However, this is not surprising in view of the fact that, in the application of the more complicated Beattie-Bridgeman equation, more data are required in order to establish the constants.

The author has applied Berthelot's equation of state to the

[10] Satisfactory only at temperatures high enough to warrant setting the rotational energy equal to its equipartition value.

[11] "On the Geometrical Representation of the Expansive Action of Heat, and the Theory of Thermodynamic Engines," by W. J. M. Rankine, Philosophical Trans. of the Royal Society of London, 1854, pp. 115–176.

[12] "Die Theorie des Sättigungsgesetzes," by M. Planck, *Wiedemann's Annalen*, vol. 13, 1881, pp. 535–543.

"Über die Theoretische Bestimmung des Dampfdruckes und der Volumina des Dampfes und der Flussigkeit," by R. Clausius, *Wiedemann's Annalen*, vol. 14, 1881, pp. 279–290 and 692–704.

"Die reduzirten Gibbs'-schen Fläcken," by K. Onnes, Communications from the Physical Laboratory of the University of Leiden, no. 66, 1900.

"Note on van der Waals' Equation," by H. Hilton, *Philosophical Magazine*, vol. 1, 1901, pp. 579–589 and vol. 2, pp. 108–118.

"Der Satz vom Thermodynamischen Potential beim Gleichgewichte eines heterogenen Systems mit Anwendung auf die Theorie von van der Waals und das Gesetz des Siedepunktes," by E. Riecke, *Wiedemann's Annalen*, vol. 53, 1894, pp. 379–391; "Über die Zustandsgleichung von Clausius," by E. Riecke, *Wiedemann's Annalen*, vol. 54, 1895, pp. 739–744.

[13] Assistant Professor of Chemical Engineering, California Institute of Technology, Pasadena, Calif.

prediction of the relation of the vapor pressure of a pure substance to temperature, employing the equality of the "thermodynamic potentials," pressures, and temperatures of the coexisting gas and liquid phases as the criteria of equilibrium. This thermodynamic potential is usually called "chemical potential" in American usage.[14] The method of solution utilized seems somewhat complicated and apparently is of no greater accuracy than has been obtained in the solution of other equations of state. The uncertainty of prediction as illustrated is comparable in magnitude to the differences to be found when the behavior of various substances is compared on a reduced basis.

The author is to be complimented upon an interesting discussion of an inherently complex problem for which he has apparently found a solution which may be of engineering utility in many instances. It is the writer's belief that the correlation of volumetric and phase-equilibrium data in accordance with the relationships set forth by Gibbs, such as the Duhem equation, will yield one of the most satisfactory bases for the prediction of the thermodynamic behavior both of pure substances and of complex mixtures.

J. A. Goff.[15] The essence of the author's paper is his hypothesis

$$u = \frac{f}{2}\, pv + u^\circ(T) \quad \ldots\ldots\ldots\ldots\ldots\ldots [81]$$

where f is a constant. The author attempts to establish a physical basis for this hypothesis by stating that the contribution to internal energy from intermolecular forces is

$$u_{\rm mol} = \frac{f}{2}\,(pv - RT) \quad \ldots\ldots\ldots\ldots\ldots [81a]$$

but clearly this is merely an alternative statement of the hypothesis and, so far as the writer is aware, is not a prediction of statistical mechanics.

The well-known identical relations of thermodynamics can be applied to the hypothesis Equation [81] directly and simply without the aid of unfamiliar variables to derive

$$pv/RT = F(Tv^{2/f}) \quad \ldots\ldots\ldots\ldots\ldots\ldots [82]$$

The form of the function F is not determined by Equation [81], although of course, its argument is. Equation [82] is equivalent to the author's Equation [10]; but why it should be dignified as a definition of "the perfect vapor" is not at all apparent.

As explained, Equation [12] is corollary to Equation [1] and must be true in any range of the physical variables where Equation [1] is true. The author assumes that this range includes the zero-pressure isobar. If it does, then

$$u^\circ(T) = \int \left(C_{v=\infty} - \frac{f}{2} R \right) dT + u^\circ \quad \ldots\ldots [83]$$

which still leaves the constant f undetermined. The author chooses f so that, at sufficiently high temperatures, the integrand will represent the contribution to $C_{v=\infty}$ from all motions excepting translation and rotation; but of course there is nothing compelling this particular choice, and it is entirely possible that a different choice would strike better agreement with experimental data. Furthermore, in some cases, electronic motions make an appreciable contribution to the internal energy, in which cases the author would not be justified in assuming that the integrand arises solely from vibrational motion as he has done.

[14] "Thermodynamic Relations in Multicomponent Systems," by R. W. Goranson, Carnegie Institute of Washington, 1930.

[15] Dean, Towne Scientific School, University of Pennsylvania, Philadelphia, Pa. Mem. A.S.M.E.

The value of the paper would have been greatly enhanced if the author had stated his hypothesis Equation [81], its corollary Equation [82], his assumption that their range of validity includes the zero-pressure isobar, Equation [83], and if he had been somewhat more apologetic for his particular choice of f. But of course the use of unfamiliar, unnecessary, and confusing variables makes this difficult. In this connection, it might be appropriate to ask what set of "elementary properties" the author would have employed if he had wanted to arrive, in similar manner, at

$$pv/RT = \varphi\left(Tp^{-\frac{2}{2+f}}\right) \quad \ldots\ldots\ldots\ldots [82a]$$

which is equivalent to Equation [82] and, therefore, corollary to Equation [81] also.

Agreement with experimental data on steam through Equation [81] is shown in Fig. 3 of the paper, and may be regarded as good or bad, depending upon the range of physical variables in which interest lies. Fig. 4 of the paper points to the usual experience that an empirical equation of state must represent p, v, T data extraordinarily well if it is to agree only moderately well with thermal data.

Author's Closure

In the foregoing discussions, further information is desired regarding the assumptions underlying the perfect vapor and the limits of its applicability. This can be done best by deriving Equations [10] and [15] from statistical thermodynamics. During the long interval between the time the paper was submitted until it was finally published, further progress was made in the application of statistics to the potential energy of molecules, thus enabling the author to set up the characteristic molecular qualities which, in first approximation, lead to the perfect vapor. It was found from this new derivation that the quantity α in the paper has the value $^1/_3$ for all kinds of molecules, and that certain relations given in the paper have to be modified for monatomic and linear molecules. It was with the revision[16] which will now be discussed that the paper was presented at the 1940 Spring Meeting of the A.S.M.E.

The energy of a fluid system consists of the internal energy of the molecules which is a function of temperature alone, and of the translational energy which is a function of both temperature and volume of the system. Thus, the partition function Ω has the form

$$\Omega = \Omega_{\rm tr}(T,v) \times \Omega_{\rm int}(T) \quad \ldots\ldots\ldots\ldots\ldots [84]$$

The energy of translation consists of kinetic and potential energy; its contribution to the partition function is (302,5)

$$\Omega_{\rm tr} = \frac{1}{h^3 N!} \int \cdots\cdots \int e^{-\frac{U_{\rm kin} + U_{\rm pot}}{kT}}\, dp_x dp_y dp_z dx dy dz \;.\, [85]$$

where

$$U_{\rm kin} = \frac{p_x^2 + p_y^2 + p_z^2}{2m}$$

Then, Equation [85] can be written

$$\Omega_{\rm tr} = \frac{1}{h^3} \int\!\!\int\!\!\int_{-\infty}^{+\infty} e^{-\frac{p_x^2 + p_y^2 + p_z^2}{2mkT}}\, dp_x dp_y dp_z \times \frac{1}{N!} \int \underset{(N)}{\cdots\cdots} \int e^{-\frac{U_{\rm pot}}{kT}}\, dx_i dy_i dz_i \ldots . [86]$$

[16] The deduction is based on methods described in "Statistical Thermodynamics," by R. H. Fowler and E. A. Guggenheim, Cambridge University Press, London, The Macmillan Company, New York, N. Y., 1939. Numbers in parentheses throughout this closure refer to the corresponding equations in this book.

Integration of the first term gives the temperature function

$$\Omega_{\text{kin}} = \left(\frac{\sqrt{2\pi mkT}}{h}\right)^3 \ldots\ldots\ldots\ldots\ldots [87]$$

The integration of the second term has to be taken over the entire space available to each of the N molecules. The assumption is made that the potential energy consists only of the simultaneous interaction of not more than two molecules, and we write

$$U_{\text{pot}} = \epsilon_{\alpha,\beta}$$

Since N molecules can be paired in $\frac{N}{2}(N-1)$ different ways, there are as many factors under the integral. With the abbreviation

$$d\omega_l = dx_l dy_l dz_l$$

Equation [86] gives (703,1)

$$\Omega_{\text{pot}} = \frac{1}{N!}\int \underset{(N)}{\cdots\cdots} \int \prod^{\frac{N}{2}(N-1)\text{ factors}} e^{-\frac{\epsilon_{\alpha,\beta}}{kT}} d\omega_1 d\omega_2 \ldots\ldots d\omega_N \ldots [88]$$

We introduce (703,2)

$$\eta_{\alpha,\beta} = e^{-\frac{\epsilon_{\alpha,\beta}}{kT}} - 1 \ldots\ldots\ldots\ldots\ldots\ldots [89]$$

and write (703,3)

$$\Omega_{\text{pot}} = \frac{1}{N!}\int \underset{(N)}{\cdots} \int \prod^{\frac{N}{2}(N-1)} (1 + \eta_{\alpha,\beta}) d\omega_1 d\omega_2 \ldots\ldots d\omega_N \ldots [90]$$

This product must now be expanded into a power series. According to the configurations permitted, certain terms in this expansion are canceled. Thus, the selection of the mechanism of molecular interaction is one of the factors which determine the thermal properties of the substance. For low densities, pairwise interaction is a satisfactory assumption which leads to van der Waals' equation of state. For higher densities, the formation of molecular clusters must be assumed, the size of which increases with the density. At very high densities, each molecule will be confined to a cell formed by its nearest neighbors.

We consider a vapor of moderate density and assume that only the simplest type of cluster may exist, this being a tetrahedron with one molecule in each corner. Each molecule at the base of this pyramid may interact with the molecule at the tip, and there may be no interaction among the base molecules themselves, Fig. 14. Then, only the following terms remain in the series expansion (703,5)

$$\Omega_{\text{pot}} = \frac{1}{N!}\int \underset{(N)}{\cdots\cdots} \int \Big(1 + \Sigma\eta_{1,4}\eta_{2,4}\eta_{3,4} + \Sigma\eta_{1,4}\eta_{2,4}\eta_{3,4} \times \eta_{5,8}\eta_{6,8}\eta_{7,8} + \ldots\ldots\Big) d\omega_1\, d\omega_2 \ldots\ldots d\omega_N \ldots [91]$$

The first sum represents configurations with but one group of four molecules, each within the range of force of the others; the second sum represents configurations with two distinct groups of four molecules interacting, and so on for the other sums. The number of terms under each sum has now to be enumerated. In the first sum, each of the N molecules can occupy place 1, then remain $(N-1)$ molecules for place 2, $(N-2)$ molecules for place 3, and $(N-3)$ molecules for place 4. Thus, the number of permutations is

$$N(N-1)(N-2)(N-3)$$

In case of complete symmetry, it was necessary to divide this expression by 4! to eliminate identical arrangements. But in the present case, interchange of the tip molecule with each base molecule represents a different arrangement; moreover, two distinct arrangements of the base molecules are possible, Fig. 15. Thus, the number of combinations is obtained by multiplying the number of permutations by $\frac{8}{4!} = \frac{1}{3}$ as

$$\frac{N(N-1)(N-2)(N-3)}{3}$$

The number of terms under the second sum is obtained by extending this procedure to groups of two tetrahedra. The number

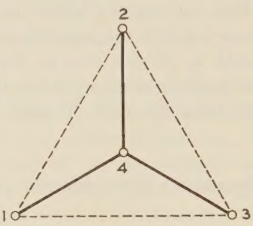

Fig. 14

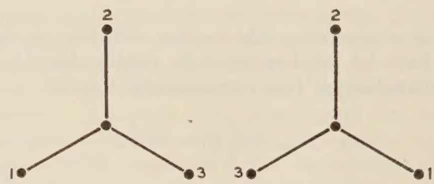

Fig. 15

of molecules available for the places 5, 6, 7, 8 in the second tetrahedron are subsequently $(N-4)$, $(N-5)$, $(N-6)$, $(N-7)$. Identical arrangements are eliminated by multiplying the number of permutations by $^1/_3$ for each of the two tetrahedra. The interchange of identical tetrahedra within each group is eliminated by division by 2!. Thus, the number of distinct sets of two tetrahedra is

$$\frac{N(N-1)(N-2)(N-3)(N-4)(N-5)(N-6)(N-7)}{2!\ 3^2}$$

In general, the number of distinct sets of r tetrahedra is

$$\frac{N(N-2)(N-3)\ldots\ldots[N-(4r-1)]}{r!\ 3^r} = \frac{N!}{r!\ 3^r\ (N-4r)!}$$

Then, after some transformation, the partition function becomes (703,6)

$$\Omega_{\text{pot}} = \frac{v^N}{N!}\sum_{0}^{\frac{N}{4}}{}_r \frac{N!}{r!(N-4r)!N^{3r}} \times \left[\frac{N^3}{3v^4}\int\int\int\int \eta_{1,4}\eta_{2,4}\eta_{3,4} d\omega_1 d\omega_2 d\omega_3 d\omega_4\right]^r \ldots [92]$$

or, if the abbreviation ξ is introduced for the term in the bracket (703,9)

$$\Omega_{\text{pot}} = \frac{v^N}{N!}\sum_{0}^{\frac{N}{4}}{}_r \frac{N!}{r!(N-4r)!N^{3r}}\,\xi^r \ldots\ldots\ldots [93]$$

To evaluate this expression, we make the further approximation (703,10)

$$\Omega_{pot} \approx \frac{v^N}{N!}\sum_0^N{}_r \frac{N!}{r!(N-r)!}\xi^r = \frac{v^N}{N!}(1+\xi)^N \ldots [94]$$

Using Stirling's theorem, we obtain (703,12)

$$ln\,\Omega_{pot} = N\left(1 + ln\frac{v}{N}\right) + N\,ln\left(1 + \frac{N^3}{3v^4}\int\int\int\int \eta_{1,4}\,\eta_{2,4}\,\eta_{3,4}\,d\omega_1 d\omega_2 d\omega_3 d\omega_4\right) \ldots [95]$$

For a perfect gas, the partition function of potential energy is given by the first term Ω_{gas} alone. The second term represents the contribution of intermolecular forces, Ω_{mol}.

Since there is no interaction between the base molecules, the potential energy of the cluster depends only upon the relative coordinates of the tip molecule, and the integration can be performed over the available space, v/N, of the three others, which yields for the second term

$$ln\,\Omega_{mol} = N\,ln\left(1 + \frac{1}{3v}\int_\omega (e^{-\frac{\epsilon}{kT}} - 1)^3\,d\omega\right) \ldots [96]$$

In order to evaluate the integral, we have to introduce a definite function for the energy of interaction. Thus, the choice of this function becomes another important factor for the thermal properties of the substance. Only molecules with no electric moments shall be considered. Then the molecular force will be a superposition of an attractive and a repulsive force. However, the range of the repulsive force is much shorter than that of the other. For the densities in question, where the molecules do not approach each other closely enough to form clusters of more than four molecules for an appreciable length of time, it may also be assumed that they do not approach each other closely enough for an appreciable length of time to allow a substantial contribution to the energy of interaction by the force of repulsion. Therefore, ϵ is assumed to consist of energy of attraction only, which may decrease proportionally to some power of the distance r between the molecules (708,5)

$$\epsilon = -\epsilon_0\left(\frac{D}{r}\right)^n$$

where D is the diameter of the molecule, representing the closest approach of the two centers. According to the neglect of the repulsion, $\epsilon = 0$ for $0 < r < D$. Expressing $d\omega$ in polar coordinates and writing $R = \frac{r}{D}$, we can extend the integration to infinity and obtain

$$ln\,\Omega_{mol} = N\,ln\left(1 + \frac{4\pi D^3 N}{3v}\int_1^\infty (e^{\frac{\epsilon_0}{kTR^n}} - 1)^3 R^2 dR\right) \ldots [97]$$

Expansion into a power series of the term under the integral and introduction of van der Waals' term $b = {}^2/_3\pi D^3 N$ yields

$$ln\,\Omega_{mol} = N\,ln\left[1 + \frac{2b}{v}\int_1^\infty \sum_3^\infty{}_\tau \frac{3}{\tau!}(3^{\tau-1} - 2^\tau + 1) \times \left(\frac{\epsilon_0}{kT}\right)^\tau \frac{dR}{R^{n\tau-2}}\right] \ldots [98]$$

Integration gives

$$ln\,\Omega_{mol} = N\,ln\left[1 + \frac{2b}{v}\sum_3^\infty{}_\tau \frac{3}{\tau!}\cdot\frac{3^{\tau-1} - 2^\tau + 1}{n\tau - 3}\left(\frac{\epsilon_0}{kT}\right)^\tau\right] \ldots [99]$$

If terms of higher order than 3 are neglected, we obtain in first approximation

$$ln\,\Omega_{mol} = N\,ln\left[1 + \frac{1}{T^3 v}\cdot\frac{2b}{3(n-1)}\left(\frac{\epsilon_0}{k}\right)^3\right]$$

With the abbreviation

$$\theta_0 = \frac{\epsilon_0}{k}\sqrt[3]{\frac{4b}{3(n-1)}}$$

the contribution of the intermolecular forces to the characteristic function is

$$\Psi_{mol} = k\,ln\,\Omega_{mol} = R\,ln\left[1 + \frac{1}{2}\left(\frac{\theta_0}{Tv^{1/3}}\right)^3\right] \ldots [100]$$

It is obvious that Equation [100] is a first-order approximation for Equation [48], when $\alpha = {}^1/_3$. Thus, the statistical foundation of the semiempirical relations in section 4 has been derived. The quantity α has the invariable value ${}^1/_3$. The complete characteristic function is now

$$\Psi = \Psi_{kin}(T) + \Psi_{int}(T) + \Psi_{mol}(Tv^{1/3}) + R\left(1 + ln\frac{v}{N}\right). [101]$$

The contribution of the molecular forces to the internal energy of a system of N molecules is

$$u_{mol} = T^2\frac{\partial \Psi_{mol}}{\partial T} = T^2 v^{1/3}\Psi'_{mol}(Tv^{1/3}) \ldots [102]$$

where the prime denotes the differentiation with respect to the argument. The pressure of the system is obtained as

$$p = T\frac{\partial \Psi}{\partial v} = \frac{RT}{v} + \frac{1}{3}\frac{T^2}{v^{2/3}}\Psi'_{mol}(Tv^{1/3}) \ldots [103]$$

From Equation [103] follows

$$pv^{4/3} = RTv^{1/3} + \frac{1}{3}(Tv^{1/3})^2\Psi'_{mol}(Tv^{1/3})$$

or

$$pv^{4/3} = F(Tv^{1/3}) \qquad \pi = F(\theta)$$

which is equivalent to Equation [10] of the paper.

Furthermore, from Equation [103]

$$pv - RT = \frac{1}{3}T^2 v^{1/3}\Psi'_{mol}(Tv^{1/3})$$

Substitution of Equation [102] gives

$$pv - RT = \frac{1}{3}u_{mol}$$

which is Equation [15] of the paper. Consequently, we have for all molecules

$$\alpha = \frac{1}{3} \ldots [104]$$

The assumptions made in the paper regarding the internal energy of the system are maintained. The necessary corrections due to the new definition of α are:

Equation [16]...... $u = 3pv + u_{osc} + \frac{f_r - 3}{2}RT \ldots [105]$

Equation [17]...... $h = 4pv + u_{osc} + \frac{f_r - 3}{2}RT \ldots [106]$

$$\text{Equation [21]} \ldots\ldots c_v = 3v\frac{\partial p}{\partial T} + c_{osc} + \frac{f_r - 3}{2}R \ldots\ldots [107]$$

$$\text{Equation [22]} \ldots\ldots c_p = 4p\frac{\partial v}{\partial T} + c_{osc} + \frac{f_r - 3}{2}R \ldots\ldots [108]$$

where f_r is the number of degrees of freedom of the fully activated rotational energy:

For monatomic molecules............ $f_r = 0$
For linear molecules.................. $f_r = 2$
For polyatomic molecules............ $f_r = 3$

Further corrections are:

$$\text{Equation [33]} \ldots\ldots\ldots \text{add} + \frac{f_r - 3}{2} R \ln T$$

$$\text{Equation [34]} \ldots\ldots\ldots \text{add} + \frac{f_r - 3}{2} RT$$

$$\text{Equation [35]} \ldots\ldots\ldots \text{add} + \frac{f_r - 3}{2} R(1 + \ln T)$$

The Joule-Thomson coefficient of a perfect vapor is obtained from Equation [32] by differentiation as

$$\mu c_p = -\left(\frac{\partial \dfrac{v}{T}}{\partial \dfrac{1}{T}}\right)_p = 4v\left(\frac{1}{2 - \left(\dfrac{\theta_0}{\theta}\right)^3 \dfrac{e^{(\theta_0/\theta)^3}}{e^{(\theta_0/\theta)^3} - 1}} - 1\right). \quad [109]$$

The changes affect the relations for the adiabatic curve in section 7 of the paper. By substitution of Equation [105] into Equation [1] follows for $d\mathfrak{s} = 0$ the equation of the adiabatic curve of the perfect vapor

$$\frac{d\pi}{\theta} = -\frac{du_{osc} + \dfrac{f_r - 3}{2}RdT}{3T} \ldots\ldots\ldots\ldots [110]$$

for monatomic vapors ($du_{osc} = 0$; $f_r = 0$)

$$\frac{d\pi}{\theta} = \frac{R}{2}\cdot\frac{dT}{T} \ldots\ldots\ldots\ldots\ldots\ldots [111]$$

for diatomic vapors at moderate temperatures ($du_{osc} = 0$; $f_r = 2$)

$$\frac{d\pi}{\theta} = \frac{R}{6}\cdot\frac{dT}{T} \ldots\ldots\ldots\ldots\ldots\ldots [112]$$

for polyatomic vapors ($f_r = 3$)

$$\frac{d\pi}{\theta} = -\frac{du_{osc}}{3T} \ldots\ldots\ldots\ldots\ldots\ldots [113]$$

In Equations [110] to [113], the left side depends upon θ only, while the right side depends upon T only, which makes the integrations practicable.

The carbon-dioxide example in section 3 requires conversion into the correct properties of state $Tv^{1/3}$ and $pv^{4/3}$. The correct diagram in these properties is shown in Fig. 16.

It has been found that there are vapors the p, v, T data of which can be represented by a single curve in π, θ coordinates, even when the assumptions made in the statistical derivation are not fulfilled. In this case, the equation of state becomes purely empirical. The points of state of steam, which consists of molecules with large electric moments, coincide surprisingly well in a single curve. In Fig. 17, the values of the empirical constant θ_0 are plotted, calculated from Equation [32] for all states in the International Steam Tables of 1935. For each state, the highest and the lowest values for v, according to the allowed tolerance,

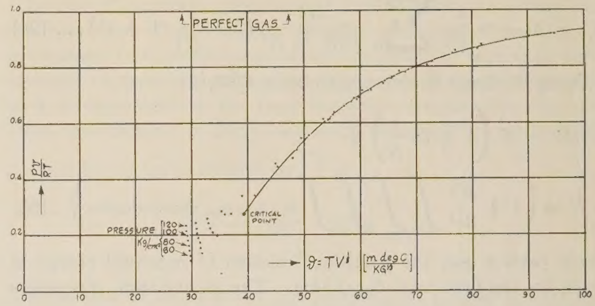

Fig. 16 Vapor Chart for Carbon Dioxide

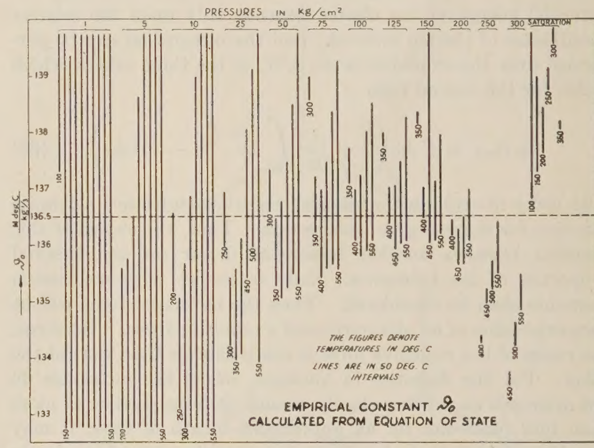

Fig. 17 Values of Empirical Constant θ_0 for Steam

have been substituted in the equation, and pertaining values θ_0 are connected by a bar in the diagram. If a line is traced across the diagram at $\theta_0 = 136.5$, it will intersect with about two thirds of all bars; which means that Equation [32] with $\theta_0 = 136.5$ will satisfy the respective states within the limits of the tolerance. For the remaining one third, the deviation is, with the exception of the highest pressures, very slight. It must be realized, that the tolerance varies only between ± 1 and ± 2 parts in 1000.

According to the title of the paper, this study is confined to the vapor region of fluids. In common usage, a state considerably above both critical pressure and critical temperature is referred to not as a vapor but as a compressed gas. These states, as well as liquids are not a subject of the paper. Nitrogen at zero C and pressures of hundreds of atmospheres, therefore, cannot be a criterion for the validity of the perfect vapor relations. The Joule-Thomson coefficient, according to Equation [109], always yields positive values. In so far as the author is aware, this is always the case in the vapor region, and the inversion of the Joule-Thomson effect occurs in a region far remote from condensation. Furthermore, it is mentioned in section 3 that the perfect vapor relations apply only to densities not higher than about one half the density in the critical point. The reason for this is evident from the statistical derivation. The perfect vapor method is intended to furnish preliminary information on the properties of vapors when experimental data are scarce. The examples in the paper show that at least fairly accurate results may be expected, and the experience available up to the present is encouraging.

The author greatly appreciates the interest shown by so many discussers and hopes that each of them may find the desired information in this closure.